UNIVERSITY OF LIVERPOOL

Characterisation of Potential Therapeutic Molecules for Neuroblastoma Using Chick Chorioallantoic Membrane Xenograft Model

Thesis submitted in accordance with the requirements of the University of Liverpool for the degree of Doctor in Philosophy

By
Rasha Swadi

September 2018

Declaration

This thesis entitled: “Characterisation of New Potential Therapeutic Molecules for Neuroblastoma Using Chick Chorioallantoic Membrane Xenograft Model”

is entirely my own work, except where indicated in the text.

This material contained within this thesis has not been presented for any other degree qualification.

This research was undertaken at the Department of Cellular and Molecular Physiology at the University of Liverpool and under Supervision of Dr Diana Moss.

Table of Contents

Abstract

Neuroblastoma is a paediatric cancer derived from the sympathoadrenal cell lineage that commonly presents as a high-risk metastatic disease with a poor prognosis.

Currently, differentiation therapy with retinoic acid is an effective therapeutic option used in the clinic, however not all tumours respond. New therapeutic agents that can control not only tumour growth but also metastasis are urgently needed and drugs that promote differentiation are particularly appropriate for neuroblastoma treatment.

Preclinical models are required to aid the development of novel therapeutics for this challenging childhood malignancy, however current systems are complex and inherently costly. Here we employ a 3Rs-compliant cost-effective preclinical chick embryo model to act as a tool for neuroblastoma therapeutic research.

Neuroblastoma cell lines were engrafted on the chorioallantoic membrane (CAM) of chick embryos and allowed to form tumours over a 7 day period. If cells were preconditioned in hypoxia they metastasised into the chick embryo. First, we validated the chick embryo model using retinoic acid and then investigated the potential of CDK inhibitors on neuroblastoma cell differentiation, tumour progression and metastasis. With retinoic acid and the CDK inhibitors we observed a reduction of tumour cell proliferation and an increase in differentiation markers. The CDK inhibitors were particularly effective in inhibiting metastasis with a single injection reducing the number of embryos with metastasis by 60%. In addition, the expression of a panel of genes with known roles in metastasis, which increased upon hypoxia-preconditioning, was largely reduced by RO-3306 (CDK1 inhibitor). These results demonstrate that CDK inhibitors are a promising alternative to currently existing therapies. We have also begun to establish the chick embryo model as an alternative to the mouse xenograft model for short term analysis of cell differentiation, proliferation, apoptosis and metastasis in response to drug therapy.

Acknowledgements

There are many people I would like to thank for their support and assistance throughout this project. I began this project with little experience in laboratory based work, and it is largely through the excellent teaching and patience of Dr Diana Moss that I have become confident in conducting lab work independently.

So for this incredible opportunity my deepest gratitude goes to my supervisor Dr Diana Moss who has been excellent at guiding me throughout the PhD research and her advice and encouragement has been fundamental to this project. Thank you for affording me the opportunity to work in your laboratory and for being ever-willing to answer my questions.

I would like also to thank Dr Rabiu Inuwa for enabling such a pleasant working environment, always being ready to offer advice and feedback and has also provided warm friendship throughout the project. I wish him the very best for the future.

I am hugely grateful for the help and friendship I have received from Dr Anne Herrmann. I would like to thank Dr Helen Kalirai for her help in conducting Ki67 staining.

Special thanks must go to the **Ministry of Higher Education and Scientific Research (MOHESR) in Iraq** for providing me with this unique and invaluable opportunity to complete my PhD study at the University of Liverpool.

Lastly and most importantly I would like to thank my family for their unwavering love and support. Thanks to my parents who have helped me reach where I have in life and for putting up with me during my thesis writing - I could not have done this without you. A big thank you hugs to my lovely sons, Munty and Moamel, whose gave me the absolute inspiration to complete this thesis. The biggest thanks of all goes to my best friend, my husband, Hayder, who has been there throughout for me; and being ever so patient, for giving me his time and effort to complete my thesis on time, and for helping me see things in perspective at every step of my life.

List of abbreviations

A260	Absorbance at 260nm
A280	Absorbance at 280nm
AHSCT	Autologous haematopoietic stem cell transplant
ALK	Anaplastic lymphoma kinase
ASCL1	Achaete-scute homolog-1
ATP	Adenosine triphosphate
ATRX	Alpha thalassemia/mental retardation syndrome X-linked
BMOV	Bis(maltolato)oxovanadium(IV)
BMP	Bone morphogenetic protein
BSA	Bovine serum albumin
CAM	chorioallantoic membrane
cDNA	Complementary deoxyribonucleic acid
CDK	Cyclin dependent kinase
CNS	Central nervous system
CO_2	Carbon dioxide
C_t	Cycle quantification
DAPI	4', 6-Diamindino-2-Phenylindole,Dihydrochloride
DMEM	Dulbecco's modified Eagle's medium
DMSO	Dimethyl sulfoxide
E	Embryonic day
EDTA	Ethylenediaminetetraacetic acid
FBS	Fetal bovine serum
GAPDH	Glyceraldehyde-3-phosphate dehydrogenase

GEMM	Genetically engineered murine model
GFP	Green fluorescent protein
H&E	Haematoxylin and eosin
HIF	hypoxia inducible factor
HPRT1	Hypoxanthine phosphoribosyltransferase 1
HRP	Horseradish peroxidase
HSR	Homogeneously staining region
IHC	Immunohistochemistry
IDRF	Imaging defined risk factor
INPC	International Neuroblastoma Pathology Classification
INRGSS	The International Neuroblastoma Risk Group Staging System
KLF4	Kruppel-like factor 4
LOH	Loss of heterozygosity
mIBG	metaiodobenzylguanidine
MMPs	matrix metalloproteinases
MYCN	Neuroblastoma-derived v-myc avian myelocytomatosis viral related oncogene
NRT	No-reverse transcriptase
NTC	No-template control
PHOX2A	Paired-like homeobox 2a
PHOX2B	Paired-like homeobox 2b
PS	Penicillin streptomycin
RA	Retinoic acid
RAR	Retinoic acid receptor
RARE	Retinoic acid response elements
ROBO2	Roundabout, axon guidance receptor, homolog 2

RXR	Retinoid X receptor
STMN4	Stathmin-like 4
TGF-β	Transforming growth factor-β
UBC	Ubiquitin C

Chapter One: Introduction

1.1. Neuroblastoma: an introduction

Neuroblastoma is a paediatric cancer derived from the neural crest cells destined to form the sympathetic nervous system. These neural crest cells give rise to the sympathetic neural ganglia and the adrenal medulla (Park *et al.*, 2013). The neuroblastoma tumour forms in the adrenal glands or the sympathetic ganglia and disseminates to other parts of the body including bone, bone marrow, liver and skin (Maris *et al.*, 2007). Neuroblastoma is a peculiar disease characterised by various biological and histological heterogeneity ranging from spontaneous regression without treatment to advanced resistant and metastatic disease (Weinstein, 2003; Maris *et al.*, 2007).

1.1.1. Epidemiology, genetic predisposition and aetiology

Neuroblastoma is a rare tumour, nevertheless it is the most commonly occurring extra-cranial solid tumour in children within 2 years of age (Heck *et al.*, 2009; Cheung and Dyer, 2013) and the third most common paediatric malignancy, following leukaemia and brain tumours. It has an incidence of 10.2 per million birth (Schwab *et al.*, 2003; Maris *et al.*, 2007). Most cases (90%) are diagnosed in children before 5 years of age; and rarely in older children up to about 14 years old; or even occasionally in adults up to 19 years of age (Izbicki, Mazur and Izbicka, 2003; Maris, 2010; Schleiermacher, Janoueix-Lerosey and Delattre, 2014). Despite the fact that, neuroblastoma has the highest rate of spontaneous regression of all human cancers (Brodeur, 2003) the metastatic form of the disease has survival probabilities of less than 40% and it thus accounts for approximately 15% of childhood oncology deaths (DeBerardinis *et al.*, 2008; Maris, 2010). Neuroblastoma can be of either familial (1-2%) or sporadic in origin (98%) (Friedman *et al.*, 2005). Familial neuroblastoma is usually diagnosed at an earlier age, often within the child's first year of life and multiple primary tumours at diagnosis is much more common in those with a genetic predisposition than in patients with sporadic disease (Mullassery and Losty, 2016). Hereditary neuroblastoma is often associated with mutations in the anaplastic lymphoma kinase (ALK) gene and in the paired-like homeobox 2B

(PHOX2B) gene, together they account for approximately 90% of hereditary neuroblastoma (Mossé *et al.*, 2008; Deyell and Attiyeh, 2011).

In contrast to most adult malignancies, very few causative factors have been identified in paediatric malignancies and this applies to neuroblastoma. The embryonal origin of tumour cells and young age at onset suggest pre- and perinatal environmental effects may be of significance. Several factors has been investigated including gestational weight and age, prenatal hormone exposure, alcohol consumption, maternal smoking, however no consistently associated factor has been identified in large studies (Bluhm *et al.*, 2008; McLaughlin *et al.*, 2009).

1.1.2 The neural crest

The neural crest (NC) is a multipotent embryonic cell population that arises from the embryonic ectoderm cell layer at the neural plate border (***Figure1.1 a***) and in turn give rise to a number of diverse cell lineages including melanocytes, craniofacial cartilage and bone, smooth muscle, peripheral and enteric neurons and glia (Patel *et al.*, 2012). A network of migration pathways and microenvironmental cues act together to control and maintain the mobility, directionality and specificity of cellular movement in migratory neural crest cells (NCCs) and disruption of which may predispose multipotent neural crest precursors to malignant transformation (Cheung and Dyer, 2013).

1.1.2.1. Development of sympathetic nervous system

During embryo development, at the third and fourth weeks of gestation in human, the ectoderm differentiates into the neural ectoderm (neural plate) and the non-neural ectoderm, the two regions interact at the neural plate border (Gammill and Bronner-Fraser, 2003). Inductive changes within the neural plate border produced by the ectoderm, the neuroepithelium and the underlying mesoderm induce the expression of a series of transcription factors, such as those encoded by the Snai1/2, Slug, Twist, Foxd3 and Sox10 genes, that define the formation of the neural crest territory and control subsequent NC development (Mayor and Theveneau, 2013).

Prior to migration, neural crest cells (NCCs) undergo complete or partial epithelial-to-mesenchymal transition (EMT), which confer enhanced migratory ability (Mayor and Theveneau, 2013; Shyamala *et al.*, 2015).

NC specifier genes such as Snai1/2, Slug and Twist form a transcriptional network to promote EMT through degrading the basement membrane and downregulating the cell-adhesion molecules such as N-CAM, N-cadherin, cadherin-6B and integrins, resulting in NCCs delamination enabling migration (Friedl, 2010; Mayor and Theveneau, 2013). whilst other NCCs specifiers such as Sox10 and Foxd3 are responsible for cell survival, migration and maintaining multipotency (Kim *et al.*, 2003; Stewart *et al.*, 2006). Compared to non-migratory NCCs, early migratory NCCs possess high level of MYCN protein that in turn facilitates migration. Expression of MYCN reduces in differentiating sympathetic neurons and therefore is found to be absent in adult tissues (Zimmerman *et al.*, 1986; Dzieran *et al.*, 2018).

After delamination, NCCs migrate from different positions along the anterior-posterior axis developing into various tissues. Thus NCCs can be categorised into cranial NC, cardiac NC, vagal NC trunk NC and sacral NCC based on their axial position of origin together with the cell and tissues they contribute to during terminal differentiation (Gilbert, 2000).

Cranial NCCs form the craniofacial mesenchyme that differentiates into various cranial ganglia and craniofacial cartilages and bones as well as smooth muscles, connective tissue and melanocytes (Friedl, 2010). The majority of cranial NCCs population enter the pharyngeal pouches and arches where they contribute to the thymus, bones of the middle ear and jaw and the odontoblasts of the tooth primordia whist some enter the frontonasal region to give rise to the frontal and nasal bones (Gilbert, 2000). Cardiac NCCs give rise to regions of the heart such as the musculo-connective tissue of the large arteries, and part of the septum, which divides the pulmonary circulation from the aorta as well as participate in the formation of semilunar valves (Gilbert, 2000; De Lange *et al.*, 2004). The vagal NCCs from the enteric nervous system, which innervates the gastrointestinal digestive tract (Gilbert, 2000). Trunk NCCs give rise to two populations. Cells destined to become

melanocytes migrates dorsolaterally into the ectoderm towards the ventral midline. Whilst cells destined to form dorsal root ganglia, sympathetic ganglia and adrenal medulla migrate ventrolaterally through the anterior portion of each sclerotome (Gilbert, 2000). Sacral NCC, which is a component of trunk NCCs contributes together with the vagal NCCs to form of enteric nerves system and the parasympathetic ganglia.

Several migration and microenvironmental cues act together to control and maintain the mobility, directionality and specificity of cellular movement in migratory NCCs (Gammill and Roffers-Agarwal, 2010; Theveneau and Mayor, 2012), and disruption of which may predispose multipotent neural crest precursors to malignant transformation (Cheung and Dyer, 2013). In trunk NCCs (***Figure1.1 b***), sympathetic precursor NCCs expressing chemokine receptor type 4 (CXCR4) are repelled from the intersomitic spaces by semaphorins and drawn to the dorsal aorta and the region surrounding the gut by the chemotactic CXCR4 ligand, stromal cell-derived factor 1 (SDF-1) (Kasemeier-Kulesa *et al.*, 2006; Kulesa and Gammill, 2010). Ephrins are expressed in the posterior section of each sclerotome, bind to NCC surface Eph receptors, initiate migration-promoting and -inhibitory effects, depending on the class of ephrins encountered (Krull *et al.*, 1997; McLennan and Krull, 2002), thus controlling the specificity of cellular movements (Kasemeier-Kulesa *et al.*, 2006).

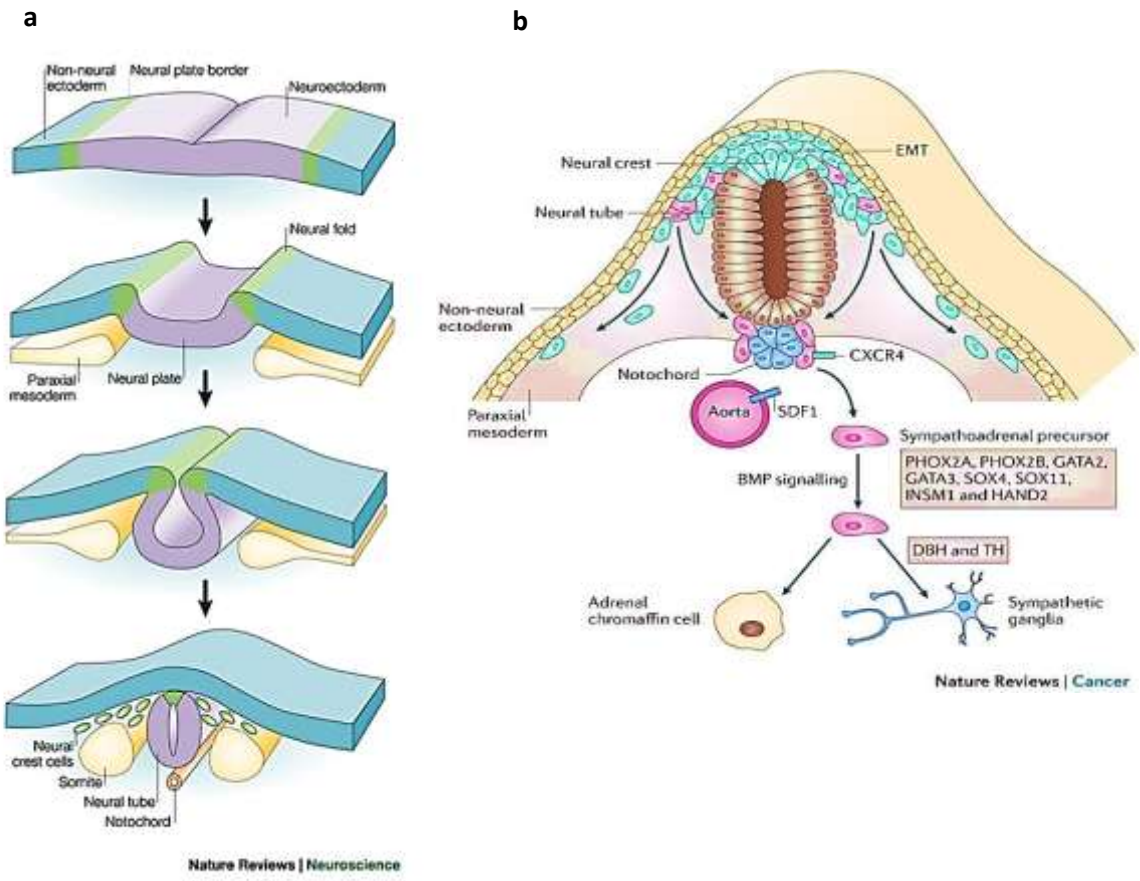

Figure1.1 Neurulation and the development of sympathoadrenal lineage of neural crest. ***a*** *The neural crest is first induced at the region of the neural plate border (green). After neural tube closure, the neural crest delaminates from the region between the dorsal neural tube and overlying ectoderm and migrates out towards the periphery.* ***b*** *Neural crest cells giving rise to the adrenal gland and sympathetic ganglia migrate to the region of the dorsal aorta and undergo differentiation. Bone morphogenetic protein (BMP), initiates differentiation of the sympathoadrenal precursor and multiple transcription factors are involved in this process. At this stage cells committed to becoming sympathetic ganglia acquire the catecholaminergic enzymes, dopamine-ß hydroxylase (DBH) and tyrosine hydroxylase (TH).* ***a*** *adapted from (Gammill and Bronner-Fraser, 2003) and* ***b*** *adapted from (Cheung and Dyer, 2013).*

Post-migratory NCCs aggregate at the dorsal aorta to form primary sympathetic ganglia prior to divergence into sympathetic ganglion neurons and adrenal chromaffin cells (Huber, 2006). In response to bone morphogenetic proteins (BMPs) secreted by dorsal aorta, NCCs destined to become sympathetic neurons undergo neuronal and catecholaminergic differentiation (Mohlin, Wigerup and Påhlman, 2011).

The dorsal aorta–derived BMPs signalling results in upregulation expression of various transcription factors that are essential for neuronal differentiation. Initially BMPs induce achaete-scute homolog 1 (ASCL1) expression (Schneider *et al.*, 1999). ASCL1 (MASH-1 in rodents, hASH-1 in humans, and CASH-1 in chicks) is the first marker of neuronal specification, however, high level of hASH-1 are seen in neuroblastoma tumours and cell lines (Söderholm *et al.*, 1999). BMPs induce the expression of PHOX2B, essential for the ASCL1 maintenance (Pattyn *et al.*, 1999) while, ASCL1 promotes the expression of PHOX2A. Together, ASCL1, PHOX2A and PHOX2B drive the expression of enzymes necessary for catecholamine synthesis, including tyrosine hydroxylase (TH) and dopamine ß-hydroxylase (DBH) (Ernsberger *et al.*, 2000). PHOX2B also initiates terminal sympathoadrenal differentiation. ASCL1 promotes further development of early precursors that are already committed to a neuronal fate, allowing the transition into a mature sympathetic neuron or chromaffin cell. Loss-of-function studies demonstrate that mice lacking PHOX2B fail to properly develop autonomic ganglia (Pattyn *et al.*, 1999). Furthermore, the PHOX2B gene is found to be mutated in some of familial neuroblastomas.

An inactivating mutation of PHOX2B is known to predispose an individual to developing neuroblastoma through dedifferentiation and increasing proliferation of sympathoadrenal cells resulting in malignant transformation (Bourdeaut *et al.*, 2005; Raabe *et al.*, 2008; Reiff *et al.*, 2010). In one study, consistent with PHOX2B role as an important neurodevelopmental gene, inducing overexpression of wild-type PHOX2B in neuroblastoma cell lines inhibited cell proliferation and synergized with all-*trans* retinoic acid to promote differentiation (Raabe *et al.*, 2008). Mutated PHOX2B has also been occasionally detected in sporadic neuroblastoma (Van Limpt *et al.*, 2004)

while overexpression of both mutated PHOX2A and PHOX2B is frequently detected in both neuroblastoma cell lines and primary tumours (Longo *et al.*, 2008). The expression of Heart And Neural Crest Derivatives expressed transcript 2 (HAND2), is dependent on PHOX2B, yet precedes PHOX2A, and in addition, is expressed independently of ASCL1. HAND2 is essential for both the proliferation of sympathetic neuron precursors and their noradrenergic differentiation. HAND2-knockout embryos showed reduced number of sympathetic neurons as well as reduced TH and DBH expression in those neurons that developed (Schmidt *et al.*, 2009). HAND2 is routinely detected in neuroblastomas, regardless of stage, suggesting that in these tumours, sympathetic differentiation is blocked at a relatively early stage in development (Gestblom *et al.*, 1999). GATA2 and GATA3, zinc finger transcription factors, are expressed after ASCL1, PHOX2B, HAND2 and PHOX2A, but before the expression of the noradrenergic enzymes TH and DBH (Tsarovina, 2004), and are both critical for the generation and differentiation of sympathetic neurons. In the absence of embryonic GATA3, a lack of TH and DBH in the sympathetic ganglia of embryos was observed (Lim *et al.*, 2000). GATA3-null embryos also showed reduced ASCL1, PHOX2B and HAND2 in the chromaffin cells, implying that feedback from GATA3 is required to maintain expression of supposed upstream transcription factors (Moriguchi, 2006).

Although the five transcription factors mentioned above are expressed in an ordered manner (ASCL1 before PHOX2B and HAND; PHOX2B before PHOX2A, HAND and GATA2/3), they are cross-linking and operate as a network that eventually results in sympathetic or adrenal cell formation. From the primary sympathetic ganglia, the prospective chromaffin cells then migrate toward the adrenal gland, and the cells destined to become sympathetic neurons travel dorsally to the position of the secondary sympathetic ganglia. Once they reach their desired destination, a change in gene expression will commence accordingly to induce differentiation further (Simoes-Costa and Bronner, 2015).

Further downstream, neurotrophins (NT), including nerve growth factor (NGF), brain-derived neurotrophic factor (BDNF), neurotrophin4/5 (NT-4/5), and neurotrophin-3 (NT-3), are heavily

involved in the formation of the neural phenotype via binding to their respective receptors family of tyrosine kinases (TrK) (Nakagawara, 2001, 2004). TrkC is the first to be expressed, TrkB is transiently expressed around the time or the primary sympathetic ganglia and TrkB needs to be down regulated and upregulation of TrkA is required for differentiation to proceed (Banfield *et al.*, 2001). Under normal levels of expression, each of these promotes and supports survival and differentiation of the sympathetic neurons (Banfield *et al.*, 2001). However, if TrkB downregulation is impaired during development, this may contribute to the genesis of neuroblastoma (Straub, Sholler and Nishi, 2007). The expression of full length TrkB with its ligand BDNF, is linked with poor outcome and undifferentiated tumours strongly associated with MYCN-amplification (Nakagawara and Ohira, 2004). However, full length TrkA expression is associated with neuroblastoma tumours destined to undergo spontaneous regression or increased differential state of tumours (Straub, Sholler and Nishi, 2007). Taken together, this suggests the role of TrkA in maintaining the differentiation process in sympathetic neurons and are classified as positive markers of neuroblastoma tumours.

1.1.3. Molecular biology

Numerous studies in molecular biology have been conducted to identify and to better understand the genetic events involved in development and progression of neuroblastoma. Neuroblastoma tumours demonstrate significant clinical heterogeneity; this perhaps reflects the absence of a single genetic alteration common to all tumours (Pugh *et al.*, 2013).

1.1.3.1. DNA ploidy

Ploidy is defined as the number of sets of chromosomes in each cell. Virtually, all cancers demonstrate aneuploidy, an abnormal number of chromosomes (Rajagopalan and Lengauer, 2004). Diploid is the normal occurrence of two copies of each chromosome: one maternal and one paternal, hence 46 chromosomes in total. The majority of neuroblastoma tumours have either near-diploidy (37-57 chromosomes) or hyper-diploidy (58-80 chromosomes) (Sakurai, Maseki and Sakurai, 1987). Malignant tumours with DNA aneuploidy are thought to form as a result of genomic stability defects resulting in chromosomal rearrangement with unbalanced translocations. Near-diploidy cases tend to confer a worse prognosis compared to hyper-diploid tumours. Thus, DNA ploidy is one of the genetic variables used in the International Neuroblastoma Risk Group (INRG) Classification System (Cohn *et al.*, 2009).

1.1.3.2. Segmental chromosome aberrations

Acquired somatic mutations and associated DNA copy number aberrations, are frequently found in high risk neuroblastomas (Pugh *et al.*, 2013). 25-35% of neuroblastoma tumours have a loss/deletion of chromosome 1p (Thorner, 2014) whereas >70% of cases have 1-3 additional copies of 17q (17q gain). Both chromosome 1p deletion and 17q gain are associated with unfavourable prognostic features such as MYCN amplification and an older age of diagnosis (Ambros *et al.*, 2009). Also, a deletion in 11q chromosomal region has been found in 15% of high risk neuroblastomas, and rarely coincides with MYCN amplification, therefore it is a powerful prognostic marker in non-MYCN amplified tumours and been included as a prognostic criterion in INRG system (Attiyeh *et al.*, 2005).

1.1.3.3. MYCN gene amplification

The most widely researched gene associated with neuroblastoma is MYCN. Approximately 35% of neuroblastoma cases are characterized by amplification of MYCN and it is firmly associated with advanced disease and poor prognosis regardless of the stage of disease or age at diagnosis (Cohn *et al.*, 2009). In children aged less than 18 months with metastasis and MYCN amplification, the overall 5 years survival rate is 34% however in the same cohort lacking MYCN amplification it was found to be 82% (Cohn *et al.*, 2009).

The MYCN gene is found in chromosome 2p24, and remains a single copy at this location even in MYCN amplified cells. Amplification (increased number of copies) of this gene can be present at an alternate locus either as extra-chromosomal chromatin bodies (double minutes) or intrachromosomally as homogeneously staining region (HSR). HSR are generally located on different chromosomes, not at the resident site, 2p24, of MYCN (Moreau *et al.*, 2006).

MYCN encodes for the N-myc protein, which together with C-myc and L-myc form the myc family of basic helix-loop-helix (bHLH) proteins which function as transcription factors (TF). The myc family play a fundamental role in the control of the normal (and oncogenic) proliferation, growth, metabolism, differentiation and apoptosis of cells. N-myc oncoprotein possesses a leucine zipper motif that is important for forming a heterodimer complex with myc-associated factor X (MAX) causing transcriptional activation of target genes (Kamijo and Nakagawara, 2012; Gherardi *et al.*, 2013). MYCN can act as a transcriptional enhancer by forming a heterodimer with the MAX protein; this dimer binds to E-box sequences (CANNTG) in the promoter regions of target genes. MYCN-MAX complex executes their function through recruiting histone acetyltransferase enzymes (HATs) (McMahon, Wood and Cole, 2000). MAD dimerises with MAX, MAD-MAX heterodimers recruit histone deacetylates (HDACs) to repress transcription of MYCN target genes. The MAD-MAX complex also reduces the amount of MAX available for MYCN binding, as well as competing with the MYCN-MAX complexes for the same promoter E-boxes. Thus MAD-MAX acts as a transcriptional repressor while MYCN appears to function as an activator (Grandori *et al.*, 2000; Nikiforov *et al.*, 2003). In

addition, MYCN can also repress transcription by forming a heterodimer with myc-interacting zinc finger protein 1 (MIZ1) and thus inhibiting transcription of its target genes (Eilers and Eisenman, 2008).

Amplification of the MYCN gene typically leads to overexpression and increased transcriptional activation /inhibition of over 200 genes resulting in tumour survival and progression. It upregulates genes involved mainly in proliferation, angiogenesis and drug resistance and downregulates number of genes involved in differentiation and apoptosis (Huang and Weiss, 2013).

MYCN overexpression alone was not efficient to induce tumorigenesis in genetically engineered murine models (Chesler and Weiss, 2011). However, MYCN overexpression associated ALK mutation induced spontaneous development of neuroblastoma tumours in mice. The second modification, induced ALK mutation, is thought to block apoptosis and maintain MYCN stability resulting in neuroblastoma growth. Of note, the resulted tumours in mice mirrored the histology, chromosomal aberrations and localisation of those formed in human (Heukamp *et al.*, 2012; Marshall *et al.*, 2014).

Downregulation of MYCN is required for terminal differentiation of neuronal precursors so the control of MYCN protein is tightly controlled in a cell-cycle–specific manner. Knockdown of MYCN expression in murine models of neuroblastoma demonstrated an increase of cellular differentiation and a reduction in cell proliferation (Chesler and Weiss, 2011). Therefore, MYCN inhibition is an attractive therapeutic approach for MYCN amplified tumours (***see section 1.1.3.3.1***).

1.1.3.3.1. Therapeutic mechanisms targeting MYCN activity

Because the MYCN structure is highly conserved making direct inhibition difficult, much attention is being directed to target molecules that interfere and modulate the activity of MYCN. Indeed four approaches have been identified to target MYCN activity. The first mechanism is by targeting DNA-binding functions of MYCN through inhibiting MYC: MAX protein interactions using a dominant

negative MYC mutant (Omomyc). Omomyc protein binds to all MYC family members and prevents dimerization with MAX (Soucek *et al.*, 2008; Prochownik and Vogt, 2010).

Targeting transcription of MYCN is the second mechanism. This involves inhibiting bromodomain and extra terminal (BET) family adaptor proteins (BRD2, BRD3, BRD4) that localize to MYC promoters (Mujtaba, Zeng and Zhou, 2007), with for example BET inhibitor JQ1 (Puissant *et al.*, 2013). BET proteins contain acetyl-lysine recognition motifs, or bromodomains, that bind acetylated lysine residues in histone tails usually correlated with euchromatin state and transcriptional activation (Mujtaba, Zeng and Zhou, 2007). JQ1 supresses the transcriptional activity of MYCN and hence downregulates MYC/MYCN transcriptional program (Puissant *et al.*, 2013).

The third mechanism is targeting the oncogenic stabilization of MYCN. In proliferating cells, MYCN is initially phosphorylated at serine 62 by Cyclin dependant kinase 1/Cyclin B. The S62-phosphorylated protein is stabilized and competent to enter the nucleus. Nuclear MYCN binds to its partner MAX and stimulates the transcription of target genes important in cell cycle, proliferation, differentiation and apoptosis (Gustafson and Weiss, 2010). This priming phosphorylation at S62 allows the binding of GSK3β, as well as Pin1 and PP2A in a complex also containing Axin. Active GSK3β phosphorylates MYCN at threonine 58, producing doubly phosphorylated, stabilized and transcriptionally active MYCN. In a Pin1-mediated process, PP2A dephosphorylates the S62 phosphate, enabling binding of and E3 ubiquitin ligases (F-box and WD repeat domain-containing 7 (FBXW7)) (Barone *et al.*, 2013). FBXW7 subsequently drives poly-ubiquitination and proteasomal degradation of MYCN. Aurora A kinase can bind to and stabilize polyubiquitinated/phosphorylated MYCN, potentially leaving it competent to bind to MAX and activate transcription (Huang and Weiss, 2013). mTORC1 also directly phosphorylates and inhibits PP2A, enabling the accumulation of doubly phosphorylated, and consequently drive oncogenic stabilisation of MYCN contributing to the general proliferation-promoting downstream effects of the PI3K /MYCN pathway (Cheng *et al.*, 2007).Thus inhibition of

CDK1, Aurora A kinase or mTORC1 confer MYC protein stabilisation and maintenance leading to potential degradation of MYCN (Gustafson and Weiss, 2010).

Targeting the expression or function of MYCN is the fourth mechanism. Regulation of the expression of MYC proteins or modification of MYC function have long been known and are currently used to treat neuroblastoma patient. For example, retinoic acid downregulates MYCN expression and inhibits its transcriptional oncogenic activity. Downregulation of MYCN expression induces cell-cycle arrest and stimulates neuronal differentiation (Thiele, Reynolds and Israel, 1985). MYCN expression also can be modulated through regulating the let-7 family of microRNAs, which negatively regulate MYCN expression (Molenaar, Domingo-Fernández, *et al.*, 2012).

1.1.3.4. ALK gene aberrations

Anaplastic lymphoma kinase (ALK) gene encodes a receptor tyrosine kinase protein that plays an important role in the CNS and PNS development. ALK protein has an anti-apoptotic role when bound to its ligase (pleiotrophin) (Bowden, Stoica and Wellstein, 2002) as well as a role in cellular differentiation and axon guidance (Palmer *et al.*, 2009). Overexpression of ALK has implications in the development of human cancers such as non-small cell lung cancer, anaplastic large cell lymphoma, neuroblastoma and several other anaplastic tumours (Berry *et al.*, 2012)

Activating germline mutations of ALK have been detected in the majority of familial neuroblastomas and point mutations have been found in approximately 7-10% of sporadic neuroblastoma cases (Huang and Weiss, 2013). Constitutive ALK signalling is thought to contribute to oncogenic transformation via controlling cell cycle progression, and cell survival and migration (Carpenter and Mossé, 2012).

The ALK gene is found in chromosome 2p23. The most potent ALK mutation detected is a recurrent cytosine-to-adenine change in exon 23 that results in a phenylalanine-to-leucine substitution at codon 1174 (F1174L) within the kinase domain (Yan *et al.*, 2011). ALK^{F1174L} mutation occurs in a high

proportion of MYCN-amplified neuroblastoma cases. Amplification of the ALK gene almost exclusively occurs in MYCN-amplified neuroblastoma primary tumours, and within this group it represents 15% of the cases (George *et al.*, 2008). Interestingly, ALK and MYCN (whose gene is located at 2p24) are physically linked on chromosome 2p and that may explain why amplification of ALK frequently occurs with MYCN amplification (De Brouwer *et al.*, 2010). This combined occurrence seems to be associated with a particularly poor outcome suggesting a positive correlation between both aberrations as supported by recent animal studies. When mice overexpressing ALK^{F1174L} are crossed with MYCN transgenic mice, they breed a progeny with aggressive, invasive and bulky neuroblastoma tumours coupled with poor survival rate (Berry *et al.*, 2012). A similar study on zebrafish revealed that the co-occurrence of the two aberrations of ALK^{F1174L} and MYCN accelerated neuroblastoma tumour onset and increased the frequency of tumours compared to MYCN alone (Zhu *et al.*, 2012). It should be noted that, ALK cooperates with MYCN to drive malignancy, as activation of ALK results in MYCN overexpression. ALK stabilizes the activity of the MYCN protein via activating PI3K/AKT/mTOR and MAPK pathways, as well as blocks apoptosis allowing escape route for MYCN-amplified cells of being able to apoptose (Berry *et al.*, 2012; Schönherr *et al.*, 2012; Zhu *et al.*, 2012). Thus targeting both of MYCN and ALK overexpression may provide a novel therapeutic approach for neuroblastoma patients.

1.1.4. Hallmarks of cancer and Neuroblastoma

As discussed in the previous section, there are a number of genetic aberrations responsible for the development and heterogeneity of neuroblastoma tumours. Alongside the genetic aberrations, the transition to malignant form requires the gaining of biological capabilities. In 2011, Hanahan and Weinberg have described 8 essential alterations (hallmarks) in cell biology in addition to two enabling characteristics that collectively dictate malignant growth (Hanahan and Weinberg, 2011). These capabilities/ hallmarks are mostly shared in all types of human cancers and here will be discussed in the context of neuroblastoma (***Figure 1.2***).

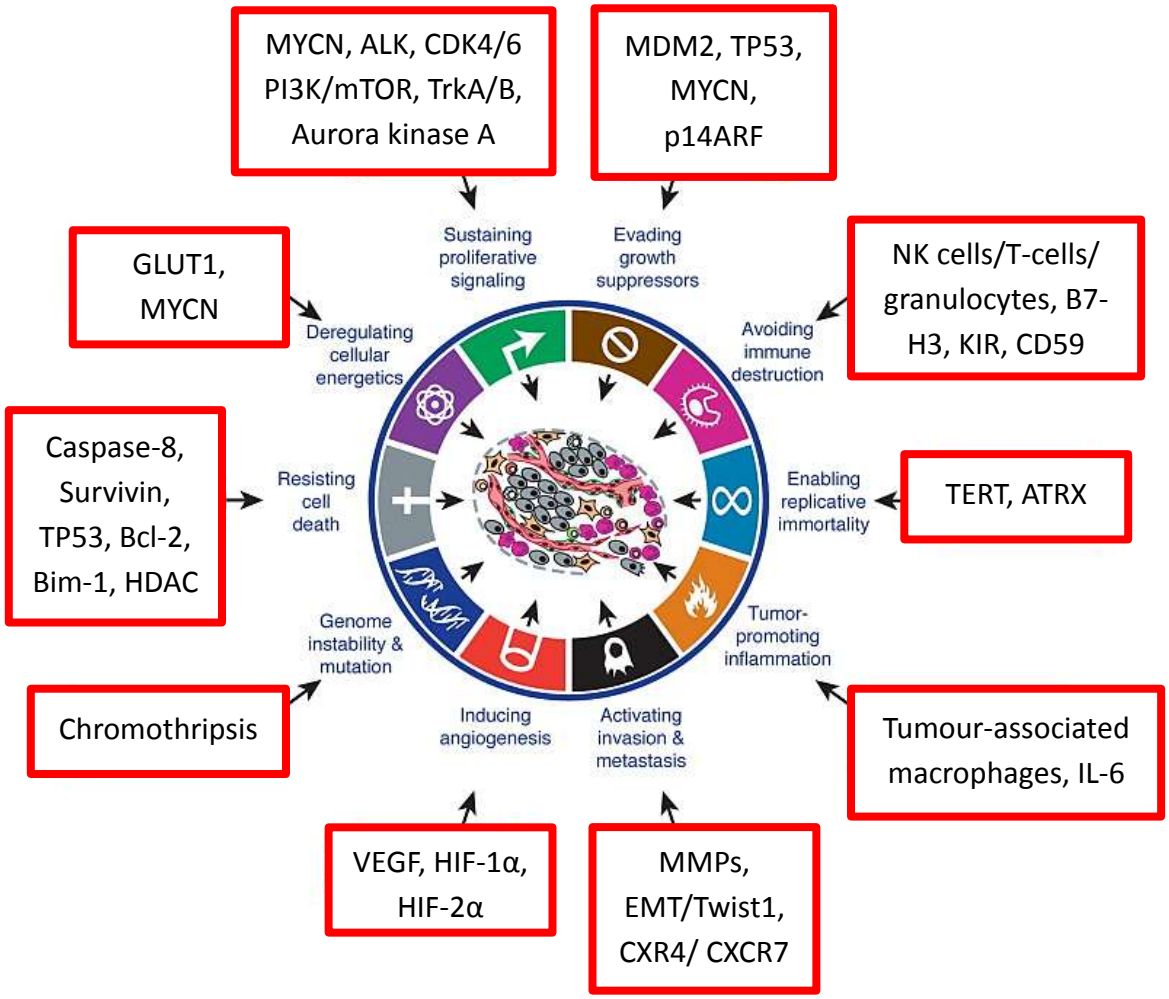

Figure1.2 hallmarks of cancer and enabling characteristic acquired by cancer cells during the process of tumorigenesis, described by Hanahan and Weinberg (2011). *Red boxes illustrate the multiple genes and genetic events contribute to the development of neuroblastoma.*

1.1.4.1. Self-sufficiency in growth signals

Self-sufficiency in growth signals is considered a defining property of stem cells. Self-renewal is important in normal tissue repair, embryogenesis and homeostasis (Horne and Copland, 2017). Cell proliferation in normal cells is strictly coordinated to maintain the function with normal architecture (Hanahan and Weinberg, 2011). Cell growth signals are largely conveyed through growth factors that bind specific cell-surface receptors on the cell membrane to transmit signals to the intracellular signalling pathways. Signals transduce to the nucleus leading to an activation of the nuclear regulatory factors that regulate DNA transcription and eventually cell cycle entry and growth (Borah *et al.*, 2015; Horne and Copland, 2017). Similar to normal cells, cancer cells also use the same

mechanism process to maintain their proliferation however they deregulate any of the aforementioned steps thereby endowing cells with sustained proliferation signalling pathways (Robbins *et al.*, 2005). Overexpressed or mutated proto-oncogenes, such as ALK and MYCN, enhance the unrestrained proliferation of cells via multiple mechanisms in neuroblastoma tumorigenesis.

In neuroblastoma, the growth is also controlled by several cytokines and growth factors that interact and bind the cell surface receptors, including receptor tyrosine kinases (Borriello *et al.*, 2016). ALK is a receptor tyrosine kinase that is normally expressed in the small intestine, testis and in developing embryonal and neonatal brain (Carpenter and Mossé, 2012). Activating ALK mutations disrupt the auto-inhibitory function, activate ligand-independent function and enhance kinases activation (Holla *et al.*, 2017), resulting in activation of plethora of stream signalling pathways which facilitate the cellular process required for tumourgesis including cell proliferation, growth and survival (Carpenter and Mossé, 2012). Oncogenic ALK mutations present in the majority of hereditary neuroblastoma and 7 to 10% in the sporadic type of neuroblastoma. Therefore, ALK provides an attractive target for neuroblastoma therapy and is currently in phase one and two clinical trials (Chen *et al.*, 2008; Carpenter and Mossé, 2012).

MYCN is known to promote cell proliferation and cell cycle progression. During embryogenesis, this function is critical to ensure a complete development of the neurons and brain (Knoepfler, 2002). MYCN amplification leads to an oncogenic activity such as playing a vital role in the inhibition of cellular differentiation through negatively regulation of tropomyosin related kinase A (TrkA) expression (Iraci *et al.*, 2011).As a consequent, cells become arrested in the proliferative stage and are unable to terminally differentiate into post-mitotic sympathetic neurons (Brodeur *et al.*, 2009).

Cyclin-dependent kinase 4 (CDK4) is found to be amplified in neuroblastoma (Gogolin *et al.*, 2013). CDK4 is a direct transcriptional target of MYCN (Westermann *et al.*, 2008). CDK4 forms a complex with cyclin D2 which hyper-phosphorylates retinoblastoma protein thereby allowing E2F1 to initiate the transcription of a cascade of genes involved in cell cycle progression leading to uncontrolled

proliferation (Westermann *et al.*, 2008; Gogolin *et al.*, 2013). Similar to CDK4, an elevated activity of the mitotic kinase CDK1 is detected in MYCN amplified neuroblastoma cell lines. CDK1 forms a complex with either cyclin A or B1 and thus the complexes mediate MYCN behaviour during mitosis through direct phosphorylation on serine 54 (Sjostrom *et al.*, 2005).Thus inhibiting CDK4 and CDK1 may offer an attractive target to treat neuroblastoma patients.

1.1.4.2. Insensitivity to anti-growth signals

In normal tissue, cell division is tightly controlled via antiproliferative mechanisms including evading the mitogenic signals, inhibition of cell adhesion molecules or tumour suppressor genes to prevent inappropriate cell growth and maintain tissue homeostasis (Ozaki and Nakagawara, 2011). Neoplastic tissues however must overcome these mechanisms to maintain cell proliferation. Tumour suppressor genes are vital component of cellular antiproliferative mechanisms through their activity in responding to DNA damage, oncogene activation, and uncontrolled cell cycle progression. TP53 is a tumour suppressor gene found to be mutated or has otherwise lost its function in most primary and relapsed cancers (Olivier, Hollstein and Hainaut, 2010; Ozaki and Nakagawara, 2011). Plethora of cellular stimuli triggers the activity of TP53 including DNA damage, oncogene activation and anoxia. The typical response of TP53 to DNA damage is by calling temporary halt for the cell cycle progression (quiescence) to allow time for DNA repair to take place. If the DNA damage is irreversible, TP53 may induce a permanent cell cycle arrest (senescence) or cell death (apoptosis) (Robbins *et al.*, 2005; Hanahan and Weinberg, 2011).

In neuroblastoma, upon diagnosis, inactivating mutations of TP53 are unlikely to be detected (<2%) in the primary tumours (Chen *et al.*, 2010). Most TP53 mutations in neuroblastoma tumours reported in relapsed or progressive tumours (Tweddle *et al.*, 2003)and these are now very common. Some alternative mechanisms of TP53 inactivation on neuroblastoma tumours have been suggested including an increase activation of mouse double minute 2 (MDM2), inactivation of p14ARF gene or cytoplasm sequestration. MDM2 is known as an oncoprotein that stabilises or sequesters TP53 thus

limiting its activity and p14ARFprotected TP53 from MDM2 mediated-degradation (Tweddle *et al.*, 2003; Van Maerken *et al.*, 2009).

The Retinoblastoma (RB) gene, the archetypal tumour suppressor gene, inhibits the cell cycle progression at the G1/S checkpoint (Hanahan and Weinberg, 2011). In the inherited form of retinoblastoma, affected children possess a germline mutation of the RB gene, a subsequent somatic mutation leads to bilateral inactivation (Knudson, 1971).

1.1.4.3. Evasion of apoptosis

In addition to unrestrained proliferation, tumour cells must evade apoptosis. Apoptosis is a mechanism used by normal cells during development and in the event of them becoming damaged. Apoptosis is characterised by a number of biochemical changes including DNA cleavage into fragments, membrane surface modification - externalization of phosphatidylserine and cleavage of intracellular substrates by Caspases (Coleman, 2010), as well as morphological changes including cell shrinkage, chromatin condensation and fragmentation, cell membrane blebbing with loss of adhesion to neighbouring cells or extracellular matrix (Kroemer *et al.*, 2009; Koff, Ramachandiran and Bernal-Mizrachi, 2015). Two pathways initiate apoptosis, intrinsic “mitochondrial pathway” or extrinsic “death receptor pathway”(Parrish, Freel and Kornbluth, 2013), both ultimately result in the activation of a proteolytic cascade of caspases leading to cell death (Elmore, 2007).

In neuroblastoma various genetic aberrations take place to secure tumour cells from apoptosis (Evan and Vousden, 2001; Hanahan and Weinberg, 2011).

The intrinsic pathway of apoptosis is initiated via multiple internal stimuli such as stress or GF deprivation. Proapoptotic members of the Bcl-2 family, BAX and BAK, undergo structural modification to become active. They then migrate to the mitochondria and homodimerise and expose the internal crypt through introducing pores on the outer surface of the mitochondria. This increases inner membrane permeability leading to the release of Cytochrome C (Tait and Green,

2013). Bcl-2 family of proteins is found to be highly expressed in neuroblastoma cell lines and tumours (Dole *et al.*, 1995; Abel *et al.*, 2005).

The extrinsic pathway, however, is initiated through death receptor binding-ligand. Death receptors are characterised by specific protein motifs that contain DD (death domain) and DED (death effector domain). Activation of a death receptor leads to the activation of Caspase 8 downstream signalling pathways (Koff, Ramachandiran and Bernal-Mizrachi, 2015). Caspase 8 plays a pivotal role in the extrinsic pathway of apoptosis. Hyper-methylation of a regulatory region (e.g. CpG island) in Caspase 8 gene has been described to elicit the loss of its function in neuroblastoma tumours (Teitz *et al.*, 2000; CASCIANO, 2004).

Unexpectedly, MYCN has been described to activate TP53 (Chen *et al.*, 2010). This may explain why MYCN amplified primary neuroblastoma tumours are more responsive to the chemical therapy, as TP53-mediated apoptosis signalling pathways are functional. However, the chemotherapy tends to induce mutations in TP53, resulting in loss of apoptotic function and consequently leading to relapse and chemo-resistance (Huang and Weiss, 2013).

1.1.4.4. Limitless replicative potential

Normal cells can only divided a limited number of times, known as the Hayflick number. After this point, cells can no longer divide and become senescent (Hayflick, 1997). At the end of the chromosomes there is a DNA sequence, termed the telomere, which shortens each time the cell divides. Short telomeres are recognised by the cell's DNA repair machinery e.g. TP53 and RB which induce cell cycle arrest and senescence. Senescence defines as an irreparable entrance into a non-proliferative but viable state. In circumstances where p53 or RB are inactivated e.g. tumour cells, the cells employ the non-homologous end joining (telomere fusion) mechanism in an attempt to rescue the cell, thus eliminating active apoptosis pathways (Hanahan and Weinberg, 2011).

Stem cells and germline cells both express telomerase; a specialised reverse transcriptase enzyme able to lengthens the telomere, and this is virtually absent from somatic cells. However, cancer cells

manage to escape from senescence via upregulation of telomerase during the period of genomic instability (Robbins *et al.*, 2005; Hanahan and Weinberg, 2011). The vast majority (~90%) of human cancer cells upregulate the expression of telomerase to propagate immortalisation trait (Sherr and McCormick, 2002; Passos, Saretzki and Von Zglinicki, 2007).

In neuroblastoma, telomerase is found to be upregulated and associated with advanced cases and poor prognosis (Hiyama *et al.*, 1995). Lack of telomerase activity has been linked to the stage 4S of neuroblastoma, explaining the spontaneous regression of the tumour (Hiyama *et al.*, 1995). Genome sequencing studies indicated that 25% of neuroblastoma patients possess rearrangement of TERT (encodes the protein component of telomerase) promotor, resulting in enhancer hijacking and activation. Of note, TERT is also a direct transcriptional target of MYCN (Peifer *et al.*, 2015). Alternative lengthening (ALT) is a telomerase independent telomere maintenance mechanism found in ~10% of human cancers (Cesare and Reddel, 2010). ATRX is an RNA helicase involved in chromatin remodelling and telomere maintenance as well as it supresses ALT (Napier *et al.*, 2015). Loss of ATRX function mutation occur in approximately 10% of sporadic neuroblastoma cases, indicating its role in eliminating the limitless replicative potential (Molenaar, Koster, Zwijnenburg, *et al.*, 2012).

1.1.4.5. Inducing angiogenesis

Despite the growth advantages gained through the previously mentioned hallmarks, tumours cannot extend beyond 1-2mm in diameter unless they are vascularised to allow delivery of O_2 and nutrients and evacuate waste products (Collet *et al.*, 2014). Neoangiogensis refers to the process in which there is a growth of new blood vessels from pre-existing vessel. This event is controlled by the balance between pro-angiogenic factors e.g. vascular endothelial growth factor (VEGF) and inhibitory factors e.g. thrombospondin-1 (TSP-1) (Muz and Azab, 2015). During tumour progression, cancer cells require access to blood vessels for growth and metastasis therefore they activate an angiogenic switch. The angiogenic switch is activated through increasing the production of the pro-angiogenic factors such as VEGF, fibroblast growth factor (FGF), angiogenin, transforming growth

factor (TGF)-α, TGF-β, tumour necrosis factor (TNF)-α, platelet-derived endothelial growth factor (PDGF), granulocyte colony-stimulating factor, placental growth factor, interleukin-8, hepatocyte growth factor, and epidermal growth factor, and concomittent loss of angiogenic inhibitors by tumour and stromal cells, leading to neoangiogenesis (Bergers and Benjamin, 2003; Wicki and Christofori, 2008; Baeriswyl and Christofori, 2009). However, tumour vasculature is abnormal; blood vessels are leaky, dilated and arbitrarily arranged (Robbins *et al.*, 2005; Hanahan and Weinberg, 2011).

Angiogenesis is prominent feature on neuroblastoma tumours (Chlenski, Liu and Cohn, 2003). Unfavourable neuroblastoma including MYCN amplification is usually associated with high vascularity and microvascular proliferation. High expression of VEGF or PDGFA is tightly correlated with the aggressive and metastatic neuroblastoma tumours (Meitar *et al.*, 1996). Unfavourable histology Schwannian stroma-poor neuroblastoma tumours demonstrate significant angiogenesis. Whilst in Schwannian stroma-rich tumours, stoma cells express an angiogenic inhibitor, identified as secreted protein acidic and rich in cysteine (SPARC). SPARC expression is found to be inversely correlated with the degree of malignant progression in neuroblastoma tumours (Chlenski *et al.*, 2002).

1.1.4.6. Tissue invasion and metastasis

The most deadly aspect of cancer is its ability to spread, or metastasize. The invasion-metastasis cascade is a complex process involving a series of sequential steps to allow spread of a primary tumour. These steps involve of local invasion, intravasation into the circulatory system, survival of the shear stress and the protective immune cells in the bloodstream, extravasation from the vessels and finally growth of micrometastases into macroscopic neoplasia (McGowan, Kirstein and Chambers, 2009; Talmadge and Fidler, 2010; Reymond, D'Água and Ridley, 2013).

Matrix metalloproteinases (MMP) family play an important role in the regulation of tumour cell adhesion and migration. A correlation between overexpression of MMP2 and MMP9 has been detected in advanced neuroblastoma (Sugiura *et al.*, 1998).

EMT is required during normal neural crest development, and also is considered an important mechanism for both the initiation of tumour invasion and subsequent metastasis (Klymkowsky and Savagner, 2009). The EMT program is orchestrated and coordinated by a number of transcription factors (TFs) notably Snail, Slug and Twist; they promote EMT in part by suppressing the expression of E-cadherin thus facilitating invasion (Micalizzi, Farabaugh and Ford, 2010; Craene and Berx, 2013; Lamouille, Xu and Derynck, 2014). An association between overexpression of TWIST-1 has been shown in a subset of neuroblastoma metastatic tumours (Valsesia-Wittmann *et al.*, 2004).

1.1.4.7. Deregulating cellular energetics

Cancer cells undergo fundamental metabolic changes maintaining energy production (ATP) to support their unchecked proliferation (DeBerardinis *et al.*, 2008). They increase their glucose uptake through upregulating glucose transporters such as GLUT 1 and GLUT 3 (Hsu and Sabatini, 2008; Kristin H Kain *et al.*, 2014), and switch their glucose metabolism form oxidative phosphorylation to glycolysis; this is termed the Warburg effect. Warburg effect has been demonstrated in neuroblastoma by the use of positron emission tomography scan to visualise the avid uptake of fluorine-18 fluorodeoxyglucose (Kushner *et al.*, 2001). Studies showed that MYCN is associated with regulation of tumour metabolism through activation of genes involved in glycolysis, glutamine metabolism, fatty acids metabolism and mitochondrial function (Qing *et al.*, 2010; Zirath *et al.*, 2013; Ren *et al.*, 2015). Amplification of MYCN supports the Warburg effect in neuroblastoma tumours by activating the transcription of several glycolytic genes such as GLUT 1 (Aminzadeh *et al.*, 2015).

1.1.4.8. Avoiding immune destruction

The immune system tightly interacts with cancer cells over the entire process of disease development and metastasis progression. This interaction between immunity and cancer can both

inhibit and enhance tumour growth. Most tumours, including neuroblastoma, arise in immunocompetent hosts (Vajdic and Van Leeuwen, 2009). Malignant cells therefore require a strategy to escape eradication by the host immune system (Vinay *et al.*, 2015). They escape the immune destruction machinery through disabling the inflammatory cells that have been sent to eradicate them. An evasive mechanism that can be used by cancer cells to evade the immune destruction is by recruiting the inflammatory cells that previously immunosuppressed such as myeloid-derived suppressor cells (MDSCs) and regulatory T cells (Tregs) to suppress the actions of cytotoxic lymphocytes (Ostrand-Rosenberg and Sinha, 2009; Mougiakakos *et al.*, 2010).

In neuroblastoma, tumour cells were found to downregulate human leucocyte antigen (HLA) class 1 and adhesion molecules thus avoiding cell recognition and destruction by the infiltrating $CD8^+$ cytotoxic T lymphocytes (CTLs) and neutral killer (NK) cells (Bottino *et al.*, 2014). In addition, MYCN amplification down regulates HLA 1 expression (Bernards, Dessain and Weinberg, 1986). Tumour-associated macrophages (***see section 1.1.4.10***) are also recruited to suppress lymphocyte activity (Liu *et al.*, 2012).

1.1.4.9. An Enabling Characteristic: Genome Instability and Mutation

Acquisition of the eight hallmarks, discussed above, depends largely on several alterations in the genomes of neoplastic cells. In addition, two enabling characteristics have been described. The first enabling characteristic for tumorigenesis is an increased tendency of alterations in genome during the tumour cell cycle (Hanahan and Weinberg, 2011). In contrast to normal cell, tumour cells acquired increased susceptibility of genomic instability (Shen, 2011). Unchecked and uncontrolled proliferation of tumour cells produces mutant clones that are genetically heterogeneous. In the presence of favourable genomic characteristics, these clones will survive and propagate, increasing tumour progression (Greaves and Maley, 2012).

Tumour cells are less genetically stable than normal cells (due to loss of a fully functioning DNA repair system) (Greaves and Maley, 2012) and one extreme example of this is Chromothripsis.

Chromothripsis is a phenomenon by which up to thousands of clustered chromosomal rearrangements occur in a single event and a single chromosome leading to structural aberrations. In a study conducted on high risk neuroblastoma tumours, the researchers reported that chromothripsis occurred in approximately 18% of these tumours, resulting in structural aberrations in genes involved in neuroblastoma pathogenesis (Molenaar, Koster, Zwijnenburg, *et al.*, 2012).

1.1.4.10. An Enabling Characteristic: Tumour-Promoting Inflammation

The second enabling Characteristic of tumorigenesis is tumour-promoting inflammation (Hanahan and Weinberg, 2011). It is firmly established that tumour cells are highly infiltrated by both adaptive and innate immune system components (Pistoia *et al.*, 2013). Although various types of immune cells are involved in supporting tumour growth, the main culprits are known as Tumour Associated Macrophages (TAMs). The presence of TAMs in neuroblastoma correlates with advanced stage, with the largest infiltration observed in children with metastatic disease (Asgharzadeh *et al.*, 2012). TAMs enhance growth of neuroblastoma tumour through increasing activation of a signal transducer and activator of transcription 3 (STAT3), enhancing tumour cell proliferation (Hadjidaniel *et al.*, 2017). Furthermore, analysis of 249 primary human neuroblastoma tumour samples revealed a significant positive correlation between that MYC up-regulation and TAM infiltration markers, CCL2 *and* CD14 (Hadjidaniel *et al.*, 2017).

1.1.5. Histological classification

As mentioned previously, tumour cells retain progenitor and stem cell markers. In general, the more differentiated tumours are less aggressive whereas tumours with more stem cell-like features are more aggressive. In respect to differentiation status, the international neuroblastoma pathology committee classification (INPC) indicated four forms of peripheral neuroblastic tumours (PNTs) that originates from sympathetic progenitor cells (Shimada, 2003). The most differentiated form of PNTs, Ganglioneuroma (GN), consists of mature ganglion cells that forms clusters and are surrounded by dense Schwannian stroma. GN often presents in older children and is less common than

neuroblastoma (Lonergan *et al.*, 2003). Ganglioneuroblastoma composes of a mixture of undifferentiated neuroblasts and mature or maturing ganglion cells. According to the development of neuroblastic and Schwannian stroma, GNB splits into two subdivision: nodular and intermixed. The nodular GNB is a more malignant form from the intermixed although it still less common than neuroblastoma (Lonergan *et al.*, 2003). Neuroblastoma, the fourth subgroup of PNTs, represents the most undifferentiated and aggressive form of PNTs. A distinguishing feature in NB tumours is the presence of pseudorosettes (small round cells arranged in nests) surrounded by neuropil (eosinophilic neuritic material) (Lonergan *et al.*, 2003). Depending on the development of Schwannian stroma, NB may be divided into undifferentiated, poorly differentiated and differentiating neuroblasts (***Figure1.3***) (Shimada *et al.*, 1999).

As discussed above, INPC classification displays the grade of maturation ranging from highly differentiated form surrounded by dense Shwannian stroma to those with mostly undifferentiated neuroblasts. The differentiated neuroblasts, generally, consist of large round cells with abundant cytoplasm that contains cytoplasmic Nissl bodies, and a prominent nucleus. However, less-differentiated neuroblasts have small round cells that contain scant cytoplasm and nuclei with dense hyperchromatic nuclei that shows mitotic activity. Tumours therefore were divided into unfavourable and favourable subgroups depending on their histological key features. Unfavourable histology confers the worst prognosis in patients (Shimada *et al.*, 1999; Peuchmaur *et al.*, 2003).

INPC system is a modified form of Shimada classification (Shimada *et al.*, 1999), a system that links the age of patient to the histological features of the tumour such as the degree of cellular differentiation and the presence or absence of Schwannian stoma (***Figure1.4***), as well as the mitosis-karyorrhexis index (MKI) (Ikeda *et al.*, 2002; Peuchmaur *et al.*, 2003).

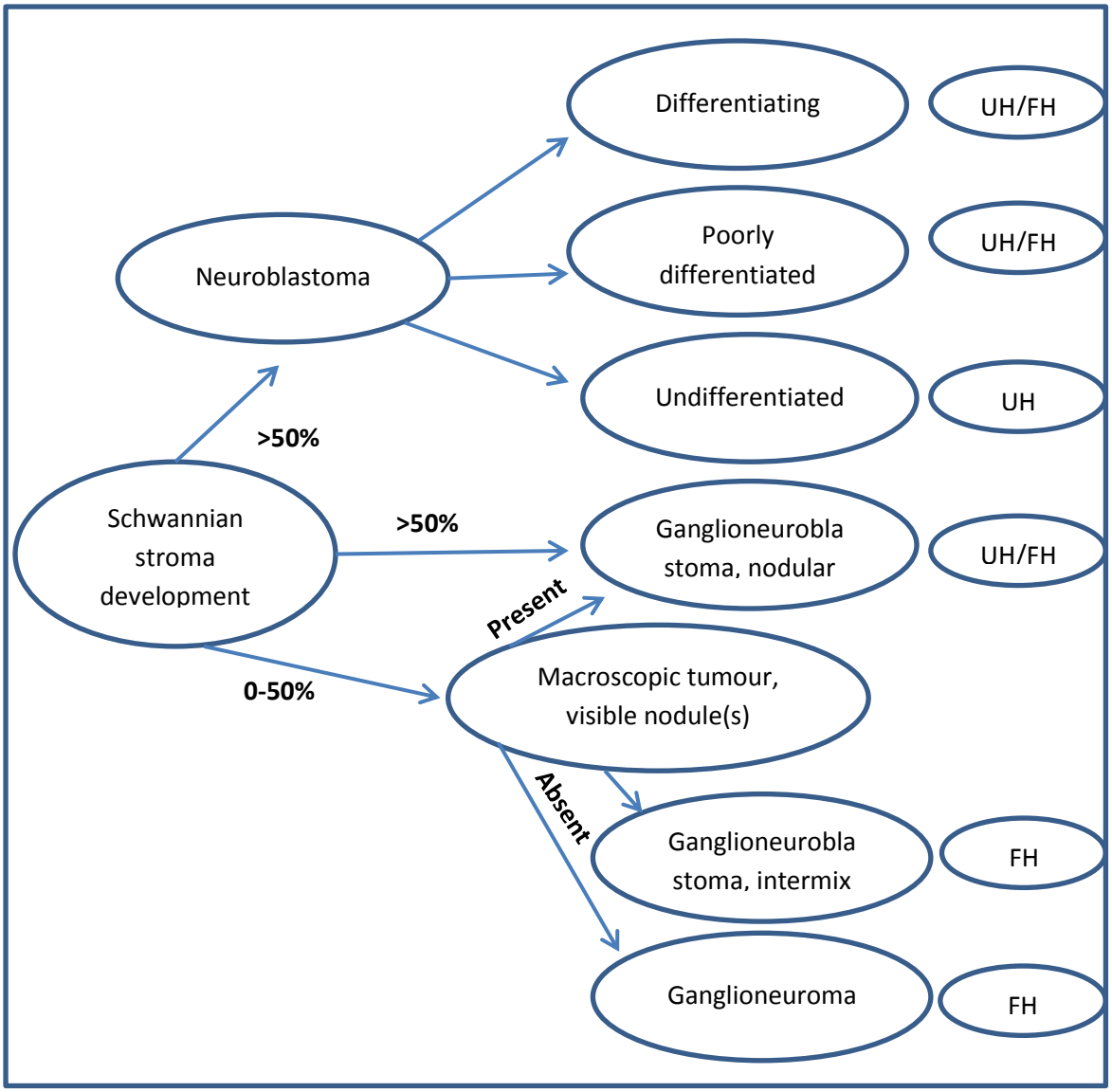

Figure1.3 International Classification System for Neuroblastoma Prognosis and Diagnosis. *Flowchart for prognostic evaluation demonstrates the histological subtypes of peripheral neuroblastic tumours based on the abundance of Schwannian stroma and the presence/absence of neuroblastic tumour nodules. There are two groups for the final evaluation of PNTs: they are favourable histology (FH) and unfavourable histology (UH). Favourable tumours demonstrate increased Schwannian stroma development. In addition, this classification illustrates those younger patients with low mitosis-karyorrhexis confer better prognosis (not shown). Adapted from* (Shimada, 2003).

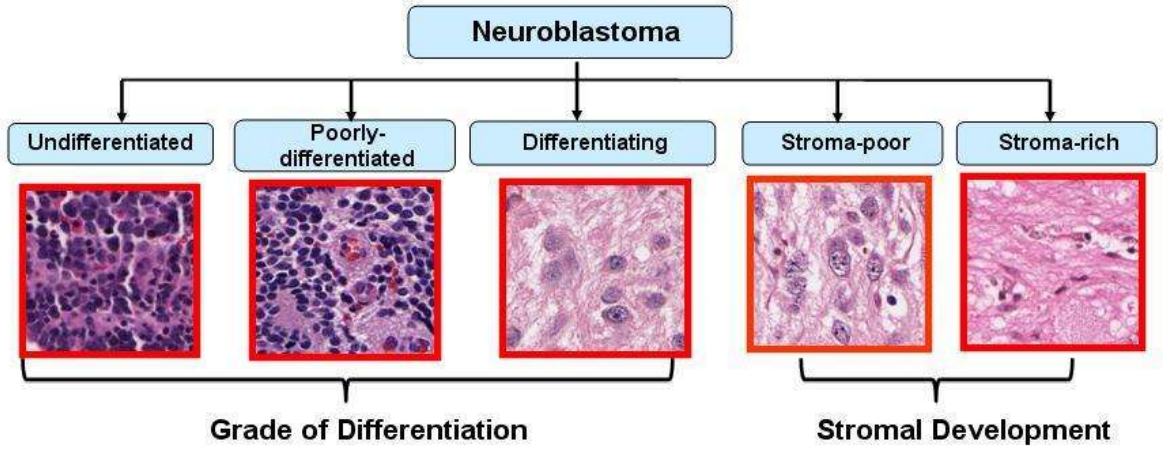

***Figure1.4 Neuroblastoma pathological classification**. Diagram displaying the three grades of neuroblastoma differentiation observed and the two levels of stromal development. Taken from http://bmi.osu.edu/cialab/mia_nb.php .*

1.1.6. Diagnosis

A combination of laboratory tests, histopathological studies and scanning can be carried out to confirm neuroblastoma diagnosis. 90% of NB tumours secrete catecholamine metabolites, homovanillic acid (HVA) and vanillylmandelic acid (VMA), in urine (Lonergan *et al.*, 2003). The relative amount of secreted catecholamine metabolites can determine the grade of cellular differentiation of neuroblastoma tumours therefore low HVA/VA is associated with poorly differentiated tumours associated poor prognosis (Strenger *et al.*, 2007). Hence, the ratio of these two markers can be then used to detect tumour relapse and progression (Mullassery and Losty, 2016). In addition, elevated dopamine level is also linked to the existence of neuroblastoma (Strenger *et al.*, 2007). Furthermore, a biopsy sample is important for the diagnosis of neuroblastoma. These tissue samples of tumour are used to investigate the histology and molecular and genetic changes, for example, identification of gene amplification or other chromosomal aberrations and mutations (Pugh *et al.*, 2013).

In addition to laboratory testing and histopathological studies, a wide range of imaging and scanning is used in the diagnosis of neuroblastoma. Patients presenting with abdominal mass may undergo an

initial investigation using ultrasonography (Matthay *et al.*, 2016).This can then followed by cross-sectional scanning using magnetic resonance imaging (MRI) or computed- tomography (CT). These will allow the size of the primary tumour to be estimated and also determining the extent of metastasis if found (Kembhavi *et al.*, 2015). Metastasis is usually determined by bone marrow aspirates from which many of the primary cells used in research are derived. To determine the primary tumour and the location of metastases, scintigraphy imaging could be performed. A tool like Meta-iodobenzylguanidine (MIBG) scanning also used to evaluate the involvement of bone and bone marrow (Shusterman *et al.*, 2011). Finally, tumour cells predominantly rely on the aerobic glycolysis to maintain their energy therefore 18F-Fluorodeoxyglucose positron emission scanning is a good tool used to measure dependency levels of glucose (Sharp *et al.*, 2009).

1.1.7. Screening

Neuroblastoma screening programmes was performed in Japan, North America and Europe using the elevated catecholamine levels as method of diagnosis in order to identify patients at a young age since these patients had a much better prognosis (Schilling *et al.*, 2002; Woods *et al.*, 2002). This programme was successful in identifying the previously undiagnosed cases of neuroblastoma however the mortality rate did not improve (Tsubono and Hisamichi, 2004). This was because most of the discovered cases had favourable clinical and biological features such as 4S stage and many underwent spontaneous regression would normally never have presented at hospital. Ultimately, the screening program did not reduce the mortality rate or the incidence of advanced cases, subsequently it was abandoned.

1.1.8. Neuroblastoma presentation

Localised primary tumours are presented in approximately 40% of neuroblastoma patients at diagnosis. The primary tumours may develop in several different sites as they reflect the diverse range of NCC derived sympathetic adrenal structures. This therefore suggests that the primary tumours may develop anywhere along the sympathetic chain or in the adrenal gland (Matthay *et al.*,

2016).The commonest site of the primary tumours is the abdominal cavity followed by thorax. The abdominal cavity primary tumours represent 70% of neuroblastoma incidences (Maris, 2010).

Approximately 50% of neuroblastoma cases presented with metastasis. The liver is the most common site for distant metastasis followed by the lymph nodes, bone and skin. The lungs and the brain are rarely involved (Taggart *et al.*, 2011).

1.1.9. Disease staging and prognosis

Neuroblastoma has been staged according to the International Neuroblastoma Staging System (INSS) since early 1990's (***Table1.1***). International Neuroblastoma Risk Group (INRG) has developed a staging system referred to as INRGSS by adding the risk stratification in order to assist in the appropriate management of patients. For that, INRG produced a standard worldwide system, through assessing several clinical trials around the world, which included both risk-based staging system (***Table1.2***) and pre-treatment classification schema (***Table1.3***) (Cohn et al., 2009). Here, the staging system includes the presence of Imaging-defined Risk factors (IDFs) such as whether the tumour is localised or has metastasised at the time of diagnosis (Brisse et al., 2011).

Risk stratification is achieved by including important prognostic features such as the age of patient at diagnosis, stage, MYCN status and DNA index in addition to International Neuroblastoma Pathology Classification (INPC) (***Table1.3***). As noted by INRG classification, low risk and localised tumours that develop in younger patients with no MYCN amplification have an excellent survival rate with or without minimal treatment. In high risk patients, however, unfavourable outcomes are expected especially when associated with MYCN amplification. Ultimately, this pre-treatment classification schema allows delivery of more adequate treatment (Cohn *et al.*, 2009).

Table1.1 *The International Neuroblastoma Staging System.*

Stage	Definition
1	Localised tumour with complete gross excision, with or without microscopic residual disease; representative ipsilateral lymph nodes negative for tumour microscopically.
2A	Localised tumour with incomplete gross excision; representative ipsilateral non-adherent lymph nodes negative for tumour microscopically*.
2B	Localised tumour with or without complete gross excision, with ipsilateral non-adherent lymph nodes positive for tumour. Enlarged contralateral lymph nodes must be negative microscopically.
3	Unresectable unilateral tumour infiltrating across the midline, with or without regional lymph node involvement; Or localised unilateral tumour with contralateral regional lymph node involvement; Or midline tumour with bilateral extension by infiltration (unresectable) or by lymph node involvement**.
4	Any primary tumour with dissemination to distant lymph nodes, bone, bone marrow, liver, skin, and/or other organs, except as defined for stage 4S.
4S	Localised primary tumour (as defined for stage 1, 2A or 2B), with dissemination limited to skin, liver, and/or bone marrow ***. (limited to infants < 18 months of age)
* lymph nodes attached to and removed with the primary tumour may be positive ** The midline is defined as the vertebral column. Tumours originating on one side and crossing the midline must infiltrate to or beyond the opposite side of the vertebral column. ** Marrow involvement in stage 4S should be minimal, ie, < 10% of total nucleated cells identified as malignant on bone marrow biopsy or aspirate. More extensive marrow involvement would be considered to be stage 4. The mIBG scan (if performed) should be negative in the marrow. **(Brodeur *et al.*, 1993)**.	

Table1.2 *International Neuroblastoma Risk Group staging system (INRGSS) - based on image defined risk factors L1 and L2 refer to localized disease whereas M and MS refer to those with metastatic spread (Cohn et al., 2009).*

Stage	Definition
L1	Imaging-defined Risk factors absent: Localised tumour confined to one body compartment and not involving vital structures, as defined by the list of image-defined risk factors
L2	Local regional tumour with presence of one or more image-defined risk factors
M	Distant metastatic disease (except stage MS)
MS	Metastatic disease in children <18 months, with metastases confined to the skin, liver and/or bone marrow.

Table1.3 *The International Neuroblastoma Risk Group Consensus Pretreatment Classification- a system designed to provide overall risk stratification based on a wide variety of patient derived and disease based features. GN, ganglioneuroma; GNB, ganglioneuroblastoma; NA, non-amplified; Amp, amplified. Modified from Cohn et al. (2009).*

INRG stage	Age (months)	Histologic category	Grade of tumour differentiation	MYCN	11q aberration	DNA content	Pre-treatment risk group
L1/L2		GN maturing: GNB intermixed					Very low
L1		Any, expect GN maturing or GNB intermixed		NA			Very low
				Amp			High
L2	< 18	Any, expect GN maturing or GNB intermixed		NA		No	Low
						Yes	Intermediate
	≥ 18	GNB nodular; neuroblastoma	Differentiating	NA		No	Low
			Poorly differentiated or undifferentiated			Yes	Intermediate
				Amp			High
M	< 18			NA		Hyper-diploid	Low
	< 12			NA		Diploid	Intermediate
	12 to < 18			NA		Diploid	Intermediate
	< 18			Amp			High
	≥ 18						High
MS	< 18			NA		No	Very low
						Yes	High
				Amp			High

1.1.10. Spontaneous regression

Neuroblastoma has a 'special' stage of aggressive disseminated growth involving liver, skin, bone marrow in addition to the primary tumour, this stage is termed 4S. The 4S tumours occur in children less than 18 months of age (Brodeur, 2018) and represent approximately 7–10% of all neuroblastoma cases. Strikingly, 4S tumours can sometimes spontaneously regress (differentiate) with little or no treatment (Schleiermacher *et al.*, 2003).The possibility of spontaneous regression

affords a good prognosis for patients however it's difficult to establish precisely what proportion of tumours undergo this phenomenon.

The mechanisms by which these tumours undergo spontaneous regression have been suggested by Brodeur and Bagatell, and include loss of telomerase activity, lack of neurotrophin, humoral or cellular immunity, and alterations in epigenetic regulation with the possibility of other mechanisms may also involve (Brodeur and Bagatell, 2014). It is likely that a better understanding of the mechanisms of spontaneous regression will help to identify targeted therapeutic approaches for neuroblastoma tumours.

1.1.11. Management of neuroblastoma

Management of patients with neuroblastoma is always dependant on the staging schema. The treatment of a localised tumour ranges from watchful waiting to surgical resection however for a metastatic tumour the treatment would require concentrated multimodal treatments.
The current approach to treat high risk neuroblastoma includes three main steps. The first step of treatment involves intensive induction of chemotherapy to reduce the tumour size and metastasis followed by surgical resection to remove the primary tumour. This step is followed by a consolidation step that includes myloablative chemotherapy with autologous haematopoietic stem cell transplant AHSCT and the final step of treatment termed "maintenance therapy" including immunotherapy and differentiation therapy (retinoic acid treatment) targeting the residual disease (Mullassery *et al.*, 2009). GD2 is a disialoganglioside found on the surface of all neuroblastoma cells, whilst little is found in normal tissues, therefore the relatively tumour specific occurrence of GD2 makes it an efficient target for immunotherapy with monoclonal antibodies. Humanized anti-GD2 monoclonal antibodies (anti-GD2 mAb) have therefore been administrated to patients to target GD2 leading to immune-mediated cell death (Castel, Segura and Berlanga, 2013; Federico *et al.*, 2017).

1.1.11.1. Retinoic acid

Retinoic Acid (RA) is a bioactive metabolite of vitamin A and has critical effects in the development of the nervous system in the embryo in addition to its role in the physiology of adults (Mark, Ghyselinck and Chambon, 2006). RA is produced normally in the body from vitamin A through two oxidizing steps to retinal and then to RA (***Figure1.5***). In addition, RA can metabolised by cytochrome enzymes (CYP26 enzymes) to hydroxylated metabolite such as 4-hydroxy-RA and 4-oxo-RA (Perlmann, 2002). At the cellular level, RA regulates the expression of target genes involved in cell growth, differentiation, apoptosis and homeostasis. Moreover, in keeping with other functions, RA has been used as an anti-proliferative drug to treat certain cancers (Niles, 2000).

RA enters to the nucleus by binding the protein cellular RA–binding protein2 (CRABP2) where it is recognised by two protein families, the RA receptors (RARs) family comprising 3 isotypes, RARα, RARβ, and RAR γ, and the retinoid X receptors (RXRs) family also including 3 isotypes, RXRα, RXRβ, and RXR γ. RARs and RXRs form heterodimers and act as RA-modulated transcription factors (Perlmann, 2002).

RA has 3 different isomers: All-trans RA (ALTR), 9-cis RA, and 13-cis RA, at some point, all three can bind to effectors but with different affinities. ALTR binds to RARs/RXRs heterodimer and then the complex binds to RA respond elements RAREs that often exist in gene promoters; therefore acting as ligand regulated transcription factors (Gyöngyösi *et al.*, 2013) (***Figure1.6***).

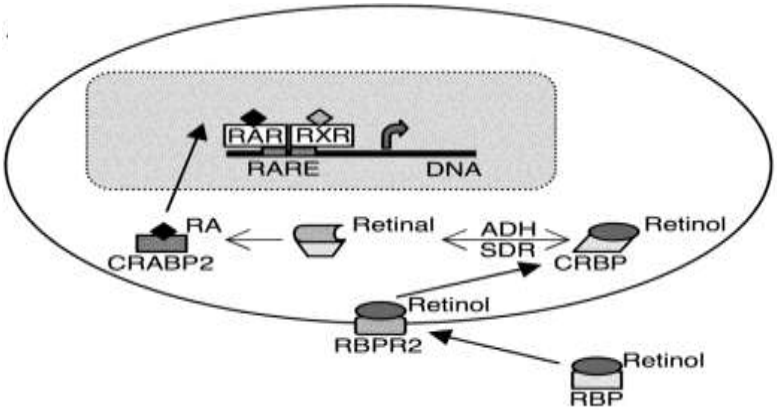

Figure1.5 The scheme of RA generation and signalling in the cell. *RA is produced intracellularly through two oxidizing steps, firstly retinol is enzymatically converted to retinal by alcohol dehydrogenase (ADH) and then retinal is oxidized to RA by aldehyde dehydrogenase (ALDH), RA is bound to CRABPs and translocated to the nucleus onto RAR/RXR heterodimers. RAR/RXR heterodimers bind to RAREs in target genes. SDR is short-chain dehydrogenases that can convert Retinal to Retinol. Adapted from (Gyöngyösi et al., 2013).*

Activation of the canonical pathway (genomic pathway) will mainly inhibit cell growth, trigger cell differentiation, and potentially apoptosis (Tang and Gudas, 2011).

Two types of DNA binding sequence (RAREs) are found in RA-regulated genes, they are DR-2 and DR-5. In the absent of ligand (RA), the transcription of the target genes is blocked. RAR/RXR heterodimer binds receptors of target genes and then nuclear receptor corepressors (NCoRs) recruits and tethered histone deacetylase (HDAC) and repressive factors such as Polycomb repressive complex 2 (PRC2) to the RAR/RXR dimer. Consequently, the chromatin is compacted so that the DNA becomes inaccessible for transcription. In the presence of ligand (RA), NCoR-binding dissociates from RAR/RXR dimer and allows interaction with co-activators of the nuclear receptor co-activator (NCoAs). These NCoAs can activate transcription by recruiting histone acetyltransferases (HATs) and Trithorax (A group of three proteins involved in gene expression maintenance such as histone modification, chromatin remodelling and DNA- binding). As a result of this, the chromatin is opened over the target gene promoter region and active transcription takes place (Niederreither and Dollé, 2008; Cunningham and Duester, 2015).

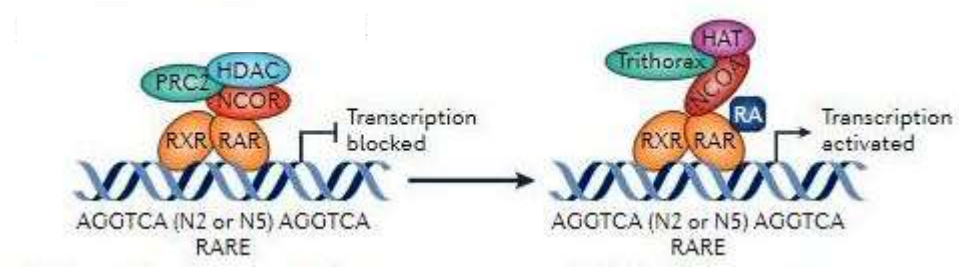

Figure1.6 Mechanisms of retinoic acid signalling. *In the absent of ligand (RA), the receptors target genes are repressed through recruiting histone deacetylase (HDAC) and repressive factors such as Polycomb repressive complex 2 (PRC2) that both are tethered through nuclear receptor corepressors (CoRs), and consequently the chromatin compacted so that the DNA become in inaccessible for transcription. In the presence of RA, NCoR-binding is destabilized in the ligand binding domain to allow interaction with co-activators of the nuclear receptor co-activator (NCoAs). These NCoAs can activate the RAR/RXR dimers by recruiting histone acetyltransferases (HATs) and Trithorax which lead to chromatin decondensation over the target gene promoter region. Adapted from (Cunningham and Duester, 2015)*

RA can be bound to other cellular proteins such as fatty acid binding protein 5 (FABP5) to activate other nuclear receptor such as peroxisome proliferator-activated receptor β/δ (PPARβ/δ). The relationship between FABP5 and PPARs is seen to be similar to that between CRABP2 and RARs. Like RARs, PPARs belong to nuclear superfamily that regulates expression of target genes are mainly involved in proliferation. RA is higher affinity to RARs compared to PPARs, and the binding affinity between RA and FABP5 is far lower compared to RA with CRABP2. In addition, certain organs and tissues are found to highly express PPARs as the proliferation and cell maintenance is an important aspect in their health, for example, in the brain, skeletal muscles, skin and adipose tissues. Moreover, keratinocytes and adipocytes have a high level of compared to CRABP2, resulting in proliferative effect following PPAR activation rather than RAR. Interestingly, RXRs can form a heterodimer with PPARs to bind receptor elements RAREs to regulate subset of genes involved in energy balance (Al Tanoury, Piskunov and Rochette-Egly, 2013).

In addition to the canonical pathways (nuclear-transcriptional pathways) of RA, discussed above, RA is involved in non-canonical pathways (extra-nuclear and non-transcriptional pathways). Some RARs present in the membrane lipid rafts, and upon binding to RA, they activate kinase cascades. In

response to RA, RARs in the lipid raft of various epithelial and fibroblast cells interact with Gαq to activate p38 MAPK through the activation of Ro-GTPases (***Figure1.7***). Alternatively, in neuron cells, in response to RA, RARs activates PI3K/ AKT pathway which in turn activates the ERKs pathway (***Figure1.7***) (Al Tanoury, Piskunov and Rochette-Egly, 2013). Activation of kinase pathways provides strong proliferative affects in both normal and cancerous cells; therefore this pathway may give the opportunity to the cancer cells to become resistance to RA treatment (Connolly, Nguyen and Sukumar, 2013).

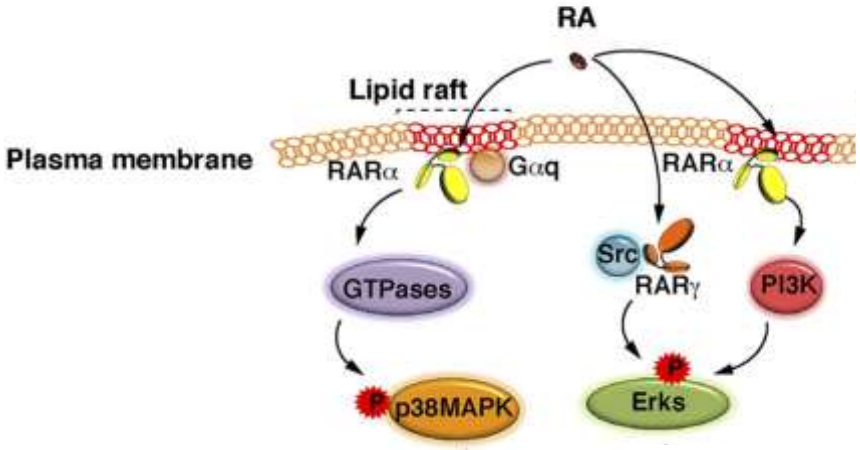

Figure1. 7 The extra-nuclear and non-transcriptional pathways of RA. *Subpopulation of RARα is present in membrane lipid rafts and initiates cascades of kinase activations upon RA binding. In various epithelial and fibroblast cells, in response to RA, RARα localized in lipid rafts interacts with Gαq proteins and activates Rho-GTPases and p38MAPK. However, in neuronal cells, in response to RA, RARα activates Erks through the activation of the PI3K/Akt pathway. Strikingly, in neuronal cells, RA has been also shown to activate Erks via RARγ in association with the Src kinase. Modified from (Al Tanoury, Piskunov and Rochette-Egly, 2013).*

1.1.11.1.1. The biological effects of Retinoic acid on cancer

RA has been investigated extensively for its potential in the chemoprevention and treatment of cancer, predominately due to its activity in arresting the cellular proliferation and inducing differentiation. Therefore, RA is a part of standard therapy for many cancers including high-risk neuroblastoma (Matthay *et al.*, 2009).

In 1982, Seeger showed that RA induced differentiation of human neuroblastoma cells growing in monolayer (Seeger, Siegel and Sidell, 1982). Similarly, some have used retinoic treatment to treat other cancer cells such as acute promyelocytic leukaemia (APL) and found that RA induced those cells to differentiate into granulocytes (Tallman *et al.*, 1997). RA therapy has since been shown to be successful in the clinic.

RA regulates the transcription of genes that play an important role in both tumour regression and tumour progression. As mentioned before, RA down-regulates MYCN expression, and hence inhibits tumour progression and increases event-free survival in some advanced stage neuroblastoma patients (Reynolds *et al.*, 2003; Matthay *et al.*, 2009). In this, RA has been investigated and found to be involved in the regulation of stem cell differentiation, this was through inducing the expression of differentiation markers which is Tuj-1 and reducing the expression of neural stem cell markers such as CD133, Msi-1, nestin, and Sox2 (Ying *et al.*, 2011). In addition, RA has also been found to inhibit expression of growth factors such as EGFR and VEGF and cell proliferation-associated markers such as cyclin D1 and human telomerase reverse transcriptase (hTERT) (Alizadeh *et al.*, 2014).

In keeping with RA's role in differentiation, a group of researchers , in China, showed that RA treatment induces cell-cycle arrest in human carcinoma cells (Zhang *et al.*, 2014) and seen to cause cell cycle arrest and apoptosis of prostate cancer cells (Chen *et al.*, 2012).

Hsu *et al.* found RA-mediated G1 arrest is associated with induction of $p27^{kip1}$ and inhibition of cyclin-dependent kinase 3 (CDK3) in human lung squamous carcinoma cells (Hsu *et al.*, 2000). Siddikuzzaman and Grace reported that encapsulated RA has the ability to inhibit lung cancer metastasis in mouse model (Siddikuzzaman and Grace, 2012). Recent research indicated that RA can suppress hepatoma cell growth and cause apoptosis (Wei *et al.*, 2014).

Taken together, these studies and trials elucidate the fact that RA is indeed a potential compound to suppress cell growth, enhance differentiation, and apoptosis in a variety of malignancies. It's also

possible that RA can work as a helper that cooperates with other treatments and attacks cancer cells.

1.1.11.2. Cyclin-dependent kinases

Protein phosphorylation is the main key that controls and regulates the eukaryotic cell cycle (Errico *et al.*, 2010). The cell progression and division critically requires the activation of a sub family of serine/threonine protein kinases known as Cyclin-dependent kinases (CDKs). This family must bind to its' corresponding cyclins for activity. During the cell cycle, cyclin abundance oscillates through scheduled synthesis and degradation as required in each phase, therefore regulating kinase activity is a timely manner (***Figure 1.8***) (Malumbres and Barbacid, 2009). In particular, at the end of M phase, ubiquitin-mediated proteolysis degrades mitotic cyclins, which leads to inactivation of CDKs and permits the return to interphase (Zachariae and Nasmyth, 1999).

To date, 9 CDK complexes have been discovered and five of them drive the cell cycle. During interphase CDK4, CDK6 and CDK2 are involved in G1, CDK2 in S and CDK1 also known as CCD2 (cell division control- protein 2) operates in both G2 and mitosis, whereas CDK3 is involved in G0. CDK activity is regulated throughout the cell cycle by binding to their activators and inhibitors. Activators includes four classes of cyclins: A, B, D and E- type (Malumbres and Barbacid, 2009). Progression through a specific cell cycle stage requires the participation of particular CDK/cyclin complex (***table1.4*** **and** ***Figure1.9***). CDK/cyclin complexes are inhibited through cyclin-dependant kinases inhibitors including the INK4 inhibitors family (p15, p16, p18, p19) and CDK inhibitory protein/kinase inhibitor protein (Cip/Kip) family (p21, p27, p57) (***Figure1.9***) (Nakamura *et al.*, 2003).

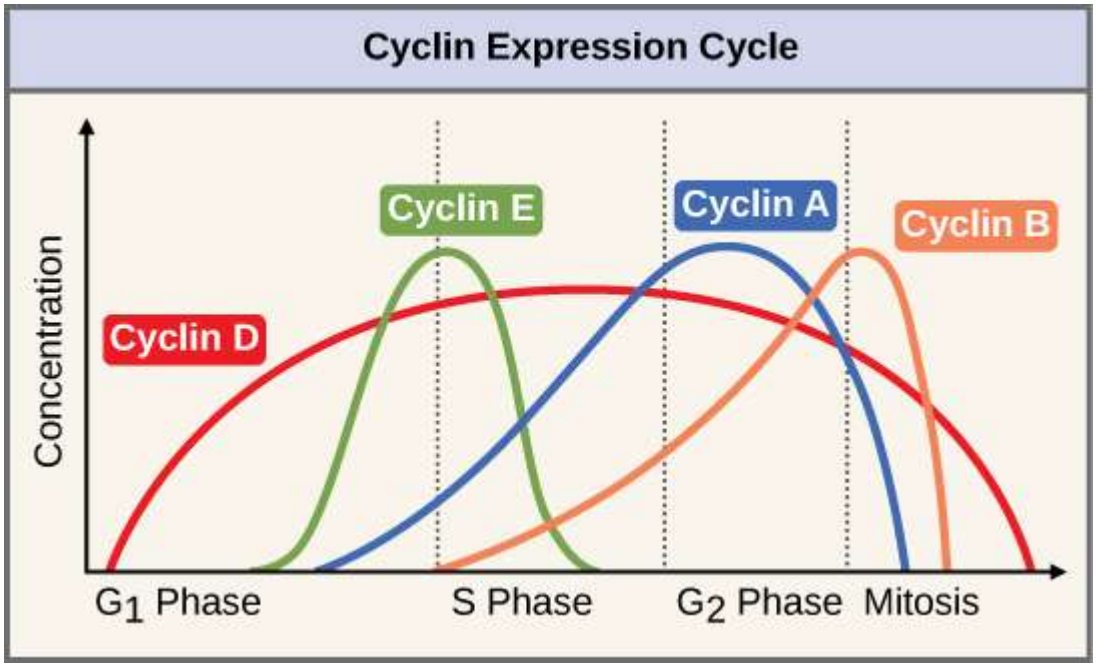

Figure1.8 Oscillation and abundance of Cyclins during the life of a cell cycle. *Taken from* https://commons.wikimedia.org/wiki/File:Figure_10_03_02.jpg .

Table1.4 *Shows the major cyclins and CDKs of vertebrates. *there are three D cyclins (D1, D2 and D3).*

Cell cycle phase activity	Cyclin	CDK Partner
G0-CDK	Cyclin C	CDK3
G1-CDK	Cyclin D*	CDK4,CDK6
G1/S transition -CDK	Cyclin E	CDK2
S-CDK	Cyclin A	CDK2,CDK1
M-CDK	Cyclin B	CDK1

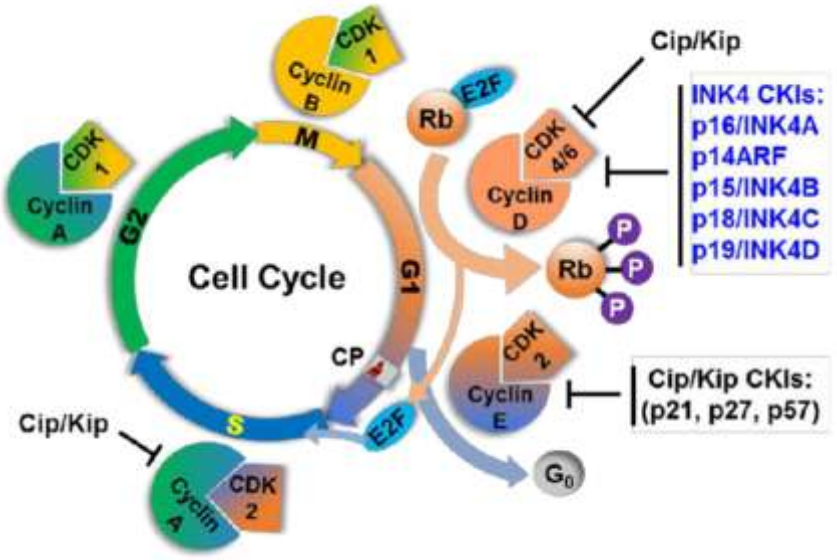

Figure1.9 Cell cycle and cyclin-dependent kinases (CDKs). *CDK-cyclin complexes have direct functions in regulating the cell cycle. CDK3/cyclin C drives cell cycle from G0. During the G1 phase, CDK4/6/cyclin D complexes initiate phosphorylation on the retinoblastoma protein (pRb) to sequester p21Cip1and p27kip1 kip1, which are both inhibitors of CDK2 thus promoting the activation of CDK2/cyclin E complex. In late G1, CDK2/cyclin E complex completes phosphorylation and inactivation of pRb, which releases the inhibition on the E2 family (E2F) transcription factors and leading to expression of the genes necessary for G1/S transition. CDK2/cyclin A complex regulates progression through S phase and CDK1/cyclin A complex through G2 phase in preparation for mitosis (M). Mitosis is initiated by CDK1/cyclin B complex. The overall rate of cell cycle progression is determined by the relative activity of the activating cyclin-CDK complexes and the inhibitory proteins of the INK4 family that inhibit CDK4 and CDK6 in G1 phase, and the Cip/Kip family that has more widespread inhibitory action through the cell cycle. Adapted from (Lutful Kabir, Alvarez and Bird, 2015).*

1.1.11.2.1. Cell cycle control and cancer treatment

The defect in balance between cellular proliferation and differentiation is believed to be a key factor in human cancers. Neuroblastoma, for example, is thought to be a result of an aberration in the regulation of the cell cycle during embryo nervous system development (Wylie *et al.*, 2015).

Indeed, multiple mechanisms operate and coordinate together to regulate the cell cycle fate. CDK/ cyclin complexes tightly control the cell cycle events and their dysregulation may result in several human cancers (Hanahan and Weinberg, 2000; Malumbres and Barbacid, 2001; Malumbres, 2011). Of note, oncogene mutations and altered – CDK activities have been reported in human cancer genomes (Aleem and Arceci, 2015), whilst, mutations in tumour suppressor genes and cyclin-

dependant kinase inhibitors (CKIs) also contribute to uncontrolled cell proliferation (Whitfield *et al.*, 2006; Malumbres and Barbacid, 2009; Santarius *et al.*, 2010).

Early work demonstrated that lengthening G1 phase of the cell cycle through CDK inhibitors induces the switch from neural progenitors (proliferative) to neuron-generating cells (Calegari *et al.*, 2005). Yang and Herrup found that the duration of G1 phase and S phase is a crucial factor in both the differentiation decision and precursor cell maintenance (Yang and Herrup, 2007).

Mechanistically, inhibition of cell cycle entry (i.e by inhibiting CDK4/6) is likely to induce cell cycle arrest or quiescence but not apoptosis. For instance, inhibition of CDK4 prevents the development of lung tumours induced by K-Ras oncogene by triggering senescence, a permanent arrest in G0/G1 (Puyol *et al.*, 2010). Recent work has demonstrated that treatment of adult neural stem cells with a cell permeable CDK4 inhibitor induced an increase in the percentage of cells in G1 and promoted neuronal differentiation *in vitro* (Roccio *et al.*, 2013). Similarly, spontaneous differentiation is preceded by cell cycle arrest in G1 phase in human embryonic stem cells (Sela *et al.*, 2012). On the other hand, accumulation of active CDK4/6/cyclin D complexes, during G1, resulted in inhibitory phosphorylation of SMAD2/3, thus preventing cell specification (Pauklin and Vallier, 2014).

In a study conducted on neuroblastoma primary tumours, CDK4 was found to be amplified and associated with genomic aberrations in the G1 regulatory genes such as MYCN, and hence inducing overexpression of E2F target genes (Molenaar, Koster, Ebus, *et al.*, 2012). Recently, there were some attempts to inhibit CDK4/6 /cyclin D1, using Palbociclib a small selective molecule inhibitor of cyclin D1 associated kinases. CDK4/6 inhibition induced cell cycle-arrest in G1, supressed the D1-pRb pathway via inhibition of phosphorylation of Rb and the expression of E2F target genes. This eventually resulted in proliferation inhibition of neuroblastoma cells *in vitro* (Rihani *et al.*, 2015). This suggests that targeting CDK4/6 may provide a new and alternative therapeutic approach for neuroblastoma patients.

In contrast to cell cycle entry CDKs, the mitotic kinase CDK1 is essential for the cell division, and inhibition of CDK1 arrests cells in G2 phase and prevents entry into mitosis (Santamaría *et al.*, 2007). Using genetically engineered mouse models, Santamaria and colleagues also showed that in the absence of interphase CDKs, CDK1 can recapitulate the function of other CDKs involved in regulating cell cycle transitions, for example CDK1 can bind to cyclin D and E, resulting in the phosphorylation of the retinoblastoma protein pRb and the expression of genes that are regulated by E2F transcription factors (Santamaría *et al.*, 2007) and hence substitutes the effect of CDK4/6. Furthermore, CDK1 binds to its ordinary cyclins (A or B) and phosphorylate more than 70 substrates in order to promote centrosome separation, chromosome condensation, nuclear envelope breakdown and mitotic entry (Malumbres and Barbacid, 2005).

CDK1 knockout mouse germ line results in arresting embryonic development around the blastocyst stage and induced embryonic lethality, demonstrating the importance of CDK1 in early development (Diril *et al.*, 2012). Overexpression of CDK1 has been described in many cancers including lymphoma, advanced melanoma and lung cancer (Zhao *et al.*, 2009; Abdullah, Wang and Becker, 2011). However, CDK1 inhibitor treatment of MYC-dependent mouse hepatoblastoma and lymphoma tumours decreased tumour growth and prolonged their survival (Goga *et al.*, 2007).

1.1.11.2.2. Rationale for therapeutically targeting CDKs in cancer

The activity of CDK/cyclin complexes activity is known to be frequently deregulated in variety of human cancers (Lapenna and Giordano, 2009). Some CDKs can be considered oncogenic, for example, CDK4 is found overexpressed in many cancers including melanoma (Sheppard and McArthur, 2013), lung carcinoma (Puyol *et al.*, 2010), breast cancer (Peyressatre *et al.*, 2015) and prostate cancer (Comstock *et al.*, 2009), or amplified in others including osteosarcoma (Wei *et al.*, 1999), glioblastoma (Schmidt *et al.*, 1994)and pancreatic cancer (Eggers *et al.*, 2011), whereas CDK6 was found mutated in a wide variety of cancers such as lymphoma (Chilosi *et al.*, 1998), glioma (Bellail, Olson and Hao, 2014), medulloblastoma(Mendrzyk *et al.*, 2005) and neuroblastoma (Easton

et al., 1998). In addition, CDK1 was found to be mutated in ovary carcinoma (Peyressatre *et al.*, 2015). Hence, controlling the cell cycle through targeting cyclin-dependant kinases and their associative regulators may provide a potential therapeutic approach for cancers.

Due to the importance of CDK4/6 activity in regulating the cell cycle, targeted therapies aimed at cell cycle pathways of CDK4/6 have been conducted. Palbociclib (PD0332991, Pfizer) is an orally administered small molecule inhibitor of CDK4/6 (Fry *et al.*, 2004), and is undergoing active clinical trial testing. In the myeloma mouse model, Palbociclib treatment induced tumour suppression with significant improvement in survival (Menu *et al.*, 2008). The Food and Drug Administration designated Palbociclib a breakthrough therapy in April 2013 (Brower, 2014). Therefore the use of highly selective CDK4/6 inhibitor, Palbociclib, is used to treat many patients with breast cancer leading to cellular senescence- like activity and cell cycle arrest at G1 (Flaherty *et al.*, 2012; Hamilton and Infante, 2016).

The use of selective inhibitors for other CDKs was also trialled following the success of Palbociclib treatment. CDK1 inhibitor (RO-3306) was tested on mitotic Hela cells as a starting point to test its efficacy. *In vitro* experiments on HeLa cells confirmed again that CDK inhibitors are one of the most successful cancer treatments (Vassilev *et al.*, 2006).

Other small-molecule CDK1 inhibitors decrease tumour growth and prolong survival in mouse models of Myc-dependent lymphoma and hepatoblastoma (Goga *et al.*, 2007). CDK1 inhibition induced a reduction of MYCN activity, which thereby decreased the transcriptional activation of MYCN on the survivin promoter, resulting in apoptosis induction (Chen, Tsai and Tseng, 2013). Similarly, targeting CDK1, but not CDK4/6, is selectively lethal to MYC-dependent human breast cancer cells (Kang *et al.*, 2014). Hence, because there are currently no compounds directly targeting Myc, CDK1 inhibition may be an important therapeutic approach for human malignancies that overexpress MYC protein (***see section 1.1.3.3.1***).

CDK1 also phosphorylates ASCL1 in Xenopus at serine-proline (SP) motifs, inhibiting the ability of ASCL1 in driving differentiation. The overexpression of CDK1 and MYCN inhibits the wild type ASCL1 driven-differentiation (Ali *et al.*, 2014; Wylie *et al.*, 2015). This suggests that the use of CDK1 inhibitor may lead to ASCL1 dephosphorylation induced-differentiation, offer new approach for differentiation therapy in neuroblastoma.

1.1.11.3. Tyrosine phosphatase inhibitors

ALK, a receptor tyrosine kinase (RTK) oncogene identified in both familial and sporadic neuroblastoma (Mukherjee *et al.*, 2004). ALK act through AKT, a common consequence of activation of phosphotyrosine signalling. Phosphotyrosine signalling is regulated by two protein families; protein tyrosine kinases and protein tyrosine phosphatases (PTPs), with PTPs being key positive and negative modulators of this signalling pathway (Badmaev, Prakash and Majeed, 1999; Bishayee *et al.*, 2010). PTPs consists of 107 family members, some of them were reported to have implications in the biology of tumour cell (Bishayee *et al.*, 2010). Approximately 70% of PTPs are considered as tumour suppressors, however, the rest of them are shown to contribute in tumour progression and resistance (MacKeigan, Murphy and Blenis, 2005), and may also act oncogenically in neuroblastoma (Shang *et al.*, 2010).

Oxovanadium, pan-inhibitors of PTP enzymes, is found to have an anticancer effect on several malignant cell lines and many preclinical *in vivo* cancer models (Evangelou, 2002; Ray *et al.*, 2006; Klein *et al.*, 2008; Kostova, 2009). Inside cells, oxovanadium complexes exist largely in two forms; vanadyl V(IV) and vanadate V(V) states, although the latter predominates and being associated with PTP inhibition (Ray *et al.*, 2006). Vanadate to vanadyl transformation in cells can be brought about by reducing agents such as glutathione (GSH) (Bishayee *et al.*, 2010).

Bis(maltolato) oxovanadium (IV) (BMOV), is found to inhibit tumour cell growth and induce senescence in Rhabdomyosarcoma cells (Dąbroś *et al.*, 2011) while inducing senescence or differentiation in certain neuroblastoma cell lines (Clark, Daga and Stoker, 2013; Clark *et al.*, 2015).

In this research we sought to investigate the effect of effect of BMOV as tyrosine phosphatase inhibitor on neuroblastoma tumours.

1.2. The Drug discovery and model systems

Drugs discovery programs are both costly and lengthy. Before designing a pharmaceutical compound, the potential targets that interact with the compound must be identified and evaluated. Following this, the compound has to confirm its reproducibly on their intended targets *in vitro* and later in a preclinical model organism. The compound must considered as effective, safe and has a suitable therapeutic window before reaching human subjects in the clinical trials (Hughes *et al.*, 2011). Increased knowledge of human biology and the process of disease helps expand the number of potential therapeutic targets. However, only one in five to ten thousands compound enters research development and finally becomes licensed for human use (Azmi and Mohammad, 2014). Therefore, it is not surprising that pharmaceutical companies report the cost of developing a compound requires a cost of many millions of dollars and takes up to 15 years to complete (Paul *et al.*, 2010; Hughes *et al.*, 2011; Mestre-ferrandiz, Sussex and Towse, 2012). A crucial step in the process of validating a new compound is the use of a pharmaceutically relevant preclinical model system.

Animal models are vital to the development of novel anti- cancer agents. Over time, animal models have been used in therapeutic research to understand mechanisms, evaluate efficacy, optimise dose timing, determine in vivo distribution and characterise the metabolism of the drug. As our understanding of many areas of cancer biology and therapeutic approaches has increased, and so has those model organisms. Each model organism has some approximattion of reality, but also some inherent limitations; limitations might include time-consuming, and cost (Vandamme, 2014).

1.2.1. The Mouse Model

The mouse model is the most common one used in therapeutic research. Several characteristics recognise the mouse model as an attractive organism for laboratory investigation, including its small size, propensity to breed in captivity, lifespan of 3 years, extensive physiological and molecular similarities to humans, as well as entirely sequenced genome (Frese and Tuveson, 2007).

The mouse genome can be manipulated to produce a genetically engineered mouse model (GEMM). This involves delivering a foreign gene to the mouse germline and allowing consistent expression (Gordon and Ruddle, 1981). This technique is used to explore many oncogenes and tumour suppressor genes and their role in tumorigenesis and treatment (Capecchi, 1989).

Improvement of several techniques relating to GEMM have led to significant increase in the use of GEMM over the past twenty years. For example, the degree of manipulation in terms of timing and the location of gene expression is ever evolving. In neuroblastoma the well-characterized TH-MYCN GEMM is increasingly used for a variety of molecular-genetic, developmental and pre-clinical therapeutics applications (Chesler *et al.*, 2007; Hogarty *et al.*, 2008; Rounbehler *et al.*, 2009). The TH-MYCN GEMM created in 1997 by Weiss and colleagues overexpresses MYCN and acts as a model for high risk neuroblastoma tumours (Chesler and Weiss, 2011).

TH-MYCN was constructed using a first-generation, “transgenic” approach. This involved introducing exogenous DNA to the nucleus of fertilised murine oocyte resulting in random integration of transgenic construct into genomic DNA. The construct incorporates exogenous human cDNA for MYCN, ligated downstream of the rat tyrosine hydroxylase (TH) promotor. A rabbit beta globin intron element enhancer was used to enhance expression, and a herpes simplex virus thymidine kinase gene sequence was used as a transcription terminator (Weiss *et al.*, 1997). The use of rat TH promoter targets the expression of MYCN to the neuronal precursors of sympathoadrenal origin, the cell-of-origin for the initiation of neuroblastoma. In addition to investigating the specific role of MYCN in driving neuroblastoma tumorigenesis, this modelling approach has been used extensively

for molecular genetics, developmental biology, imaging technology and gene interaction and therapeutics (Chesler and Weiss, 2011). In neuroblastoma, other GEMM have been constructed using similar approach including ALK^{F1174L} and ALK^{F1174L} and these have been crossed with the MYCN transgenic mouse model (Berry *et al.*, 2012).

GEMM models have many strengths, including the spontaneous growth of tumour in an immunocompetent host and in appropriate tissue and microenvironment (Chesler and Weiss, 2011). Thus, they give a better representation of the tumour reality in human patients and provide meaningful therapeutic research which can translate effectively in a clinical setting. Conversely, GEMM models have many criticisms that limit its significance. It is difficult to reproduce the heterogeneity of gene mutations and expression seen throughout primary tumours in this model (Ruggeri, Camp and Miknyoczki, 2014). Another problem is that they often fail to recapitulate the metastatic patterns observed in patients (Teitz *et al.*, 2013). The neuroblastoma cells are also mouse cells and not human cells. This presents a significant limitation and the extent to which therapeutic effect can be modelled successfully using this model. Several other practical issues including cost, patents, long latencies to tumour development, low tumour penetrance as well as the difficulty in monitoring tumour development and therapeutic response limit the use of this model, especially in routine preclinical drug screening (Chesler and Weiss, 2011).

Transplantation mouse models are another commonly cancer research tool. Various systems and techniques have been used to propagate tumour tissues in different hosts. Allograft mouse model is one of these model systems that involves transplanting of tumour tissues derives from the same host species (Yang *et al.*, 2017). Similar to GEMM, these tumours and tissues is not humans and thus limit the value of the results obtained using this model system.

Xenograft model is another transplant model system that involves transplantation of human tumour tissue into a mouse that must be immunodeficient to avoid host immune rejection (Vandamme, 2014). Xenografting can be subcutaneous where cells injected under the host skin or orthotopic

whereby the tissue transplanted in the region form which it would have originated or intravenous. A subcutaneous mouse model allows monitoring the growth of the tumour without the need for sophisticated imaging techniques (Kumar *et al.*, 2012). However, orthotopic model recapitulates the nature of tumour better in terms of cell-cell interactions of the local microenvironment in which the tumour grows, invade and metastasise (Ruggeri, Camp and Miknyoczki, 2014). The technique by which orthotopic models produced requires a highly and precise skills, time consuming and do not allow to direct visualisation of the tumour. Some non- invasive techniques have been developed to overcome the visualisation problem but still it adds more complexity and cost to the model (Albanese *et al.*, 2013).

The mouse models discussed have both strengths and limitations to their use in therapeutic research. One common limitation of all these models is the growing complexity and cost associated with their use. In the context of rapidly increasing potential targets new models are required which can help to screen which drugs should be used in these more complex and expensive systems.

1.2.2. The Chick Embryo Model

As discussed earlier, drug screening programs demand the use of huge number of animals mostly rodents; however, these models are expensive, time-consuming, sometimes difficult to handle, and there are important ethical and legal issues (Vargas *et al.*, 2007). There is a need for a preclinical model that is relatively cheap, cost-effective, easy to handle and ideally do not required a Home Office licence. The chick embryo model represents an alternative model to rodents for some types of experiments and also has advantages over the other preclinical models (Ribatti, 2010, 2014; Rovithi *et al.*, 2017).

The chick embryo is a well-known model system with a long and fascinating history since Aristotle, who monitored the progression of chick embryo development by opening the egg shell daily (Stern, 2005). Chick embryos have been instrumental not only to the field of developmental biology, but have also made significant contributions to research in cancer biology, virology, immunology and cell

biology (Kristin H. Kain *et al.*, 2014). An example of several Nobel Prize winning discoveries made using the chick embryo model is that by Rita Levi-Montalcini who discovered Nerve growth factor (Kristin H Kain *et al.*, 2014).

As embryology advanced, more histological studies were carried out using the chick embryo. For example, in 1889, a first comprehensive morphological atlas of chick development was produced by Mathias Duval. Mathias's works provided the foundations for Viktor Hamburger and Howard Hamilton's to published their 46 morphologically distinct stages of chick development, which is still widely in use (Hamburger and Hamilton, 1992). The development time of the embryo is 21 days as illustrated by the Hamburger and Hamilton stages (***Figure1.10***) (Kristin H. Kain *et al.*, 2014) . All the above mentioned work on chick embryo has been further built upon making the chick embryo a well characterised model with a fully sequenced genome (Vergara and Canto-Soler, 2012).

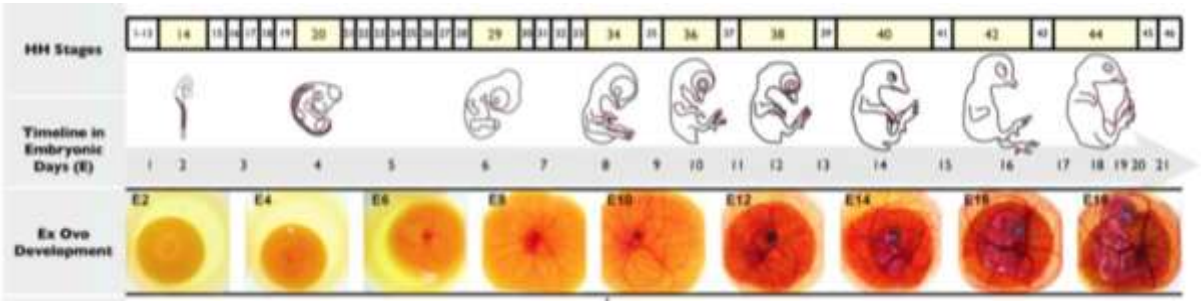

Figure1.10 The stages of chick development. *Image displaying the 46 Hamburger and Hamilton (HH) stages of chick development, and how they relate to the length of incubation (E). Adapted from (Kristin H. Kain et al., 2014)*

The chick embryo has an advantage over other (non-mammalian) preclinical models, due to the similarities of the chick to the human embryo at the anatomical, cellular and molecular levels. They may be less similar than the mouse but much more so than drosophila or zebrafish. The accessibility of the developing embryo for visualization and experimental purposes is other key advantage of this model (Vergara and Canto-Soler, 2012; Kristin H. Kain *et al.*, 2014). Like other vertebrates, chick embryos possess an immune system that contains both T-cells and B-cells. Its immune system begins to develop around E9 but then it requires until E18 to be fully developed (Vargas *et al.*, 2007). This

gives the chick embryo model extra advantage of being immunodeficient when performing experimental work before E14.

There are also many economical and practical advantages of the model which should be mentioned. Fertilised eggs are available almost anywhere in the world and they can be purchased in specific quantities and may be stored easily for several days prior to incubation. This, allows researchers to conveniently obtain embryos at the specific developmental stage that serve their research needs. Current UK legislation on protection of animals for scientific purposes allows experimentation on chick embryos without authorization up to the age of development day 14 (E14) (Vergara and Canto-Soler, 2012). This makes the model extremely feasible to use and conduct experimental work up to E14.

Furthermore, ethical considerations such as the 3Rs principle (reduce, refine and replace animal experiments) are also important to consider. This principle highlights the need to consider using none protected animal species when conducting research wherever possible. Humane protocols have been optimised to eliminate the distress on the chick up to E14 when performing experiments. Chick embryo model can serve as a replacement for other higher preclinical models however experiments that require a long time period cannot be conducted on the model, thus, the chick embryo could partially *replace* some model systems (Bjornstad *et al.*, 2015). Altogether, the chick embryo provides an alternative potential model that can be used in increasing our understanding of tumour biology and testing new therapeutic agents.

1.2.2.1.The Chorioallantoic membrane

The most common use of the chick embryo model in cancer biology involves growing xenograft tumours on the CAM. Three extra-embryonic membranes protect and nourish the chick embryo until the hatching (***Figure1.11***). The chorioallantoic membrane (CAM) is one of them and serves multiple functions. The CAM serves as the respiratory organ for the embryo, has a role in calcium transport

from the eggshell, and is involved in acid-base homeostasis in the embryo and in ion and water reabsorption from the allantois sac.

The CAM is formed by the fusion between of the allantois and the chorion membrane around days five to six of incubation. It develops progressively adhering to the inner side the eggshell and surrounds the embryo by day 11 (Ribatti *et al.*, 2001; Gabrielli and Accili, 2010). The CAM is transparent and highly vascularised tissue composed of arteries and veins and with intricate capillary plexi (***Figure1.12***) (Vargas *et al.*, 2007).

Histologically, the CAM contains three major layers, from outside to inside they are; the ectodermal chorionic epithelium attached to the shell membrane ; an intermediate mesoderm enriched in blood vessels and stromal components; and the endodermal allantoic epithelium facing the allantoic cavity (Ribatti *et al.*, 2001; Gabrielli and Accili, 2010).

The CAM is a very thin structure ~100µm across the entire three layers. Haematoxylin–eosin staining of paraffin sections clearly identifies the ectoderm, represented by 1-2 cells epithelial layer; the capillary plexus visualized as tiny circular openings in the ectoderm frequently filled with erythrocytes; the mesoderm filled with the stromal cells, collagen fibres and blood vessels of different diameters, including terminal capillaries localized right under the ectoderm; and the one cell-layer of flat endoderm (***Figure1.13***).

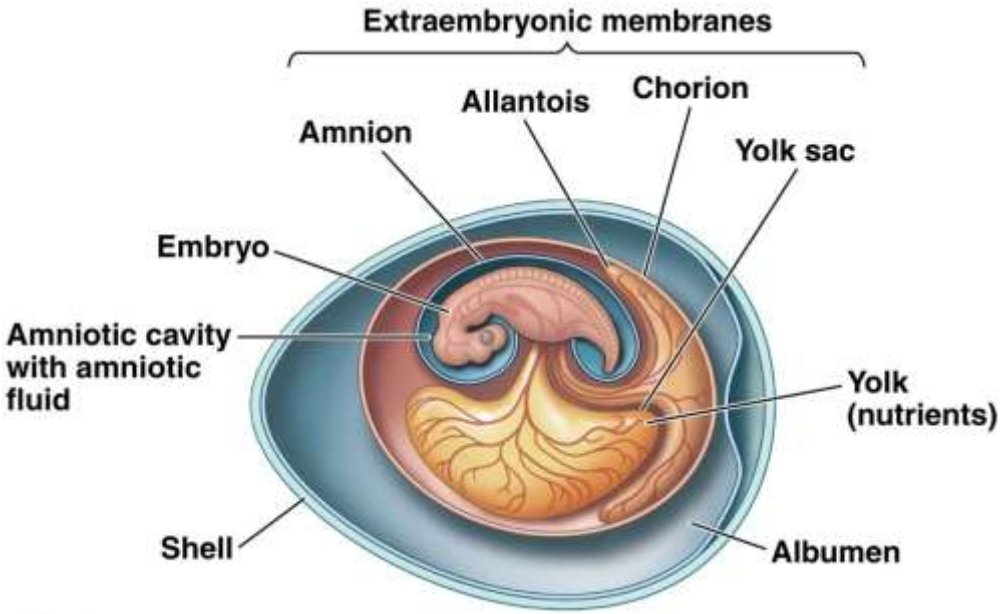

Figure1.11 Diagram of the chick embryo highlighting the extraembryonic membranes. *The chorion and allantosis (labelled in grey) fuse to form the chorioallantoic membrane at day 5-6 of embryonic development. Adapted from http://abacus.bates.edu/acad/depts/biobook/Verteb2.htm .*

Figure1.12 The chick chorioallantoic membrane (CAM) - this image, taken 8 days after incubation (E8) demonstrates the highly vascular CAM by Grace Mather.

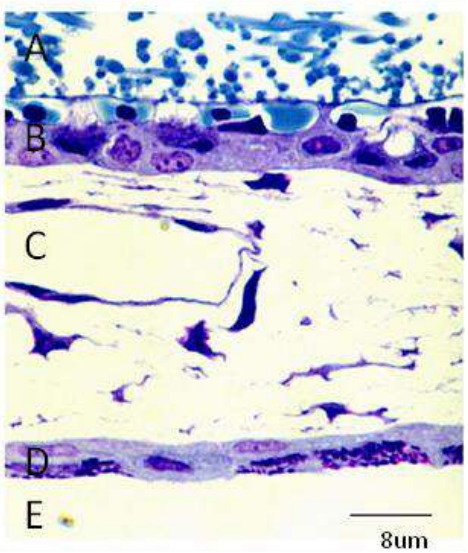

Figure1.13 A section through the CAM demonstrating the three tissue layers (B-D). A: *shell membrane. B:chorionic epithelium****. C:*** *mesoderm layer****. D*** *allantoic epithelium* ***E:*** *allantoic cavity. Adapted from (Gabrielli and Accili, 2010).*

Given the highly vascular nature of the CAM, the CAM has been used widely for angiogenesis and wound healing studies however it has also been used in cancer research for decades (Vogel and Berry, 1975). Since the young embryos are not fully immunocompetent, they then provide a perfect host platform for cancer cell and biopsies. In 1982 Armstrong et al reported the ability of several different types of tumour cells to invade the CAM's epithelial layer and form tumour beneath it. The authors illustrated that following light trauma to the CAM surface, tumour cells readily invaded the superficial epithelial layer to form the tumour nodule (Armstrong, Quigley and Sidebottom, 1982). Tumours grown on the CAM, were shown to express the typical features of a tumour in terms of complexity, angiogenesis and metastasis (Zijlstra *et al.*, 2002; Bobek *et al.*, 2004; Fergelot *et al.*, 2013; Kristin H Kain *et al.*, 2014).

Indeed, CAM model as a biological platform with all the advantages mentioned above provides an opportunity for transplanting human tumours (Bader, Kang and Vogt, 2006), tumour xenografting (Klingenberg *et al.*, 2014; Swadi *et al.*, 2018), tumour-induced angiogenesis (Nowak-Sliwinska *et al.*, 2012; Nowak-Sliwinska, Segura and Iruela-Arispe, 2014), and cancer metastasis (Deryugina and Quigley, 2008; Kristin H. Kain *et al.*, 2014; Herrmann *et al.*, 2015). Here we aim to develop the CAM model as a high through-put, economically viable yet highly informative model system in the context of neuroblastoma drug discovery.

1.3. Hypothesis and Aims

Differentiation is a key prognostic factor in neuroblastoma as the most differentiated pattern leads to favourable outcomes for patients. Neuroblastoma is thought to result from aberrations that occur during development leading to cells that have arrested in an undifferentiated form. The ability of cells in the 4S tumour to spontaneously regress to a more differentiated form, GN, supports this hypothesis (Park *et al.*, 2013). Thus therapies that promote differentiation are a particularly useful approach. Here we hypothesise that reducing or blocking cell division will promote differentiation leading to tumour regression.

To test our hypothesis we aimed to address the following points:

1) Optimise drug delivery to the CAM tumours in the chick embryo using the well-characterised small molecule RA
2) Characterise the effect of potential therapeutic molecules using in *vitro* assays.
3) Study the effect of these molecules *in vivo* using the CAM model and identify whether they are promising and should be prioritised for further investigation.
4) Determine the efficacy of these molecules in inhibiting neuroblastoma metastasis.

Chapter Two: Materials and Methods

2.1. Introduction

This chapter will introduce neuroblastoma cell lines and the techniques that been used to assess the efficacy of different drugs/ treatments on them. In addition, chick embryo work will also be presented later to illustrate the effect of those drugs/ treatments *in vivo*.

2.1.1. Cell lines

Several Neuroblastoma cell lines were established from samples of primary or metastatic tumours which are obtained from patients during bone marrow aspiration, surgical resection and occasionally from peripheral blood. Four cell lines were used in this research; each has different features that can be seen in ***Table 2.1***. These cell lines were chosen as they are characteristic of two types of clinically high risk neuroblastoma tumours: MYCN amplified and chromosome 11q deleted. Wild type cells and cells transduced with green fluorescent protein (GFP) were used.

Table2.1 *Information on the origins and characteristics of the cell lines used in this project.*

Cell line	Source	Characteristics
BE2C	BE(2)-C is a sub-clone of SK-N-BE(2), a neuroblastoma cell line that was established from a bone marrow biopsy taken from a 2 year old child with disseminated neuroblastoma after repeated courses of chemotherapy and radiotherapy.	MYCN amplified Chromosome 1p deletion Chromosome 17 translocation.
IMR32	Isolated from an abdominal NB in a 13-month-old child.	MYCN amplified 1p deletion
KELLY	Isolated from a metastatic brain lesion in a 13-month-old child.	MYCN amplified ALK ^{F1174L} mutation
SKNAS	Metastatic site: bone marrow biopsy of a 6 year old child.	Single copy MYCN Chromosome 1p deletion Chromosome 11q deletion

2.1.1.1 Culturing Neuroblastoma cell lines

Cell lines were generally cultured as monolayers in 25cm^2 or 75cm^2 culture flasks (Corning, UK), in their appropriate media (***see Table2.2***). Flasks were kept in a humidified incubator at 37°C, 5%CO_2. In order to persistently supply the NB cells with the nutrients that they needed, 5ml of medium were regularly removed and replaced with 5mL of fresh medium.

When cells were approaching 90% confluency, calcium- and magnesium-free Hanks Balanced Salt Solution (HBSS) (H9394, Sigma-Aldrich, UK) was used to wash the culture surface, followed by treatment with 1ml 0.05% trypsin EDTA 1x Solution (Gibco) per 75cm^2 flask. Following 5 minutes incubation at 37°C, 9ml culture medium was added to the dislodged cells and pipetted in and out to disrupt cell clumps. The resulting cell suspension was then split into two to four 75cm² flasks and a further 10ml of fresh medium added to each flask.

A haemocytometer was used to count cell after producing a single-cell suspension using 1ml pipette. The average number of cells was calculated from 4 counts, to give (average) x 10^4 cells/ml. Cells were then seeded at an appropriate density according to each experiment requirements. Cells were routinely tested for mycoplasma to ensure they remained free of contamination. GFP-labelled cells and wild type cells were cultured in the same medium using the same methods.

For Hypoxia studies, cells were maintained at 37°C with 5%CO_2 and 1%O_2 (Don Whitley Scientific, Shipley, UK; Hypoxystation-H35) for 72hr, or cells were treated with a hypoxia mimic (Dimethyloxalylglycin DMOG) (Enzo Laboratories, Farmingdale, NY, USA) at 0.5mM and incubated at 37°C with 5%CO_2 for 24hr.

Table2.2 *Neuroblastoma cell lines and their culturing requirements.*

Cell line	Culture media
BE2C	FCS - 10% , Pen Strep - 1%, and NEAA - 1% in DMEM
IMR32	FCS - 10% ,Pen Strep - 1% and NEAA - 1% in RPMI
KELLY	FCS - 10%, Pen Strep - 1% in RPMI
SKNAS	FCS - 10% , Pen Strep - 1% and NEAA - 1% in DMEM

2.1.1.2. Thawing of Neuroblastoma cells

Cells were stored in 2ml cryovials (Starlab, UK) in liquid N2 tank. When needed, vials were removed from the storage and placed in the cabinet hood briefly to just thaw (but not warmed to room temperature). Upon thawing, cell suspension (1ml) was removed from the vial and placed into 20ml sterile universal bottle (Starlab, UK), and 1ml of the appropriate media added drop-wise with gentle mixing. A further 18ml medium was added over 30-60 seconds, following which the diluted cell suspension was spun using a GLC-4 General Laboratory Centrifuge (Sorvall Instruments) at 1000rpm for 10 minutes. After centrifugation the supernatant was discarded and the cell pellet resuspended in 7ml fresh media. Cells were seeded in 25cm^2 flasks and transferred into 75cm^2 flasks once 80-90% confluency was reached.

2.1.1.3. Freezing of Neuroblastoma cells

Following trypsinisation (*see cell line culture*), cells were diluted in 10ml of fresh media and centrifuged at 1000rpm for 5-10 minutes, the supernatant was removed and the cell pellet was resuspended on ice in “freezing medium” (10% dimethylsulfoxide DMSO in Foetal Bovine Serum FBS). Aliquots of 1ml were placed in cryogenic vial (Starlab, UK) and 2-3 vials per 90-100% confluent 75cm^2 flask of cells were produced. Vials were kept overnight in gas phase over liquid N_2 to lower

the temperature slowly and limit cell damage. Next day, vials transferred to the liquid N_2 tank for long-term storage.

2.2. Therapeutic compounds

2.2.1. All-trans retinoic acid

All-Trans retinoic acid (RA) (Sigma-Aldrich) was dissolved in DMSO to make a 0.16M stock solution, which was stored at -80°C light protected.

2.2.2. Bis(maltolato)oxovanadium(IV)

Bis(maltolato)oxovanadium(IV) or BMOV (Sigma-Aldrich) was dissolved in DMSO to make 10mM aliquot and stored at -20^0C.

2.2.3. Palbociclib (PD-0332991) HCl

Palbociclib (Selleckchem, US) was reconstituted in Dulbecco's Phosphate Buffered Saline DPBS (Life Technologies) to obtain 10mM stock solution and then stored at -80^0C according to the manufacturer's instructions.

2.2.4. RO-3306 (SML0569)

RO-3306 (Sigma-Aldrich) was reconstituted in DMSO to obtain either 10mM or 14mM stock solution and stored at -80^0C according to the manufacturer's instructions.

2.3. Functional assays

2.3.1. Cell proliferation and morphological changes detection

2.3.1.1 Seeding the cells and treatments

Neuroblastoma cells were grown on 13mm glass cover slips (Appleton Woods Ltd, UK) in 24 well plates (Corning, UK). Cells were seeded at 2.5x 10^4 and 5x 10^4 cells/ml density for BE2C and IMR-32 respectively and incubated with their appropriate cell culture medium (500µl per well) for 18-24hr to adhere and settle prior to treatment.

RA treatment

A final 10µM concentration of RA was obtained by diluting the stock solution with the appropriate cell culture medium (***see Table2.2***).

BMOV treatment

Cells were cultured in 10µM BMOV alone and in combination with RA (10µM) in an appropriate cell culture medium (***see Table2.2***).

Palbociclib treatment

A final 7.5 or 5µM concentration of Palbociclib alone and in combination with RA were obtained using the appropriate cell medium (***see Table 2.2***).

Following the treatments, cells were observed and imaged for morphology changes using Leica DMIRB microscope linked to a camera (Leica DFC420C) prior to staining with proliferation marker, Ki67.

2.3.1.2. Fixing, quenching and permeabilisation of cells

Cells grown on coverslips (*section 2.3.1.1*) were removed from the well containing medium using bent syringe needle and put in a staining plate; cells were fixed using 100µL of 4% paraformaldehyde (PFA) for 10 minutes and then washed with DPBS ($+Ca^{2+}/Mg^{2+}$). Subsequent to paraformaldeyde removal, fixation was quenched with 50µl of 0.1M glycine pH7.4 for 15 minutes at room temperature. Cells were permeabilised with 100µL of blocking buffer (1% BSA, 0.1%Triton X100, 0.12M phosphate PH 7.4) for one hour at room temperature to allow blockage of non-specific binding sites for antibodies.

2.3.1.3. Antibody labelling and counterstaining

Following the removal of the blocking buffer the primary antibody, Rabbit anti Ki67 (Abcam, Ab15580), was diluted in the blocking solution at 1:50, added and left at 4°C overnight. A control

coverslip was prepared by omitting the primary antibody. Ki67 was then removed and cells were washed 3X with DPBS (+Ca^{2+}/Mg^{2+}). Secondary antibody, Alexa 594 Goat anti Rabbit IgG (Thermo Fisher Scientific, A-11037) at concentration 1:500 diluted in 1% BSA, 0.1% Triton X100 in 0.12M phosphate pH7.4, plus 0.1µg/ml of 4',6-diamidino-2-phenylindole DAPI (Thermo Fisher Scientific,D3571) were added and incubated, protected from light, for one hour at room temperature. Secondary antibody were removed in dip wash in DPBS 2X and in dH2O once and left to dry for 10min. A drop of Dako fluorescent mountant medium was applied to each sample before the addition of a cover slip to each slide. Slides were again stored at 4°C and protected from light until analysis.

2.3.1.4. Cell proliferation quantification

Cell proliferation was quantified manually under a Leica fluorescent microscope using a x40 oil immersion objective. The number of Ki67 positive cells (red) in each field were counted and expressed as percentage of the total number of DAPI stained cells (blue) in the same field. For each coverslip a minimum of four fields were examined and 100-200 cells were counted in each field. To eliminate bias, counting was performed blind; this was achieved by covering the identity of the cover slip and assigning cardinal numbers to each slide and checking the identity of the cover slip only after counting. Each experiment was conducted independently 3 times.

2.3.2. Cell viability detection

2.3.2.1. Determination of cell number to be used

SKNAS and BE2C cells were set at ten 2-fold dilutions in triplicates in a 96 well plate (corning, UK), from 5 x 10^6 cells/ml to 4.88 x 10^3 cells/ml. The procedure was carried out as described in table2.3.

Table2.3 *Ten 2-fold dilutions procedure used to optimise the cell number for MTT assay.*

Label Tubes (cells/mL)	**Add Cell Culture Medium**	**Add Cells**
5.00×10^6	_	400 µl of 5.00×10^6 cells/ml stock
2.50×10^6	400µl	400 µl of 5.00×10^6 cells/ml stock
1.25×10^6	400µl	400 µl of 2.50×10^6 cells/ml stock
6.25×10^5	400µl	400 µl of 1.25×10^6 cells/ml stock
3.13×10^5	400µl	400 µl of 6.25×10^5 cells/ml stock
1.56×10^5	400µl	400 µl of 3.13×10^5 cells/ml stock
7.81×10^4	400µl	400 µl of 1.56×10^5 cells/ml stock
3.91×10^4	400µl	400 µl of 7.81×10^4 cells/ml stock
1.95×10^4	400µl	400 µl of 3.91×10^4cells/ml stock
9.77×10^3	400µl	400 µl of 1.95×10^4 cells/ml stock
4.88×10^3	400µl	400 µl of 9.77×10^3 cells/ml stock
Medium (Control)	400µl	_

Cells were plated at 100 µl /well including 3 control wells of cell culture medium alone. Cells then incubated at 37°C with 5% CO_2 for 12 - 18hr. 10µl of aqueous MTT solution (5mg/ml) was added to each well, the plate was shaken gently with a shaker for 1 minute. The plate was wrapped in foil to prevent light exposure and incubated for 4hr at 37°C. 100µl stop solution (5% sodium dodecyl sulphate SDS 0.01 M HCl) was added to each well, without mixing, and incubated at 37°C overnight.

Absorbance was detected at 570nm using Spectrophotometer (FLUOstar Omega microplate reader) (Molecular Devices, UK). Average values from triplicate readings were adjusted by subtracting the 'blank' average value reading (MTT dye and media only) to determine the optical density OD of viable cells. Absorbance plotted on the y-axis versus cell number per ml on the x-axis providing a curve that has a linear portion. Selection of a cell number that falls within the linear portion of the curve (i.e. providing values between the range of 0.75 and 1.25) allows for the measurement of both stimulation and inhibition of cell proliferation.

2.3.2.2. Determination of cell viability following CDK4/6i and CDK1i

Following optimisation the cell density (*section 2.3.2.1*), BE2C and SKNAS cells were seeded in triplicate at 7.81 x 10^4cells/ml density in 96 well plates (Corning, UK) and left to settle and adhere for 12-18 hrs in presence of three blank wells for each cell line (culture medium only).

Palbociclib and RO-3306 treatment

After cells adhered, culture medium was removed and replaced with medium containing 1µM, 5µM, 10µM and 20µM of Palbociclib and RO-3306. Controls were cultured with medium supplemented with DPBS or DMSO at the same concentration of Palbociclib and RO-3306 respectively in each cell line. Cells were treated for a total of 3 days prior to analysis with MTT assay.

DMOG treatment

In some, after cells adhered; cells were treated with further 24hr with DMOG (Enzo Laboratories, Farmingdale, NY, USA) at 0.5mM and incubated at 37°C with 5%CO_2. In parallel, controls were cultured with medium containing DMSO at the same concentration for each cell line. Following DMOG treatment, cells were treated with 5µM Palbociclib and RO-3306 for 3 days prior to analysis with MTT assay.

Analysis of cell viability

MTT assay was used to measure cell viability following treatments as described previously (*section 2.3.2.1*). The average of absorbance values were adjusted by subtracting the 'blank' reading (MTT and media only). Absorbance values from treated wells were compared with control wells (i.e. cells treated with DMSO/DPBS) to determine the effect of the treatment on the number of viable cells. Each experiment was performed in triplicates and repeated 3 times.

2.3.3. Determination of Apoptosis in cultured cells in response to Palbociclib and RO-3306

BE2C and SKNAS cells were grown on 13mm glass coverslips (Appleton Woods Ltd, UK) in 24 well plates (Corning, UK) at density of 2.5x 10^4 cells/ml and incubated with their appropriate cell culture medium (500µl per well) for 18-24hr to adhere and settle prior to treatment. After cells adhered, culture medium was removed and replaced with 5µM of Palbociclib and RO-3306 containing medium and incubated for further 3 days. Controls were cultured with medium supplemented with DPBS or DMSO at the same concentration of Palbociclib and RO-3306 respectively in each cell line. Apoptosising cells were identified using Apoptotic/Necrotic/Healthy Cells Detection Kit from Promokine (PK-CA707-30018) according to the kit instructions. Cells grown on coverslips were removed from wells using bent syringe needle and put in a staining plate; cells washed twice with 1X Binding Buffer and then incubated, without prefixation, with a staining solution (5µl of FITC-Annexin V, 5µl of Ethidium Homodimer III and 5µl of Hoechst 33342 in 100µl 1X Binding Buffer, 1:20 dilution) for 15 minutes at room temperature, protected from light. Coverslips were then washed a further 2 times with 1X Binding Buffer and mounted on a glass slide with Dako fluorescence mountant. Images were taken within 24hr using Leica LEITZ DMRB florescent microscope together with camera Leica DFC450C.

2.4. Quantitative PCR (qPCR)

The Polymerase Chain Reaction (PCR) allows amplification of small amounts of DNA. SYBR green is a fluorescent dye which specifically binds to double-stranded DNA and fluoresces only when bound to dsDNA. This property can be used to assess the relative changes in gene expression of samples compered to control. During the exponential phase of the reaction, fluorescence is directly proportional to amplification, thus allowing measurement of copy number. The cycle at which fluorescence exceeds the pre-determined threshold value is termed the cycle of quantification (C_t) value.

2.4.1. RNA extraction

RNA extraction was completed using the RNeasy Mini Kit (Cat no. 74104, QIAGEN). All reagents were stored in a dedicated RNase-free area in the lab, all surfaces and pipettes were decontaminated using RNAzap cleaning agent (R2020, Sigma-Aldrich), and samples kept on ice throughout to prevent degradation. Cells were first trypisinised and pelleted as for at 1000rpm for 10 minutes. The supernatant was then removed and the pellet disrupted by gentle tapping of the tube. RNA was extracted using spin-column based isolation and utilised 3 buffers: RLT, RW1 and RPE. To inactivate RNases, 1%ß-Mercaptoethanol was added to buffer RLT. 350µL of the buffer RLT was then added to lyse the cells. The cells were repeatedly drawn up and down using a 19G needle and 1ml syringe to simultaneously disrupt and homogenise the cells. A 1x volume of 70% ethanol was subsequently added to the lysate and mixed by pipetting, the resulting solution transferred to an RNeasy Spin Column and centrifuged at 800 x g for 15 seconds. The flow through was then discarded and 700µL of buffer RW1 was added to the column and centrifuged at 800 x g for 15 seconds. The flow through was again discarded and 500µl of buffer RPE was added and spun as before. The RNeasy Spin Column was transferred to a fresh collection tube and 40µl of RNAase free water was applied to the column membrane before spinning for 1 minute at 8000 x g. RNA concentration (ng/µl) and quality

(A260/280) were recorded using a NanoDrop spectrophotometer (Thermo Scientific, USA) and RNA was stored in aliquots at -80°C.

2.4.2 cDNA synthesis

cDNA synthesis was completed using a GoScript reverse transcription system (A5000, Promega, UK) according to the manufacturers protocol. A total of 1µg of RNA was used per reaction. Volume and reagents indicated in the table below (***Table2.4***). For the no reverse transcriptase controls nuclease-free water was added instead of reverse transcriptase. 1µg of RNA were mixed, on ice, with Oligo dT primers to give a volume of 5µl, and heated (block heat) at 70°C for 5 minutes then chilled on ice prior to the addition of the other reagents. After combining the reagents, the reaction mix was placed in a thermocycler to anneal for 5 minutes at 25°C, extend for 60 minutes at 42°C and the reverse transcriptase was inactivated at 70°C for 15 minutes. The resulting cDNA was aliquoted and stored at -20°C.

Table2.4 *Reagents and corresponding volumes used during reverse transcription according to the manufacturer's protocol. $MgCl_2$ (Magnesium Chloride), OligodT primers and RNAsin Ribonuclease Inhibitor were optimised.*

cDNA reaction mix reagents	**Volume per reaction**
RNA + Oligo dT primers	5µl
GoScript Reaction Buffer	4µl
$MgCl_2$	2µl
PCR Nucleotide Mix (NdTP)	1µl
Reverse Transcriptase	1µl
RNAsin Ribonuclease Inhibitor	0.5µl
Nuclease Free Water	6.5µl
Final reaction mix	20µl

2.4.3. Reference gene selection

Reference genes were selected to allow normalised relative quantification of genes of interest to be calculated. According to a literature search on reference genes in neuroblastoma cells,(Vandesompele *et al.*, 2002), three genes, glyceraldehyde-3-phosphate dehydrogenase (GAPDH), hypoxanthine phosphoribosyltransferase 1 (HPRT1) and ubiquitin C (UBC) were reported to be stably expressed in neuroblastoma cell lines and therefore were selected by Grace Mather from our lab as a reference genes to assess the effect some drugs on neuroblastoma cells (Grace Mather, University of Liverpool).

2.4.4. Target gene selection

The effect of retinoic acid on gene expression in several cell lines in culture has been described (Sung *et al.*, 2013). We selected the three genes having the largest fold increase/decrease (at least one in each direction)from this paper; Kruppel-like factor 4 (KLF4), roundabout, axon guidance receptor, homolog 2 (ROBO2), stathmin-like 4 (STMN4). MYCN is also included due to its significance in neuroblastoma differentiation.

2.4.5. Primers

Primer sequences were identified in published papers using the same target or reference genes in qPCR experiments (Vandesompele *et al.*, 2002; Sung *et al.*, 2013). Primer sequences were ordered from Sigma-Aldrich.Once the primers were received they were reconstituted in nuclease-free water (ThermoFisher Scientific, UK) and stored at -20°C in small 10mM aliquots to avoid freeze-thawing process. ***Table2.5*** below details all primer pairs used.

Table2.5 *List of the primers used in qPCR experiments.*

Gene	Forward 5'-3'	Reverse 5'-3'
GAPDH	AATCCCATCACCATCTTCCA	TGGACTCCACGACGTACTCA
HPRT1	TGACACTGGCAAAACAATGCA	GGTCCTTTTCACCAGCAAGCT
UBC	ATTTGGGTCGCGGTTCTTG	TGCCTTGACATTCTCGATGGT
KLF4	CGCCGCTCCATTACCAAGAGC	CGGTCGCATTTTTGGCACTG
MYCN	CACAAGGCCCTCAGTACCT	ACCACGTCGATTTCTTCCTCT
ROBO2	GATGTGGTGAAGCAACCAGC	TGGCAGCACATCTCCACG
STMN4	CCTAGCAGAGAAACGGGAACA	GGCGTGCTTGTCCTTCTCTT

2.4.5.1 Primer Efficiency

Primer efficiency for GAPDH, HPRT1, UBC, KLF4, MYCN, ROBO2 and STMN4 had been previously determined (Grace Mather, University of Liverpool).

2.4.6. qPCR Protocol design

Protocols were designed according to the recommendations of the ITaq SYBER green mastermix manufacturer (BioRad) specifically for the CFX Connect system. Each reaction comprised of 7.5µl of ITaq Universal SYBR® Green (1x) (172-5121, BioRad), 0.75µl of the forward primer (500nM final concentration), 0.75µl of the reverse primer (500nM final concentration), 2µl of the diluted cDNA, and the volume was adjusted to 15µl with nuclease free PCR grade water. The samples were vortexed to mix the cDNA with the SYBR green and were plated into hard shell white-coated 96 well plates (HSP-9645, BioRad). The cycling programme used is shown in ***Table2.6***. All samples were run as triplicates for each gene per reaction plate. Target experimental values were normalized to 3 housekeeping genes using the relative quantification method with 3 independent biological samples per condition.

Table2.6. *qPCR cycling conditions*

Step		**Details**
1	Polymerase activation and DNA denaturation	95°C (30 seconds)
2	Amplification (Denaturation)	95°C (5 seconds)
3	Amplification (Annealing/Extension + plate read)	60°C (30 seconds)
4	Amplification (Cycles)	40
5	Melt curve	65 C to 95 C (0.5 C increment) 5 seconds/step

2.4.6.1. Controls

For all experiments a no template control (NTC) was included to monitor genomic DNA contamination and primer-dimer formation. A no reverse transcriptase control (NRT) was also included whenever a new preparation of RNA was used, to monitor genomic DNA contamination (***see Figure2.1***).

GAPDH	NTC	NTC	NRT	NRT	RA	RA	NTC	NTC	NRT	NRT	DMSO	DMSO
UBC												
HPRT1												
KLF4												
MYCN												
ROBO2												
STMN4												

Figure2.1 Example plate layout for controls. *NTC, no template control, NRT, no reverse transcriptase.*

2.4.6.2. Plate design

Reaction supermixes were prepared in triplicates and 15µl of reaction supermix was carefully pipetted into a single well of a 96-well hard-shell PCR plate (HSS9641, BioRad, UK). The plate was covered by a clear seal (MSB1001, BioRad, UK) and centrifuged briefly in a microplate centrifuge. An example plate design can be seen in ***Figure2.2***. The plate was transferred to a CFX connect

thermocycler (BioRad, UK), which was used for all experiments. The thermocycler employed precise temperature control and rapid temperature changes for optimal cDNA amplification. ***Figure 2.3*** outlines the cycling control for PCR amplification.

				T1			T2			T3		
RG1	NTC	NTC	NTC	cDNA	cDNA	cDNA	cDNA	cDNA	cDNA	cDNA	cDNA	cDNA
RG2												
RG3												
TG1												
TG2												
TG3												
TG4												
TG5												

Figure2.2 Example plate layout for qPCR. *T, treatment, RG, reference gene; TG, target gene; NTC, no template control.*

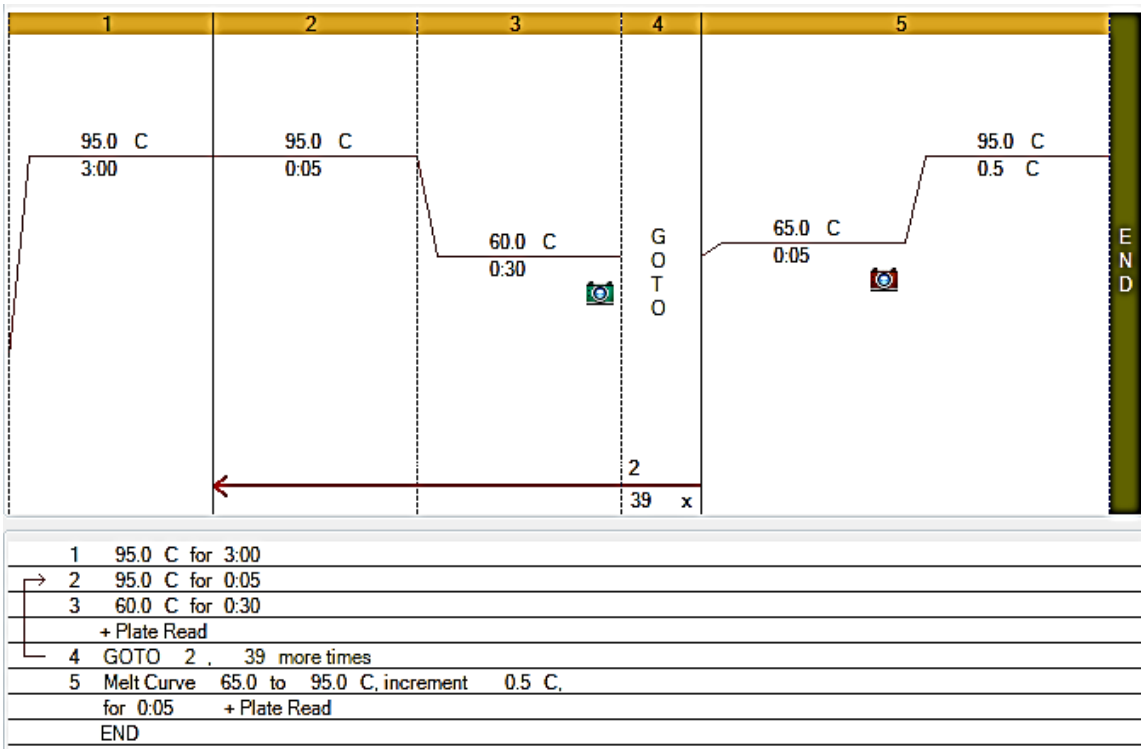

Figure2.3 Outlines the cycling control for PCR amplification.

2.4.7. Analysis of qPCR data

Data was viewed using Bio-Rad CFX Manager 3.1 software. An initial inspection of both the amplification plot and melt curve ensured that there were no obvious anomalous results. Fold change in target gene expression was calculated relative to the control. Results were normalised to the three reference genes (GAPDH, HPRT1 and UBC).

The mean C_t value for 3 technical replicates from a single biological replicate was calculated, followed by the mean C_t value for 3 independent biological replicates. A commonly used method of calculating relative gene expression using qPCR data is the $2^{-\Delta\Delta Ct}$ method (Schmittgen and Livak, 2008). To conduct statistical analysis NRQ data of 3 independent biological replicates were compared to control to standardise the fold change.

$$\Delta C_t = C_t\,(TG) - C_t\,(RG)$$

$$\Delta\Delta C_t = \Delta C_t \text{ Treatment} - \Delta C_t \text{ control}$$

$$\text{Fold change due to treatment} = 2^{-\Delta\Delta Ct}$$

C_t, threshold cycle; TG, target gene; RG, reference gene.

2.5. Chick embryo work

Chick embryo experiments were carefully carried out according to the current UK Home Office legislation, 2013. All the steps are illustrated in ***Figure2.4.***

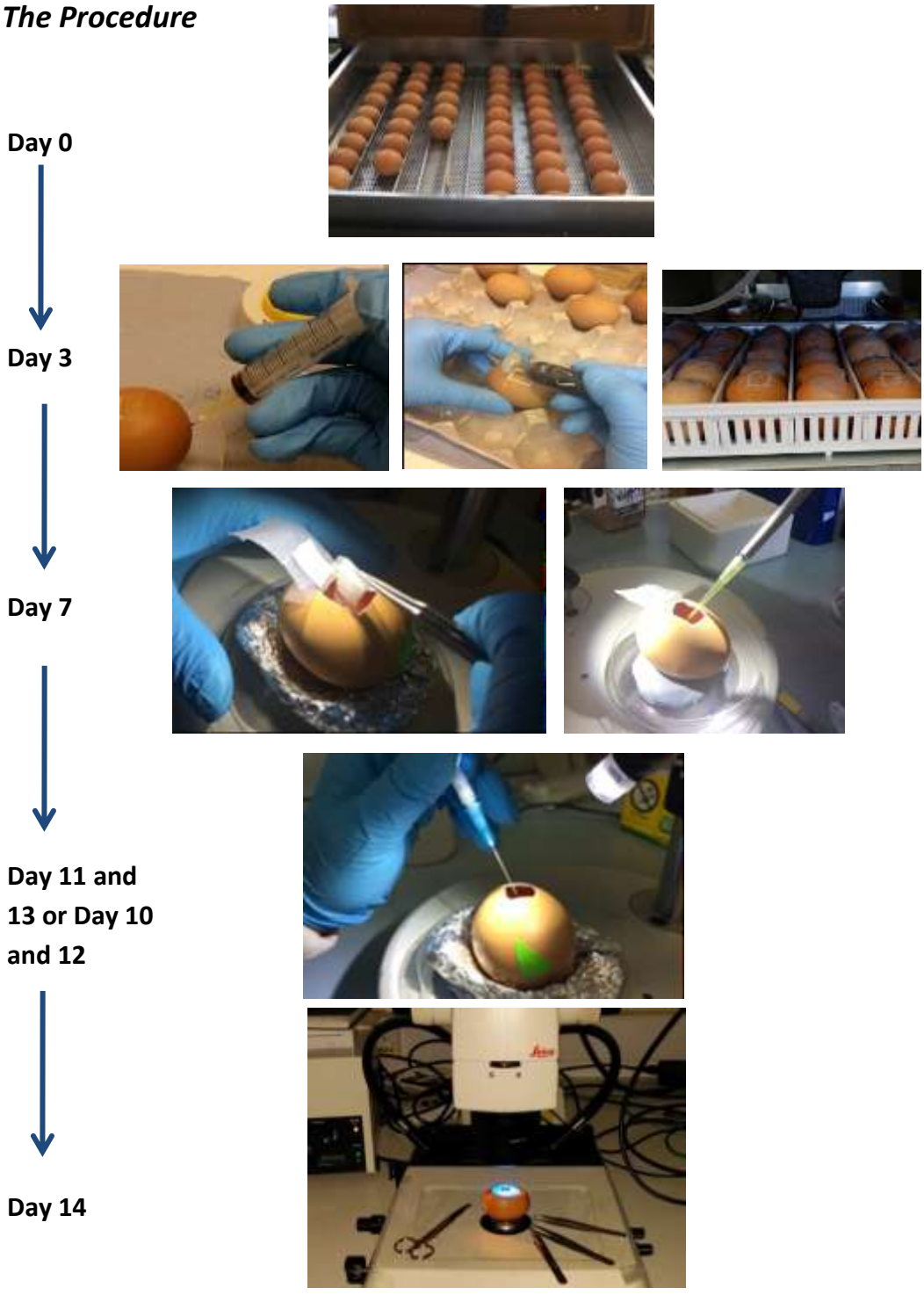

Figure2.4 Visual display of the steps in chick embryo experiment. *E0: fertilised white leghorn eggs were incubated in Multihatch Mark II. E3: albumen removal with subsequent "windowing" of the shell with power tool, and resealing window with adhesive tape. E7: the CAM was lightly traumatised using sterile lens tissue improves tumour formation followed by topical implantation of BE2C cells onto surface of CAM. E10- E13 was injection of drug solution into allantois. E14: Visualisation and dissection of any resultant tumours occurred.*

2.5.1. Egg preparation

Fertilised white leghorn chicken eggs were obtained from Lees Lane Poultry, Wirral, or Tom Barron, Preston, UK. The eggs were placed into and egg incubator (Multihatch Mark II, Brinsea, UK) and maintained at approximately 38°C and 35% relative humidity. In order to ensure easy access to the embryo at later stages in development, eggs were laid horizontally as they would be in normal physiological settings. The day the eggs were placed in the incubator was “day 0” and referred to as “Embryonic day 0”.

2.5.2. Egg Fenestration

On embryonic day 3 (E3), the eggs were removed from the incubator and gently cleaned using 70% ethanol, a small hole was poked in the rounded base of the egg, and 4ml of albumin were removed using a 19G needle (Terumo) and 5ml syringe (Terumo) inserted at 45° angle. The removal of albumin was to prevent the embryo and surrounding vessels from fusing to the inner surface of the shell. The hole was then sealed using a small triangle of adhesive tape to prevent any further seepage from the hole site. A small rectangular window approximately 1cmx1.5cm was cut into the top of egg’s shell using Power Craft PKW-160N Combitool. Next windows were resealed tightly using Scotch Magic adhesive tape and eggs were again incubated under the same conditions until E7.

2.5.3. Cell preparation

Prior to implantation, cells were harvested from 75cm^2 culture flasks using 1ml 0.05% trypsin EDTA, and following 5 minutes incubation at 37°C, diluted into 10ml total volume with the appropriate medium containing, triturated using 1 ml pipette tip to obtain a single-cell suspension. An appropriate number of cells (typically 2x10^6 cells per egg) in culture medium were transferred into a sterile 1.5ml eppendorf tube and centrifuged at 1000 rpm for 5 minutes. After centrifugation the supernatant was discarded and the cell pellet resuspended in 5-10µl fresh media and kept in ice until implantation.

2.5.4. Implantation of cells on to the CAM

At E7, eggs were removed from the incubator and assessed for survival. GFP-labelled BE2C, IMR32, Kelly and SKNAS cells were harvested and counted as described previously. Eggs were removed individually from the incubator and the surface of the chorioallantoic membrane (CAM) was lightly traumatised using a small piece of sterilised lens tissue. 5µl of 0.05% trypsin was applied to the surface of the CAM and $2x10^6$ cells (10-12µl) were implanted.

2.5.5 Drug delivery

2.5.5.1 Retinoic acid delivery optimisation in chick embryos

The initial dose was measured on the presumption that each egg weighed 50g, 10% of this value was deduced to represent the weight of the shell, giving 45g (45ml assuming the density is one) of the actual weight. Doses were given as 30mg/kg equivalent to 100µM, 3mg/kg equivalent to 10µM and 12mg/kg equivalent to 40µM.

Two methods were tested to optimise drug delivery starting with 100µM dose. A 28µl of RA (0.16M) diluted to 56µl with DMSO, 1:1 dilution, and made up to 200µl in DPBS, was initially administered topically onto the surface of the CAM. RA is soluble to 40mg/ml in DMSO, however is extremely insoluble in water (Sigma-Aldrich). The topical administration was abundant because of precipitation issues.

The other method used was diluting the required amount of RA up to 200µl in DPBS and injecting it under the CAM into the allantois. A cloudy solution was resulted when RA mixed with DPBS therefore a serial of needle with different sizes (19, 21and 23G) attached to a 5ml syringe were used to triturate and homogenise the solution before injection. In addition, the embryo movement, inside the egg, also assist RA to dissolve more. Injection was initially on E11, E12 and E13 before reducing the dose to two, at E11 and E13. A 23G needle attached to a 1ml syringe was used. Careful attention was made to avoid injecting into and damaging any large blood vessels to prevent major bleeding.

For the control 28ul of DMSO was diluted up to 200ul and injected. Following RA administration, fresh adhesive tape placed over the window and the eggs were returned to the incubator. This procedure carried out at approximately the same time after each day. The drugs administrated using the latter procedure (injection) in this project.

2.5.5.2. Palbociclib and RO-3306 administration to chick embryos

Palbociclib and RO-3306 were given at 6mg/kg equivalent to 20µM. 90µl of 10mM stock Palbociclib and 65µl of 14mM stock RO-3306were both made up to 200µl of DPBS. Drugs were injected to the allantois of embryos at E11 and E13 or E10 and E12 using 23G needle connected to 1ml syringe. Control groups were injected with either 200µl DPBS (control for Palbociclib) or 65µl DMSO diluted up to 200µl DPBS (control for RO-3306). Following drug administration, eggs were resealed and returned to the incubator until E14.

2.5.6. Harvesting of tumours

On E14, each surviving embryo was observed under the fluorescent light of a Leica M165 FC stereo microscope for the presence of any tumours. The visual field was maximized by breaking away shell surrounding the egg "window". Eggs were examined thoroughly for the presence of tumour formation and fluorescently labelled cells. Tumours present were dissected using 6" straight tips dissection forceps and Castro-Viejo 4"straight tips dissecting scissors. Once the tumour was removed it was placed in HANKS' and the embryo was humanely destroyed or for some dissected to assess for the presence of metastatic cells. Tumours were imaged before and after dissection using the Leica DFC425C camera and imaged using the LAS V4.0 software system. Tumours then weighed and stored in RNAlater (QIAGEN), or fixed in PFA or formalin.

2.5.7. Chick embryo dissection and metastasis detection

Following tumour harvesting, chicks were pulled out the shell using a curved tweezers, and placed in a 60mm petri dish (Appleton Woods). They were decapitated using 4"straight scissors, washed with Hanks' to remove blood and NB cells slicked to the skin/feathers before opening the abdomen.

Organs were removed into 35mm petri dish (Appleton Woods), washed with Hanks and images in bright field and fluorescent were captured using a Leica DFC425 C camera connected to the microscope.

2.6. Immunohistochemistry (IHC)

2.6.1. Tumour block preparation and sectioning

The tumours were embedded in paraffin in the histology lab of the University of Liverpool. Following fixation, tumours were dehydrated in 70% ethanol in dH2O for one hour and then 100% ethanol for another hour. 100% ethanol was replaced twice and left overnight. The 100% ethanol was replaced with two changes of 100% isopropanol, agitated gently for 15 min each time on rocking platform. Tumours were placed in a glass vial, and immersed with 50% paraffin in isopropanol and incubated for 1hr at 65°C, agitating gently every 10-15 min. Following this, the tumours were placed in 100% fresh paraffin from the embedding station (Shandon Histocentre 3, ThermoFisher, UK) and left overnight at 65°C. Next tumours were placed in a preheated stainless steel mould (filled with some molten paraffin) and orient accordingly, mould was put on a small cooling plate to allow the tumour to adhere to the mould. Cassette was placed onto the mould and filled fully with paraffin, then carefully the mould placed on large cooling plate and then left to harden for 30 min and then the mould is removed. The embedded specimens were then sectioned using the Shandon FINESSE 325 Microtome and S35 microtome blade (JDA-0100-00A, Feather). The blocks were initially cooled on ice prior to sectioning, to prevent the cut sections from rolling up. After initially trimming the blocks by cutting thick 20-25µm sections to expose the specimen, thin 4µm sections were cut in a ribbon of approximately four and transferred to a water bath set at 37°C. Once in the water bath, curved forceps were used to separate each section before mounting onto APES coated microscope slides (Leica). The slides were placed in metal racks and “baked” overnight at 37°C to remove any remaining water. The following day, slides were kept in a plastic container at 4°C until time for staining.

2.6.2. Antigen retrieval and deparaffinisation

Prior to performing immunohistochemistry, slides were placed in a slide rack compatible with the Dako PT Link (Dako, UK) in order to deparaffinise, rehydrate and heat induced antigen retrieval. The slide rack was inserted into pre-heated high pH retrieval solution (Tris/EDTA, pH 9.0) for deparaffinisation, high-pH (buffer, pH 9.0) antigen retrieval was performed at 96 °C for 20 minutes. Slide racks were allowed to cool in the PT Link, after which slides were rinsed with FLEX wash buffer (50mM Tris-base, 150mM NaCl, 0.05% Tween 20, pH 7.6) to remove excess paraffin.

2.6.3. Ki67 staining

Slide racks were transferred to the automated Dako autostainer system. IHC was performed using FLEX EnVisionTM reagents (Dako, UK). All steps were carried out at room temperature. Endogenous peroxidase was blocked by incubating slides with Peroxidase-Blocking Reagent (phosphate buffer containing hydrogen peroxide, 15mM NaN3) (DM821) for 5 minutes. Primary antibody, mouse anti Ki67 (Leica Biosystems, KI67-MM1-L-CE), was diluted (1:250) in antibody diluent (K8006) and slides were incubated the primary antibody for 30 minutes, followed by incubation a goat anti-mouse secondary antibody conjugated with horseradish peroxidase HRP (Dako, DM822) for 20 minutes. Negative control was stained by replacing Ki67 with mouse IgG1 Negative control (Dako, X0931) at 1:250. Positive staining was visualised with the chromogen, 3,3'-Diaminobenzidine (DAB), prepared by adding 1 drop of stock solution to 1 ml of substrate buffer (DM823). Slides were washed with FLEX wash buffer (50mM Tris-base, 150mM NaCl, 0.05% Tween 20, pH 7.6) between steps of staining.

2.6.4. Counterstain and mounting

Haematoxylin has a deep blue-purple colour and stains the nucleus of the cells within the tissue. Counterstaining with haematoxylin helps identifying chick cell-type- from neuroblastoma cell-type.

Slides were immersed in haematoxylin solution for 20 seconds, washed with running tap water, cleared in 0.5% acid alcohol and incubated in Scott's tap water blueing agent for 30 seconds. Slides

then underwent dehydration in a series of alcohol and xylene incubations before mounting with DPX mountant (Sigma, UK) on 22 x 50mm cover slips (630-2210, Menzel Gläser, UK). Tissue known to express the protein of interest (ki67) was included as a positive and negative control.

2.6.5. Cell proliferation quantification of sections

Slides were observed under bright field microscopy and manual counting of histological sections was used to determine Ki67 proliferative index. For each section ≥4 fields were assessed and ~ 200 cells were counted per field. Ki67 positive nuclei are stained in brown. Negative nuclei are counterstained in blue by haematoxylin. The percentage of the brown-stained nuclei of the total number of cells determined the Ki67 index. Haematoxylin staining allowed identification of both chick tissue and tumour nuclei. Chick tissue cells could be identified as they had a small nucleus whereas tumour tissue cells had a relatively larger nucleus with less cytoplasm**.**

2.7. Tumour mounting for morphology studies

For some experiments the CAM was seeded with 90% wild type BE2C cells and 10% GFP BE2C cells and the resultant tumour used to analyse the morphology of the GFP cells in response to RA.Tumour specimens <2mm were mounted on a glass slide using DAKO fluorescence mounting medium. A circular cover slip was laid over the top with slight pressure to both remove trapped air and flatten the specimen.The morphology of cells within the tumours was observed using confocal microscopy with the Leica DMIRE2 microscope and X40 objective, together with the Leica Confocal Software program.

2.8. Apoptosis assay by TUNEL (Terminal Deoxynucleotidyl Transferase Mediated Nick End Labelling)

Paraffin sections were prepared as described previously (*section 2.6.1*). TUNEL is used to assay apoptotic (programmed) cell death by measuring nuclear DNA fragmentation. Biotinylated nucleotide is incorporated at the 3'end of the fragmented DNA using a Terminal Deoxynucleotidyl

Transferase, (TdT) enzyme. Streptavidin HRP (HRP Horseradish peroxidase-labelled) is bound to the biotinylated nucleotides and detected using hydrogen peroxide and diaminobebzidine (DAB). Hence nuclei of apoptotic cells stained dark brown. The Dead End™ Colorimetric TUNEL System (Promega) was used. Paraffin sections underwent deparaffination with Histo-clear II. Slides were washed with 100% ethanol followed by rehydration in a decreasing ethanol series (95%, 70%, and 50%) and washed in 0.85% NaCl at room temperature (RT). After washing with phosphate-buffered saline (PBS) the tissue was fixed in 4% (PFA) and washed with PBS. The tissues were permeabilised with Proteinase K solution (20µg/ml) for 10 minutes at RT and washed again in PBS before re-fixing in 4% PFA. The sections were washed in PBS and equilibrated with 1 x TdT buffer at RT. The slides were incubated at 37°C for 1hr in a humidified chamber with TdT reaction mix containing 98µl equilibration buffer, 1µl biotinylated nucleotide mix and 1µl TdT enzyme (1U/µl), per slide. For negative control a slide was prepared without TdT and for positive control a slide was treated with 1 µl DNase 1 (1U/µl, Promega). The slides were washed in PBS and treated with 0.3% hydrogen peroxide to block endogenous peroxidases and washed in PBS. Slides were treated with streptavidin HRP for 30 minutes at RT and washed in PBS before the colour reaction. DAB was added to the slides and allowed to develop (6 minutes), before washing with deionised water. Covers slips were mounted using DPX Mountant (44581, Sigma-Aldrich).

2.8.1. Cell apoptosis quantification

Slides were observed and imaged under bright field Leica microscopy, ~ 600 cells counted in ≥4 fields per section. TUNEL positive nuclei are stained in brown. The percentage of the brown-stained nuclei of the total number of cells determined the TUNEL index.

2.9. Quantitative PCR (qPCR) in tumours

2.9.1. RNA extraction

Tumours dissected from the chick CAM were placed in RNAlater (QIAGEN) and stored at 4°C for up to 2 weeks prior to RNA extraction. The tissue was first removed from the RNAlater and transferred to a clean RNase free falcon tube. Liquid nitrogen was used to freeze the tissue before a pestle and mortar was used to disrupt it. RNA was then extracted as per the culture protocol (***section 2.4.1***).

2.8.2 cDNA synthesis

cDNA synthesis was completed using the same protocol mentioned previously (***section 2.4.2***).

2.8.3. Reference gene selection

Same reference genes described in ***section 2.4.3*** were used.

2.9.4. Target gene selection

The effects of hypoxia on several prometastatic genes on neuroblastoma cell lines *in vitro* and *in vivo* has been described (Herrmann *et al.*, 2015). We selected eight genes having the largest fold increase/decrease from this paper; glucose transporter 1 (GLUT1), vascular endothelial growth factor (VEGF), matrix metallopeptidase 9 (MMP9), A disintegrin and metalloproteinase with thrombospondin motifs 1 (ADAMST1), vascular cell adhesion molecule 1 (VCAM), integrin alpha V (ITGαV), integrin beta 5 (ITGβ5), versican (VCAN).

2.9.5. Primers

Primer sequences were identified in published papers using the same target or reference genes in qPCR experiments ((Vandesompele *et al.*, 2002; Herrmann *et al.*, 2015). Reference primer sequences were ordered from Sigma-Aldrich, whereas target genes were kindly given by Anne Herrmann, University of Liverpool. Once, primers received, they were reconstituted in nuclease-free water (ThermoFisher Scientific, UK) and stored at -20 C in small 10mM aliquots to avoid freeze-thawing process. ***Table2.7*** below details all primer pairs used.

Table2.7 List of the primers used in qPCR of tumours experiments

Gene	Forward 5'-3'	Reverse 5'-3'
GAPDH	AATCCCATCACCATCTTCCA	TGGACTCCACGACGTACTCA
HPRT1	TGACACTGGCAAAACAATGCA	GGTCCTTTTCACCAGCAAGCT
UBC	ATTTGGGTCGCGGTTCTTG	TGCCTTGACATTCTCGATGGT
ADAMST1	CCCTCACTCTGCGGAACTTT	GGACCCACACAAGTCCTGTC
GLUT1	GAACTCTTCAGCCAGGGTCC	ACCACACAGTTGCTCCACAT
ITGαV	CGCTTCTTCTCTCGGGACTC	AGAAACATCCGGGAAGACGC
ITGβ5	GGGAGCCAGAGTGTGGAAAC	GGATCGCTCGCTCTGAAACT
MMP9	TTCTGCCCGGACCAAGGATA	ATGCCATTCACGTCGTCCTT
VCAM	TGTTTGCAGCTTCTCAAGCTTTTA	GTCACCTTCCCATTCAGTGGA
VCAN	ACCAGACAGGCTTCCCTCCCC	GGGTGATGCAGTTTCTGCGAGGA

2.9.6. qPCR Protocol design

Protocols were designed as described previously in ***section 2.4.6***.

2.9.7. Analysis of qPCR data

Data was viewed using Bio-Rad CFX Manager 3.1 software. An initial inspection of both the amplification plot and melt curve ensured that there were no obvious anomalous results. Fold change in target gene expression was calculated relative to the control. Results were normalised to the three reference genes (GAPDH, HPRT1 and UBC). Fold change calculated by comparing the C_t value of each tumour condition and then taking the mean from 3 independent biological replicates. $2^{-\Delta\Delta Ct}$ method was used to calculating relative gene expression using the normalised qPCR data (Schmittgen and Livak, 2008). To conduct statistical analysis NRQ data of 3 independent biological replicates were compared to control to standardise the fold change.

2.10. Statistical analysis of data

The data from each experiment were first averaged and presented as means with standard error bar (±SEM). The statistical analysis was performed using either a student T test or a one-way ANOVA to determine statistical significance between groups. This was followed by a post-hoc Tukey test multiple-comparison test to determine significance between data sets. A p value of <0.05 was considered significant. All statistical data was analysed using GraphPad Prism version 6.00 for Windows.

Chapter Three: Results I
Optimisation of the chick embryo model system for neuroblastoma treatment

3.1. Introduction

Neuroblastoma is a neural crest-derived malignancy which has an unusually high rate of spontaneous regression. Differentiation status is a key prognostic factor in neuroblastoma with the least differentiated phenotypes displaying the worst prognosis for patients (Craig *et al.*, 2016). Interestingly, Park et al reported in his review that neuroblastoma is an aberration of normal development and 4-S stage tumours may spontaneously regress to leave more differentiated benign ganglioneuromas (Park *et al.*, 2013). This therefore indicates that drugs that stimulate differentiation may also offer a potential therapy for in neuroblastoma (Thiele, Reynolds and Israel, 1985).

Retinoic acid (RA) is a differentiation agent known to induce a more neuronal phenotype of some neuroblastoma cell lines, especially MYCN amplified cells. RA is been used in clinic, as a standard treatment for patients with high risk neuroblastoma (Reynolds *et al.*, 2003). Therefore, differentiation therapy including RA was a prime target on which to verify the effectiveness of the chick embryo model.

Commonly, mouse model is used for the *in vivo* assessment of potential new therapeutic targets in many cancers (Cekanova and Rathore, 2014). However, mouse models are expensive and time consuming. Other models, such as the chick embryo chorioallantoic membrane (CAM), are therefore an attractive alternative model of cancer studies. The chick embryo model has many advantages includes 1) the nature of the CAM highly vascularized which promotes the efficiency of tumour cell grafting, 2) immuno-deficient nature which means that the chick can eccept the cancer cells regardless their origin, 3) high reproducibility, simplicity and cost effectiveness (Ribatti, 2008; Lokman *et al.*, 2012).

The CAM model has been used extensively to study angiogenesis and tumour xenografting (Richardson and Singh, 2003; Balciūniene *et al.*, 2009; 2014; Durupt *et al.*, 2012; Lokman *et al.*, 2012; Yuan *et al.*, 2014; Kavaliauskaite *et al.*, 2017). However, to date, there have been few studies that

have used CAM assays to assess the effect of therapeutic agents on cancer behaviour (Richardson and Singh, 2003; Rytelewski *et al.*, 2014; Sathe *et al.*, 2016).

Interestingly, MYCN amplified neuroblastoma is closely correlated with unfavourable prognostic features and therefore patients with MYCN amplification denotes high risk neuroblastoma (Rubie *et al.*, 1997; Chan *et al.*, 2007). Thus these are the cells that are known to be more aggressive and therefore would be expected to form tumours more readily on the CAM (Mather, 2014). Moreover in representing high risk disease, new therapies are required to treat these cells.

3.1.1. Aims of the chapter

The work described in this chapter aimed to establish the value of the CAM model by demonstrating the effect of the known differentiation agent RA on MYCN amplified neuroblastoma cells. This was divided into the following sub-aims.

- Set up assay systems *in vitro* to analyse the response of neuroblastoma cells to RA.
- Develop neuroblastoma tumours *in vivo*.
- Determine an appropriate method of drug delivery to tumours.
- Analyse the effect of RA on tumour assays set up *in vivo*.

3.2. Results

3.2.1. Retinoic acid reduces cell proliferation and induces changes in morphology in BE2C and IMR32 cells

To investigate the effect of Retinoic acid on MYCN amplified cell lines, in culture, in terms of proliferation and cell morphology, cells were treated with RA for a period of 72hr and observed under the Leica DMIRB microscope before carrying out Ki67 staining.

Morphology assessment

Following 3 days with RA, both BE2C and IMR32 cells showed a change in morphology compared to DMSO treated cells. RA- treated cells showed more elongated shape with neurites outgrowth (refers to any projection from the cell body which length equals or exceeds the cell body diameter) as can be seen in ***Figure3.1***.

Proliferation assessment

Assessment of cell proliferation (Ki67) was crucial in determining the behaviour of the neuroblastoma in culture first before assessing their behaviour *in vivo,* in response to RA treatment.

Ki67 is expressed during the G1, S, G2 and M phases of the cell cycle, whereas, in G0 stage of the cell cycle it found to be absent (Gerdes *et al.*, 1984) . Many subsequent studies have reported that Ki67 expression level is crucial for normal proliferation across various cell lines (Kausch *et al.*, 2003; Zheng *et al.*, 2006, 2009; Rahmanzadeh *et al.*, 2007) .

Cell proliferation appeared to be reduced in the RA treated cells relative to control based on visual inspection of the culture. We therefore performed Ki67 staining on these cells to quantify this effect. Cells were stained with a rabbit anti-Ki67 antibody and labelled with goat anti-rabbit (secondary antibody) conjugated with Alexa Fluor 594 (red) to enable identification of proliferating cells whilst counterstaining with DAPI allowed identification of the total number of nucleus cells present. Cell counts were performed comparing the number of Ki67 positive cells to the number of DAPI stained cells in the treated as well as in control cells (***Figure3.2 A&B***). Overall a 68% reduction was observed in the level of Ki67 staining in the IMR32 cell line and a 70% decrease in BE2C cell line (***Figure3.2 C***).

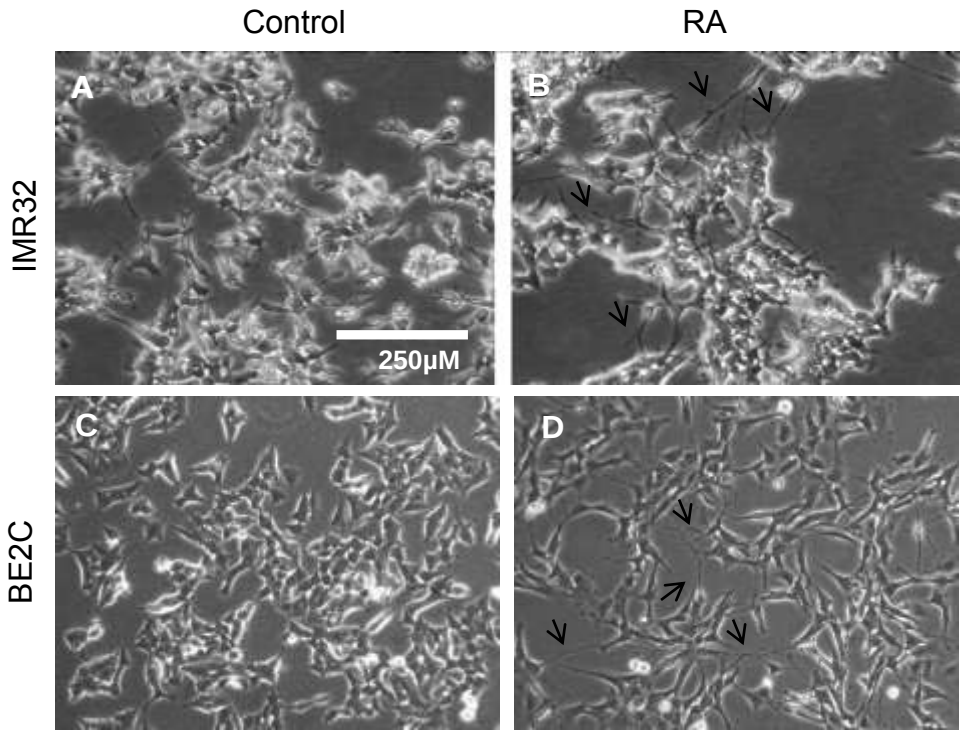

Figure3.14 Changes in cell morphology after72 hrs of RA treatment. ***A*** *and* ***B*** *are IMR32 cells,* ***C*** *and* ***D*** *are BE2C cells.* ***A*** *and* ***C*** *are images taken of the control cells and* ***B*** *and* ***D*** *are the treatment. Black arrows indicate morphological changes as neurite outgrowth.*

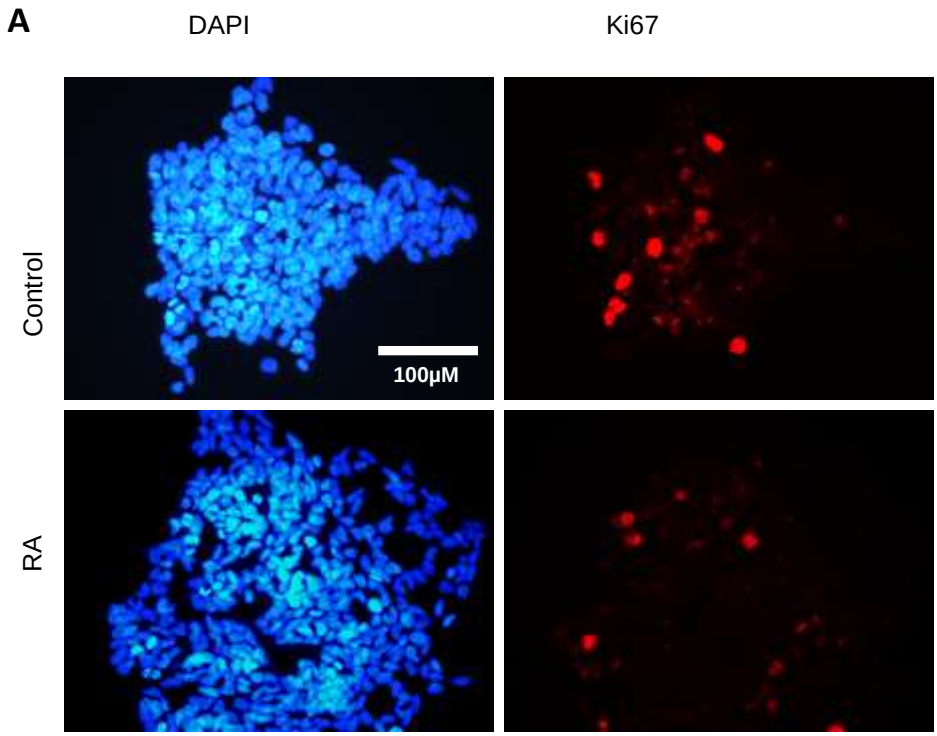

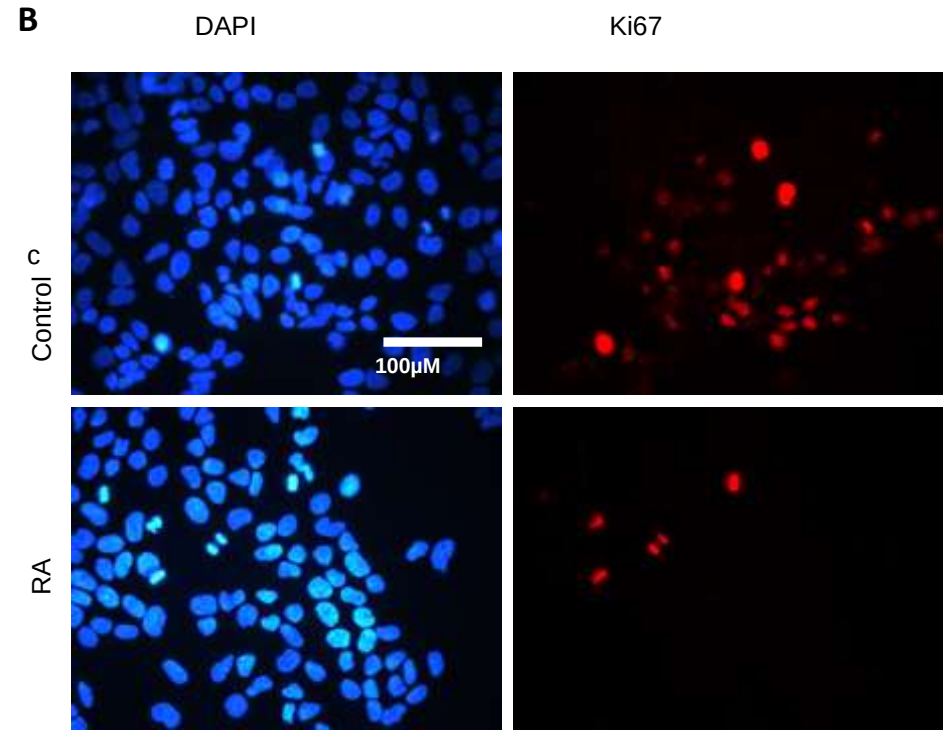

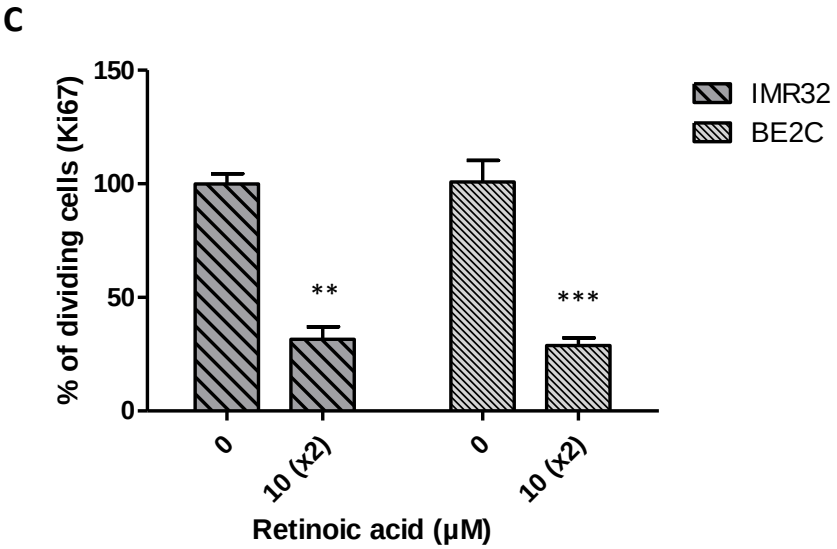

Figure3.2 Effect of RA treatment on IMR32 and BE2C cell proliferation. ***A*** *DAPI stained (blue) and Ki67 stained (red) IMR32 cells following three days of treatment with 10µM RA (*RA was replenished following 48hr of treatment hence 10 (X2)) *or DMSO.* ***B*** *DAPI stained (blue) and Ki67 stained (red) BE2C cells following three days of treatment with 10µM RA or DMSO.* ***C*** *Graph to show the reduction in cell proliferation following treatment with RA. Ki67 displayed by setting the control to 100%, Ki67 index= number of Ki67 positive expressed as a percentage of the total number of cells. Data presented relative to control. Data represents mean ± SEM (n=9). Each bar represents the mean ± SEM of three biological replicates and at least 9 fields per experiment. ** P< 0.01 and ***P<0.001.*

3.2.2. Retinoic acid change the gene expression of differentiation markers in IMR32 and BE2C cells

To further investigate the effect of RA on gene expression, quantitative assessment of cellular differentiation was undertaken using qPCR. Genes which demonstrate large fold changes upon neuroblastoma cell differentiation were selected: KLF4, STMN4 and ROBO2 (Sung *et al.*, 2013) and MYCN (Huang and Weiss, 2013). KLF4 is a stem cell marker involved in the regulation of differentiation and its expression would be expected to decrease in differentiated cells (Zhang *et al.*, 2010). STMN4 and ROBO2 are involved in neuronal differentiation. ROBO2 is also involved in regulation of the actin cytoskeleton and axon development and guidance. Expression of both would be expected to increase in differentiated cells (Beilharz *et al.*, 1998; Andrews *et al.*, 2008). MYCN is an oncogene, and is known to be involved in the regulation of the neural crest development and initiation of neuroblastoma (Olsen *et al.*, 2017).

In keeping with previous results, there was a significant change in the expression of the differentiation markers KLF4 and STMN4 but not ROBO2 and MYCN in RA treated cells compared with DMSO treated cells. In IMR32 cells, KLF4 decreased by 5.5 fold and STMN4 increased more than 6 fold, ROBO2 also showed an increase which was not significant and MYCN showed a slight decrease (***Figure3.3 A, B***). Similar to IMR32 cells, BE2C cells results showed a decrease by more than 4 fold in KLF4 and an increase of 14.5 fold in STMN4 and they both were significant. ROBO2 showed an expected trend but did not reach significance whereas a small decrease in MYCN (***Figure3.3 C, D***).

A

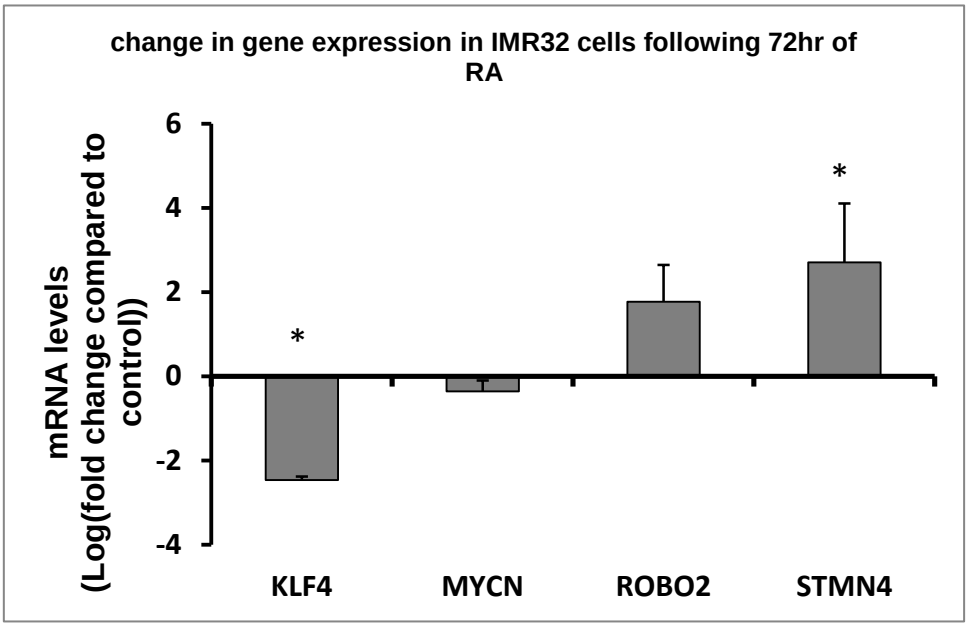

B

	KLF4	MYCN	ROBO2	STMN4
Fold change	-5.53	-1.28	3.41	6.52
Log fold change	-2.47	-0.36	1.77	2.70
Regulation	down regulated	no change	no change	up regulated

C

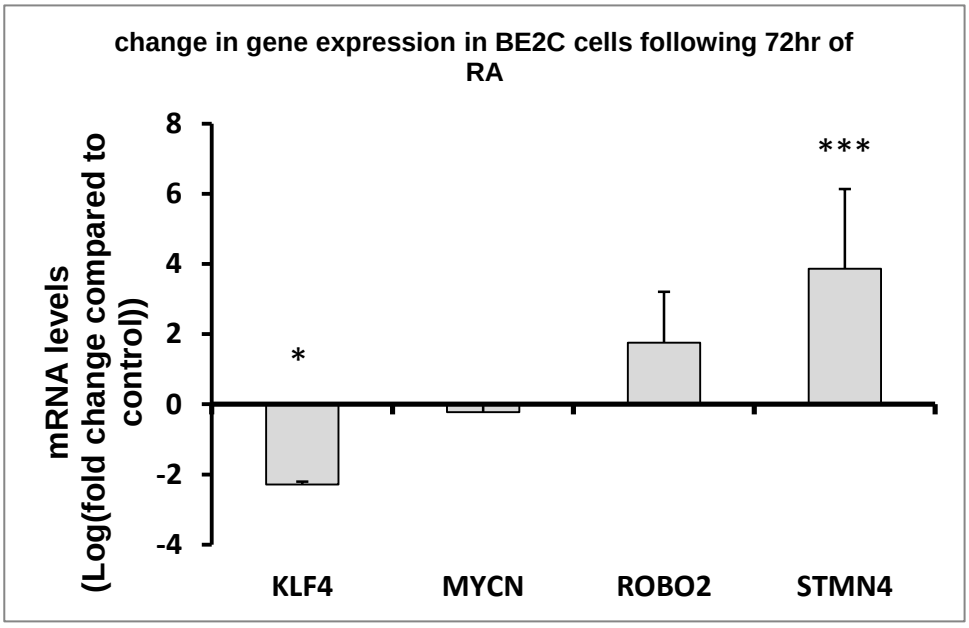

D

	KLF4	MYCN	ROBO2	STMN4
Fold change	-4.89	-1.17	3.37	14.6
Log fold change	-2.29	-0.23	1.75	3.87
Regulation	down regulated	no change	no change	up regulated

Figure3.3 Graphs showing the level of target gene expression in IMR32 (A) and BE2C (C) cells following 72hr of RA treatment. *Graphs display the results of three biological repeats. Results are displayed relative to control. Error bars were calculated using standard error (SE). Tables give a summary of the QPCR data for the 4 target genes for IMR32 (**B**) and BE2C (**D**).*

3.2.3. Assessing the effect of RA on MYCN amplified cell lines *in vivo* using the chick embryo model

3.2.3.1. Efficiency of tumour formation on the CAM among MYCN amplified cell lines

In culture RA has behaved as expected and we have established differentiation markers that are sensitive to RA treatment. Next we aim to confirm that neuroblastoma cells respond to RA *in vivo* in our model and that these assays can successfully detect the response. Preliminary experiments started with the two MYCN amplified cell lines; IMR32 and BE2C cells; to test the potential of these cells to form tumours on the CAM successfully. The outcomes revealed, in the majority of experiments, that MYCN amplified cells were seen as a flat sheet on the surface of the CAM (***Figure3.4 a & b)*** indicating that those cells failed to invade the CAM and form a tumour therefore they remained on the surface. This was surprising as MYCN amplified cell lines are known to be very invasive and extravasate following intravenous injection (Carter *et al.*, 2012). In some instances, cell lines had formed tumours beneath the CAM (***Figure3.4 c-f***).

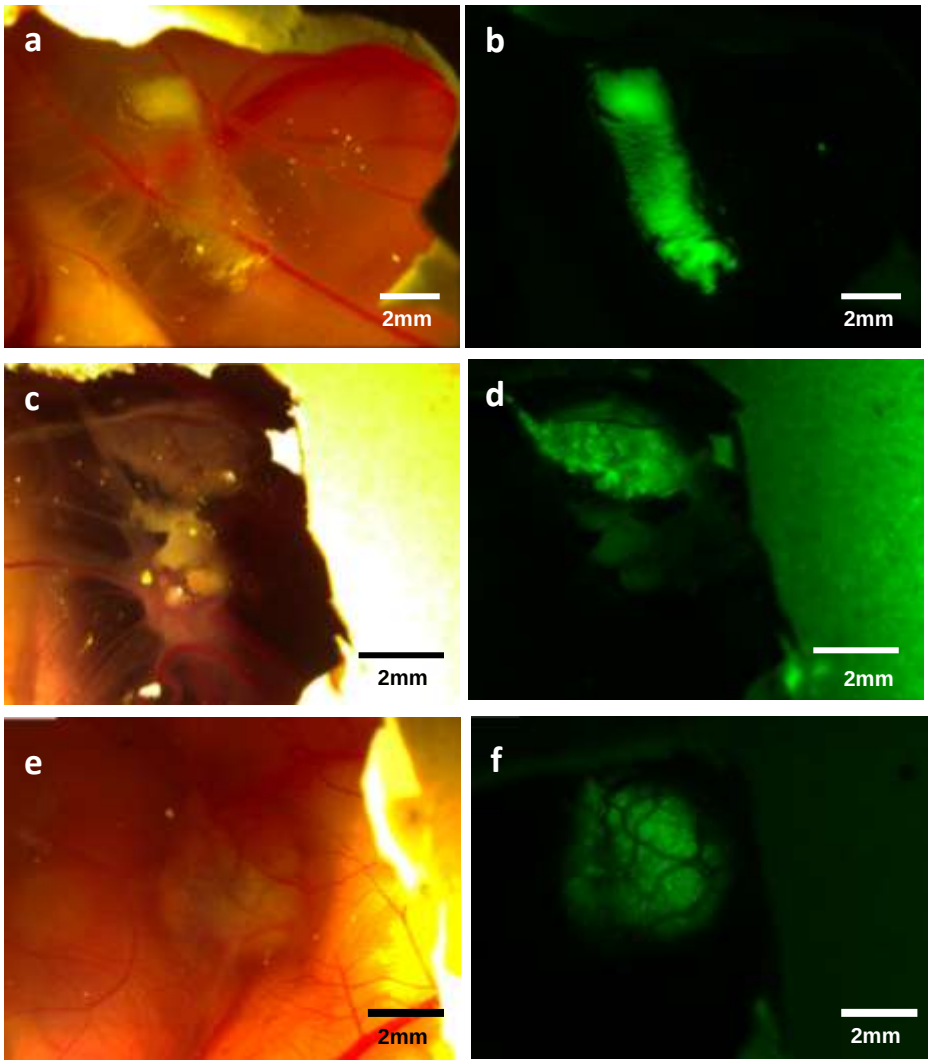

Figure3.4 MYCN amplified neuroblastoma tumours formed on the CAM of chick embryo model. *Left side is bright field images, right side is GFP images.* ***a*** *and* ***b*** *are GFP-labelled neuroblastoma cells dried on the surface of the CAM indicating that those cells failed to invade the CAM and form a tumour.* ***c-f*** *tumours formed successfully beneath the CAM of the chicks.*

The efficiency of tumour formation was 27% of surviving embryos had formed a BE2C tumour and only 7% in IMR32. The efficiency of tumour formation quantified for each cell line during dissection (E14), was achieved by dividing the number of the number of eggs with tumours by the number of eggs surviving until this time to give the tumour success rate for each cell line (***Figure3.5 A***). Due to the poor efficiency shown by IMR32 and BE2C cells, another MYCN amplified cell line, Kelly cells, was included to investigate whether this cell line could form tumours on the CAM more efficiently than the other two cell lines. Unfortunately, this cells line seemed to have similar efficiency to the IMR32 cells in forming tumours (***Figure 3.5 A***).

A work done by others, in our laboratory illustrated that SKNAS cells (non-MYCN amplified cells) form tumours much more efficient on the CAM than BE2C, IMR32 and Kelly cells (MYCN amplified cells), therefore they sought to enhance the ability MYCN amplified cells to form tumours on the CAM by mixing them with SKNAS. Their results were showing a significant increase in the yield of tumour formation within this environment suggesting that the problem lay with the invasion ability of MYCN amplified cells (Mather, 2014).This prompted us to treat the CAM surface with trypsin prior to adding the cells. Trypsin is a protease whose cleaves peptides on the C-terminal side of lysine and arginine amino acid residues and therefore we asserted that it may aid the penetration of xenografted tumour cells through the superficial epithelial cell surface of the CAM (Olsen, Ong and Mann, 2004). Trypsin addition indeed improved the efficiency of the tumour formation for MYCN amplified cells to more than 70% for BE2C cell, IMR32 is 33% and Kelly 37% (***Figure3.5 B***). Tumours grown on the CAM became visible under the fluorescent stereomicroscope three to four days following implantation (***Figure3.6 a-f***). Large tumours (~5mm) were occasionally identifiable without fluorescence by E14, It was noticed that where dried blood was evident on the surface of the CAM tumours were present; however the vast majority of tumours were only identifiable under the fluorescent microscope (***Figure3.6 g-h***). In most instances, one tumour formed however in rare cases multiple smaller masses could be seen (***Figure3.7 a-b***). Tumours were highly vascular with blood vessels clearly recognisable on their surface (***Figure3.7 c-j***). Among cell lines, tumours showed

or revealed different morphological features, IMR32 tumours had an elongated appearance (***Figure3.6 a-b***), BE2C tumours were more rounded (***Figure3.6 c-d***), and Kelly were irregular shape (***Figure3.6 e-f***).

To be consistent with the *in vitro* experiments and as the Kelly cells did not add to the efficiency of tumour formation rate, it was decided that IMR32 and BE2C cell lines would be used in experiments designed for testing the effects of RA *in vivo*.

A

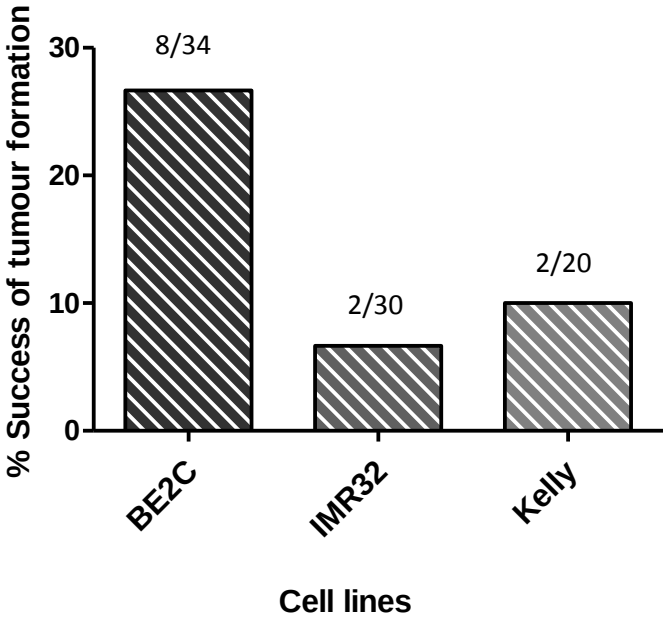

B

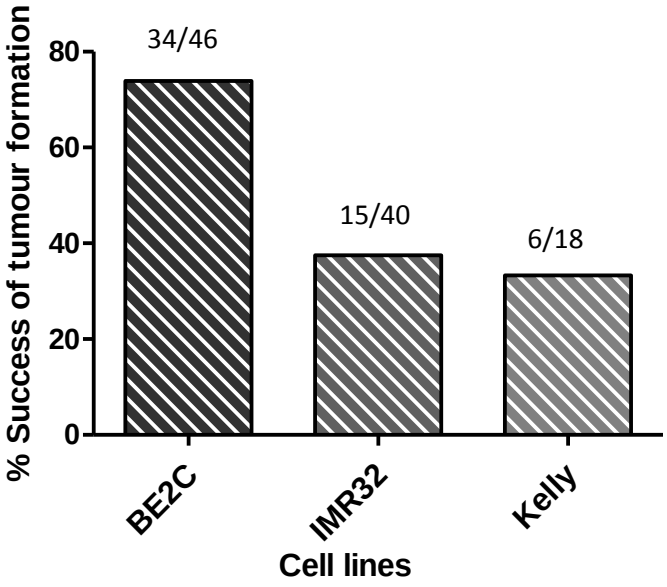

Figure3.5 Graph of the tumour success rate of IMR32, BE2C and Kelly without and with trypsin treatment. A *is the tumour success rate without trypsin treatment, the success percentage was between 7-27% indicating a low yield of tumour formation, BE2C tumour production compared to IMR32 and Kelly is evident.* ***B*** *is the tumour success rate with trypsin treatment, the success percentage increased dramatically over the three cell lines, BE2C tumour production compared to IMR32 and Kelly still evident though.*

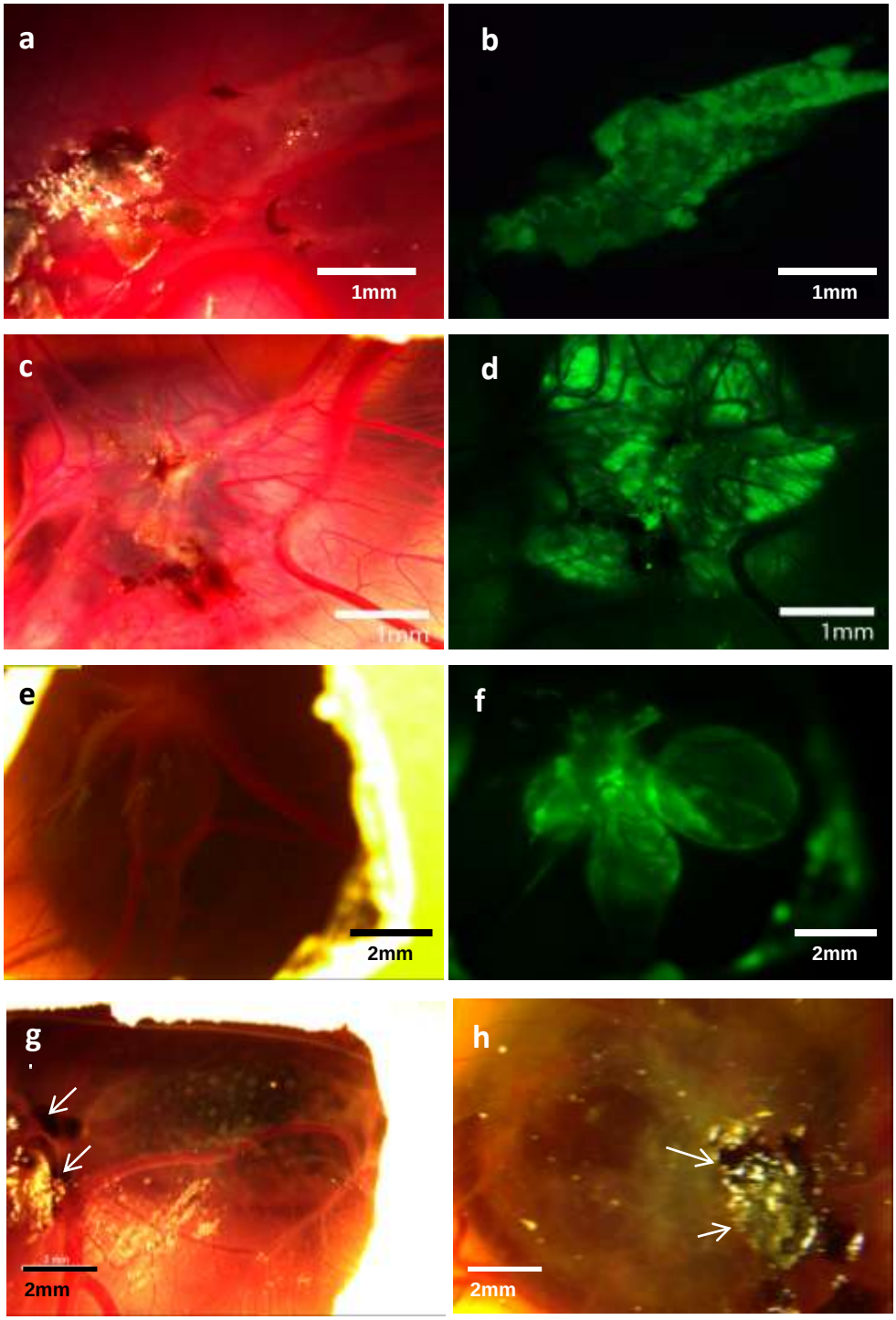

Figure 3.6 Images of tumours formed on the CAM of chick embryo. ***a-f*** *in vivo GFP and corresponding bright field images of 100% GFP labelled tumour cells-* ***a and b*** *are IMR32,* ***c and d*** *are BE2C, and* ***e and f*** *are Kelly tumours.* ***g and h*** *are Large tumours (~5mm) were identifiable without fluorescence by E14 where dried blood on the surface of the CAM tumours were present. White arrows indicate the evidence of tumour formation.*

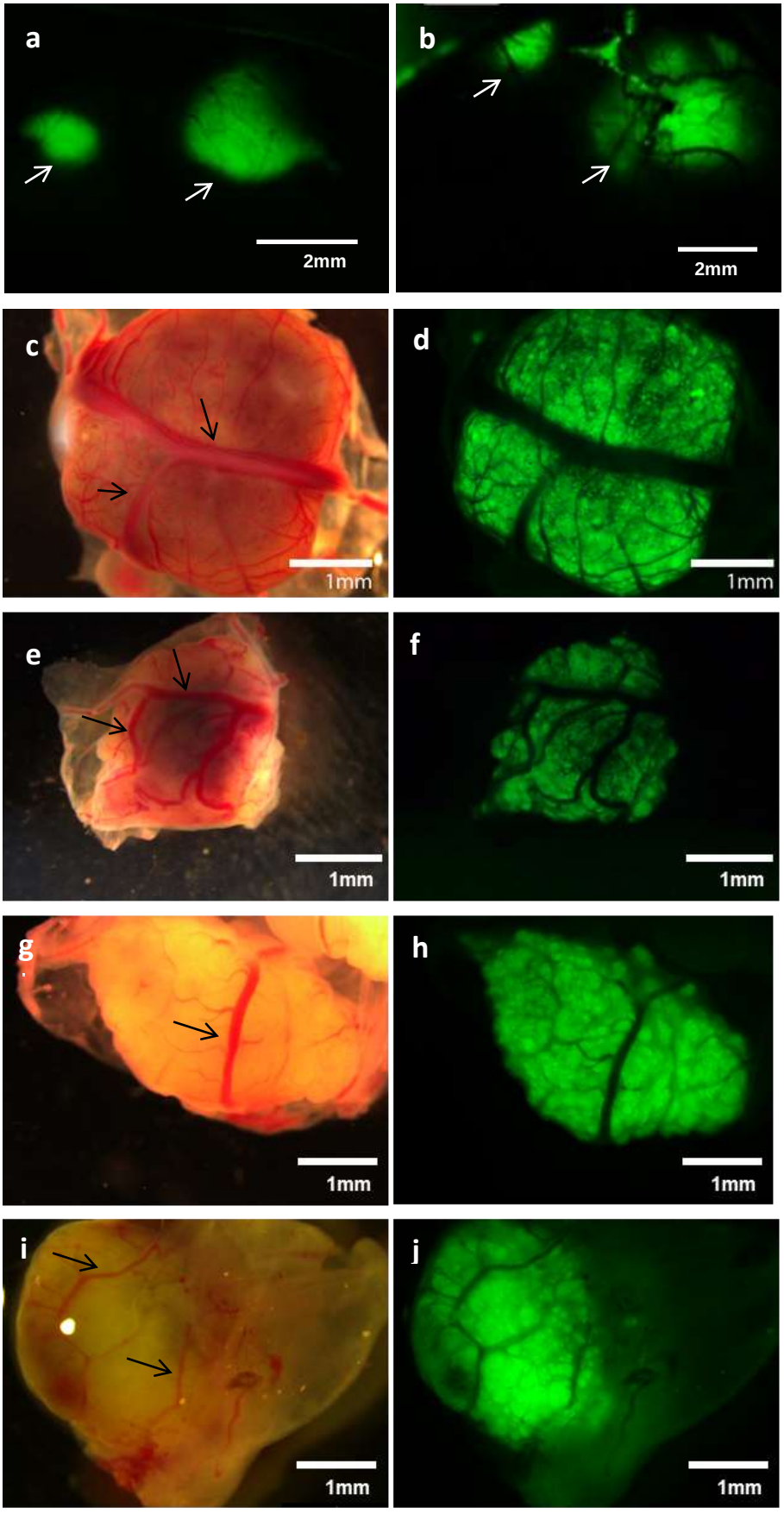

Figure3.7 In vivo and harvested CAM tumours in GFP and its corresponding bright field. ***a-b*** *more than one tumour grown in the CAM can be seen , white arrows indicate the tumours.* ***c-j*** *a group of harvested tumours . Tumours were highly vascular with blood vessels clearly recognisable on their surface. Black arrows indicate the blood vessels.*

3.2.3.2. Histology characterisation of CAM tumours

To characterise the histology of the CAM tumours, tumours were harvested out of the egg and fixed in 4%PFA. After harvesting, the tumours were processed into paraffin sections and haematoxylin and eosin (H&E) staining was performed to observe the histological appearance of the tumour. Dissected tumours were seen as separate masses which had a smooth outer surface (***Figure3.8 a & b***). They were typically covered by and penetrated by evident network of blood vessels (***Figure3.8 a & b***).

Paraffin sections demonstrated that the tumours were made up of densely packed tumour cells form of solid mass (***Figure3.8 c, d & e***). This indeed reflects the histology of patient tumours suggesting that the CAM tumours are a good model for preclinical studies (Dr Rajeev Shukla, Alder Hey Children's Hospital, personal communication).

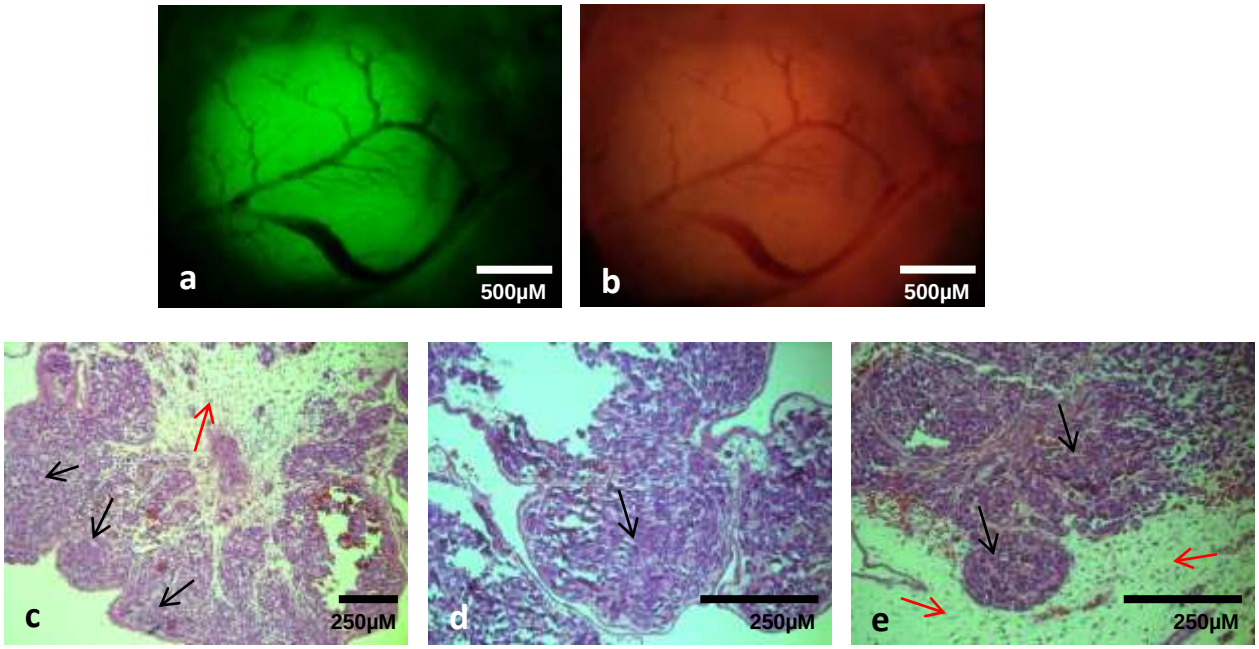

Figure3.8 Harvested CAM tumours and their sections stained with haematoxylin and eosin (H&E). a *and* ***b*** *GFP CAM tumours with its relative bright field showing that tumours have a smooth outer surface that penetrated by evident network of blood vessels.* ***c*** *,* ***d*** *and* ***e*** *are tumour sections stained with H&E. Black arrows indicate tumour tissue. Red arrows indicate chick tissue.*

3.2.3.3. Proliferation reduction and morphological alterations in CAM tumours caused by RA

RA had demonstrated a reduction in cell proliferation and induced changes in morphology in both IMR32 and BE2C cells; here we sought to investigate the effect of RA *in vivo* on tumours generated using same cell lines.

Tumours could be reliably observed by E11 therefore RA treatment was initiated at E11 and repeated at E13. RA treatment was started by replicating the dose used for cell culture experiments (10µM). Dose calculations used the weight of an average egg less the weight of its shell. Although the survival of embryos at 10µM was good, the effect of RA on proliferation was not significant. In order to observe therapeutic effects of RA in tumours, we decided to apply the dose that used to treat xenograft mouse models which was 30mg/Kg (100µM)(Shalinsky *et al.*, 1995). 100µM dose showed a significant reduction in CAM tumours proliferation. Survival of the embryos was unaffected by the introduction of three injections of 28µl (Ξ100µM) of RA or DMSO compared to no treatment (***Figure3.9***). Later, we sought to reduce the dose and the number of drug application; therefore we used 40µM with two injections. The effect of RA on cell proliferation of BE2C cells within the tumour was assayed. A notable reduction on proliferation of cells within tumours that were treated with RA could be seen in ***Figure3.11*** compared to ***Figure3.10***. The percentage of dividing cells was reduced significantly by 43% following three injections of 100µM RA whereas 10µM RA reduced proliferation by 22% while two doses of 40µM reduced proliferation significantly by 37% (***Figure3.12***). Interestingly, our results showed that decreasing the dose to 40µM (x2) reduced the proliferation almost effectively as the 100µM(x3) did and the percentage increase of Ki67 positive cells in the 40µMRA treatment group was only 6.67% higher than the percentage of stained cells in the 100µM treatment group(***Figure3.12***). Thus four fold the dose used in culture was sufficient to reduce the proliferation statistically. This result prompted us to investigate whether 40µM RA had an effect on differentiation state within the tumour.

Here, CAM tumours generated from 90% wild type BE2C cells mixed with 10% of GFP-labelled BE2C cells were examined (***Figure3.13***). RA treated cells exhibited a more elongated body shape of cells with small extensions resembling neurites, suggesting a more differentiated state compared to cells treated with DMSO (***Figure3.14***).

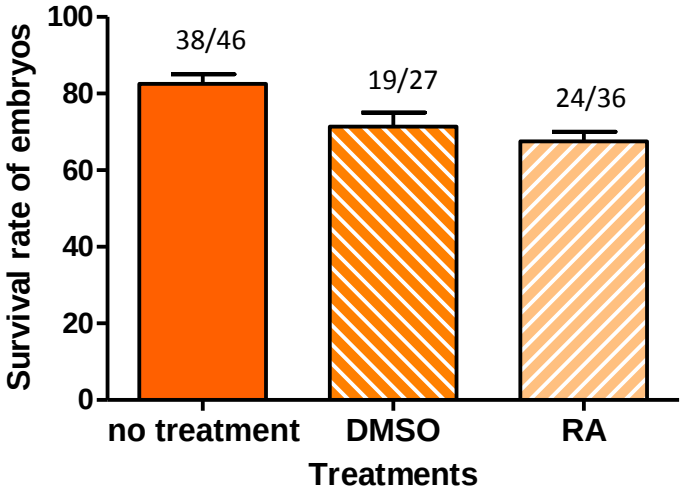

Figure3.9 Embryo survival rate following RA and DMSO treatments compared to those were non-treated*. Neither DMSO (28 µl injections X3) nor RA (100 µM injections X3) affected the survival of the chick embryos (n > 50 for all conditions). Each bar represents the mean ±SEM of three biological replicates.*

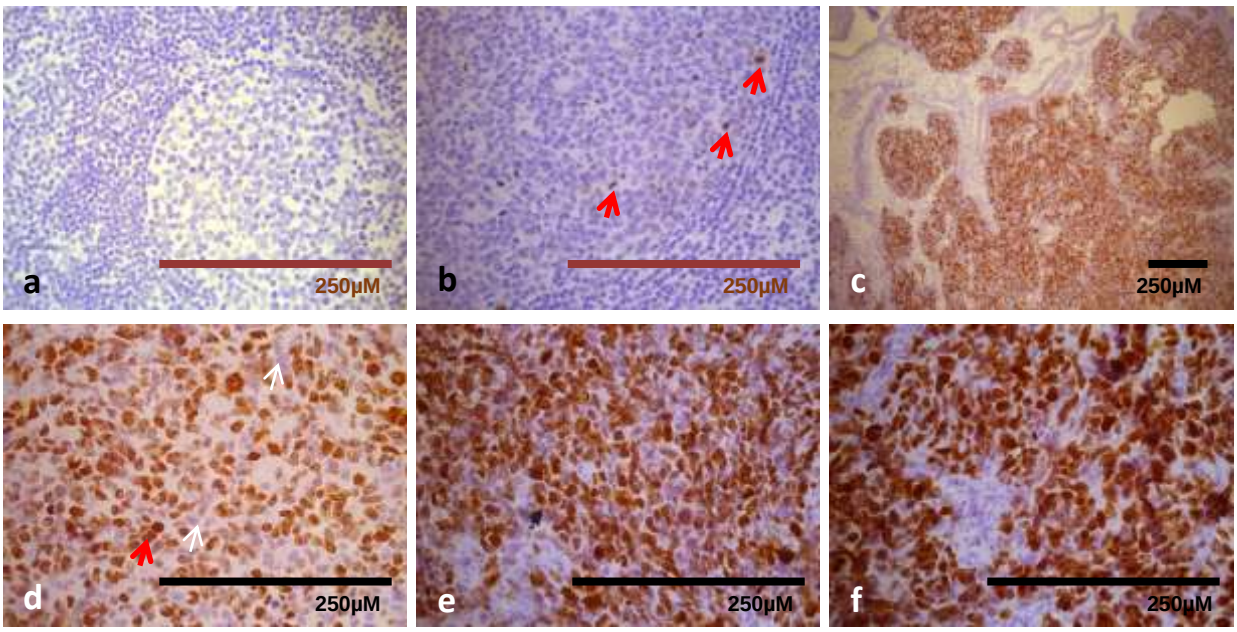

Figure3.10 Ki67 treated sections. a *and* ***b*** *tonsil tissue used as a Ki67 negative (without Ki67) and positive (with Ki67) control respectively. Cells undergoing mitosis could be seen (red arrow).* ***c-f*** *tumour sections treated with DMSO injected into the allantois. Red arrow indicates Ki67 stained nucleus, white arrow indicates unstained cell.*

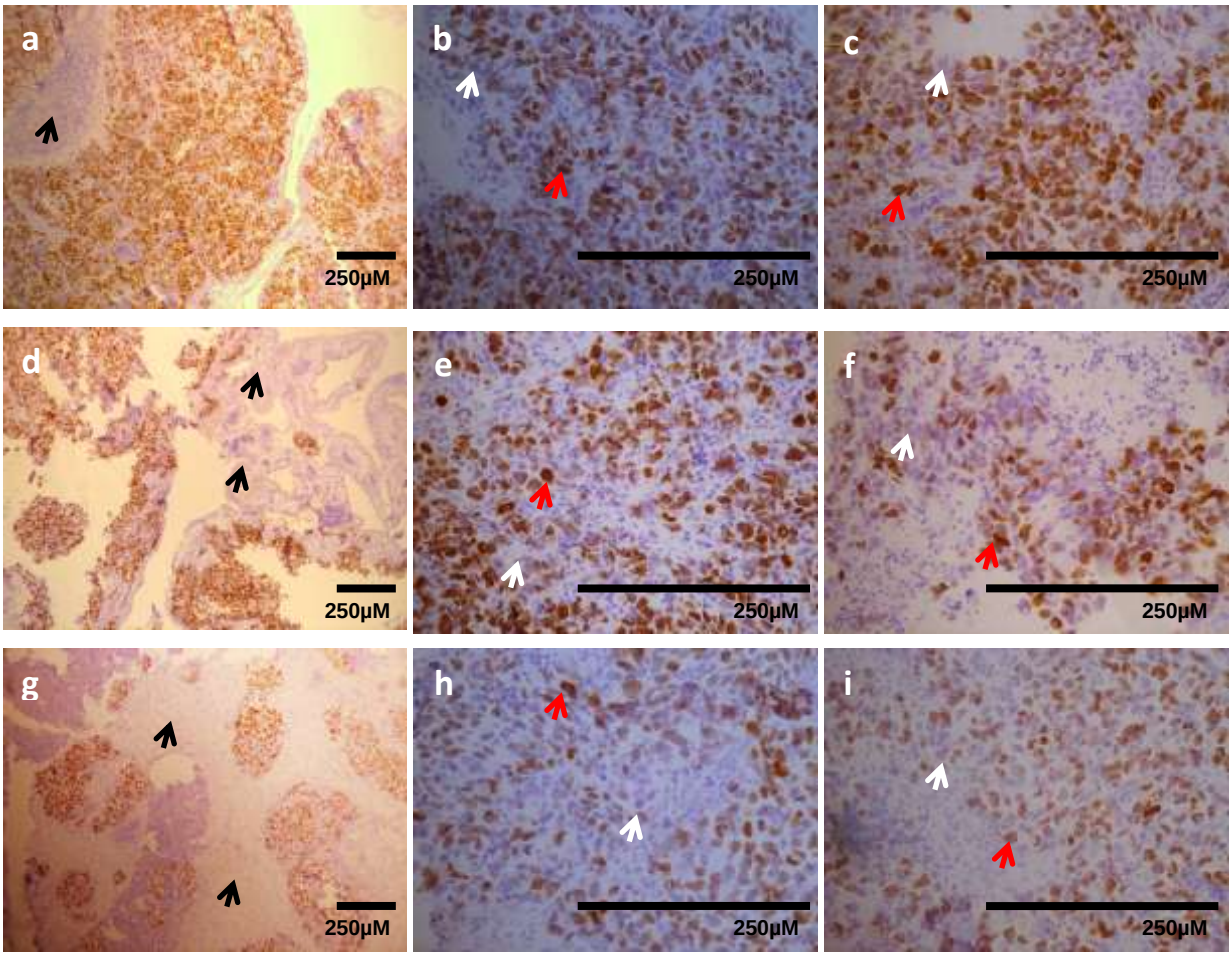

Figure3.11 RA treated BE2C tumours. a-c *tumour sections treated with 10μM RA,* ***d-f*** *tumour sections treated with 40μM RA ad* ***g-i*** *tumour sections treated with 100μM RA injected into the allantois. Note the decreasing number and staining intensity of the cell nuclei as the concentration of RA is increased. Red arrow indicates Ki67 stained nucleus, white arrow indicates unstained cell and black arrow indicates chick tissues.*

A

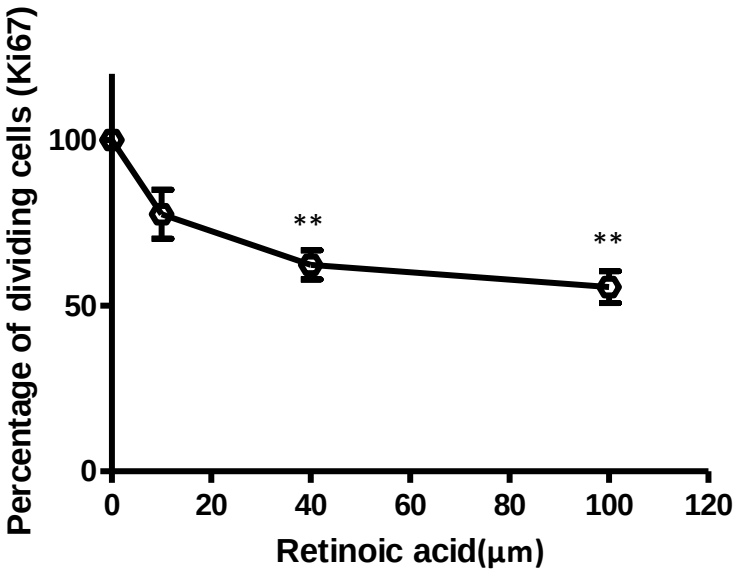

B

RA µM	No. of injections	% proliferation	% proliferation reduction
0	3	76.95±1.13	**0**
10	3	59.99±5.79	**22.33**
40	2	48.31±3.45	**37.67**
100	3	43.21±3.67	**44.33**

Figure3.12 Ki67 quantification of BE2C tumours after different RA treatments. A *graph showing the percentage of proliferation in RA treated tumours compared to DMSO.* ***B*** *table summarising the details of RA doses, percentages of proliferation and percentage reduction. Results suggested that both 40µM of RA (2 injections) and 100µM (3 injections) reduces the number of proliferative cells significantly (*p < 0.05) compared to the control.*

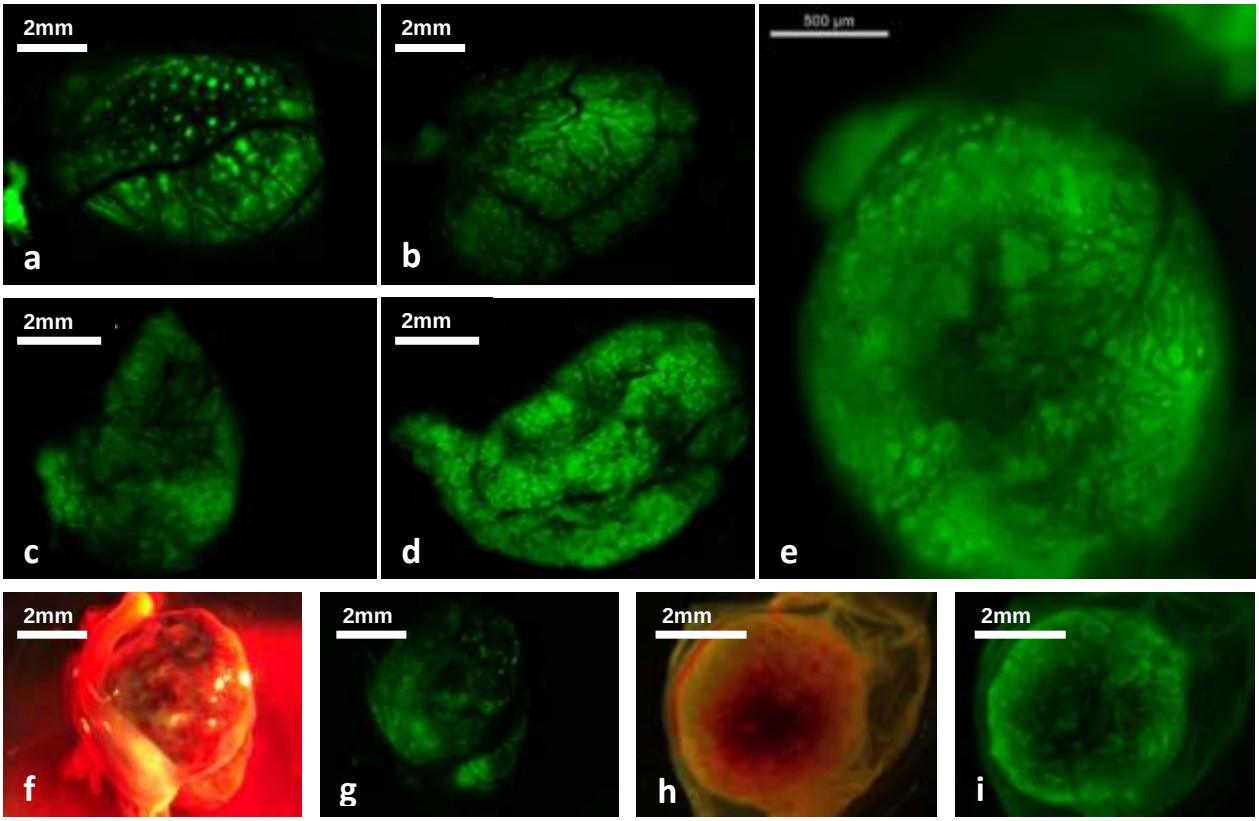

Figure3.13 In vivo and dissected 10% GFP-labelled tumours formed on the CAM of chick embryo model. ***a*** *and* ***b*** *images of 10% GFP BE2C tumours are taken in vivo.* ***c*** *and* ***d*** *images of 10% GFP BE2C tumours are taken following dissection.* ***e*** *is enlarged image of a harvested 10% GFP IMR32 tumour.* ***f-i*** *images of harvested 10% GFP tumours with their relative bright field.* ***f*** *and* ***g*** *are BE2C,* ***h*** *and* ***i*** *are IMR32.*

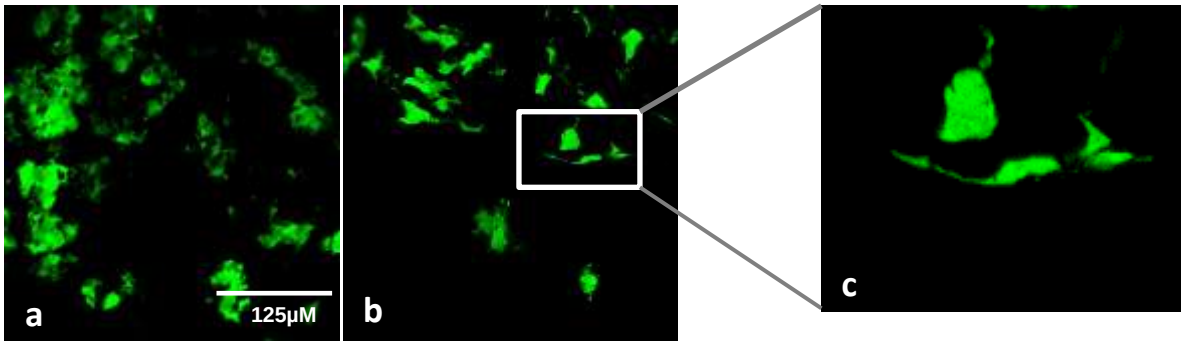

Figure3.14 confocal image of tumour treated with 40µM twice with RA or DMSO. ***a*** *is DMSO treated,* ***b*** *is RA treated and* ***c*** *is enlarged image of RA treated tumours. Tumours were formed from BE2C cells of which 10% expressed GFP. RA treated tumours exhibited a more elongated body shape of cells with small extensions resembling neurites, suggesting a more differentiated state compared to cells treated with DMSO.*

3.2.3.4. RA promotes differentiation of CAM tumours

A further validation, done by Grace Mather, University of Liverpool, to investigate the effect of RA on differentiation of CAM tumours, tumours treated with and without RA were evaluated for changes in the differentiation markers and also for MYCN. For IMR32 cells the results were similar to those observed in culture with KLF4 down regulated 4.2 fold and STMN4 upregulated 4.4 fold. ROBO2 and MYCN showed an appropriate trend but it was not statistically significant (***Figure3.15 a &b***). For BE2C cells both ROBO2 and STMN4 were significantly upregulated (5.9 fold and 5.0 fold respectively) and KLF4 and MYCN were down regulated by 3.4 and 2.2 fold respectively although these latter results were not statistically significant (***Figure3.15 c &d)***. Nevertheless the cells within the tumours shown a similar change in expression of the differentiation markers compared to cells in culture.

Taken together, the CAM tumours respond as expected to RA treatment confirming the value of the CAM tumour model for screening new therapeutic agents.

A

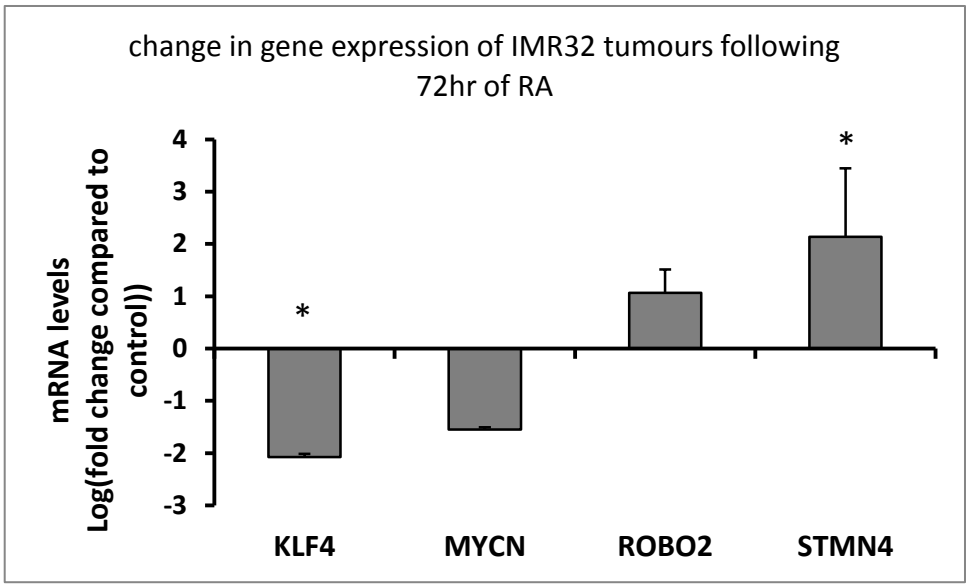

B

	KLF4	MYCN	ROBO2	STMN4
Fold Change	-4.22	-2.93	2.09	4.4
Log fold change	-2.08	-1.55	1.06	2.14
Regulation	down regulated	no change	no change	up regulated

C

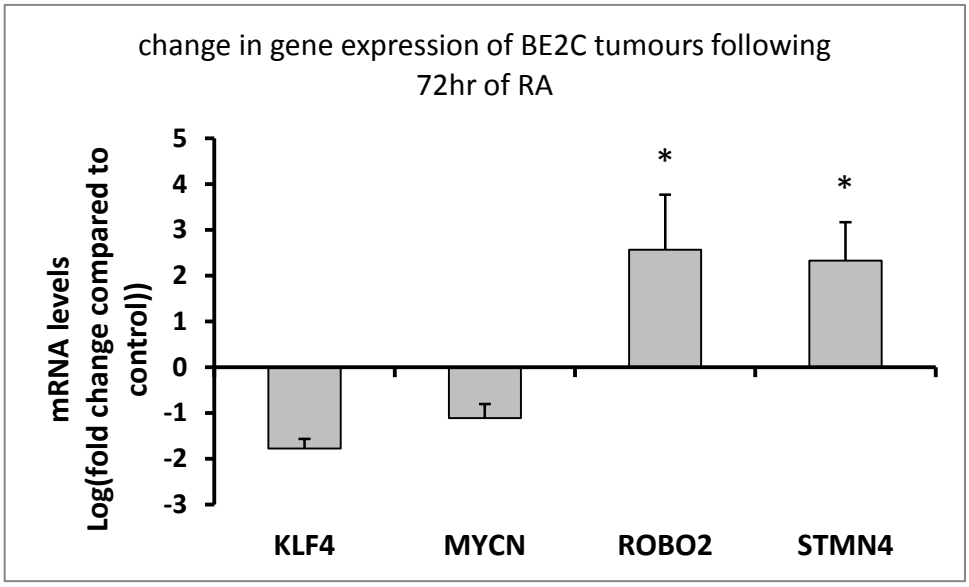

D

	KLF4	MYCN	ROBO2	STMN4
Fold Change	-3.44	-2.17	5.91	5.02
Log fold change	-1.78	-1.12	2.56	2.33
Regulation	no change	no change	up regulated	up regulated

Figure3.15 Graphs showing the level of target gene expression in IMR32 (A) and BE2C (C) tumours following 72 hr of RA treatment. *Graphs display the results of three biological repeats. Results are displayed relative to control. Error bars were calculated using standard error (SE). Table gives a summary of the QPCR data for the 4 target genes for IMR32 (**B**) and BE2C (**D**).*

3.3. Discussion

In this chapter we aimed to establish the potential of the chick embryo to act as a therapeutic model system for neuroblastoma research. By optimising the protocol for tumour production within the CAM, the tumour success growth rate with the MYCN amplified cell line BE2C reached 72%. We hoped to show the effect of RA on neuroblastoma tumour cells in this system, and then detect the effects exerted by other drugs in a quantifiable way. A simple but effective drug delivery system was developed ensuring complete distribution of the drug treatment to any tumours present. Ultimately we wished to validate the model by confirming the efficacy of existing standard therapy, RA, on neuroblastoma tumours within chick embryo model.

3.3.1. Growing tumours on the chick CAM

We used the shell windowing technique in the chick embryo experiments as it has been used by others for different means (Wang, Wang and Cai, 2009; Sys *et al.*, 2013). This technique allows us visualise the embryo and tumour growth throughout the experiments. While the windowing method allows us continual visualisation and access to great area of the CAM, it has been reported to compromise the survivals (Lokman *et al.*, 2012). We were able to detect tumour formation after 3-4 days following the cell implantation as well as being able to apply treatment and monitor the effect on tumours following the treatments. This ability confers significant advantage of chick embryo model over murine models that require palpable tumour growth and a more complex technique of imaging in order to establish the presence of a tumour and monitor tumour growth (Young *et al.*, 2009; Puaux *et al.*, 2011; Miller *et al.*, 2012).

To graft cells into the CAM, various methods has been used such as matrigel grafts (Celik *et al.*, 2005; Lokman *et al.*, 2012), plastic rings (Balke *et al.*, 2010) and collagen implants (Zijlstra *et al.*, 2006; Tiemi Egoshi *et al.*, 2015). Furthermore, cancer cells can also be administered intravenously to study metastasis of cancer cells in the chick embryos (Palmer, Lewis and Zijlstra, 2011). In our research, we

were applying the cells directly into the CAM surface avoiding any unnecessary complexity or manipulation.

Furthermore, we were placing the cells on the CAM at E7 and allowing 7 days for tumour to grow. Others however were grafting cells or explanting tumour to the CAM at late stage as E9 or E10 (Jefferies *et al.*, 2017; Vu *et al.*, 2018). Nevertheless, others have found that this period of time did improve the survivals of embryos and increased the tumour formation (Wang, Wang and Cai, 2009). Our data showed a good rate of tumour formation achieved when placing the cells on the CAM at the earlier stage. In addition, it allows us to complete experimental work on chick embryos prior to E14 without the need for the Home Office licence. This perhaps makes the model more accessible for many laboratories. Considering the 21 days of the embryo development, tumours formed earlier provide longer period to test therapeutic compounds and allows analysing the consequent effect of these compounds within the model. In either case, the time of conducting and obtaining the results using this model is faster than murine models.

Implantation of several neuroblastoma cell lines on to the surface CAM allowed us observe the ability of the cells to form tumours in this environment. Interestingly, we observed low yield of tumour formation (less than 25%) in BE2C, IMR32 and Kelly cells. This contradicts with the clinical classification that considers MYCN amplified tumour as aggressive and metastatic disease (Dzieran *et al.*, 2018), and thus MYCN amplified cells are expected to form tumours in the CAM more readily. When MYCN cell failed to form tumours in the model, they were seen as a flat sheet on the surface of the CAM rather than beneath it as a mass.

The degradation of basement membrane to penetrate into the underlying stroma is known to be one of the hallmarks of cancer (Hanahan and Weinberg, 2011). Matrix metalloproteinases (MMPs) are a group of zinc-dependent endopeptidases that show proteolytic activity for many components of the extra-cellular membrane (Al-Dasooqi *et al.*, 2010). Among the proteases, MMPs are believed to be involved in tumour invasion and metastasis (Hanahan and Weinberg, 2011).

The expression profile of MMPs and their inhibitors has been studied in several neuroblastoma cell lines (Ara *et al.*, 1998; Sugiura *et al.*, 1998; Bjørnland *et al.*, 2001; Roomi *et al.*, 2013; Arumugam *et al.*, 2016).For instance, Sugiura et al reported that a number of neuroblastoma cell lines such as IMR32, BE2, SKNSH, LAN1, LAN2, LAN5, LAN6, and HT1080 were seen to overexpress certain MMPs but in an inactive proform (Sugiura *et al.*, 1998). Interestingly, in another study conducted in other neuroblastoma cell lines, SKNAS were found to have the highest expression of MMPs among other cell lines, and of those tested, was the only cell line expressed the biological activator of MMP (Bjørnland et al., 2001).

The above findings may explain why the cells we used in experiments failed to form tumours as the lack of active MMP enzymes affects cell ability to penetrate through superficial epithelial layer of the CAM, and so they remained on the surface, fail to grow and consequently died. In support to this, a significant improvement of tumour formation was noticed following the addition of Trypsin, a proteolytic enzyme. Trypsin allowed for the invasion of cells under the superficial epithelial layer of the CAM, the neuroblastoma cells had a near optimum environment to expand, draw in blood vessels and exponentially grow.

Following the addition of Trypsin, tumour success formation of BE2C increased to 70% whereas in IMR32 and Kelly increased to almost 40%. These results supports what seen in other studies that also observed variable levels of cell line specific success when investigating the tendency of malignant cell lines to form tumours in the chick embryo model (Balke, Neumann et al. 2010).

Ultimately, the success of tumour formation demonstrate that human neuroblastoma cells, like many other malignancies (Khanna *et al.*, 2002; Balciūniene *et al.*, 2009; Cecilia Subauste *et al.*, 2009; Fergelot *et al.*, 2013; Sys *et al.*, 2013; Manjunathan and Ragunathan, 2015; Jefferies *et al.*, 2017; Vu *et al.*, 2018), are able to form tumours in CAM model. The improvement of tumour yield following the addition of Trypsin may have significance, not only in establishing the chick embryo as a suitable

in vivo model system for neuroblastoma, but may aid research into other malignancies being used in the model.

3.3.2. Retinoic Acid in culture

In culture, three days of RA administration showed some morphological changes such as neurites outgrowth in both IMR32 and BE2C cells. Many in the literature have described these morphological changes as being a differentiation characteristic (Sidell, 1982; Sidell *et al.*, 1983; Wu *et al.*, 1998). Cell proliferation has been quantified using Ki67 staining. A reduction in Ki67 positive cells was seen in both cell lines, also suggesting that cell differentiation is taken place.

Changes in the level of target gene expression after exposure to RA were detected using qPCR. In keeping with previous results, showing the reduction of proliferation and the morphological changes, there was a significant change in the expression of the differentiation markers KLF4 and STMN4 but not ROBO2 and MYCN in RA treated cells compared with DMSO treated cells.

Expression levels of KLF4 fell significantly after 3 days of RA treatment in both cell lines. KLF4 results further support Sung et al observation and extend it to show similar changes in the BE2C cell line (Sung *et al.*, 2013). KLF4 is a stem cell marker and expected to be down regulated when differentiation is taken place. Interestingly, human neural stem cells (NSCs) exhibits high endogenous expression levels of KLF4, and together with other genes, KLF4 can be reprogram NSCS to become a pluripotent termed Induced Pluripotent Stem Cells (iPSCs) (Kuan *et al.*, 2017). Cotterman and Knooepfler have reported that N-myc regulates the expression of KLF4 in both tumours and stem cells. They suggest that N-myc may enforce expression of stem-like state of KLF4 driving undifferentiated phenotype of neuroblastoma (Cotterman and Knoepfler, 2009) .Thus, together with our results; the more differentiated pattern of neuroblastoma displays a decreased KLF4 expression.

Against our expectations, MYCN expression level remained unchanged after 3 days of RA treatment in culture. MYCN is a transcription factor known to be involved in the regulation of expression of many target genes. RA treatment is thought to down-regulate MYCN expression prior to enhancing differentiation. However, our results indicated no change in MYCN expression under RA influence. A paper has been published by Guglielmi et al in which the authors indicated a crucial need for MYCN in the onset of neuroblastoma differentiation (Guglielmi *et al.*, 2014). In contrast to others (Thiele, Reynolds and Israel, 1985; Varlakhanova *et al.*, 2010; Huang *et al.*, 2011), Guglielmi et al reported that in the first few days of RA treatment- induced differentiation, MYCN expression elevates prior to differentiation. The authors suggested that MYCN expression is necessary for the initiation of neuronal differentiation as well as is important in the regulation of some target genes involved in the subsequent phases (Guglielmi *et al.*, 2014). Our results did not support the increased level of MYCN expression, however as we observed expression after 3 days only, it is possible that a rise in MYCN could have occurred prior to day 3 and levels may have begun to fall again by day 3.

Expression of ROBO2 was increased by almost 4 fold in both cell lines; however the rise was not statistically significant following 3 days of RA in cell culture. Nevertheless, our results follow the trend of what seen in Sung et al paper and extended them to demonstrate similar changes in the BE2C cell line (Sung *et al.*, 2013). ROBO gene has been studied extensively to have an important role in the axon guidance (Andrews, Barber and Parnavelas, 2007; Andrews *et al.*, 2008; Curinga and Smith, 2008). In particular, ROBO2 is shown to be involved in the regulation of axonogenesis and actin cytoskeleton pathways (Oe *et al.*, 2005).The morphological changes observed in response to RA also support the trend towards an increase in ROBO2.

Following the RA treatment, STMN4 was up regulated in both BE2C and IMR32 cells. Again this result was very similar to that published by Sung et al. STMN4 is identified to be essential in the regulation of dynamic microtubules which are known to be aid growth cone advance and responses to guidance cues (Duncan *et al.*, 2013; Lin and Lee, 2016)

Changes observed in the gene expression of KLF4, STMN4 and ROBO2 correlated with the proliferation reduction and the morphological changes of the cells, and thus the results are largely consistent. Furthermore our results were in line with other published works indicating the significance of those markers in determining the differentiation status in neuroblastoma cells.

3.3.3. RA drug delivery

Because of the precipitation issue with RA, mentioned ***in section 2.5.5***, and after exploring multiple methods for the delivery of drugs onto the CAM, it was found that the most successful was the injection of treatment underneath the allantois. As the allantois is filled with approximately 5-10ml of fluid, the injected solution of RA in PBS was hypothesised to be evenly distributed (Corral *et al.*, 2007). From experimentation with RA solubility it was found that by adding 1µl of 10mM RA solution to 1000µl of PBS resulted in no RA crystal formation. This provided evidence that the distribution of RA in the allantoic fluid would result in the RA crystals dissolving in this volume.

3.3.4. Retinoic Acid in tumours

In order to demonstrate the suitability of the chick embryo xenograft model for therapeutic research, the model was assessed using RA.

In line with culture experiments, tumours treated with RA had a reduction in proliferation seen through IHC staining using the antibody Ki67.

Confocal microscopy supported the hypothesis of there being morphological alterations in the differential state of cells as an increase in neurite extensions was seen in cells within the tumours. Interestingly, the cell shape alterations were observed at 40µM dose of RA. Cells were less rounded and less clustered in appearance compared to the DMSO control group. This supports previous work that RA is a successful treatment in the reduction of proliferation and increased differential state of cells within neuroblastoma tumours. In conclusion, RA has demonstrated the expected effect on

MYCN-amplified tumours so the need now is to find other potential therapeutic molecules of differentiation other RA resistant tumours e.g 11q deletion tumours (SKNAS cells).

Taken together, many others have suggested the suitability of the chick embryo model for therapeutic research; however this is the first time, outside the field of angiogenesis, that the efficacy of a known compound used in the treatment of neuroblastoma has been reproduced in the chick embryo model. These positive results encourage the use of the CAM model for further screening of potential molecules treating resistant neuroblastoma prior to clinical testing.

Chapter Four: Results II
Characterisation of some potential therapeutic molecules using the chick embryo model system

4.1. Introduction

The work discussed in chapter 3 suggested that chick embryo model is a reliable model system that can be used in therapeutic research for neuroblastoma. *In vivo*, Retinoic acid effect was seen to induce differentiation and reduce proliferation of neuroblastoma CAM tumours (both BE2C and IMR32 tumours).

As the principle has been proved following the use of Retinoic acid on CAM tumours, we decided to test new potential molecules that may boost the effect of RA further. Dysregulation in the phosphorylation state can lead to uncontrolled cell proliferation and survival (Tonks, 2006). Targeting the enzymes that control the phosphorylation in the cell cycle such as PTP may boost the effect of RA or open another potential route to treat neuroblastoma. Here, we hypothesised that the use of tyrosine phosphatase inhibitor, (Bis(maltolato)oxovanadium(IV) (BMOV)), may enhance the effect of Retinoic acid in decreasing proliferation and inducing differentiation of neuroblastoma tumours.

The reduction of proliferation following Retinoic acid treatment is due to increasing the levels of p27(Kip1), an inhibitor of Cyclin-Dependent Kinases 2, 4 and 6 (Borriello *et al.*, 2000) and reducing the proliferation is shown to be tightly linked with the differentiation state in normal development (Hardwick and Philpott, 2014). Furthermore, as mentioned previously, neuroblastoma may develop due to an aberration of the cell cycle that happens during normal development and prevents the cells from differentiating (Park *et al.*, 2013). Given that CDKs are important regulators of the cell cycle which facilitate cell division. Hence we hypothesise here that inhibiting the cell cycle using agents such as CDK inhibitors may provide an additional or alternative approach to promoting differentiation of neuroblastoma. The first molecules came to our attention to test was Palbociclib, a CDK 4/6 inhibitor. Palbociclib has been tested clinically in a range of cancers including breast cancer (Palanisamy, 2016). We included also another molecule to investigate which is RO-3306. RO-3306 is an inhibitor of CDK1 and has been tested in some preclinical models (Kang *et al.*, 2014).

Ultimately, we sought to investigate the effect of CDK4/6 and CDK1 inhibitors on neuroblastoma tumours using the chick embryo model.

4.1.1. Aims of the chapter

The aims of the work described in this chapter to:

- Examine the effect of BMOV alone and in combination with RA on BE2C cells, *in vitro* and *in vivo*.
- Investigate the effect of Palbociclib alone and in combination with RA on BE2C and SKNAS cells.
- Investigate the effect of Palbociclib on BE2C and SKNAS CAM-tumours.
- Determine the effect of RO-3306 on BE2C and SKNAS cells *vitro* and *in vivo.*

4.2. Results

4.2.1. Bis(maltolato)oxovanadium (IV) (BMOV) reduces cell proliferation and induces changes in morphology in MYCN-amplified cell line, BE2C cells

Cells were cultured with BMOV alone and in combination with RA for a period of 72hr. Cells then observed using Leica DMIRB microscope to identify the effect of BMOV on cell morphology prior to carrying out proliferation assessment.

Morphological assessment

Cells with BMOV appeared to have similar or less pronounced morphological changes to that noticed with RA. The combination treatment showed more neurite outgrowths but not more strikingly than RA alone. As the morphological changes were not much different following the single of BMOV or even when combined with RA, we sought to investigate whether BMOV reduced proliferation using Ki67 staining (***Figure4.1***).

Proliferation assessment

Assessing cell proliferation (Ki67) was crucial in determining the behaviour of the neuroblastoma in culture first before assessing their behaviour *in vivo,* following BMOV or BMOV+RA treatment.

To quantify cell proliferation, we performed Ki67 staining in all BMOV alone, RA alone, BMOV+RA and control-treated cells. Cells were stained with a rabbit anti-Ki67 antibody and labelled with goat anti-rabbit (secondary antibody) conjugated with Alexa Fluor 594 (red) to enable identification of proliferating cells whilst counterstaining with DAPI allowed identification of the total number of nucleus cells present. Cell counts were performed comparing the number of Ki67 positive cells to the number of DAPI stained cells in the treated as well as in control cells (***Figure4.2 A***). Overall, BMOV alone reduces the cell proliferation to 51% in BE2C cells compared to the control and a reduction of 60 % was observed in both RA treatment and the combination treatment (***Figure4.2 B***). Of note, there was no significant difference between the combination treatment compared to RA alone or BMOV alone.

Ultimately, both morphological assessment and proliferation assessment suggested that the BMOV alone or in combination with RA reduced proliferation effectively and induced morphological changes compared to the control but no more effectively that RA alone.

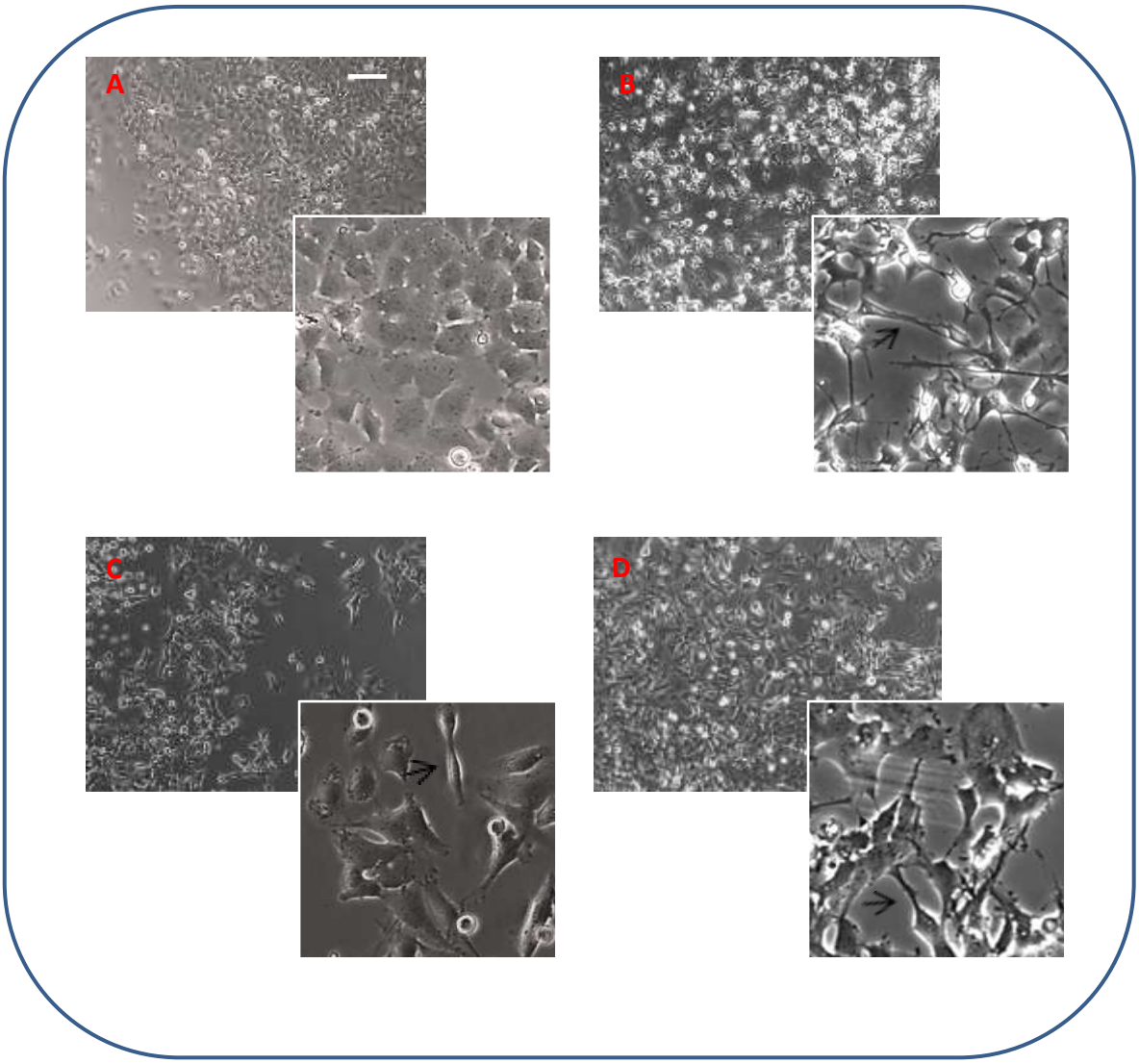

Figure4.1 Changes in cell morphology of BE2C cells after72 hr of BMOV alone or in combination with RA treatment. ***A*** *represents the control (DMSO),* ***B*** *is RA alone (10µM),* ***C*** *is BMOV alone (10µM) and the* ***D*** *is BMOV (10µM) +RA treatment (10µM). Black arrows indicate morphological changes as neurite outgrowth. Scale bar =100µM.*

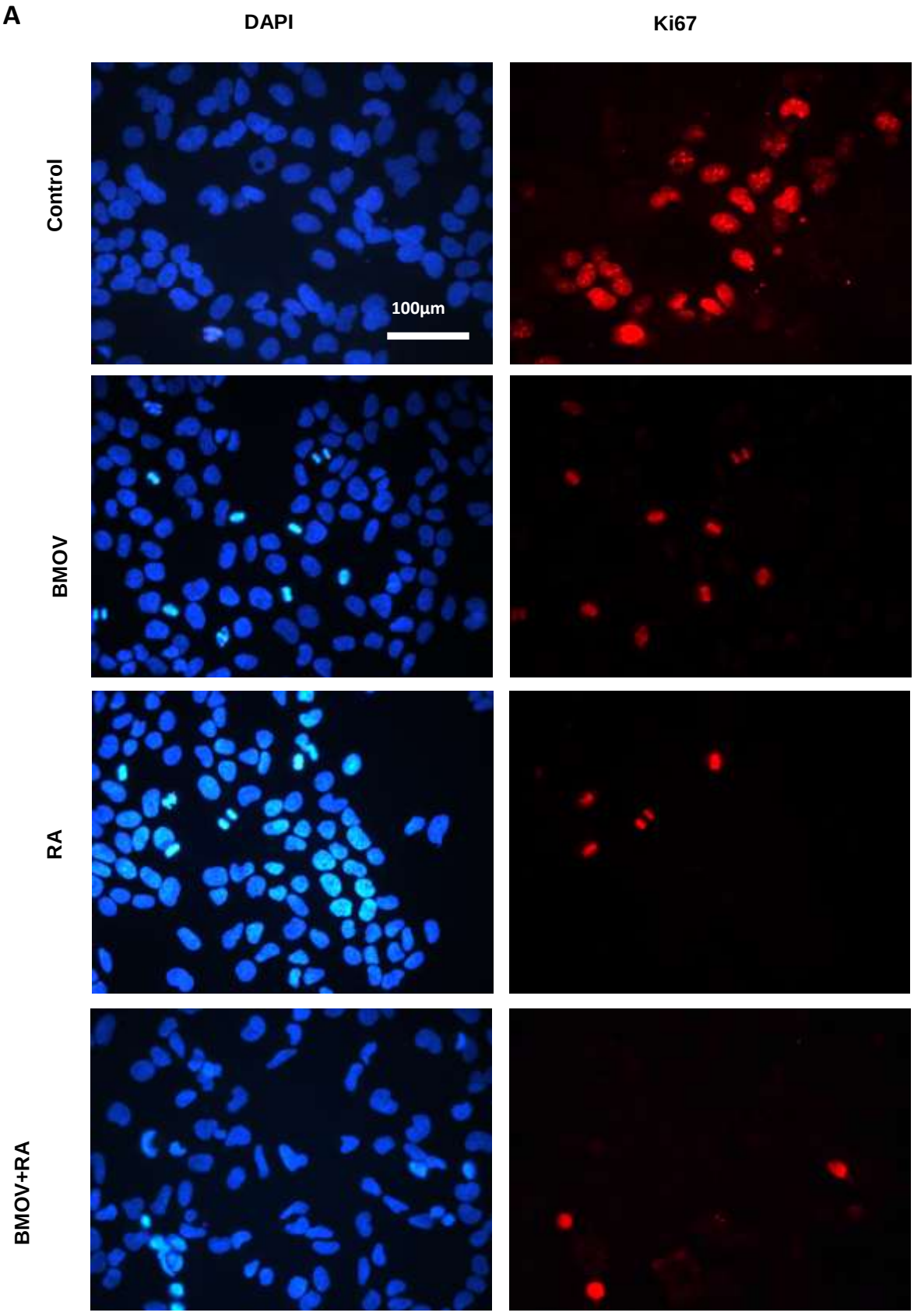
A
DAPI
Ki67
Control
BMOV
RA
BMOV+RA
100μm

B

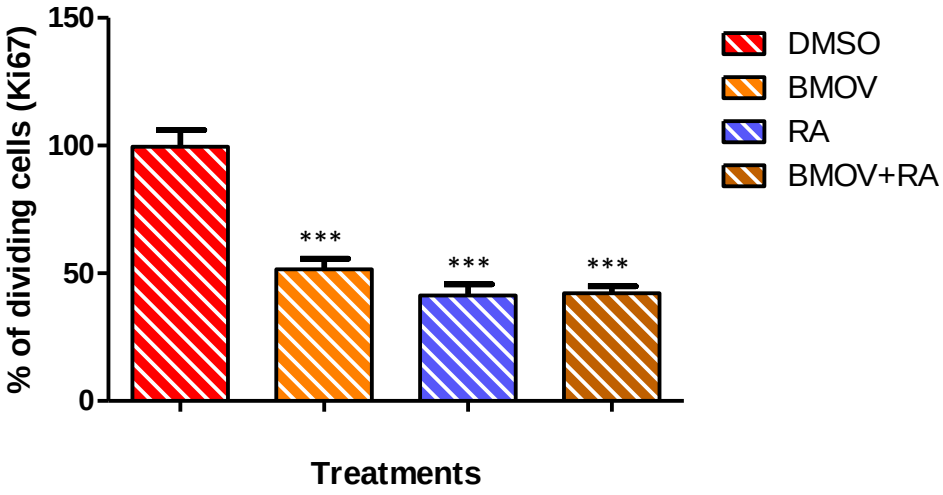

Figure4.15 Effect of BMOV alone and in combination with RA treatment on BE2C cell proliferation. ***A*** *DAPI stained (blue) and Ki67 stained (red) BE2C cells following three days of treatment with 10µM BMOV alone or in combination with 10µM RA or DMSO.* ***B*** *displayed the percentage of proliferative cells after setting the control to 100%, proliferation index = number of Ki67 positive expressed as a percentage of the total number of cells divided by the % in the control. Data presented relative to control. Data represents mean ± SEM (n=9). Each bar represents the mean ± SEM of three biological replicates and at least 9 fields per experiment. ***P⩽0.001.*

4.2.2. Effect of BMOV alone and in combination with RA on gene expression of differentiation markers in BE2C cells

To further investigate the effect of BMOV alone and in combination with RA on gene expression, quantitative assessment of cellular differentiation was undertaken using qPCR. The same genes used in assessing the effect of RA alone in chapter 3 were used: KLF4, STMN4 and ROBO2 (Sung *et al.*, 2013) and MYCN (Huang and Weiss, 2013).

In keeping with these results, there was a significant change in the expression of the differentiation marker STMN4 but not ROBO2, KLF4 and MYCN in BMOV treated cells compared with DMSO treated cells (***Figure4.3***). The combination treatment induced a significant change in the expression of STMN4, KLF4 and MYCN but not ROBO2 compared with DMSO treated cells. In BMOV and RA combination treatment, STMN4 increased by 8 fold whereas KLF4 and MYCN decreased by 4.5 fold (***Figure4.4***).

A

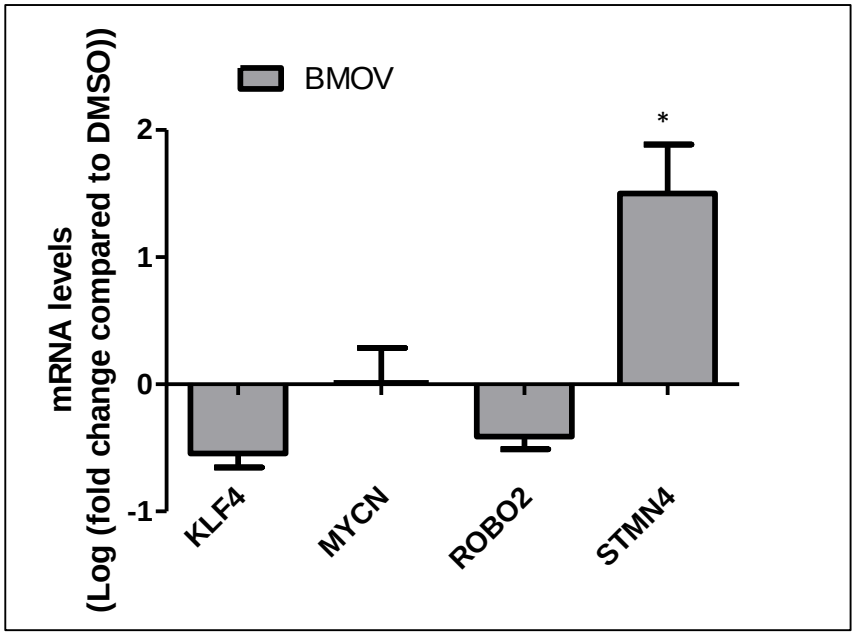

B

	KLF4	MYCN	ROBO2	STMN4
Fold change	-1.45	1.05	0.01	3.05
Log Fold change	-0.54	0.01	-0.41	1.50
Regulation	no change	no change	no change	up regulated

Figure4.16 The effect of BMOV on gene expression of BE2C cells. A *Relative mRNA levels for the target genes were determined by qPCR. Cells were cultured with 10µM of BMOV or DMSO for 3 days. At least three independent experiments (n = 3) were analysed for each gene and relative mRNA levels are displayed relative to GAPDH, UBC and HPRT1 and normalised to cells cultured for 3 days with DMSO(control). Each bar in the graph represents the log of normalised mean± SEM of three independent experiments. *P⩽0.05 compared with control.* ***B*** *Table gives a summary of the qPCR data for the 4 target genes for BE2C cells.*

A

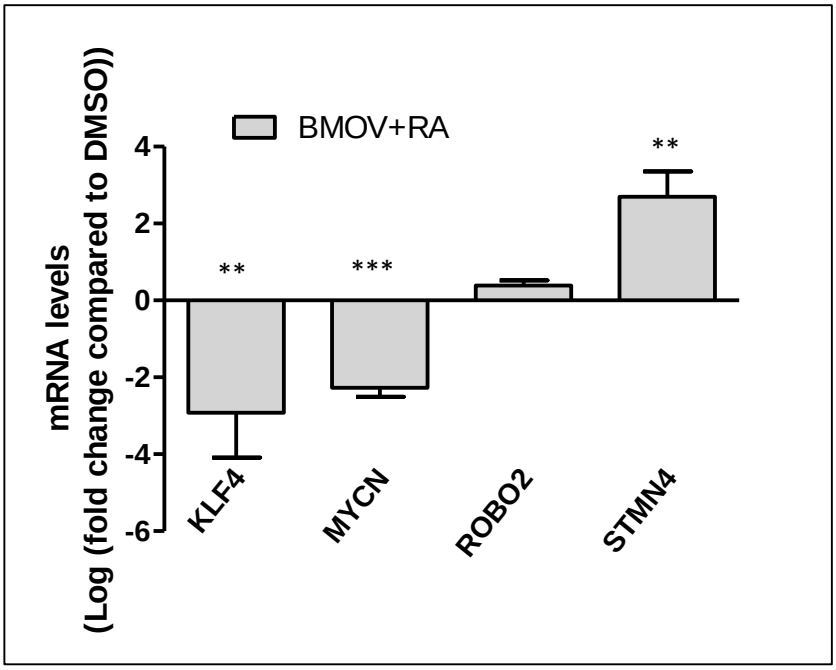

B

	KLF4	MYCN	ROBO2	STMN4
Fold change	-4.65	-4.71	0.05	8.07
Log fold change	-2.92	-2.27	0.39	2.70
Regulation	down regulated	down regulated	no change	up regulated

Figure4.4 The effect of BMOV and RA on gene expression of BE2C cells. A *Relative mRNA levels for the target genes were determined by qPCR. Cells were cultured with 10µM of BMOV+ 10µM of RA or DMSO for 3 days. At least three independent experiments (n = 3) were analysed for each gene and relative mRNA levels are displayed relative to GAPDH, UBC and HPRT1 and normalised to cells cultured for 3 days with DMSO(control). Each bar in the graph represents the log of normalised mean± SEM of three independent experiments. **P⩽0.01 and ***P⩽0.001 compared with control.* ***B*** *Table gives a summary of the qPCR data for the 4 target genes for BE2C cells.*

4.2.3. Assessing the effect of BMOV alone and in combination with RA on MYCN amplified cell line *in vivo* using the chick embryo model

In culture, treatment with the BMOV and RA has suggested that differentiation markers are sensitive to the synergic effect of BMOV and RA. Next we aimed to test whether BE2C cells respond to BMOV alone and BMOV+RA *in vivo*. Tumours were grown on the CAM as described in chapter 2 using GFP-labelled BE2C cells.

The treatment initially started using BMOV alone. Previously we have found that using four times the *in vitro* concentration of RA in the chick CAM tumours gave a significant reduction in cell proliferation and change in the differentiation markers (Swadi *et al.*, 2018). We therefore injected 40µM of BMOV to the allantois of the embryos at E11 and E13. The embryos were observed daily under the microscope following the treatment. It was noticed there was a drop in survival rate following the second treatment with BMOV. The vast majority of embryos did not survive up to E14 hence indicting a toxic effect of BMOV *in vivo*.

As the BMOV revealed a toxic effect *in vivo*, the search was started to test new active molecules that can tackle neuroblastoma. CDK4 found to be amplified in neuroblastoma cells (Molenaar, Koster, Ebus, *et al.*, 2012) and because CDK4 synergise together with CDK6 in pushing the cell cycle toward mitosis, we sought to inhibit both CDK4 and CDK6 using selective inhibitor of CDK4/6, Palbociclib. Here we tested the effect of Palbociclib on neuroblastoma cells *in vitro* and *in vivo*.

4.2.4. Palbociclib reduces cell proliferation and induces changes in morphology in MYCN-amplified cell line and cell death in non-MYCN-amplified cell line

Morphology assessment

We tested Palbociclib in two neuroblastoma cell lines, the RA-sensitive cell line (MYCN-amplified cell line, BE2C) and the RA-resistant cell line (non- MYCN-amplified cell line SKNAS). SKNAS cells have not

been found to differentiate or indeed respond at all to RA alone (Clark, Daga and Stoker, 2013) so it was interesting to test the effect of Palbociclib. GFP-labelled BE2C and SKNAS cells were cultured as described in chapter 2 using 24-well plates. Treatment of Palbociclib was used as 0, 5, 7.5,10 and 20μM to determine the optimal concentration that affects the neuroblastoma cell lines. In BE2C cells, 5μM Palbociclib induced neurite outgrowth strikingly compared to control (PBS) treated cells. Similarly, 7.5 μM Palbociclib showed a similar effect to that observed with 5μM. In contrast, this effect started to change from differentiation induction to induction of cell death following the increase of Palbociclib dose. 10 and 20μM Palbociclib resulted in massive cell death in a dose-dependent manner (***Figure4.5***). However, in SKNAS cells, the effect of cell death induction was observed even when low concentration (5μM) of Palbociclib was used (***Figure4.6***).

Following observation of cell death by phase microscopy, we sought to investigate the cell death/cell viably after applying the treatment of Palbociclib using the MTT assay. MTT is a colorimetric assay for assessing cell metabolic activity. NAD(P)H-dependent cellular oxidase enzymes reflect the number of viable cells present. Thus MTT assay measures NAD(P)H-dependent cellular oxidoreductase by converting this to formazan crystals and then the latter dissolves in SDS to form soluble solution to be measured using Spectrophotometer. Cell density was optimised using MTT assay prior to carrying out experiments.

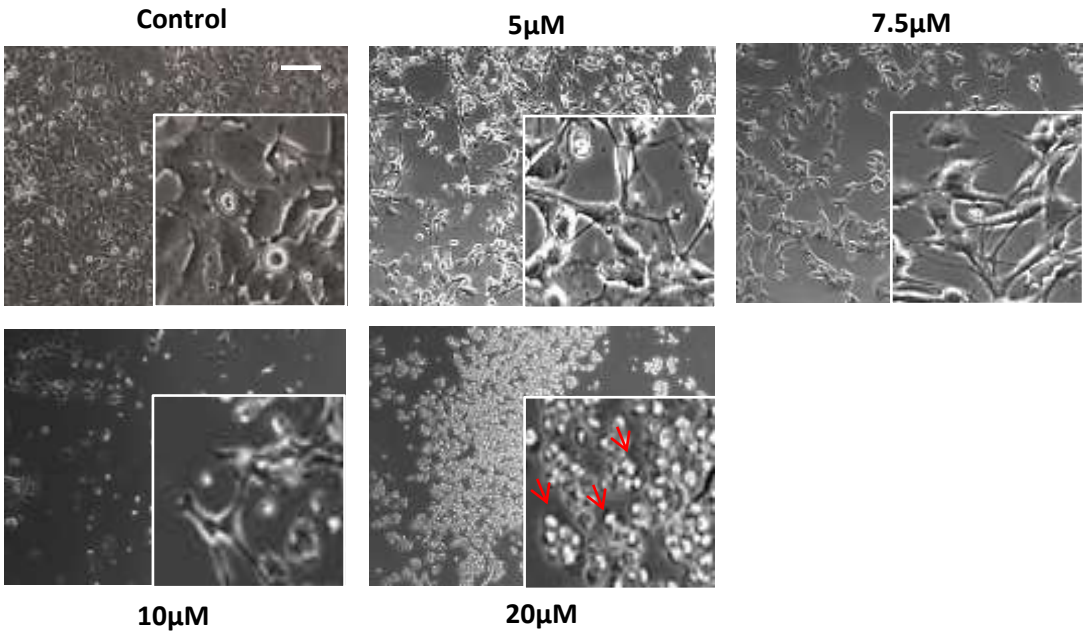

Figure4.5 BE2C cells after 72hr of treatment with different concentration of Palbociclib (CDK4/6 inhibitor). *5µM and 7.5µM are showing the morphological changes as the neurite outgrowth.10µM showing less of differentiation than cell death. The latter effect has been observed extensively within the 20µM concentration. The red arrows indicate dead cells. Scale bar is 250µm.*

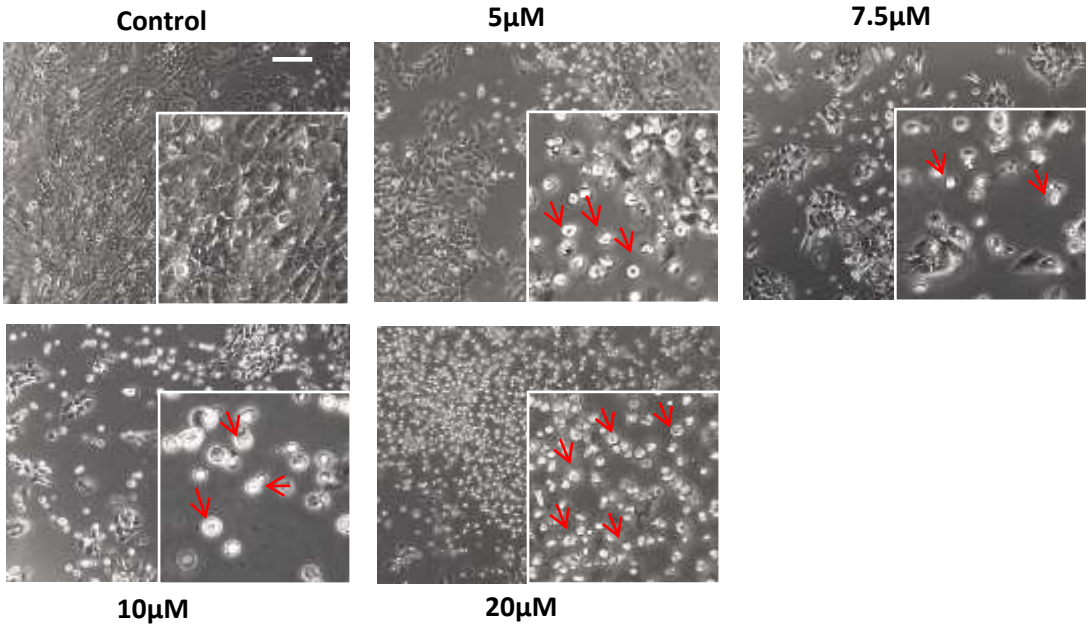

Figure4.6 SKNAS cells after 72hr of treatment with different concentration of Palbociclib (CDK4/6 inhibitor). *Palbociclib induced cell death at 5 and 7.5µM and this effect observed to be extensive at10 and 20µM concentrations. The red arrows indicate dead cells. Scale bar is 250µm.*

4.5.5. Optimising the cell density for MTT assay

To perform the MTT and for best results, an optimisation step was required to identify the optimum cell number to plate out for the experiments. Selection of a cell number that falls within the linear portion of the curve (i.e. providing values between the range of 0.75 and 1.25) limiting the lag phase following plating of the cells. Both cell lines were seeded for 24hrs in flatted bottom multi-well plate at 10 serial two-fold dilutions starting with stock solution of $5x10^6$ to end up with $4.88x10^3$. Each dilution was performed as triplicate with three wells of blank control (culture medium) and incubated at 37C° and 5%CO_2. After 24 hrs, 10 µL of MTT reagent has added to the wells and incubated for 4hrs in order to form the formazan crystals, 100µl of 10% SDS solution have added to each well and incubated at room temperature overnight. The plate was read at 570nm and the blank was subtracted from the experimental readings. The optimal density after 24hr was determined to be $1.56x10^5$cells/ml for both BE2C and SNKAS cells (***Figure4.7***).

Our results from the preliminary optimising experiment suggested that $1.56x10^5$ cells/ml is the best after 24 hr, however, because of the time of the real experiment is much longer (72hr) than the preliminary and to do not exceed the maximum reading (OD) of the plate reader, we decided to set the cells as $0.5x10^5$ cells/ml.

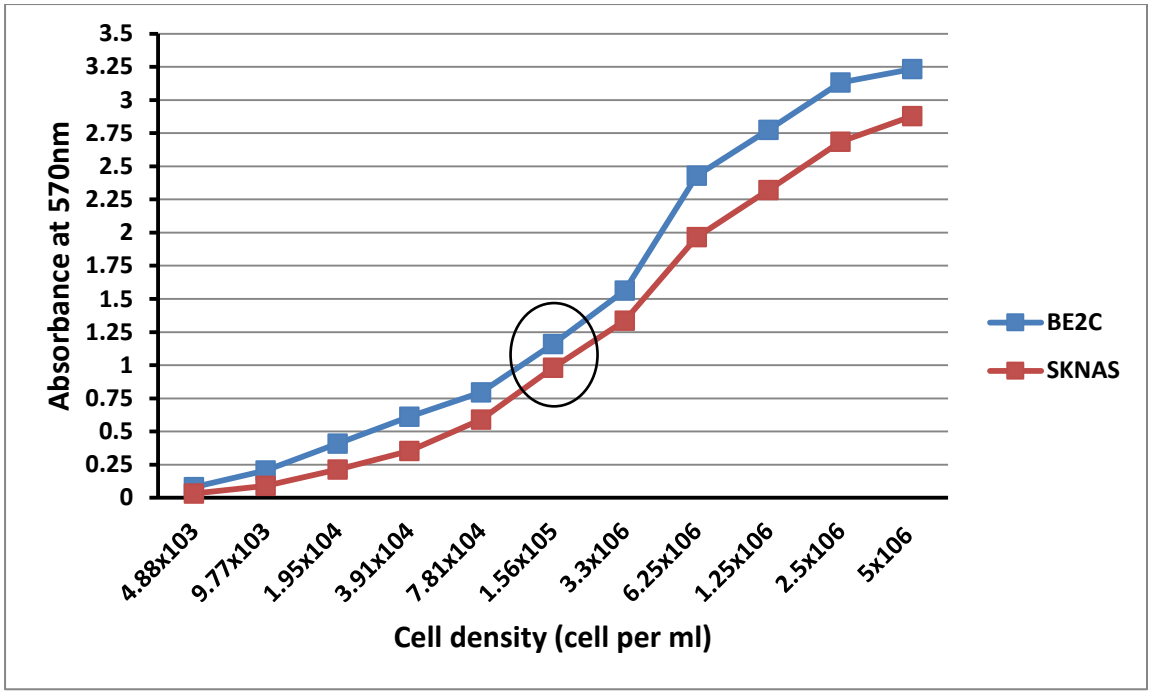

Figure 4.7 The optimisation of cell density using MTT assay. *BE2C and SKANS cells were seeded for 24hr in flatted bottom multi-well plate at 10 serial two-fold dilutions starting with stock solution from $5x10^6$ to $4.88x10^3$cells/ml. Each dilution was performed as triplicate with three wells of blank control (culture medium). The optimum cell density after 24hr was $1.56x10^5$cells/ml.*

4.2.6. Increasing Palbociclib concentration elicits a reduction in cell viability in both BE2C and SKNAS cells

SKNAS and BE2C cells were seeded in cover slips inside 96 well plate at $0.5x10^5$ cells/ml for 24hr prior to drug administration. After 24hr, cells were treated fresh medium including 0, 1, 5, 10, and 20µM of Palbociclib in order to determine the cell viability following the treatment. Palbociclib treated cells with the presence of controls were incubated for 72hr (refeed after 48hr) at 5%CO_2 and 37C°. Following this, MTT assay was carried out as described previously. MTT results indicated that increasing the concentration of Palbociclib reduces the cell viability and prompts cell death as shown in ***Figure4.8***. In BE2C cells, the cell viability has decreased by 30% compared to the control following the application of 5µM of Palbociclib whereas SKNAS cell viability was reduced by 20% under similar condition. At 20µM of Palbociclib, however, both BE2C and SKNAS cell viability has dropped significantly by more than 50% compared to the control.

In keeping with MTT assay results we sought to identify the proliferation status of BE2C and SKNAS cells following the treatment of Palbociclib.

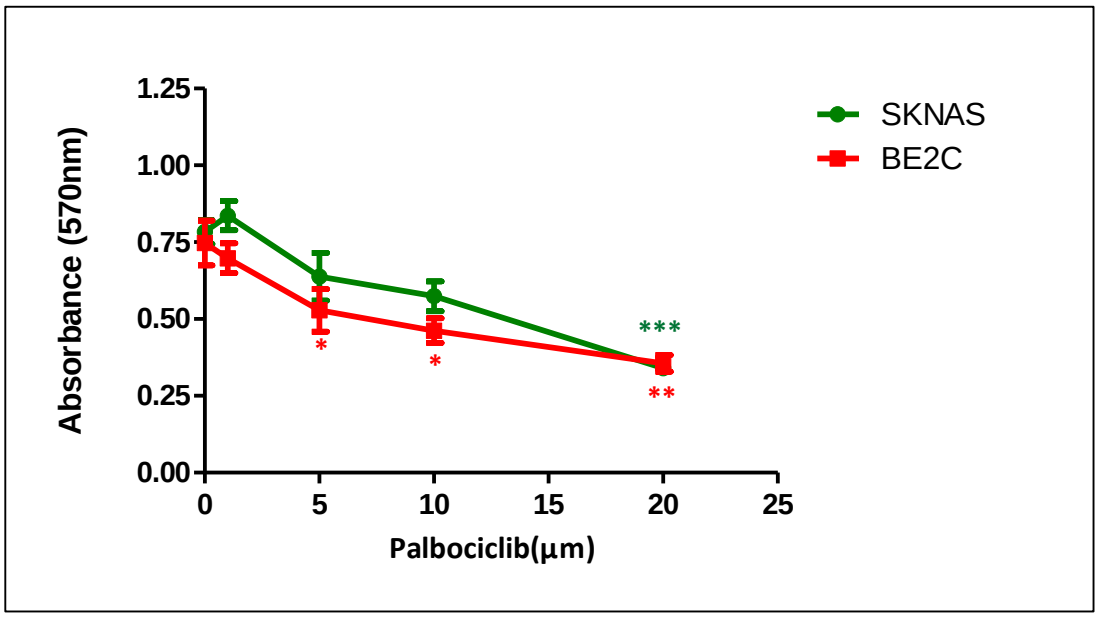

Figure4.8 Cytotoxicity of Palbociclib to Neuroblastoma cell lines (BE2C and SKNAS)*. Cells were treated with different doses of Palbociclib for 72hr as indicated in the Materials and Methods. Green line is SKNAS and Red line is BE2C. The graph represents cell viability based on the MTT assay. Each point represents a mean value and standard error of 3 experiments with 3 replicates per concentration. Cell viability of BE2C in 5, 10, and 20µM are significantly different compared to the control. SKNAS cell viability has dropped more significantly at 20 µM compared to control according to ANOVA Tukey's test. *P⩽0.05 **P⩽0.01 and ***P⩽0.001.*

4.2.7. Cell death assessment following Palbociclib

To further investigate the cell death of BE2C and SKNAS following Palbociclib treatment, we performed Annexin V staining. When apoptosis occurs, phosphatidylserine (PS) is translocated from the inner side of the plasma membrane to the outer layer exposing PS at the surface of the cell. Hence, we used Annexin V that can stain the translocated PS in cells to identify apoptotic event.

Cells were seeded as for the proliferation assessment. Apoptosis was noticed following the application of Palbociclib on both cell lines (***Figure4.12***).

Ultimately, we showed that Palbociclib induces apoptosis as well as reduces cellular proliferation and induces differentiation at the lowest concentration (5µM) for BE2C however for the SKNAS cells; Palbociclib promotes apoptosis in them.

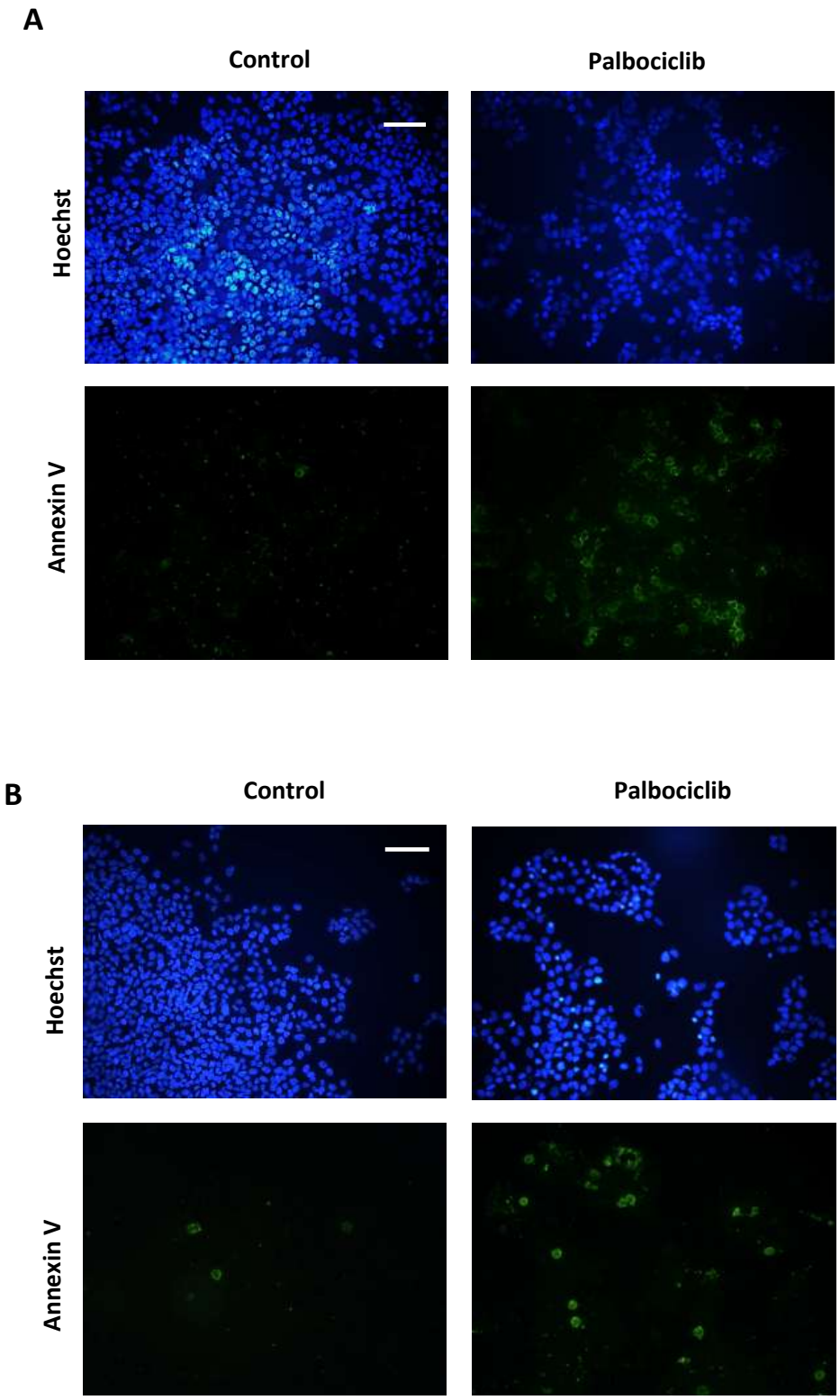

Figure4.9 Palbociclib induces apoptosis in BE2C and SKNAS cells. A *is BE2C* ***and B*** *is SKNAS. Immunofluorescent analysis of live BE2C and SKNAS cells using Annexin V-FITC Conjugate (green) and Hoechst 33342 (blue). Cells were treated for 72 h with media contains either PBS as control or Palbociclib (5µM). The staining shows apoptotic nucleus after Palbociclib application on both BE2C and SKNAS cells. Scale bar =250µM.*

4.2.8. Proliferation assessment of Palbociclib alone and in combination with RA

Palbociclib alone or in combination with RA induced changes in cell morphology on BE2C cells. Here we sought to investigate its effect on proliferation using Ki67 staining.

Prior to treatment, cells were seeded on coverslips inside 24 well plate as described in chapter 2. Cell then treated with Palbociclib and left for further 72hr at 5%CO_2 and 37C°. Following that, cells were observed first under the inverted microscope, initial observation showed lots of cells were floating in the top of the medium in each well in both cell lines except 5µM Palbociclib and BE2C. The number of floating cells increases where the concentration of the drug was higher.

Staining was carried out using Ki67 as primary antibody and Goat anti Rabbit as a secondary antibody and slide kept in dark overnight. Under the microscope it was pretty difficult to distinguish the nucleus of cells in both cell lines after Palbociclib treatment (except for 5µM in BE2C) because of the abnormality on cell shape and nuclei fragmentation. Therefore, proliferation quantification was only carried out for the 5µM concentration in BE2C cells (***Figure4.8 A&B***).

Interestingly, Palbociclib has different effect on BE2C cells from SKNAS; it induces differentiation and reduces cellular proliferation at the lowest concentration (5µM) in BE2C however for the SKNAS cells, Palbociclib promotes cell death.

As the 5µM concentration of Palbociclib indicates a significant reduction in cell proliferation, we sought to test this concentration in combination with RA (10µM) on BE2C cells. Overall, both Palbociclib alone and the combination treatment reduced the cell proliferation to 40% in BE2C cells compared to the control, suggesting there was neither a synergistic nor an additive effect between the two drugs (***Figure4.8 A&B***).

A

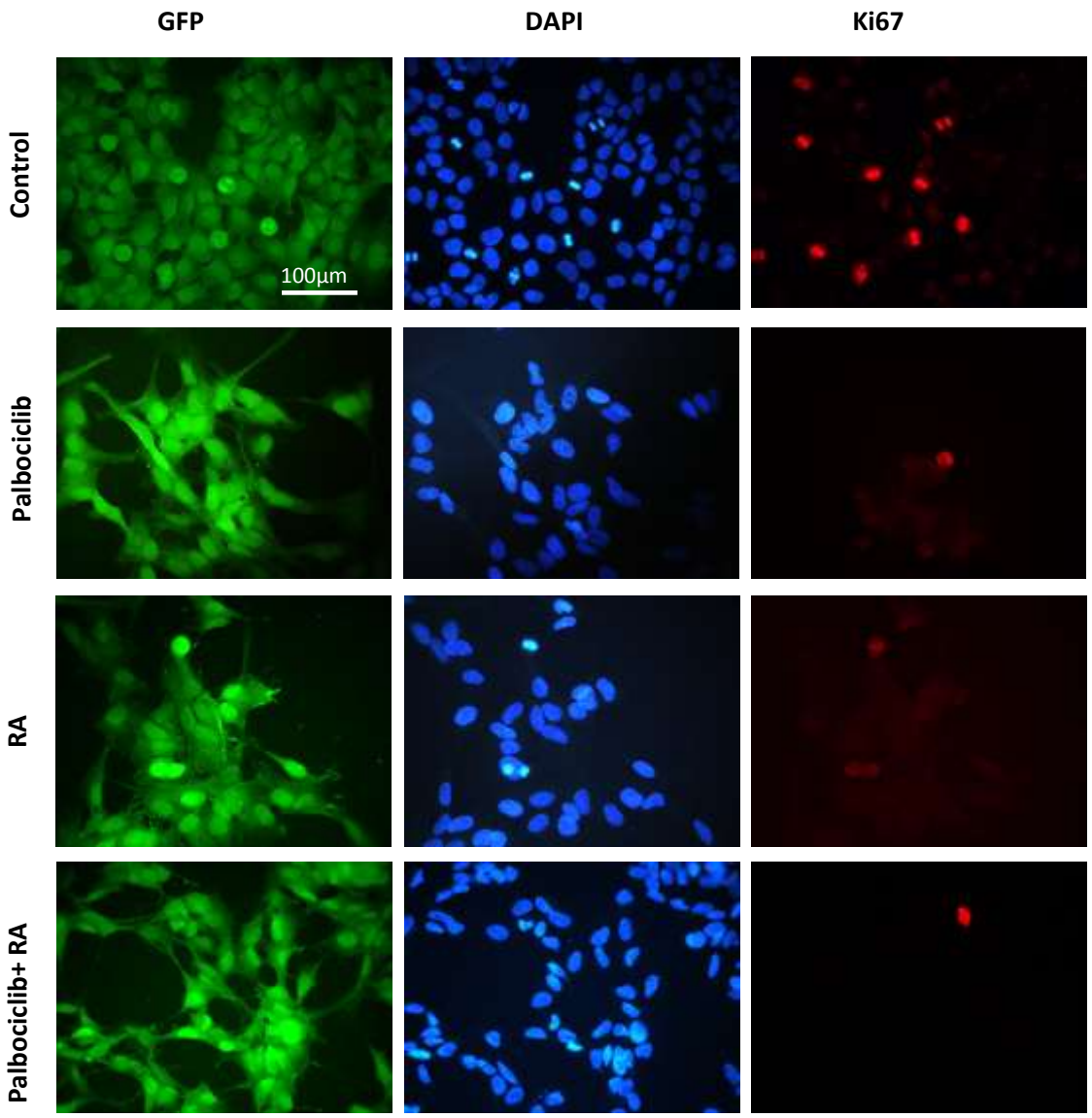

B

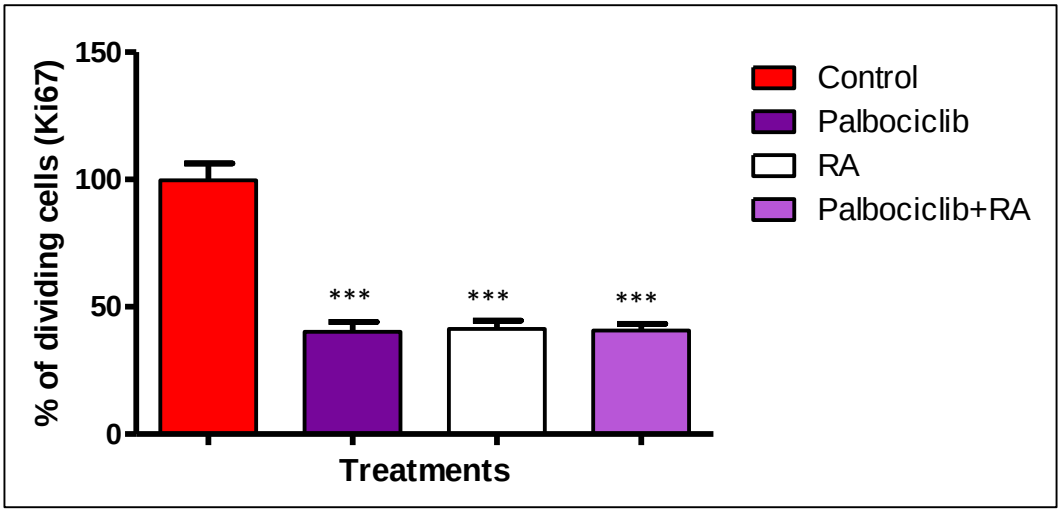

Figure4.10 Effect of Palbociclib alone and in combination with RA treatment on BE2C cell proliferation. ***A*** *GFP stained green, DAPI stained (blue) and Ki67 stained (red) BE2C cells following three days of treatment with 5μM Palbociclib alone or in combination with 10μM RA or DMSO.* ***B*** *displayed the percentage of proliferative cells after setting the control to 100%, proliferation index = number of Ki67 positive expressed as a percentage of the total number of cells divided by the % in the control. Data presented relative to control. Data represents mean ± SEM (n=9). Each bar represents the mean ± SEM of three biological replicates and at least 9 fields per experiment. ***P<0.001.*

4.2.9. Palbociclib effect on gene expression of differentiation markers in BE2C cells

To investigate the effect of Palbociclib alone and in combination with RA on gene expression, quantitative assessment of cellular differentiation was undertaken using qPCR. The same genes used in assessing the effect of BMOV and RA this chapter and in chapter 3 were used: KLF4, STMN4 and ROBO2 (Sung *et al.*, 2013) and MYCN (Huang and Weiss, 2013).

In previous results, we showed that Palbociclib alone and in combination with RA treatment reduced proliferation significantly and induced evident morphological changes at 5µM concentration. In support to these results, here we observed a significant change in the expression of the differentiation marker STMN4 and ROBO2 and stem cell marker KLF4 but not MYCN in Palbociclib alone and Palbociclib plus RA treated cells compared with control treated cells (***Figure4.10, 4.11***). In Palbociclib alone treatment, KLF4 decreased by 3 fold whereas STMN4 and ROBO2 increased by 4 fold (***Figure4.10***). Similarly, the combination treatment decreased KLF4 by 2 fold and increased STMN4 and ROBO by 5 fold. Although there was no significant difference between the single and the combination treatment, indicating that the combination do not have a synergetic or additive effects on gene expression (***Figure4.11***).

In keeping with the positive results found with Palbociclib as a CDK4/6 inhibitor on BE2C and SKNAS cells, we sought to investigate the effect of another CDK inhibitor on neuroblastoma cells.

A

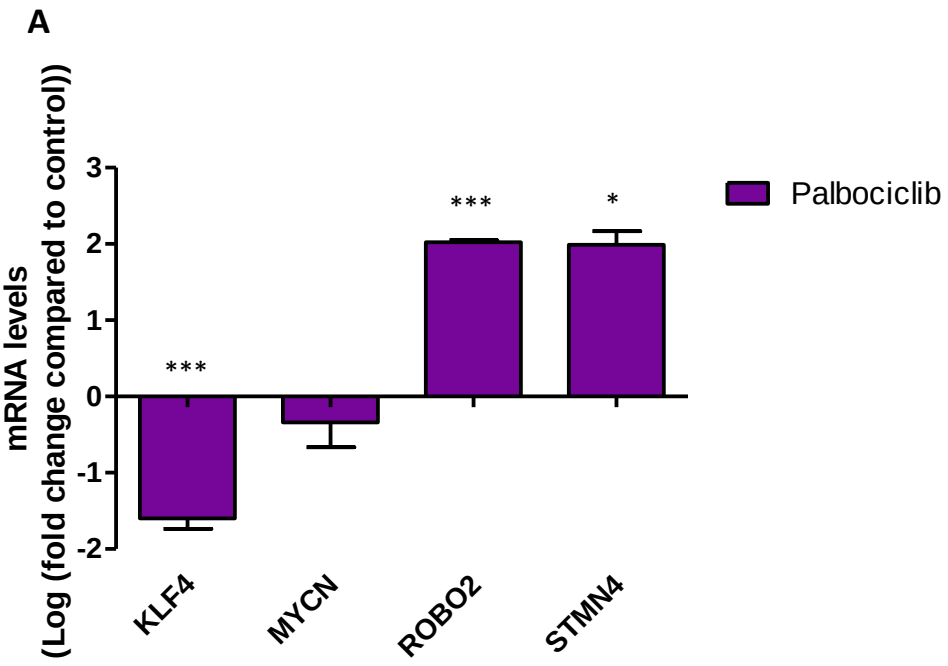

B

	KLF4	MYCN	ROBO2	STMN4
Fold change	-3	-1.21	4.07	4.26
Log fold change	-1.58	-0.28	2.03	2.09
Regulation	down regulated	no change	up regulated	up regulated

Figure4.11 The effect of Palbociclib on gene expression of BE2C cells. A *Relative mRNA levels for the target genes were determined by qPCR. Cells were cultured with 5µM of Palbociclib or PBS for 3 days. At least three independent experiments (n = 3) were analysed for each gene and relative mRNA levels are displayed relative to GAPDH, UBC and HPRT1 and normalised to cells cultured for 3 days with PBS (control). Each bar in the graph represents the log of normalised mean± SEM of three independent experiments. *P⩽0.05 and ***P⩽0.001 compared with control.* ***B*** *Table gives a summary of the qPCR data for the 4 target genes for BE2C cells.*

A

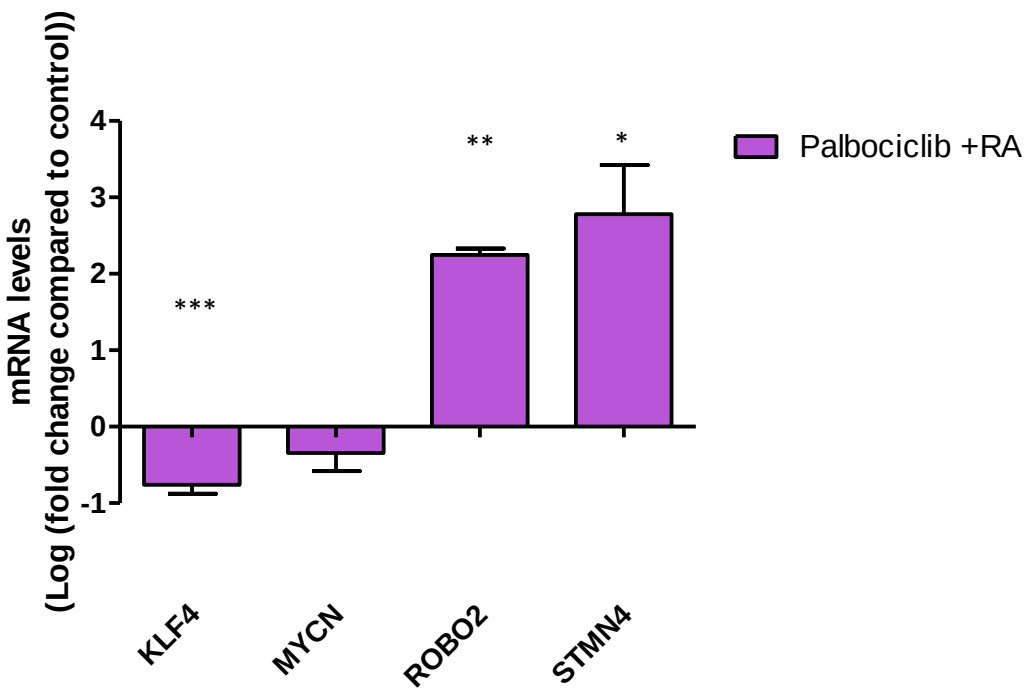

B

	KLF4	MYCN	ROBO2	STMN4
Fold change	-1.68	-1.24	4.76	4.94
Log fold change	-0.75	-0.31	2.25	2.30
Regulation	down regulated	no change	up regulated	up regulated

Figure4.12 The effect of Palbociclib in combination with Retinoic acid on gene expression of BE2C cells. A *Relative mRNA levels for the target genes were determined by qPCR. Cells were cultured with 5µM of Palbociclib+10µM of RA or PBS for 3 days. At least three independent experiments (n = 3) were analysed for each gene and relative mRNA levels are displayed relative to GAPDH, UBC and HPRT1 and normalised to cells cultured for 3 days with PBS (control). Each bar in the graph represents the log of normalised mean± SEM of three independent experiments. *P⩽0.05 **P⩽0.01 and ***P⩽0.001 compared with control.* ***B*** *Table gives a summary of the qPCR data for the 4 target genes for BE2C cells*

4.2.10. RO-3306 induces cell death in both BE2C and SKNAS cells

Both BE2C and SKNAS cells were cultured with RO-3306 for a period of 72hr at 0, 5, 10 and 20µM to determine the optimal concentration that has an effect on these cell lines. Cells then observed using Leica DMIRB microscope to identify the effect of RO-3306 on cell morphology prior to carrying out proliferation assessment.

Morphology assessment

As shown in ***Figure4 .13*** the response of both BE2C and SKNAS to RO-3306 was cell death at 5µm. A reduction of living cell was noticed to increase significantly as the concentration of RO-3306 increased. Following the observation of cell death by inverted microscopy, we sought to investigate the cell death/cell viably after applying the treatment of RO-3306 using MTT assay.

4.4.11. RO-3306 reduces cell viability in both BE2C and SKNAS cells

SKNAS and BE2C cells were seeded in cover slips inside 96 well plate at $0.5x10^5$ cells/ml for 24hr prior to drug administration. After 24hr, cells were treated fresh medium including 0, 1, 5, 10, and 20µM of RO-3306 in order to determine the cell availably following the treatment. RO-3306 treated cells with the presence of controls were incubated for 72hr at 5%CO_2 and 37C°. Following this, MTT assay was carried out as described previously. MTT results indicated that increasing the concentration of RO-3306 reduces the cell viability and prompts cell death as shown in ***Figure4.14***. In both BE2C and SKNAS cells, the cell viability has decreased by more than 40% compared to the control following the application of 5µM of RO-3306. At 20µM of Palbociclib, both BE2C and SKNAS cell viability has dropped significantly by more than 60% compared to the control.

In keeping with the morphology assessment and MTT assay results we sought to investigate the extent of cell death further following RO-3306 treatment using Annexin v staining.

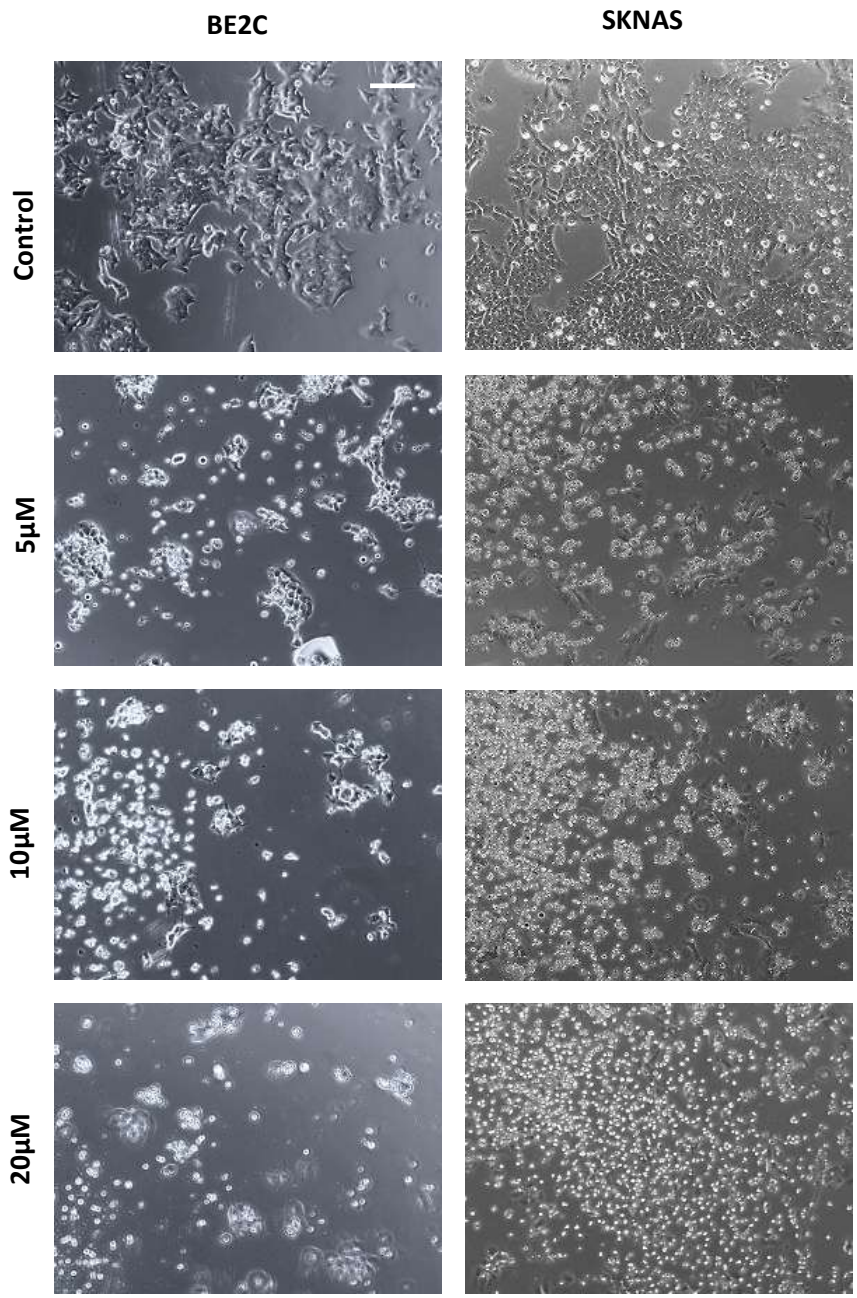

Figure4.13 The response of BE2C and SKNAS cells after 72hr of treatment with different concentration of RO-3306 (CDK1 inhibitor). *RO-3306 induced cell death at 5µM in both cell lines and this effect observed to be extensive at 10 and 20µM concentrations. Scale bar is 250µm.*

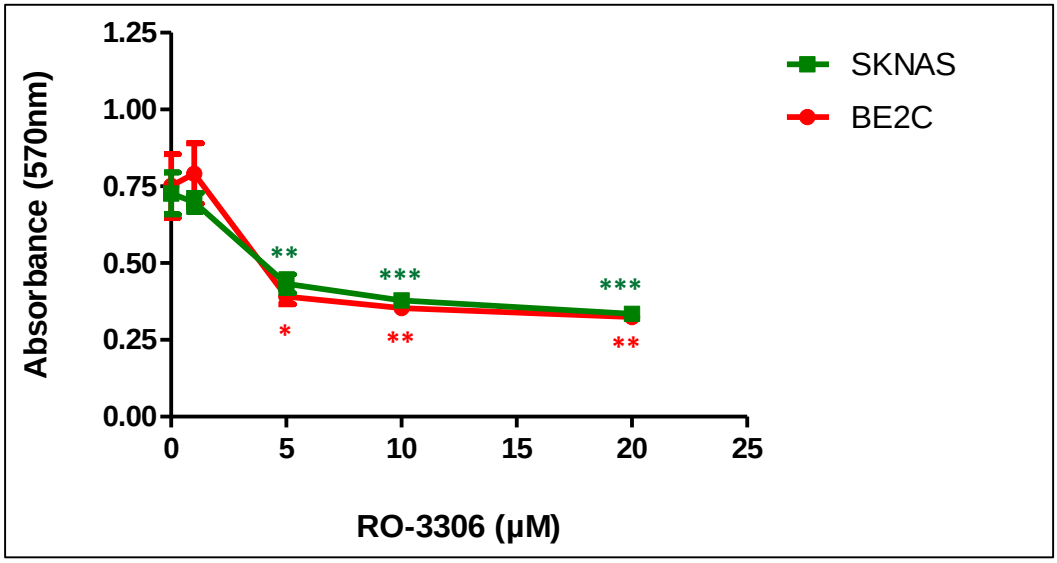

Figure 4. 14 Cytotoxicity of RO-3306 to Neuroblastoma cell lines (BE2C and SKNAS). *Cells were treated with different doses of RO-33306 for 72hr as indicated in the Materials and Methods. Green line is SKNAS and Red line is BE2C. The graph represents cell viability based on the MTT assay. Each point represents a mean value and standard error of 3 experiments with 3 replicates per concentration. Cell viability at 5, 10, and 20µM are significantly reduced in both cell lines compared to control according to ANOVA Tukey's test. *P⩽0.05 **P⩽0.01 and ***P⩽0.001.*

4.2.12 Cell death assessment following RO-3306

To further investigate the cell death of BE2C and SKNAS following RO-3306 treatment, we performed Annexin V staining. As mentioned previously in section 4.3.9, we used Annexin V to identify apoptosis event in cells. Cells were seeded as for the proliferation assessment. Apoptosis effect was noticed following the application of RO-3306 on both cell lines (***Figure4.15***).

To conclude, RO-3306 reduced cell viability and induced cell death in both MYCN-amplified cell line (BE2C) and non-MYCN amplified cell line (SKNAS). Interestingly, 5µM RO-3306, which is CDK1 inhibitor, has shown different effect on BE2C cells to that observed with Palbocilcib (CDK4/6 inhibitor) where induce differentiation.

In keeping with the effect of Palbociclib on SKNAS in terms of cell death, we decided to reduce the exposure time for both Palbociclib and RO-3306 to 24hr instead of 72 followed by 48 in normal media. Here, we sought to investigate whether 24hr of Palbociclib or RO-3306 can reduce the cell proliferation effectively and potentially prompt differentiation.

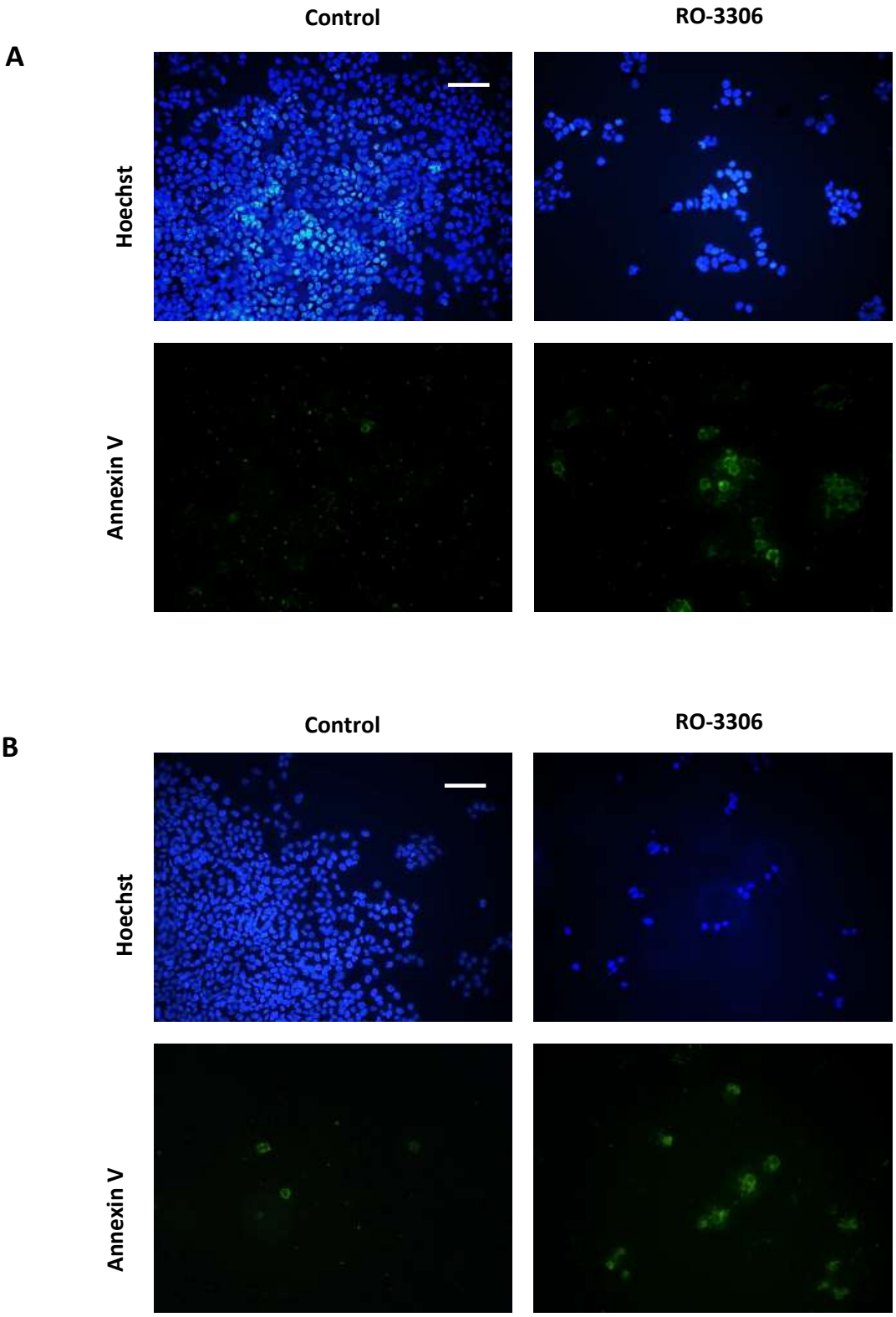

Figure4.15 RO-3306 induces apoptosis in BE2C and SKNAS cells. A *is BE2C* ***and B*** *is SKNAS. Immunofluorescent analysis of live BE2C and SKNAS cells using Annexin V-FITC Conjugate (green) and Hoechst 33342 (blue). Cells were treated for 72h with media contains either DMSO as control or RO-3306 (5μM). The staining shows apoptotic nucleus after RO-3306 application on both BE2C and SKNAS cells. Scale bar =250μM.*

4.2.13. Palbociclib and RO-3306 reduce cell proliferation of BE2C and SKNAS after 24hr treatment

Prior to treatment, cells were seeded on coverslips inside 24 well plate as described in chapter 2. Cell were then treated with 5µM Palbociclib (or PBS as a control) and RO-3306 (or DMSO as a control) and left for further 24hr at 5%CO_2 and 37C°. Following that, old medium contains drug was discarded; cells were washed and left with fresh normal medium for further 48hr.

To quantify cell proliferation, we performed Ki67 staining in all conditions. Cells were stained with a rabbit anti-Ki67 antibody and labelled with goat anti-rabbit (secondary antibody) conjugated with Alexa Fluor 594 (red) to enable identification of proliferating cells whilst counterstaining with DAPI allowed identification of the total number of nucleus cells present. Cell counts were performed comparing the number of Ki67 positive cells to the number of DAPI stained cells in the treated as well as in control cells (***Figure4.16 A***). Overall, both of Palbociclib and RO-3306 reduce the cell proliferation significantly in both cell lines. For instance, in BE2C, cell proliferation has been reduced by 45% and 60% compared to the controls following the administration of Palbociclib and RO-3306 respectively. In SKNAS, however, both Palbociclib and RO-3306 reduced cell proliferation by more than 40% (***Figure4.16 B***).

A

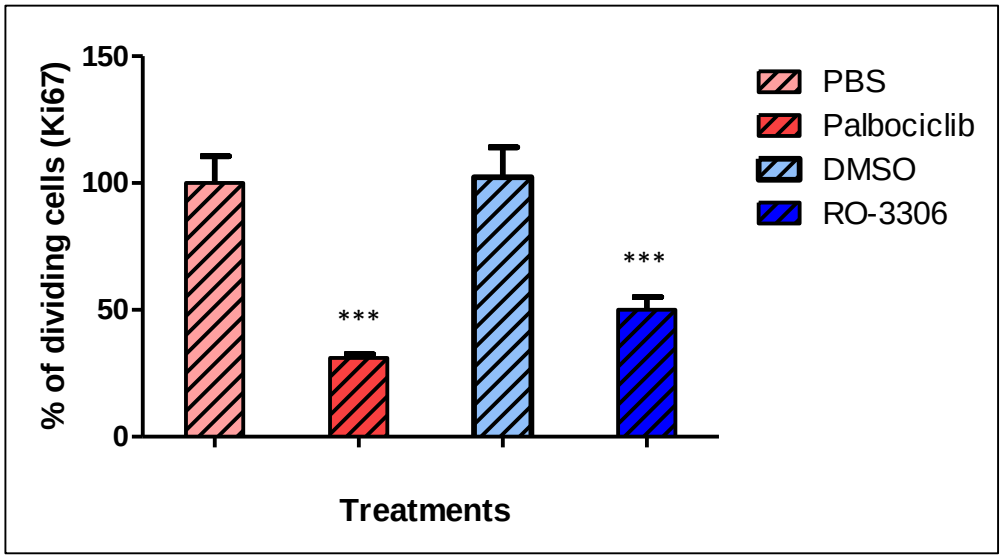

B

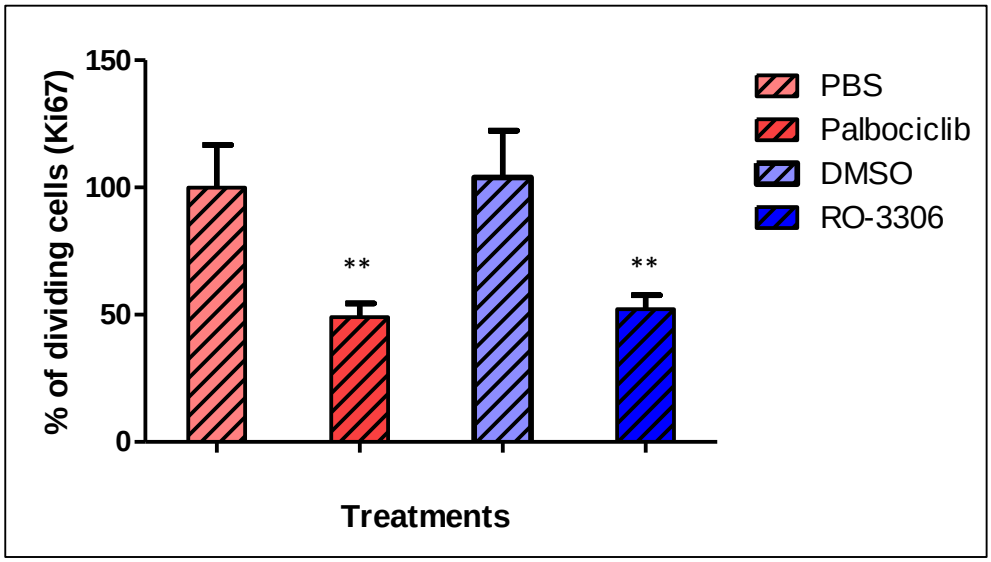

Figure4.16 Effect of Palbociclib and RO-3306 treatment on BE2C and SKNAS cell proliferation. ***A*** *displayed the percentage of BE2C proliferative cells after setting the control (PBS and DMSO) to 100%, proliferation index = number of Ki67 positive expressed as a percentage of the total number of cells divided by the % in the control. Data presented relative to control. Data represents mean ± SEM (n=9). Each bar represents the mean ± SEM of three biological replicates and at least 9 fields per experiment.* ***B*** *is same for SKNAS. **P⩽0.01.*

4.2.14. Effect of Palbociclib and RO-3306 on cell proliferation in BE2C and SKNAS tumours

Similar to RA treatment, we used two injections of 20µM (≡6mg/kg) Palbociclib and RO-3306 into the allantois sac at E11 and E13. This dose has been calculated in respect to culture experiments. The chick embryos tolerated the doses well with no significant change in embryo survival. Tumours were harvested and analysed at E14. To quantify proliferation following the treatments Ki67 staining was carried out on tumour sections.

A significant reduction in cell proliferation was revealed in response to both Palbociclib and RO-3306 (***Figure4.17 &18***). Palbociclib reduced cell proliferation of BE2C cells by 35% (***Figure4.17***). Surprisingly RO-3306 proved more efficient, reducing cell proliferation almost 50%.

Similar experiments were carried out with SKNAS cells. The reduction in proliferation was similar to that seen with BE2C cells (40-50%) although there was no statistical significance between the two inhibitors (***Figure4.18***).

Since RO-3306 reduces cell survival in culture we used TUNEL staining to test for apoptosis of cells in the tumours.

4.2.15 Cell death assessment in tumours following Palbociclib and RO-3306

Similar to proliferation assessment, TUNEL assay was carried out on tumour sections following the treatment to determine apoptotic (programmed) cell death by measuring nuclear DNA fragmentation. Surprisingly, unlike in culture, the number of apoptosing cells was very small. For BE2C cells it was less than 1% and neither inhibitor prompted a significant increase (***Figure 4.19***). For SKNAS cells, Palbociclib doubled the number of apoptosing cells to 1.3% but RO-3306 had no effect (***Figure4.20***).

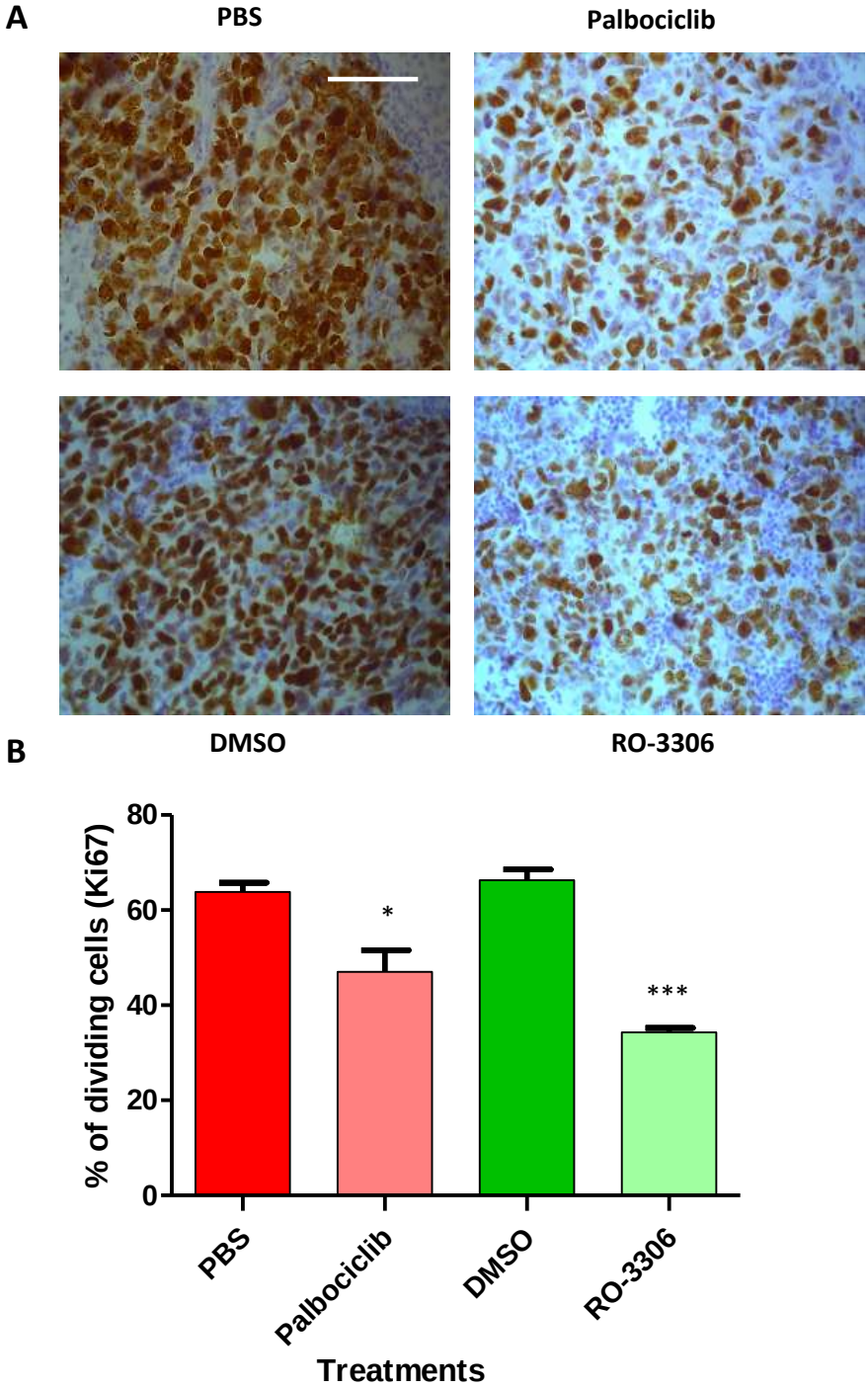

Figure4.17 Palbociclib and RO-3306 reduce cell proliferation of BE2C cells forming tumours. A *FFPE BE2C sections stained with Ki67 (brown). GFP-labelled BE2C cells were implanted on the CAM of E7 chick embryos. Treatments were two injections (20µM Palbociclib or 20µM RO-3306 CDK1i plus control (PBS or DMSO)) into the allantoic membrane of embryos at E11 and E13.* ***B*** *Quantification of Ki67-positive cells out of the total cell number indicates a reduction in cell proliferation following treatment with 20µM Palbociclib or 20 µM RO-3306 compared to their control. Each bar represents the mean ±SEM of three independent experiments and at least 9 fields counted per experiment, *P⩽0.05 and ***P⩽0.001 compared with the control. Scale bar is 100µm.*

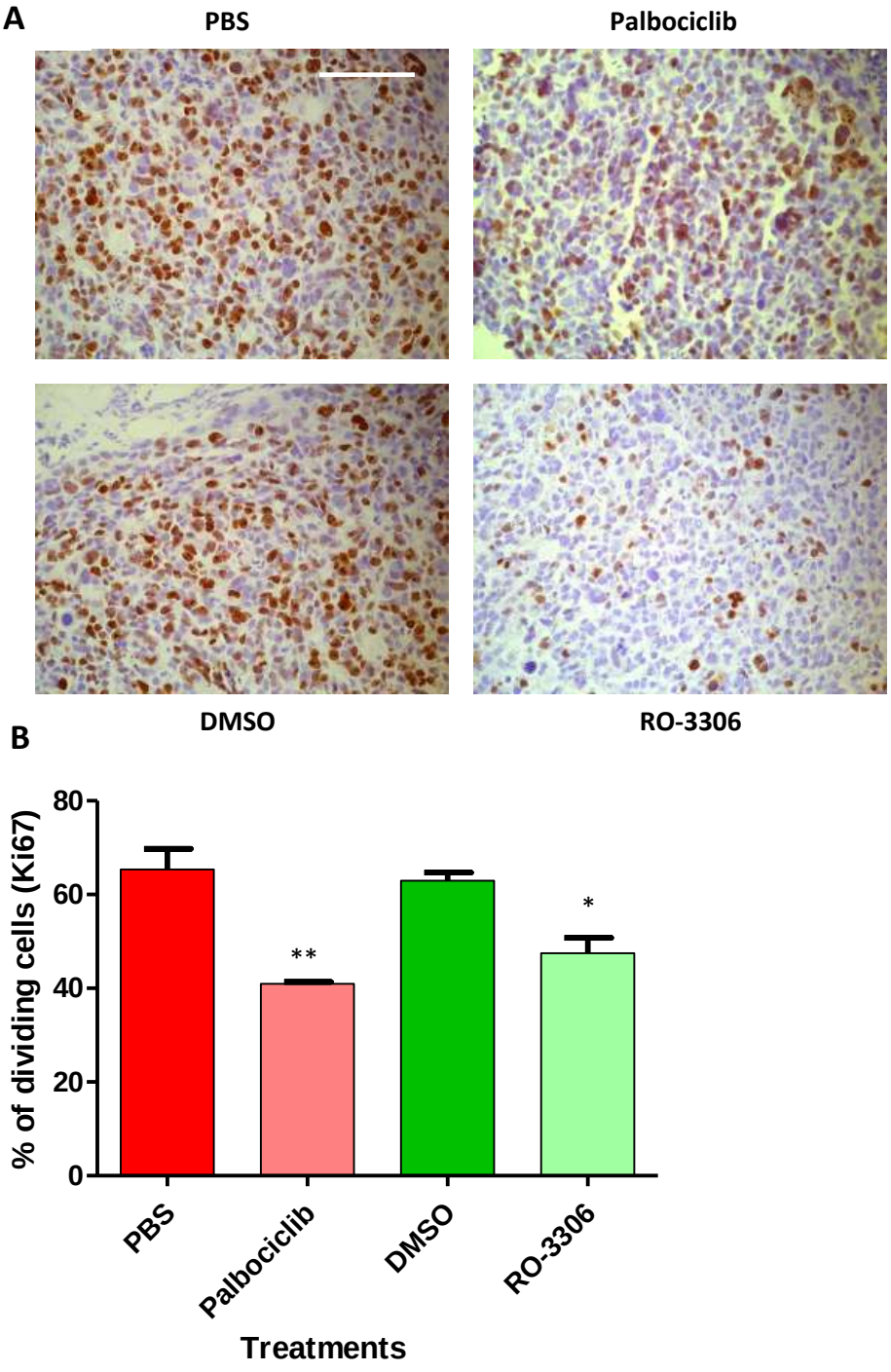

Figure4.18 Palbociclib and RO-3306 reduce cell proliferation of SKNAS cells forming tumours. A *FFPE SKNAS sections stained with Ki67 (brown). GFP-labelled SKNAS cells were implanted on the CAM of E7 chick embryos. Treatments were two injections (20µM Palbociclib or 20µM RO-3306 plus control (PBS or DMSO)) into the allantoic membrane of embryos at E11 and E13.* ***B*** *Quantification of Ki67-positive cells out of the total cell number indicates a reduction in cell proliferation following treatment with 20µM Palbociclib and 20µM RO-3306 compared to their controls. Each bar represents the mean ±SEM of three independent experiments (n = 3) and at least 9 fields counted per experiment, *P⩽0.05 and **P⩽0.01 compared with the control. Scale bar =100µm.*

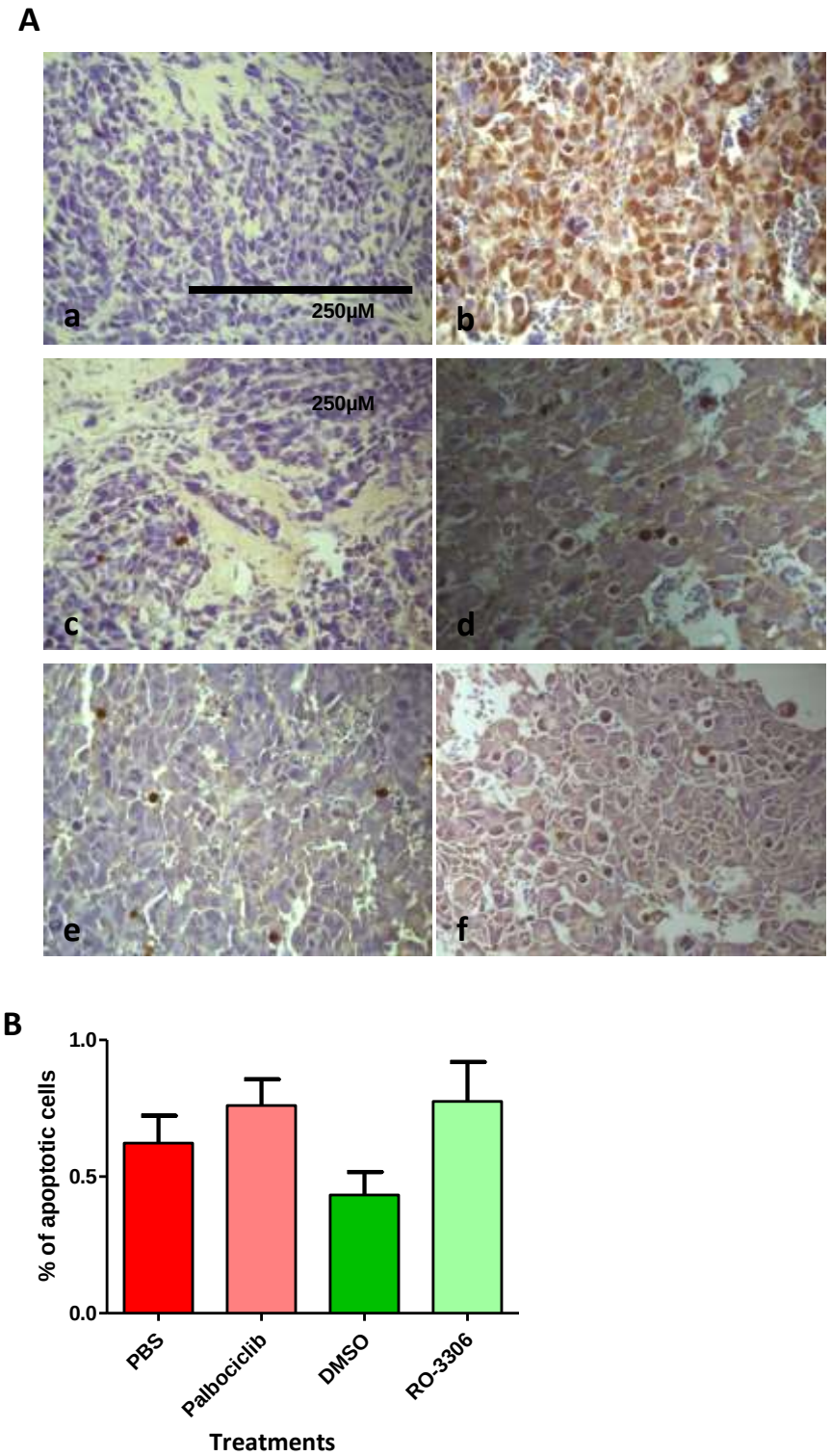

Figure 4.19 Palbociclib and RO-3306 effect on cell death of BE2C cells forming tumours. A *FFPE BE2C sections stained with TUNEL staining (brown).* ***a*** *and* ***b*** *indicate the positive (DNase-treated cells) and negative control of staining.* ***c*** *is DMSO,* ***d*** *is RO-3306,* ***e*** *is PBS and* ***f*** *is Palbociclib.* ***B*** *Quantification of TUNEL-positive cells out of the total cell number. Each bar represents the mean ±SEM of three independent experiments (n = 3) and at least 9 fields counted per experiment. Scale bar =250µm.*

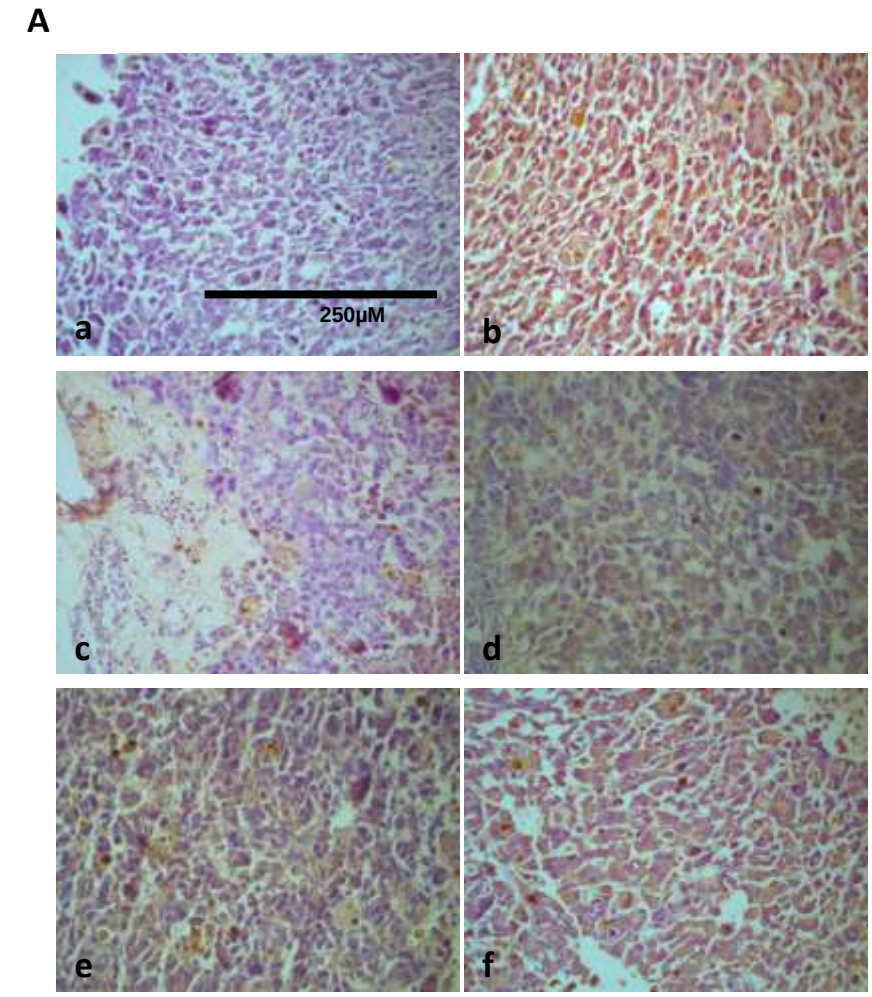

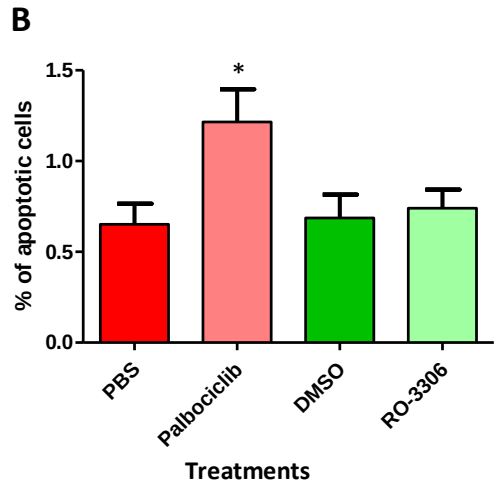

Figure4.20 Palbociclib and RO-3306 effect on cell death of SKNAS cells forming tumours. A *FFPE SKNAS sections stained with TUNEL staining (brown).* ***a*** *and* ***b*** *indicate the positive (DNase-treated cells) and negative control of staining.* ***c*** *is DMSO,* ***d*** *is RO-3306,* ***e*** *is PBS and* ***f*** *is Palbociclib.* ***B*** *Quantification of TUNEL-positive cells out of the total cell number. Each bar represents the mean ±SEM of three independent experiments (n = 3) and at least 9 fields counted per experiment, *P⩽0.05 and **P⩽0.01 compared with the control. Scale bar =250µm.*

4.3. Discussion

The chick embryo model has been proven to be a powerful tool which can be readily grow tumours and analyse the effect of drugs efficiently. Retinoic acid is a standard treatment used in clinic to treat high- risk disease although some patients did not respond to such treatment which means additional treatment is needed urgently. Here in this chapter we aimed to evaluate the effect of new and potential therapeutic molecules on neuroblastoma behaviour *in vitro* and *in vivo*.

We quantified the effect of vanadium-based PTP inhibitors such as BMOV in combination with RA *in vitro*, and found that BMOV alone or in combination with RA inhibits proliferation and induces change in gene expression of BE2C cells, but there was no significant difference between BMOV and RA. Thus we begun to investigate the effect of other targets and molecules such Cyclin- dependent kinase inhibitors. By introducing Palbociclib (CDK4/6 inhibitor) and RO-33306 (CDK1 inhibitor) into tumours formed on the CAM, the proliferation has been reduced significantly by25% and 50% respectively in BE2C tumours whereas in SKNAS tumours the reduction in proliferation 40% following Palbociclib treatment and 25% following RO-33306. We showed that CDK4/6 inhibitor changes the expression of differentiation markers in BE2C cells. The effect of CDK inhibitors was more pronounced than the effect of RA and in addition CDK inhibitors shown to have an effect on RA- resistant cell line, the SKNAS cells. Thus, Cyclin- dependent kinase inhibitors seen to have the potential to provide an alternative treatment for the RA- resistant neuroblastoma tumours.

4.3.1. Bis(maltolato)oxovanadium (IV)

In culture, three days of 10µMBMOV alone administration showed small morphological changes compared to the combination between BMOV and RA in BE2C cells. The combination of BMOV with RAis thought to enhance both differentiation and senescence in neuroblastoma cells (Clark, Daga and Stoker, 2013). The reduction in proliferation is thought to be tightly associated with the initiation of differentiation during normal development (Hardwick and Philpott, 2014). Hence, cell proliferation has been quantified to more accurately provide insight into the differentiation status.

The results indicated a reduction in cellular proliferation in BE2C cells following 72hr with 10μM BMOV alone or BMOV in combination with RA. Thus, it is suggested that differentiation is taken place.

Interestingly, Clark et al found that all the tested cell lines exhibited a robust p21 response to BMOV, and a further p21 elevation after the combination treatment, indicating the role of RA in inducing an increase of p21 (Clark, Daga and Stoker, 2013). Some *in vitro* studies reported a cytotoxicity of prolonged exposure to BMOV against three human cancer cells lines (Cruz et al, 1995). Nevertheless, in the same study, continuous exposure of human bone marrow cells to BMOV was seen to have only a slight myelosuppressive effect at concentrations of BMOV that were cytotoxic to all three tumour cell lines. These findings confirmed the potential anticancer effect of BMOV against cancer cells.

Change in the levels of target gene expression after exposure to BMOV alone was detected, although the change was not significant except for STMN4. However, BMOV in combination with RA showed a more pronounced change in the expression of the differentiation markers KLF4 and STMN4 and MYCN but not ROBO2 compared with DMSO treated cells. This supports what seen in the morphology as the combination treatment showed more of outgrowth neurites compared to the single treatment of BMOV.

As we showed the effect of BMOV *in vitro*, *in vivo* effect of BMOV could not be observed on tumours because of toxicity. We have used 12mg/Kg (40μM) of BMOV injected to the allantois cavity of chick embryos at E11 and E13. The survival dropped significantly following the first injection. These findings are in support to the toxicity observed with intraperitoneal administration of (200 mg/kg) BMOV in which rats were lethargic and under stress immediately following injection and this was followed by weight loss (Chakraborty *et al.*, 2006). Similarly, rapid bolus intravenously injections of BMOV at 10mg/kg to rats induced sluggish and mild cyanotic and had diarrhoea for 2-4hr after administration of the drugs (Jackson *et al.*, 1997). In contrast, 10mg/kg of BMOV; five times per

week for 4weeks, delays tumour progression and prolongs survival time in severe combined immunodeficient mouse xenograft models of human malignant glioblastoma (D'Cruz and Uckun, 2002). Despite numerous pharmacokinetic and toxicity studies in animal models, more clear understanding of the relevant biological and biochemical basis of vanadium is needed to the contribution in cancer treatment.

4.3.2. Palbociclib (CDK4/6 inhibitor)

RA-induce differentiation is commonly used in clinic to treat high-risk neuroblastoma patients however it has failed sometimes to treat resistant tumours. CDK4/6 is shown to be involved in the tumorigenesis of neuroblastoma (Cheung and Dyer, 2013; Rader *et al.*, 2013), suggesting that neuroblastoma tumours may result in response to activated oncogenes in the process of cell cycle regulation. Thus, inhibiting CDK4/6 could play a role in neuroblastoma treatment.

Within differentiation context and to tackle resistance to RA of neuroblastoma, we selected Palbociclib, a selective CDK4/6 inhibitor that shown promising antitumor activity in several clinical trials in other cancer types (Musgrove *et al.*, 2011). Currently, Palbociclib is used in clinic to induce differentiation and treat the aggressive form of breast cancer (Finn et al., 2015). In culture, we have shown that 5µMof Palbociclib alone or in combination with the well characterised drug RA (10µM) induced neurites outgrowth strikingly compared to control, and moreover, reduced proliferation in BE2C cells. Neuroblastoma cell lines have been shown to have a variable sensitivity to Palbociclib with BE2C being more resistant than most (Rihani *et al.*, 2015). Nevertheless Palbociclib proved to reduce cell proliferation and induce differentiation for BE2C cells and whilst for SKNAS cells it reduced cell viability and initiated apoptosis. Of note, BE2C cells harbour a p53 mutation which may be one of the reasons why this cell line showed less level of apoptosis (Carr *et al.*, 2006). Interestingly, at lower concentrations (1µm) in culture there was no change in either proliferation or decrease in cell viability.

Since Palbociclib reduced cell proliferation in BE2C cells and induced some morphological changes, it was logical to investigate the differentiation pathway. MYCN expression did not change in response to the treatment however KLF4 was decreased by 3 fold. Both STMN4 and ROBO2 were increased by almost 5 fold following the treatment of Palbociclib or Palbociclib with RA.

In support to previous result, although Palbociclib dose used in mouse models is far much than that we used (75-120mg/kg)(Bollard *et al.*, 2017; Cook Sangar *et al.*, 2017) our *in vivo* experiments showed that four times (20µM≡6mg/kg)) the concentration used in culture decreased cell proliferation significantly by 25% in BE2C and by 40% SKNAS tumours.

Interestingly, Palbociclib inhibited tumour progression and reduced proliferation by >80% in a preclinical trail performed on myeloma patients (Niesvizky *et al.*, 2018). Others, have found that inhibiting CDK4/6 using another CDK4/6 inhibitor such as LEE011 on MYCN amplified neuroblastoma tumours formed in murine xenograft models reduced the tumour growth effectively (Rader *et al.*, 2013).

4.3.3. RO-3306 (CDK1 inhibitor)

RO-3306, CDK1 inhibitor, was thought to prompt cell differentiation in neuroblastoma cell lines (Wylie *et al.*, 2015), however, in culture, RO-3306 at 5µM promoted cytotoxicity and apoptosis in both MYCN amplified and non-MYCN amplified neuroblastoma cells. CDK1 plays a key role in regulating the cell cycle by governing the transition from G2 to M phase, and the use of CDK1 inhibitors induce G2 arrest in various cell types including fibroblasts, retinal pigmented epithelial cells, lymphoma cells, and hepatoblastoma cells (Goga *et al.*, 2007). In this study, the authors showed that apoptotic events were only detected in the cells expressing MYC proto-oncogene. In neuroblastoma, MYCN expression level denotes aggressive and invasive form of neuroblastoma, and moreover MYCN amplification is the primary adverse prognostic indicator for neuroblastomas (Shimada, 2003). MYCN amplification is significantly associated with low level of p21 induction which is a CDK1 inhibitor, and failed G1 arrest in neuroblastoma cell lines (Tweddle *et al.*, 2001; Bell *et al.*,

2006). However, CDK1 inhibition by RO-3306 induced cellular apoptosis only in tumour cells with MYCN amplification but not in MYCN single copy cells (Otto *et al.*, 2009). In contrast to the previous study, we observed that CDK1 inhibitor induced cellular apoptosis irrespective to MYCN status. In support to our findings, a study conducted mRNA profiling of primary neuroblastoma tumours showed that high expression of CDK1 linked to significantly worse outcome and this was independent of the MYCN amplification status. Nevertheless, CDK1 expression was significantly higher in MYCN-amplified tumour. Of the tested genes, only CDK4 was significantly associated with MYCN amplification status (Schwermer *et al.*, 2015). In the same study, Schwermer et al also reported that viability was dropped significantly in neuroblastoma cell lines following knocking down CDK1 *in vitro,* and similar effect was noticed when using inhibiting CDK1 with RO-3306. Because the cell lines in our study were either an amplified or single copy of MYCN showed apoptosis after RO-3306, then MYCN copy number is not necessarily correlated with its expression levels (Cohn *et al.*, 2000; Hansford *et al.*, 2004; Chen, Tsai and Tseng, 2013).The copy number might not be the most critical factor in CDK1 inhibition induced apoptosis. However, the expression levels of MYCN might be more important (Chen, Tsai and Tseng, 2013).

Whilst two doses of 20µM (≡6mg/kg) of RO-3306 reduced cell proliferation significantly in tumours others demonstrated that using 4mg/kg, seven injection per mice at four-day intervals reduced tumour volume significantly (Yang *et al.*, 2016).

Surprisingly there was little or no increase in apoptosis *in vivo*. This may be due to differing concentration of inhibitor experienced by the cells however at lower concentrations in culture (1µm) there was no change in either proliferation or decrease in cell viability. Therefore, the cellular response to agents in 3D tumour environment can be different to that seen in 2D culture environment as described by others (Gandellini *et al.*, 2015; Anastasiou, 2017).

Overall, in order to boost the differentiation therapy of RA and to tackle the aggressive and resistant form of neuroblastoma tumours, it is highly significant employing new agents involved in mediating cell cycle and differentiation.

Chapter Five: Results III
Hypoxic preconditioning promotes metastasis of neuroblastoma cells and cyclin-dependent kinase inhibitors reverse this *in vivo*

5.1. Introduction

The ability of the chick embryo chorioallantoic membrane to efficiently support the growth of grafted-tumour cells greatly facilitates further analysis of drug efficacy against tumour growth. Upon tumour progression, cells become invasive and penetrate surrounding tissues to colonise distant tissues. This phenomenon is termed metastasis and involves several steps beginning with initial separation from the primary tumour, diffusion through surrounding tissues and penetration of their basement membranes, intravasatation into the blood vessels and survival within blood, and extravasation to proliferate in the metastatic site to form secondary tumours. It has been reported that more than 60% of neuroblastoma cases are invasive (Jogi *et al.*, 2002)and despite treatment advances in the last decade, metastasis is still one of the major obstacles to overcome. Hypoxia occurs in solid tumours such as neuroblastoma and has been suggested to promote reprogramming of neuroblastoma cells leading to metastatic dissemination and tumour aggressiveness (Herrmann *et al.*, 2015). Increased cancer dissemination has been shown to tightly associated with poorly oxygenated (hypoxic) regions in primary tumours (Lu and Kang, 2010). Taken together, in this chapter we aimed to develop a system to test drugs (Palbociclib and RO-3306) for ability to inhibit the metastatic process.

5.2. Aims of the chapter

The work described in this chapter aimed to examine the effect of RA, Palbociclib and RO-3306 on hypoxic and metastatic CAM formed tumours using both MYCN amplified and non-MYCN amplified neuroblastoma cell lines. Specifically:

- Test the effect of RA, Palbociclib and RO-3306 on hypoxic neuroblastoma cells
- Confirm the behaviour of hypoxic tumours specifically with respect to metastasis
- Analyse the effect of RA, Palbociclib and RO-3306 on hypoxic tumour.
- Assess metastasis in response to RA, Palbociclib and RO-3306.

5.3. Results

During normxic conditions, in cells, prolyl-hydroxylated 2 (pOH) (PHD2) activated-degradation and hypoxia factor inhibiting HIF (FIH) degrades and inactivate Hypoxia induced factor HIF-1α. In contrast, this mechanism is inhibited when cells are incubated under hypoxic conditions (1% O_2 for 3 days). This enables HIF-1α accumulation and activation permitting the expression of specific hypoxia induced genes. In the absence of hypoxia, HIF-1α may be stabilised by treating cells with Dimethyloxalyl Glycine (DMOG) for 24hr. DMOG is a PHD inhibitor hence its presence permits a direct HIF activation (***Figure5.1***).

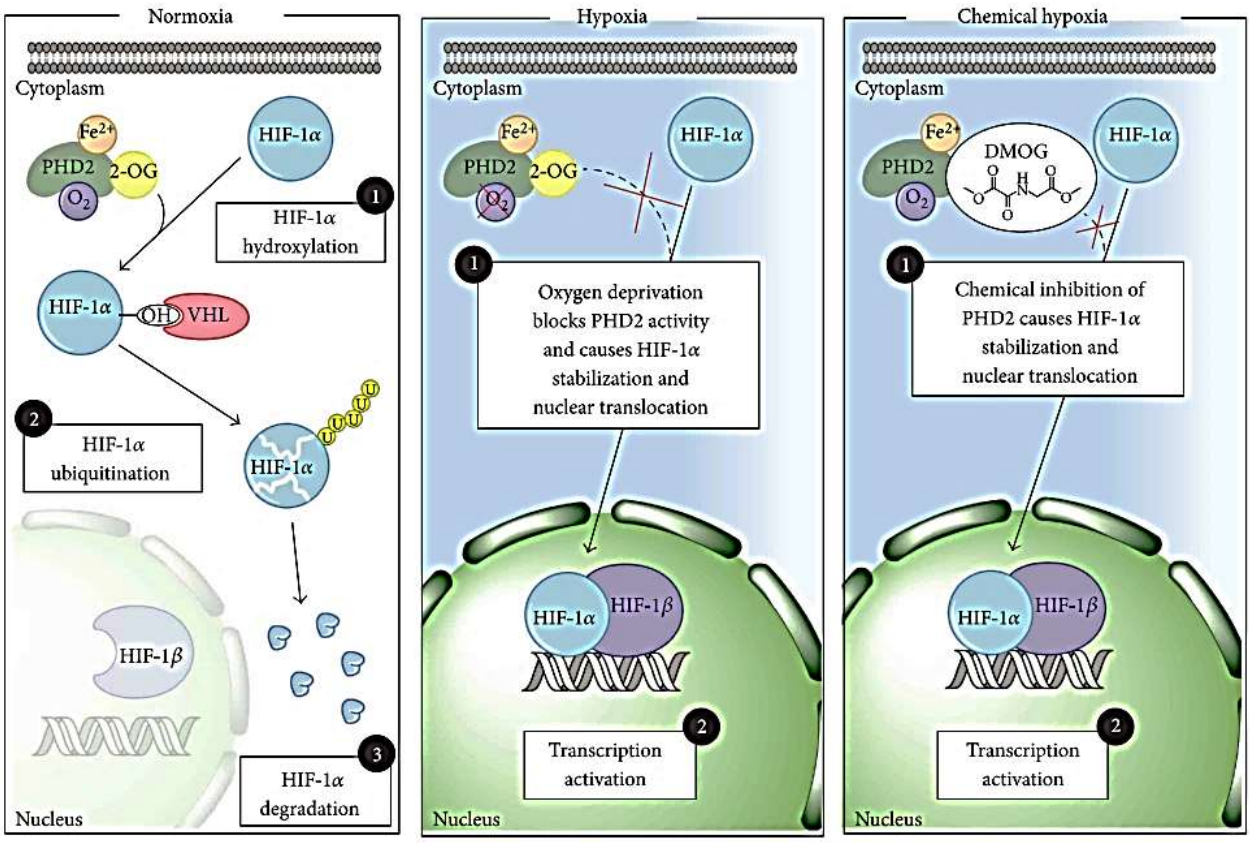

Figure5.1 Mechanisms of HIF-1α degradation and activation*. Left panel represents PHD2 targets HIF-1α for ubiquitination by the von Hippel–Lindau ubiquitin ligase complexand subsequent proteasomal degradation HIF-1α degradation by proteasome under normoxic conditions. Middle panel represents HIF-1α stabilization under hypoxic conditions mediated by the oxygen deficiency which causes the inhibition of PHD2 activity, leading to increased stability of HIF-1α, enhanced binding of coactivators, and increased transcription of HIF-1 target gene. The right panel represents chemical-induced HIF-1α stabilization under normoxic conditions by the inhibition of PHD2 activity through DMOG treatment. Adapted from (Menon et al., 2018).*

Furthermore, preconditioning neuroblastoma cell lines for three days in 1% oxygen or pre-treating them for 24hr with DMOG promote metastasis of cells into the embryo (Herrmann *et al.* 2015). We were interested to discover whether treatment with the differentiation agent (RA) or CDK inhibitors (Palbociclib and RO-3306) may have an effect in inhibiting metastasis.

5.3.1. Effect of the Retinoic acid on DMOG pre-treated BE2C cells

We started by assessing the effect of RA on cell proliferation of DMOG-treated BE2C cells *in vitro* to see whether RA has an effect on DMOG-treated cells. DMOG treatment increased cell proliferation significantly by 45% in DMOG- treated cells compared to non-DMOG treated cells (***Figure5.2***). Interestingly, 3 days with RA reversed this increase to the level of control cells but not RA treated normoxic cells.

DMOG- treated BE2C cells were sensitive to RA treatment. Because RA so far has not been reported to have any effect on SKNAS cells, we did not test RA on them and instead sought to investigate the effect of Palbociclib and RO-3306 on cell viability in both SKNAS and BE2C cells.

A

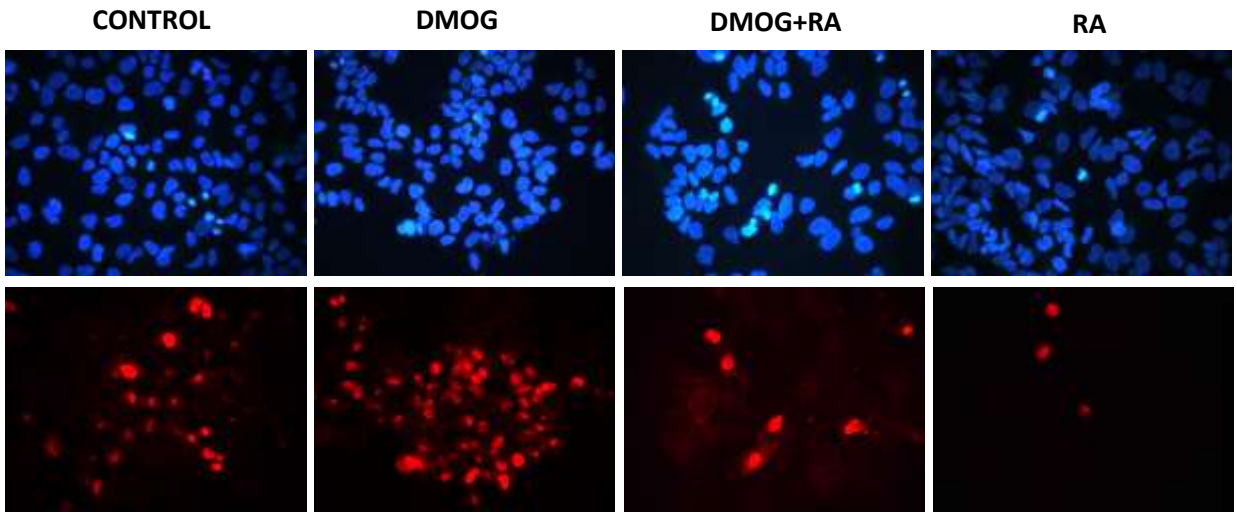

B

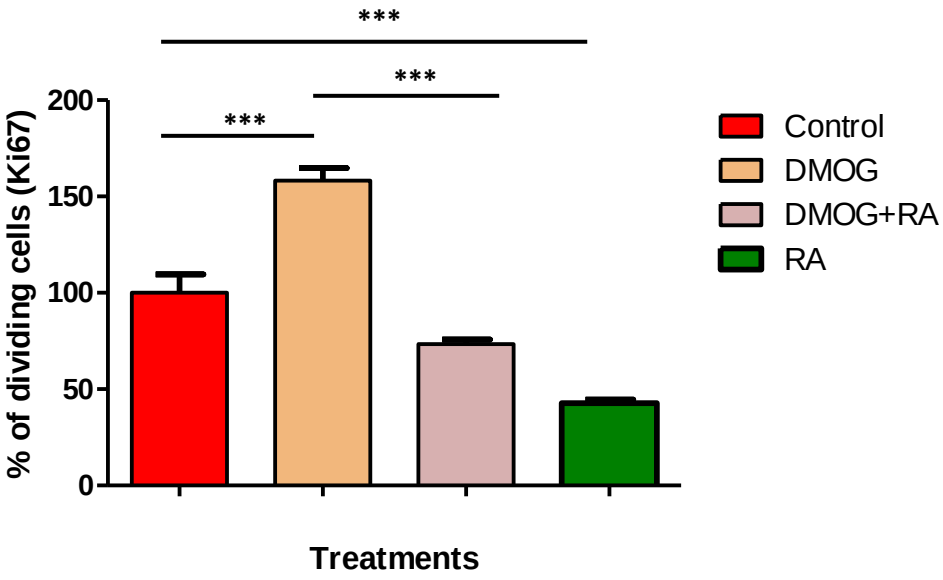

Figure5.2 The effect of Retinoic acid on DMOG-treated BE2C cells. A *BE2C cells were pretreated with DMOG for 24hr followed by 3 days with or without 10 µM ATRA. For comparison cells without DMOG were also treated with ATRA. Cells were then stained with Ki67 (red) and DAPI stained (blue) Scale bar =100 µM.* ***B*** *Quantification of percentage of Ki67-positive cells indicates a reduction in cell proliferation following treatment with 10 µM of ATRA in both DMOG- treated and control BE(2)C cells. Each bar represents the mean ±SEM of three independent experiments (n = 3) and at least 9 fields per experiment. ***p⩽0.001 compared with the control.*

5.3.2. Effect of Palbociclib and RO-3306 on the viability of DMOG pre-treated cells

The effect of Palbociclib and RO-3306 on the viability of normoxic cells was shown in the last chapter. In the presence of normoxic cells as a control, here we assessed the effect of Palbociclib and RO-3306 on the viability of DMOG pre-treated cells using MTT assay.

In RA-sensitive cell, BE2C cells, both inhibitors reduced the viability of cells irrespective of the DMOG treatment (***Figure5.3***). In normoxic BE2C cells, Palbociclib and RO-3306 reduced cell viability between 49% and 67% whereas to 38% and 23% in DMOG- treated BE2C cells, compared to their controls.

Similar results were observed in SKNAS cells, although RO-3306 was more effective than Palbociclib (***Figure5.4***). In normoxic SKNAS cells, Palbociclib reduced the cell viability by 42% whereas RO-3306 reduced it by 68%. However, in DMOG-treated SKNAS cells, Palbociclib decreased cell viability to 39% while RO-3306 by 45%.

Ultimately, Palbociclib and RO-3306 showed a pronounced effect on cell viability of both cell lines regardless hypoxic preconditioning.

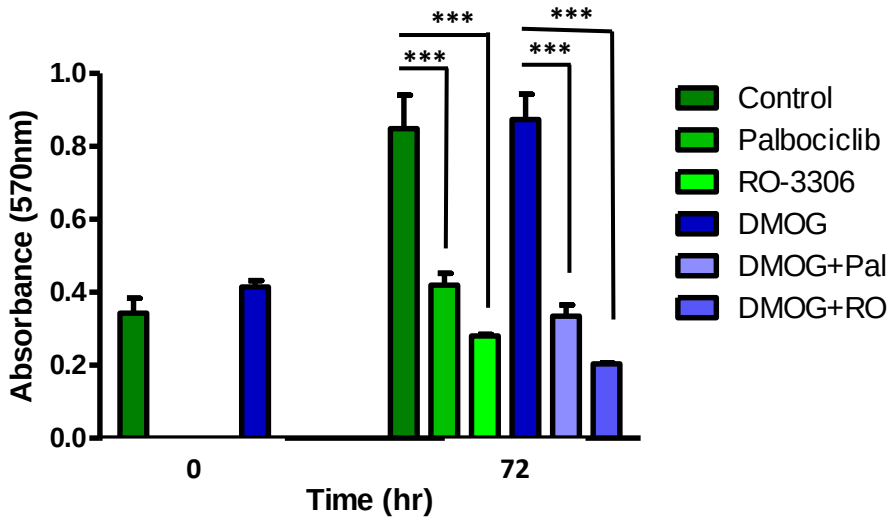

Figure5.3 The effect of Palbociclib and RO-3306 on cell viability of DMOG-treated and normoxic BE2C cells. *BE2C cells were grown +/- DMOG for 24 h and then treated with Palbociclib, RO-3306 or medium with now drug for 3 days. The number of viable cells was assessed using the MTT assay. Palbociclib and RO-3306 both reduced the cell number irrespective of whether the cells were precondition in DMOG. Displayed is the mean ±SEM of at least three independent experiments (n = 3), with 3 technical replicates in each treatment.*P⩽0.05 and **P⩽0.01 compared with the control.*

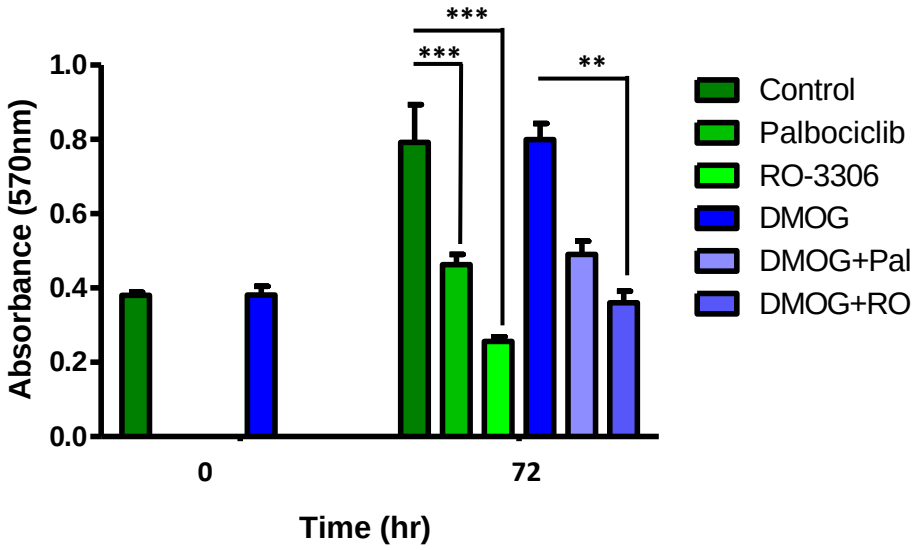

Figure5.4 The effect of Palbociclib and RO-3306 on cell viability of DMOG-treated and normoxic SKNAS cells. *SKNAS cells were grown +/- DMOG for 24 h and then treated with Palbociclib, RO-3306 or medium with now drug for 3 days. The number of viable cells was assessed using the MTT assay. Palbociclib and RO-3306 both reduced the cell number irrespective of whether the cells were precondition in DMOG. Displayed is the mean ±SEM of at least three independent experiments (n = 3), with 3 technical replicates in each treatment.*P⩽0.05 and **P⩽0.01 compared with the control.*

5.3.3. SKNAS and BE2C tumours formed on CAM model

5.3.3.1. Tumour differences – Normoxic versus DMOG or hypoxia-Precultured cells

SKNAS is found to form tumours efficiently without the need to trypsin addition but for comparison and to be consistent, we added 5µl of Trypsin to the CAM before implanting the SKNAS cells similar to the procedure for BE2C cells.

In the presence of normoxic controls, both SKNAS and BE2C cells were cultured with 0.5mM DMOG for 24hr at 37C° and 5%CO_2. Cells were then spun down and counted. Cells were grafted on CAM following the addition of trypsin and left to grow up to E14. Untreated BE2C cells were overall less efficient at forming tumours on the CAM than SKNAS cells (65% vs 85% for SKNAS). Following treatment with DMOG the efficiency of BE2C tumour formation fell to 30% whereas SKNAS. We therefore tried growing BE2C cells in 1% oxygen for 3 days. Following this modification, the efficiency of BE2C tumour formation returned to almost 65%.

On E14, tumour cells surviving upon the CAM were observed under the microscope, imaged and harvested. They were washed, imaged again in different planes determining tumour characteristics, and stored appropriately for further analysis.

Compared to normoxic SKNAS tumours, hypoxic tumours were found to be heavily vascularised. Some tumours depict haemorrhagic lesions forming upon the CAM, and moreover were often accompanied by a large sac filled with blood (***Figure5.5***). Although the primary tumour morphology was variable, they were often leaky and surrounded by haematoma, a morphology commonly present in neuroblastoma (Fletcher, 2013) (***Figure5.6***). For BE2C, however, no difference were noticed between hypoxic and normoxic BE2C tumours in terms of size and characteristics (***Figure5.7***).

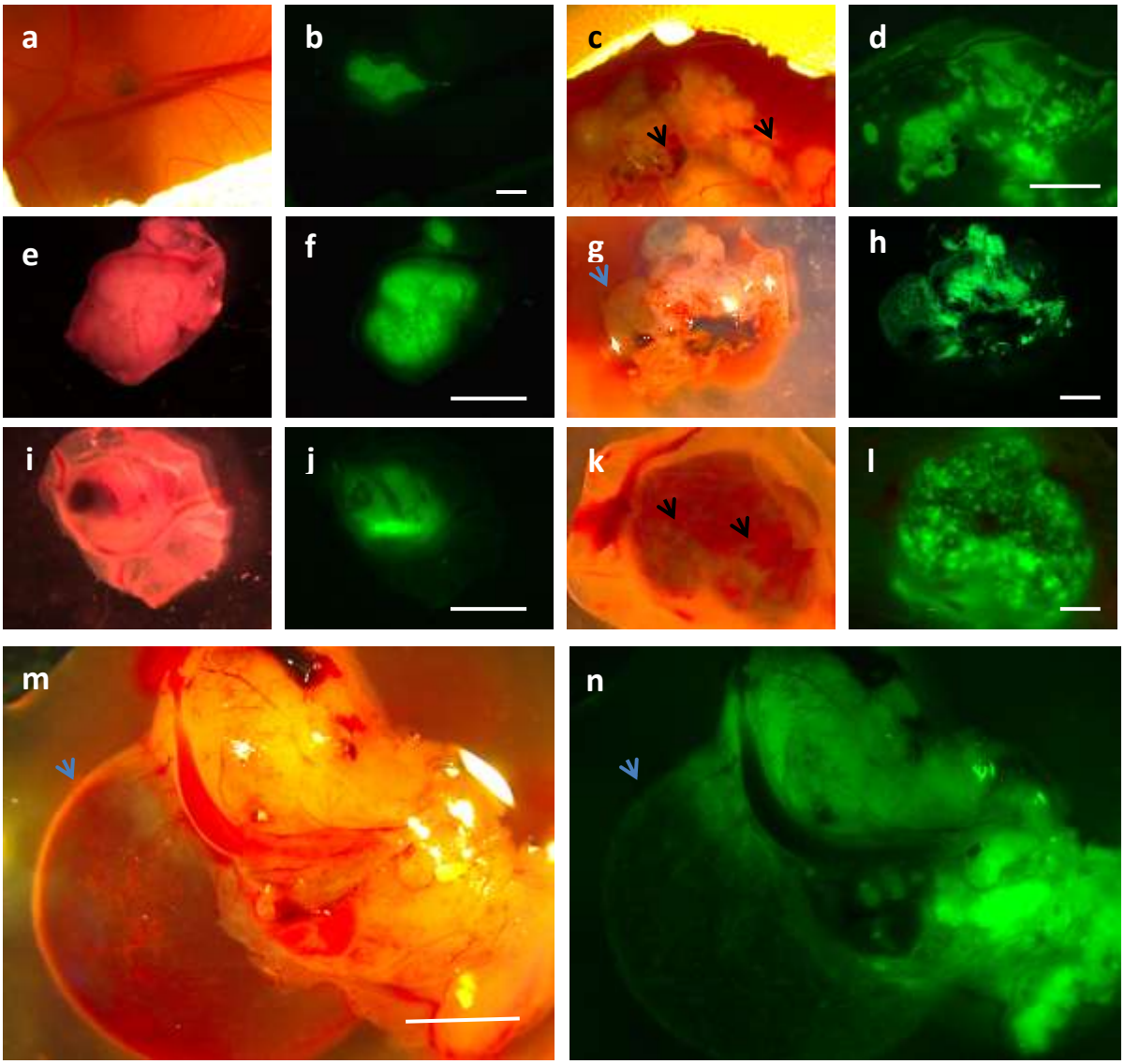

Figure5.17 SKNAS tumours formed on the CAM of chick embryo model. a,b,e,f,I and j *are tumours formed on the CAM from normoxic SKNAS cells.* ***c,d,g,h,k ,l,m and n*** *are tumours formed on the CAM from DMOG-treated SKNAS cells. Black arrows depict hematoma/haemorrhagic lesions. Blue arrows indicate big blood sac attached to tumours. Scale bar is 2mm.*

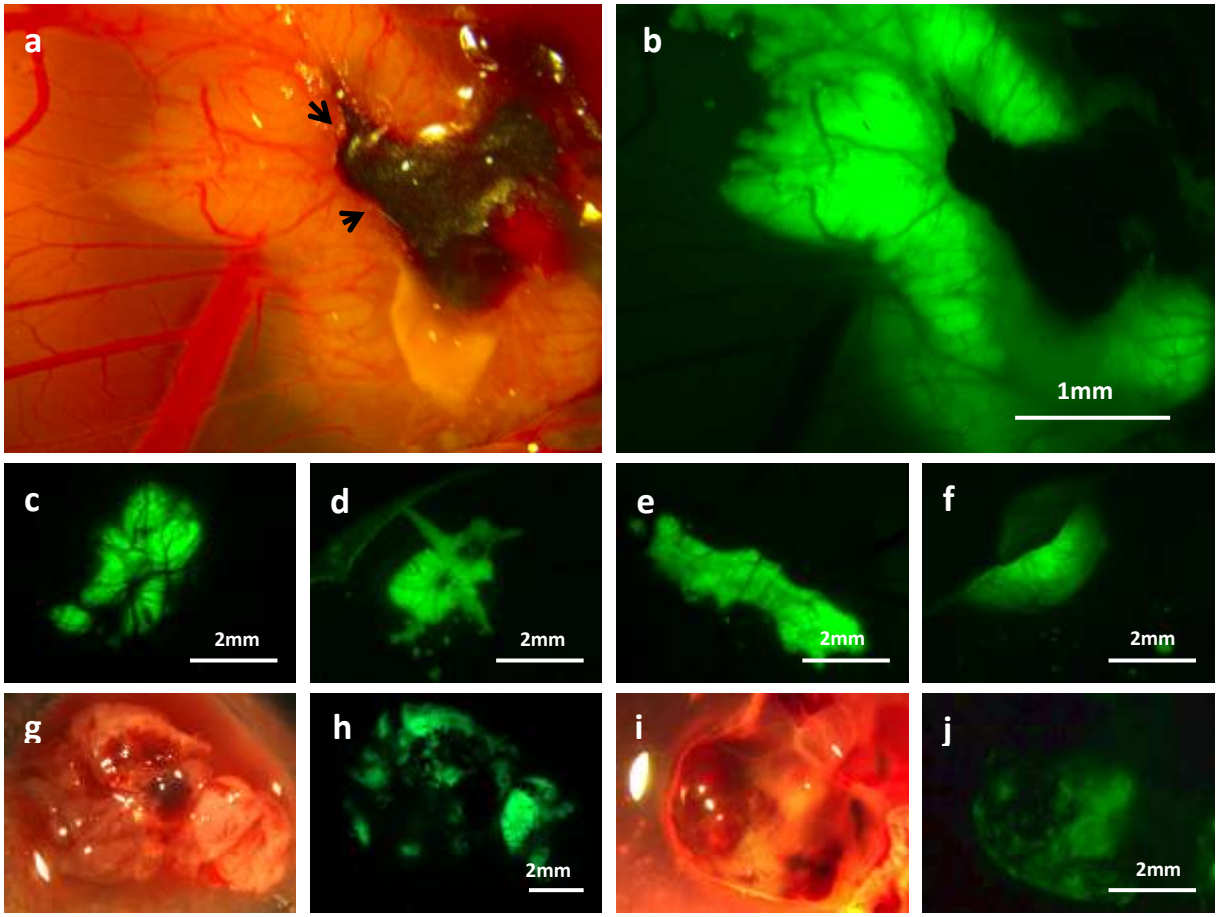

Figure5.6 Images of DMOG-treated SKNAS tumours formed on the CAM of chick embryo. a and b *in vivo GFP and corresponding bright field .* ***c, d,e and f*** *are in vivo GFP tumours shows variable morphology of SKNAS tumours formed on the CAM.* ***g and i*** *are bright fields of dissected tumours with their corresponding GFP* ***, h and j****. Black arrows depict a leaky tumour.*

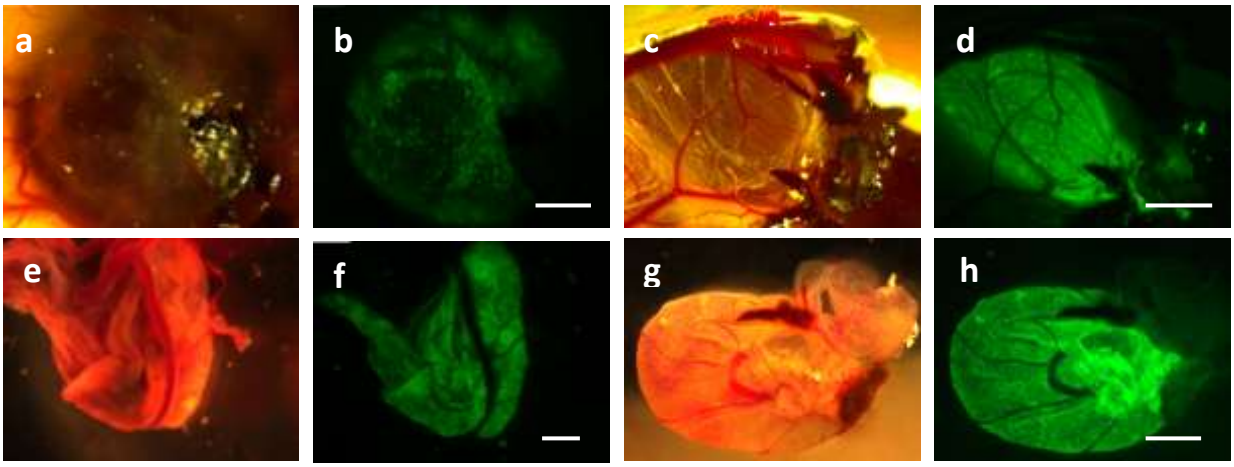

Figure5.7 BE2C tumours formed on the CAM of chick embryo model. a-d *are in vivo CAM tumours.* ***e-h*** *are dissected tumours****. a,b, e and f*** *are normoxic BE2C tumours formed on the CAM before and after dissection .* ***c,d,g and h*** *are hypoxia-treated BE2C tumours formed on the CAM in vivo and following dissection. Scale bar is 2mm.*

5.3.3.2. Invasion differences – Normoxic versus hypoxic tumours

Following identification and harvesting of SKNAS and BE2C tumours. The chick was decapitalised and removed from egg shell, washed 3 times with DPBS and placed in a clean 60mm petri dish. At this point, the chick was systematically dissected with each organ carefully removed and analysed for the presence of migrated/ invading tumour cells and more importantly, to identify metastatic secondary tumours.

Rigorous examination of all chick tissues/ organs was unsuccessful in identifying metastatic SKNAS or BE2C cells precultured in normoxia. Therefore, although the CAM was proven to be an excellent supporter of normoxic tumorigenesis, formation of metastatic secondary tumours did not occur within the chick over 7 days post-implantation. Invasion could not be found in any organ or tissue of the chick embryo upon implantation of normoxic precultured SKNAS or BE2C cells as had been seen previously.

In contrast, both DMOG-treated SKNAS and hypoxia –preconditioned BE2C cells were successful in forming tumour metastasis. Cells had the ability to migrate and invade embryonic tissues or organs. Subsequently this resulted in the formation of multiple metastatic foci. Highly favoured locations for tumour cell invasion were the intestines, adjoining tissues in the trunk and crucially, the liver which is a very common site for tumour metastasis in patients with neuroblastoma. Other less frequently affected regions of the embryo were gizzard and meninges (***Figure5.8***).

Although, we induced hypoxic effect pathologically for 24hr using 0.5mM DMOG for BE2C and physiologically in SKNAS using hypoxia chamber equipped with 1% O_2 for 3 days, there were no significant difference between the two approaches in tumorigenesis and invasion induction (***Figure5.9***).

Location of Metastastic deposits		Frequency of Presentation
Gizzard	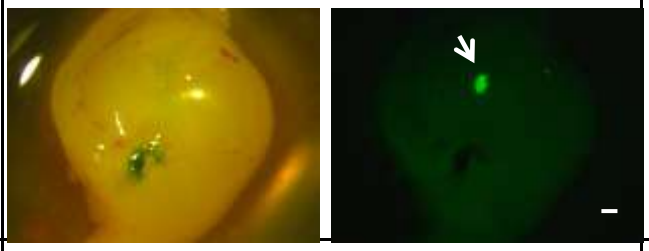	32%
Intestine		75%
Liver	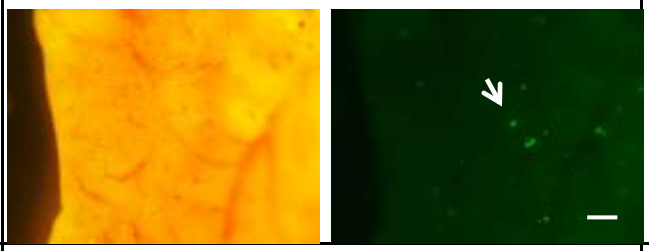	80%
Trunk	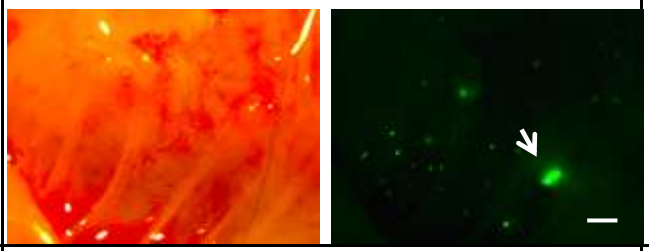	65%
Meninges	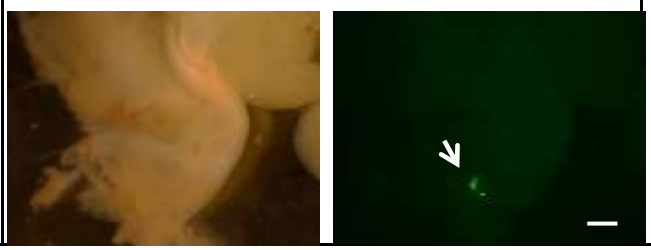	26%

Figure5.8 Invasion of organs/tissues following implantation of DMOG-treated SKNAS and hypoxia-treated BE2C. *Left side is bright field images, right side is GFP images. All embryos with CAM tumours formed from DMOG-treated SKNAS and hypoxia-treated BE2C were dissected at E14 and the percentage of metastatic cells in each organ or tissue was calculated. A minimum of 25 embryos per condition was analysed (n=25-30). GFP panel exhibits the metastatic foci proliferating within chick organs. Invasion on the liver and intestinal mesentery was the highest among other organs and tissues. Scale bar is 100um.*

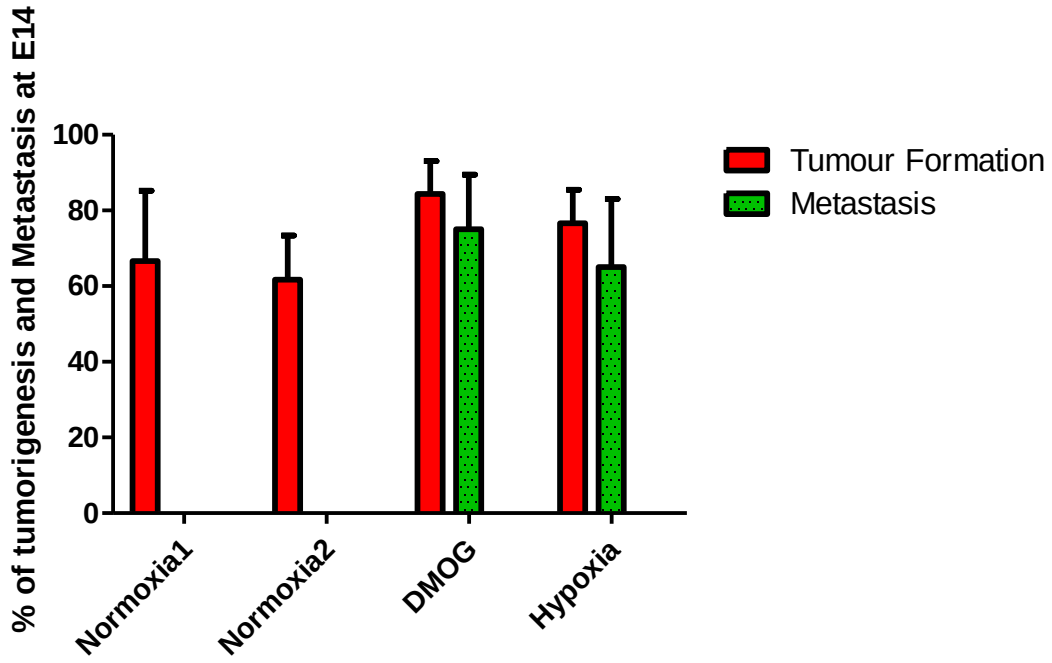

Figure5.9 SKNAS and BE2C tumourigenesis and metastasis assayed at E14. *Tumourigenesis (red), Metastasis (green). Normoxia1 is the control for DMOG-SKNAS treated. Normoxia2 is the control for hypoxic BE2C. Tumourgensis occurred regardless of preculture condition in both cell lines. Metastasis in each condition was investigated over 3 independent experiments, n>15 per condition. Error bars express Standard Error (SE).*

5.3.4. Effect of Retinoic acid, Palbociclib and RO-3306 on hypoxic tumours

5.3.4.1. Quantifying tumour invasion for drug delivery

Before testing the effect of the drugs we first screened embryos at E9 – E13 for tumour formation. Next, embryos were dissected to determine time taken from implantation of cells to the first metastatic cells being observed. Tumour formation could first be detected at E10 for SKNAS and E11 for BE2C, and no metastasising cells were ever observed before E10 and were more often after E12. Following this observation, we therefore changed the dose regime from injections at E11 and E13 to E10 and E12 to ensure that the drugs were introduced before cells had begun to metastasise. RO-3306 and Palbociclib were used as 20µM whereas RA was used as 40µM.

5.3.4.2. Effect of drugs on proliferation in DMOG- treated SKNAS and hypoxia-treated BE2C tumours

Following Palbociclib and RO-3306 treatment at E10 and E12, DMOG - treated SKNAS tumours were harvested and analysed for Ki67 staining at E14. Approximately 80% of tumour cells were Ki67 positive in the control tumours (PBS or DMSO) which was similar to the proportion of Ki67 positive cells in tumours that had never been exposed to DMOG (***Figure4.16A & Figure5.10***). Both of Palbociclib and RO-3306 treatments reduced cell proliferation in tumours by between 24-39%.

For BE2C, Retinoic acid, Palbociclib and RO-3306 were injected to the allantois of embryos at E10 and E12, and the cell proliferation in the tumours was assessed by Ki67 staining at E14. Approximately 65% of tumour cells were Ki67 positive compared to 70% for cells grown in normoxia (***Figure4.16B & Figure5.11***). As shown in ***Figure5.11*** approximately 8% decrease in proliferation was observed following RA treatment compared to 12% decrease with Palbociclib and a 14% decrease with RO-3306, all reductions are not significant though. Thus a similar but smaller trend is observed with these agents on tumours formed from cells grown in normoxia.

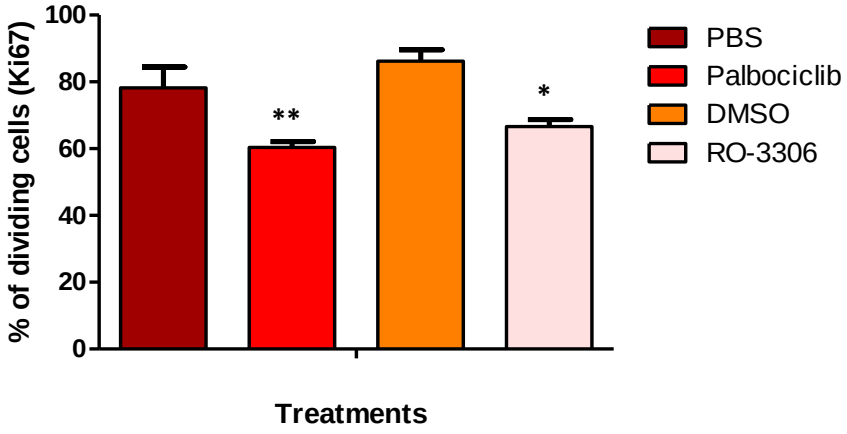

Figure5.10 The effect of Palbociclib and RO-3306 on cell proliferation of DMOG-preconditioned SKNAS cells in tumours. *SKNAS cells were pre-treated with DMOG for 24 hr prior to implantation at E7 on the CAM of chick embryos. Two doses of 20μM of Palbociclib and RO-3306, or PBS, or DMSO as control respectively were made up to 200μl injected into the allantoic sac of embryos at E10 and E12. Tumours were sectioned and stained for Ki67. The percentage of Ki67 positive cells is shown and each bar represents the mean ±SEM of three independent experiments (n = 3) and at least 9 fields per experiment.*P⩽0.05 and **P⩽0.01 compared with the control.*

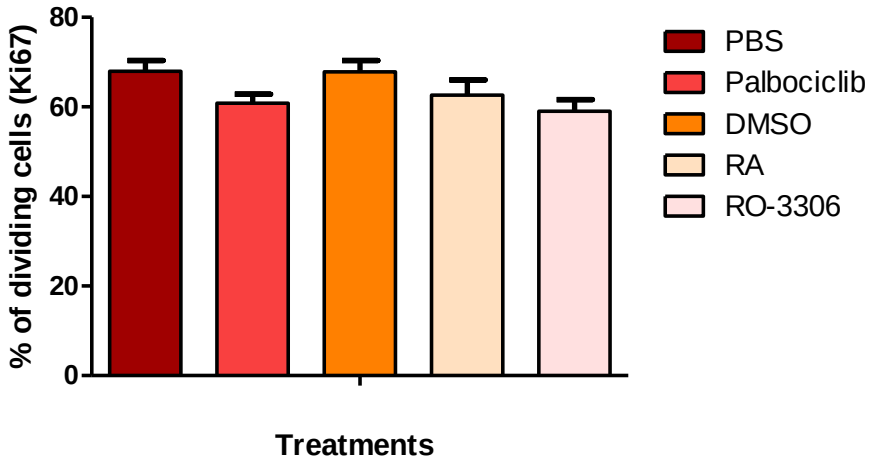

Figure5.11 The effect of Retinoic acid, Palbociclib and RO-3306 on cell proliferation of hypoxia-preconditioned BE2C cells in tumours. *BE2C cells were cultured in 1% O_2 for 3 days prior to implantation at E7 on the CAM of chick embryos. Two doses of 40μM RA or 20μM of Palbociclib and RO-3306 or DMSO, or PBS as controls were made up to 200μM were injected into the allantoic sac of embryos at E10 and E12. Tumours were sectioned and stained for Ki67. The percentage of Ki67 positive cells is shown and each bar represents the mean ±SEM of three independent experiments (n = 3) and at least 9 fields per experiment.*

5.3.5. Effect of drugs on metastasis

DMOG-treated SKNAS cells were treated with either RO-3306 or an equivalent volume of DMSO. Injections at E10 and E12 reduced metastasis from 95% (no injection) to 25% for both DMSO alone and RO-3306. DMSO above 100µl in total is reported to compromise chick survival (Wyatt and Howarth 1976) and although chick survival was not affected we concluded that a final volume of 130µl might be affecting the ability of tumour cells to metastasise. Next we gave a single injection of RO-3306 at E10 and as shown in ***Figure5.12*** a reduction of embryos with metastasis from 80% (with 65ul of DMSO) to 33% (with RO-3306) was observed. Palbociclib was dissolved in PBS but for comparison we also gave only one injection at E10. Here the metastasis was reduced from 92% to 44%.

Similar experiments were conducted with BE2C cells and again RO-3306 reduced metastasis by almost 60% while Palbociclib reduced metastasis by 56% (***Figure5.13***). RA could be introduced into the allantoic sac in 28µl of DMSO so the effect of one and two injections was compared. One injection reduced metastasis from 80% to 60% while two injections reduced it from 64% to 27% (***Figure5.14***).Thus RA was less efficient at reducing metastasis than either of the CDK inhibitors but it was interesting that the 2nd injection was able to significantly reduce metastasis supporting the notion that metastasis was gathering pace between E12 and E14 in this model.

In conclusion, all drugs were showing a significant tendency to inhibit invasion and metastasis of CAM tumours. At this point, because of time limitation, we sought to investigate the effect of only RO-3306 on gene expression of hypoxic CAM tumours.

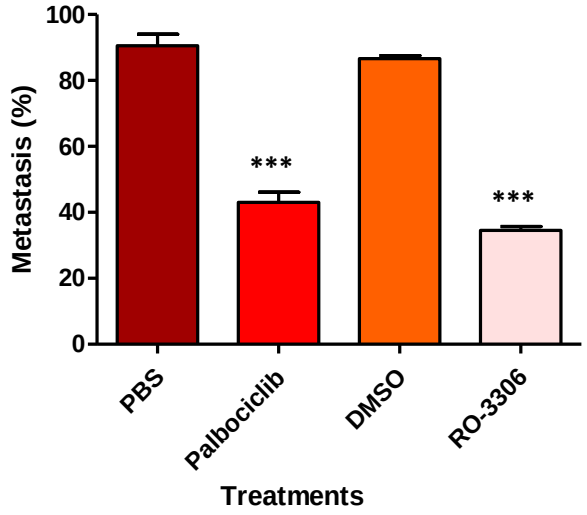

Figure5.12 The effect of Palbociclib and RO-3306 on SKNAS metastasis. *Embryos with SKNAS cells implanted on the CAM at E7 were treated with a single injection of 20µM Palbociclib and RO-3306 made up to 200µl or PBS or DMSO at E10. All embryos with CAM tumours formed from DMOG-treated SKNAS were dissected at E14 and the percentage of embryos with metastatic cells for each treatment was calculated. The percentage of metastasis is shown and each bar represents the mean ±SEM of three independent experiments and a minimum of 15 embryos per condition was analysed (n=15-18). ***P⩽0.001 compared with the control.*

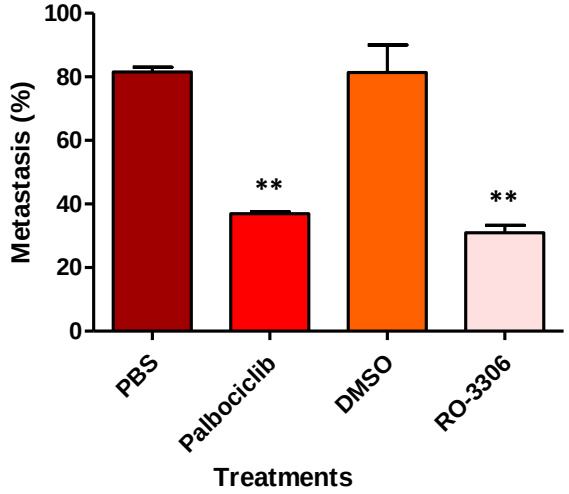

Figure5.13 The effect of Palbociclib and RO-3306 on BE2C metastasis. *Embryos with BE2C cells implanted on the CAM at E7 were treated with a single injection 20µM Palbociclib and RO-3306 made up to 200µl or PBS or DMSO at E10. All embryos with CAM tumours formed from hypoxia-treated BE2C were dissected at E14 and the percentage of embryos with metastatic cells for each treatment was calculated. The percentage of metastasis is shown and each bar represents the mean ±SEM of three independent experiments and a minimum of 12 embryos per condition was analysed (n=12-19). **P⩽0.01 compared with the control.*

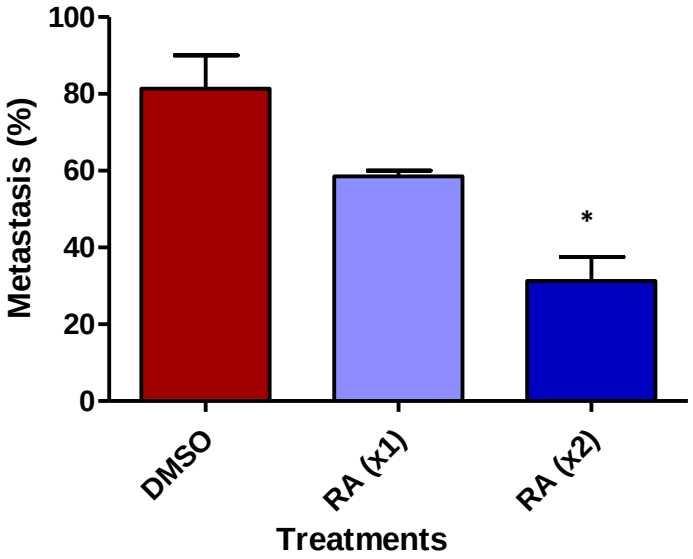

Figure5.14 The effect of different doses of Retinoic acid on BE2C metastasis. *Embryos with BE2C cells implanted on the CAM at E7 were treated with either a single of 40µM of RA made up to 200µl DMSO at E10 or two injections at E10 and E12. All embryos with CAM tumours formed from hypoxia-treated BE2C were dissected at E14 and the percentage of embryos with metastatic cells for each treatment was calculated. The percentage of metastasis is shown and each bar represents the mean ±SEM of three independent experiments and a minimum of 12 embryos per condition was analysed (n=12-19).*P⩽0.05 compared with the control.*

5.3.6. Gene expression in hypoxic tumours

Because we observed profound metastatic effects triggered by pre-culture in DMOG or hypoxic environment, we sought to investigate the transcriptional outputs of the primary hypoxic tumours using qPCR. Genes which demonstrate large fold changes in response to hypoxia were selected: hypoxia induced genes such as GLUT1 and VEGF, intravasation genes such as MMP9 and ADAMST1, and extravasation genes such as VCAN, ITGβ5, ITGαV and VCAM (Herrmann *et al.*, 2015). GLUT1 is the predominant glucose transporter and found to be overexpressed in neuroblastomas compared to maturing ganglioneuromas or intermixed ganglioneuroblastomas (Ramani, Headford and May, 2013), reflecting the altered metabolism and proliferation in neuroblastoma tumours. VEGF is a specific mitogen for cells of endothelial origin that stimulates angiogenesis and is found to be overexpressed in neuroblastomas (Jakovljević *et al.*, 2009). MMP9 is endopeptidase that belongs to zinc-dependent metalloproteinases family that degrade several components of the extracellular matrix. Of interest, elevated expression of MMP9 drives cell division in human neuroblastoma cells (Sans-Fons *et al.*, 2010). ADAMTS1 belongs to A Disintegrin and Metalloprotease with Thrombospondin motifs metalloprotease family. Increased ADAMTS1 expression enhances pro-metastatic alterations such remodelling of the extracellular matrix environment promoting tumour progression and metastasis (Tan, Ricciardelli and Russell, 2013). VCAN is anti-adhesive belongs to hyaluronan-binding proteoglycans family. VCAN is found to be negatively regulated in migratory neural crest cells (Henderson, Ybot-Gonzalez and Copp, 1997). ITGβ5 and ITGαV are transmembrane receptors that facilitate cell - extracellular matrix (ECM) adhesion; both of them are reported to be linked to tumour invasion and metastasis (A., Graf and G., 2013; Hoshino *et al.*, 2015). VCAM belongs to the cell adhesion molecules family and is found to facilitate firm adhesion and transmigration to cancer cells (Wu, 2007).

There was a significant change in the expression of the tested genes in both DMOG- and hypoxia-treated tumours compared to normoxic tumours as was reported previously. DMOG-treated SKNAS tumours showed a significant increase by more than 7 fold for VEGF, 6 fold for ADAMTS1 and 10 fold

for VCAM compared to normoxic SKNAS tumours. GLUT1, MMP9 and ITGαV were also upregulated by approximately 3 fold whereas VCAN was reduced by 50% (***Figure5.15***). Similar to DMOG –treated tumours, in hypoxic BE2C, VEGF possesses the highest fold change with almost 5 fold increase while MMP9 increases by ~4 fold. GLUT1, ADAMTS1 and VCAM also found to be upregulated by roughly 3 fold increase compared to MMP9 in normoxic tumours. ITGβ5 and ITGαV expressed small increase while a significant decrease was observed for VCAN (***Figure5.16***).

Taken together, we confirmed that preculture in DMOG or hypoxia chamber induced a long-lasting change in 8 premetastatic genes involved in tumour progression and metastasis. As RO-3006 showed a significant reduction in invading and metastatic BE2C and SKNAS cells *in vivo*, we sought to investigate whether this drug has an effect in changing or reversing the alterations of transcriptional outcomes caused by hypoxia signature.

A

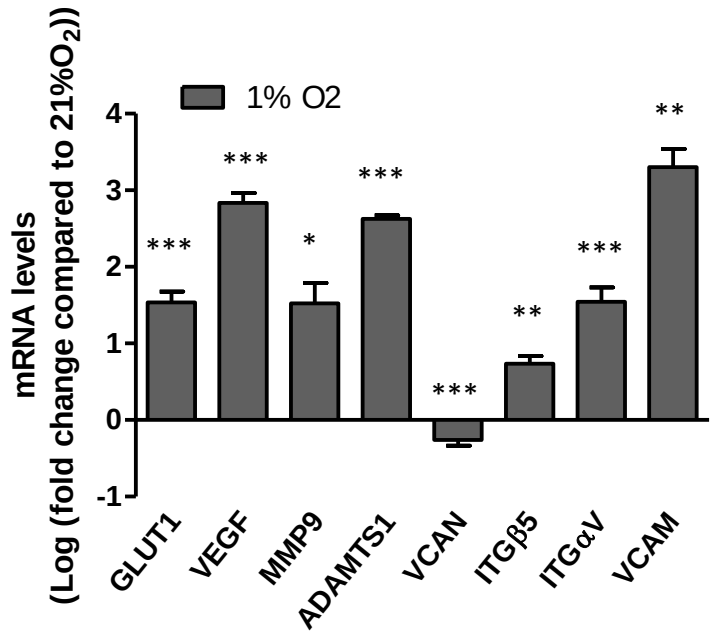

B

	GLUT1	VEGF	MMP9	ADAMTS1	VCAN	ITGβ5	ITGαV	VCAM
Fold change	2.94	7.23	3.04	6.19	-1.20	1.68	2.99	10.31
Log fold change	1.54	2.84	1.52	2.63	-0.26	0.73	1.54	3.30
Regulation	up regulated	up regulated	up regulated	up regulated	down regulated	up regulated	up regulated	up regulated

Figure5.15 The effect of DMOG preconditioning on gene expression of SKNAS tumours. A *Relative mRNA levels for the target genes were determined by qPCR. Cells were cultured for 24hr with DMOG prior to implantation on CAM at E7. At least three independent experiments (n = 3) were analysed for each gene and relative mRNA levels are displayed relative to GAPDH, UBC and HPRT1 and normalised to cells cultured for 3 days with DMSO (control). Each bar in the graph represents the log of normalised mean± SEM of three independent experiments. *P⩽0.05 **P⩽0.01 and ***P⩽0.001 compared with control.* ***B*** *Table gives a summary of the qPCR data for the 8 target genes for DMOG-treated SKNAS tumours.*

A

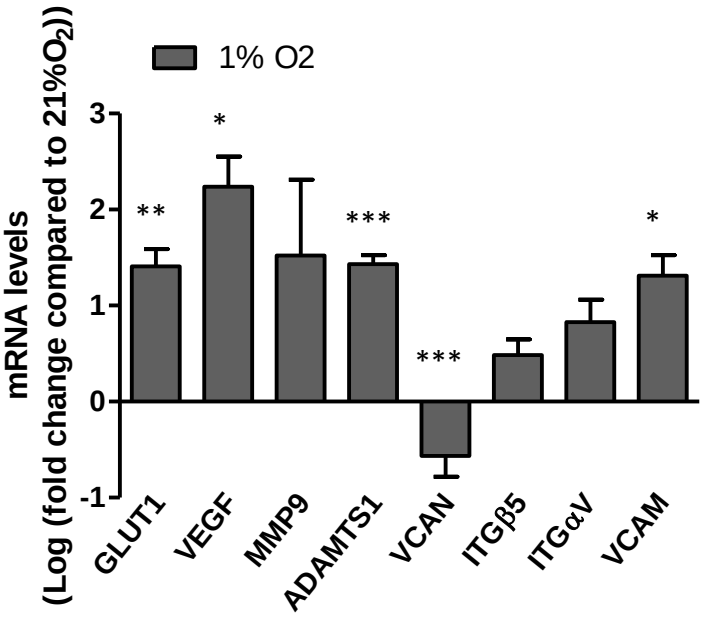

B

	GLUT1	VEGF	MMP9	ADAMTS1	VCAN	ITGβ5	ITGαV	VCAM
Fold change	2.7	4.95	3.96	2.71	-1.51	1.42	1.83	2.54
Log fold change	1.41	2.24	1.52	1.43	-0.56	0.49	0.83	1.31
Regulation	up regulated	up regulated	up regulated	up regulated	down regulated	no change	no change	up regulated

Figure5.16 The effect of hypoxia preconditioning on gene expression of BE2C tumours. A *Relative mRNA levels for the target genes were determined by qPCR. Cells were cultured for 3 days at 1% O_2 prior to implantation on CAM at E7. At least three independent experiments (n = 3) were analysed for each gene and relative mRNA levels are displayed relative to GAPDH, UBC and HPRT1 and normalised to cells cultured for 3 days with DMSO (control). Each bar in the graph represents the log of normalised mean± SEM of three independent experiments. *P⩽0.05 **P⩽0.01 and ***P⩽0.001 compared with control.* ***B*** *Table gives a summary of the qPCR data for the 8 target genes for hypoxia-treated BE2C tumours.*

5.3.7. Effect of RO-3306 on gene expression of hypoxic tumours

QPCR quantification on hypoxia or DMOG –treated tumours indicated significant changes in the expression of genes thought to be important in the metastatic process (***Section 5.3.6***). Here we aimed to identify the effect of RO-3306 on the gene expression of those tumours. RO-3306 was introduced to the allantois at E10. Following one injection of 20μM RO-3306, in DMOG-treated SKNAS tumours, seven genes were reduced significantly (except VCAN) showing a reversal of expression towards the normoxic levels. Expression of VEGF, MMP9 and VCAM dropped by more than 4 fold while GLUT1, ADAMTS1, ITGβ5 and ITGαV reduced by 2 fold approximately compared to the levels seen in hypoxic tumours (***Figure5.17***).

The effect of RO-3306 on BE2C hypoxia –treated tumours was similar to that observed in DMOG-treated SKNAS tumours, a significant reduction of expression was noted in all genes, except VCAN. Glut1, ITGαV and VCAM reduced by more than two fold while ADAMTS1 fell by 3 fold. A small reduction of VEGF expression by < two fold whereas MMP9 reduced by almost 20 fold, both were significant though (***Figure 5.18***).

Taken together these result strongly suggest that a single injection of RO-3306 reduces the metastatic activity of cells pre-conditioned in hypoxia by reducing the increase in expression of genes that are implicated in hypoxia-driven metastasis.

A

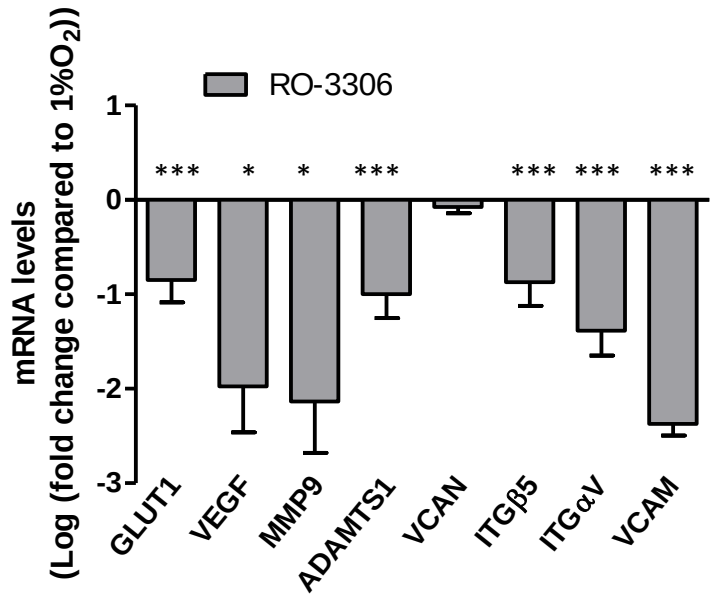

B

	GLUT1	VEGF	MMP9	ADAMTS1	VCAN	ITGβ5	ITGαV	VCAM
Fold change	-1.85	-4.37	-4.97	-2.06	-0.39	-1.89	-2.69	-5.22
Log fold change	-0.85	-1.98	-2.14	-1.00	-0.07	-0.87	-1.38	-2.37
Regulation	down regulated	down regulated	down regulated	down regulated	no change	down regulated	down regulated	down regulated

Figure5.17 The effect of RO-3306 on gene expression of DMOG-Preconditioned SKNAS tumours. A *Relative mRNA levels for the target genes were determined by qPCR. Tumours were treated with single injection of 20μM RO-3306 at E10. At least three independent experiments (n = 3) were analysed for each gene and relative mRNA levels are displayed relative to GAPDH, UBC and HPRT1 and normalised to cells cultured for 3 days with DMSO (control). Each bar in the graph represents the log of normalised mean± SEM of three independent experiments. *P⩽0.05 and ***P⩽0.001 compared with control.* ***B*** *Table gives a summary of the qPCR data for the 8 target genes for DMOG-treated SKNAS tumours following RO-3306 treatment.*

A

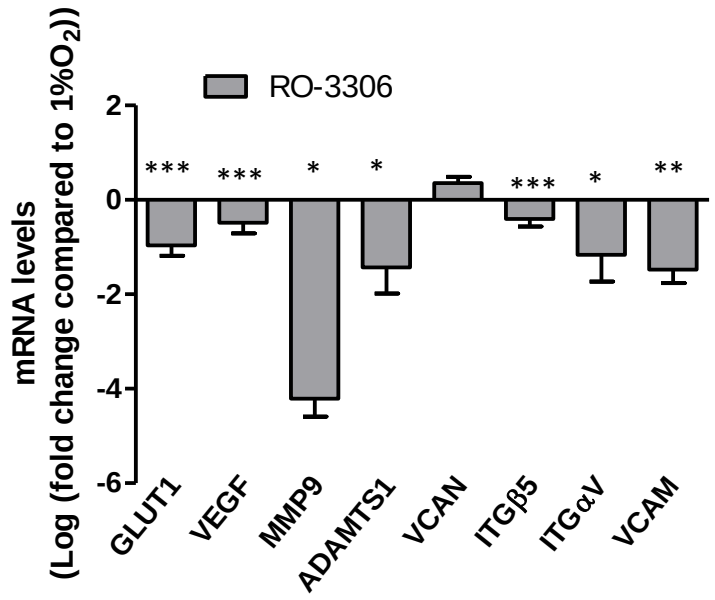

B

	GLUT1	VEGF	MMP9	ADAMTS1	VCAN	ITGβ5	ITGαV	VCAM
Fold change	-2.00	-1.43	-19.85	-3.08	1.29	-1.34	-2.64	-2.90
Log fold change	-0.96	-0.48	-4.21	-1.43	0.35	-0.54	-1.16	-1.48
Regulation	down regulated	down regulated	down regulated	down regulated	no change	down regulated	down regulated	down regulated

Figure5.18 The effect of RO-3306 on gene expression of hypoxia-Preconditioned BE2C tumours. A *Relative mRNA levels for the target genes were determined by qPCR. Tumours were treated with single injection of 20μM RO-3306 at E10. At least three independent experiments (n = 3) were analysed for each gene and relative mRNA levels are displayed relative to GAPDH, UBC and HPRT1 and normalised to cells cultured for 3 days with DMSO (control). Each bar in the graph represents the log of normalised mean± SEM of three independent experiments. *P⩽0.05, **P⩽0.01 and ***P⩽0.001 compared with control.* ***B*** *Table gives a summary of the qPCR data for the 8 target genes for hypoxia-treated BE2C tumours following RO-3306 treatment.*

5.4. Discussion

Our previous findings indicated that Palbociclib and RO-3306 reduced cell proliferation and induced cell death *in vitro* under normoxic conditions. It was demonstrated in previous studies that hypoxic cells are more aggressive and invasive with better ability to metastasize (Azab *et al.*, 2012; Herrmann *et al.*, 2015). Here we aimed to test the effect of Palbociclib and RO-3306, alongside the well-characterised treatment RA, on reducing metastatic behaviour of hypoxic tumours. We found that treating tumours grown from hypoxic cells with Palbociclib and RO-3306 reduced meatstasis and reversed the change of gene expression caused by hypoxia. Thus Palbociclib and RO-3306 showed a significant suppression activity on tumour growth and metastasis.

5.4.1. Response of DMOG-treated SKNAS and BE2C cells in response to Palbociclib and RO-3306 treatment

Our results indicated that culturing SKNAS and BE2C in the hypoxia mimetic, DMOG, for 24hr increased cell proliferation compared to untreated cells similar to that seen by Herrmann (Herrmann *et al.*, 2015). In contrast to this, cell growth analysis using MTT assay on DMOG-treated human tendon stem cells (hTSCs) revealed that 1mM of DMOG for 24hr decreased proliferation by almost 51% compared to control cells (Menon *et al.*, 2018). This suggests that DMOG may have a different activity on normal cells, compared to cancer cells.

We demonstrated that three days with 5µM Palbociclib significantly reduces cell viability of both DMOG-treated SKNAS and BE2C cells. Others also showed that inhibition of CDK4/6 with 5µM LEE011 resulted in cell cycle accumulation of BE2C in G0/G1 phase and significantly decreases the percentage of cells in S and G2/M. In the same study, however, the authors reported that SKNAS cell line was resistant to CDK4/6 inhibition and arrested in G1 only at significantly higher doses (10µM) of LEE011 (Rader *et al.*, 2013).

Palbociclib was found to reduce cell viability and promotes apoptosis in a panel of 5 human colon cancer cell lines regardless of the presence of hypoxia, after treatment for 48hr at 10µM (Zhang *et*

al., 2017). Fry et al demonstrated that Palbociclib could arrest the transition of the G1-S phase of the cell cycle in MDA-MB-453 breast carcinoma cells under hypoxia (Fry *et al.*, 2004). The authors in this study found also that Palbociclib destabilizes HIF-1α and reduces Glycogen Synthase Kinase 3β (GSK-3β) expression under hypoxic conditions. GSK-3β is an essential serine/threonine kinase in cell survival and NF-κB pathway activation; inhibition of GSK-3β also induced cell death of glioma cells (Kotliarova *et al.*, 2008). Considering the therapeutic effect of Palbociclib against aggressive and metastatic tumours, Palbociclib effect is the same but the mechanism by which inducing this effect is more complex as it acts and interacts with many other pathways.

Our results showed that inhibiting CDK1 with R0-3306 resulted in reduction of cell viability and apoptosis in DMOG-treated SKNAS and BE2C cells. Interestingly, it is reported that CDK1 regulates the expression of HIF-1α via direct phosphorylation on Serine 668. Phosphorylation of HIF1-α by CDK1 stabilizes HIF1α levels, even during normoxia (Warfel *et al.*, 2013). This is likely to be due to a reduction in lysosomal degradation of HIF-1α and therefore increases HIF-1α protein stability (Hubbi *et al.*, 2014). Increased stabilization of HIF-1α associated with an increase in transcription activity of HIF-dependent target genes, which functionally resulted in enhanced levels of angiogenesis, cell proliferation and invasion (Warfel *et al.*, 2013; Ortmann, Druker and Rocha, 2014). Knockdown of CDK1 decreases HIF-1 protein levels and eventually its transcriptional activity in HeLa cells (Hubbi *et al.*, 2014). Taken together, inhibiting CDK1 is shown to negatively regulate the cell cycle as well as HIF-1α activity leading to decreased proliferation and increased apoptosis and eventually inhibition of tumour progression.

5.4.2. Hypoxia versus Normoxia tumours

Reduced oxygen availability, hypoxia, stimulates metabolic adaptation in cancer cells and promotes tumour growth. Hypoxic conditions increase overexpression of HIF1-α in tumours leading to metastases which is associated with the aggressiveness of a majority of human cancers and correlates with poor overall survival (Semenza, 2010; Muz *et al.*, 2015; Påhlman and Mohlin, 2018).

HIF-α accumulation and activation alters blood vessel formation, metastasis, and metabolism via a number of genes including VEGF, MMPs, EMT, E-cadherin, CXCR4, GLUT1 and GSK (Muz and Azab, 2015).

Our results indicated that culturing SKNAS or BE2C cell lines under normoxic condition prior to implantation on the CAM did not prompt metastasis from the SKNAS or BE2C CAM tumours and invasion could not be found in any organ or tissue of the chick embryo. In contrast, both DMOG-treated SKNAS and hypoxia-preconditioned BE2C cells were successful in forming tumour metastases. This finding supports that found by Herrmann et al (Herrmann *et al.*, 2015). These findings, together with similar observations in multiple myeloma (MM) cancer (Azab *et al.*, 2012), suggest that cells cultured in hypoxic conditions were more able to metastasise than others cultured under normoxia.

Similar observations were recorded in mice bearing sarcoma tumours, where exposure to acute hypoxia augmented the number of lung metastases (Cairns, Kalliomaki and Hill, 2001). This indicates that hypoxia influences invasive and migratory behaviour of cancer cells allowing tumour progression and dissemination.

5.4.3. Effect of Hypoxia on gene expression

Hypoxia regulates tumour metabolism, neovascularization, and cell death and cell survival. In addition, hypoxia contributes to EMT-like cancer cell migration and cancer stem-cell-like properties allowing propagation of the tumour and resistance to treatment (Muz and Azab, 2015). Our results showed that there was significant increase in the expression of HIF-1α target genes such as VEGF, MMP9 and GLUT1 in hypoxic tumours compared to normoxic tumours

Under hypoxic conditions, angiogenesis occurs due to sprouting of the pre-existing vessels caused by increased production of VEGF and MMPs and integrins (Muz and Azab, 2015). Here we showed that beside the increased levels of VEGF and MMP9 there was a significant increase in the expression of

integrins (ITGβ5 and ItαV), adhesion molecules known to facilitate cell metastasis (Bendas and Borsig, 2012). In hypoxic tumours, we showed that expression of the cell adhesion molecule VCAM was upregulated while anti-adhesive molecule, VCAN, was downregulated compared to normoxic tumours. The importance of this can be explained due to the necessity for cancer cells increase their attachment to the endothelial vessel wall to facilitate transmigration.

Furthermore, under hypoxia, in addition to HIF pathway activation, other hypoxiaassociated pathways are activated including NF-κB, PI3K/AKT/mTOR and MAPK/ERK pathways, which are involved in cell proliferation, survival, apoptosis, metabolism, migration, and inflammation.

In conclusion, hypoxia contributes to cancer metastasis by triggering HIF-1α pathway and altering many different pathways that together facilitate aggressiveness and resistance to treatment. Therefore targeting hypoxia with an inhibitor such as RO-3306 which reverses some pathways activated by hypoxia was of interest.

5.4.4. Effect of RO-3306 on gene expression of hypoxic tumours

As shown previously, hypoxia altered the expression of many genes involved in metastasis. Here we aimed to test the effect of RO-3306 on gene expression of hypoxic tumours. As discussed previously, CDK1 targets HIF-1α by direct phosphorylation at serine 668, leading to expression of HIF-1 targets, promoting tumour angiogenesis, proliferation, and tumour growth (Warfel *et al.*, 2013). We showed that inhibiting CDK1 with RO-3306 significantly reduced the expression of most of the tested genes. In support, siRNA-mediated knockdown or RO-3306-mediated inhibition of CDK1 studies reduced HIF-1α half-life whereas overexpression of CDK1 enhanced HIF-1α levels (Warfel *et al.*, 2013). Of note, in addition to HIF-1α activation, others demonstrated that overexpression of CDK1 enhanced induction of GLUT1 and VEGF mRNA expression in HeLa cells under hypoxic conditions (Hubbi *et al.*, 2014).

Together, these findings underline the importance of CDK1 inhibition in mediating HIF-1α and reverse the transcriptional activity caused by hypoxia.

Chapter Six: Discussion

6.1. Introduction

Neuroblastoma is the most common extracranial solid tumour affects the children under 5 years of age, accounting 15% of all paediatric oncology deaths. Overall, survival for patients with high risk neuroblastoma tumours is poor (<50%), thus crucially indicating a need to develop additional therapies (Matthay *et al.*, 2009; Modak and Cheung, 2010). Whilst many agents tested *in vitro* look promising, remarkably few are as successful in preclinical models or eventually patients. Thus, this project aimed to screen new and potential therapeutic agents using an *in vivo* model, the chick embryo model. The project objectives were as listed below:

1- Validate the CAM model a well characterised drug, RA.

2- Investigate the effect of some potential therapeutic agents specifically Palbociclib and RO-3306 on the behaviour of the neuroblastoma tumours grown on the CAM.

3- Investigate the effect of these therapeutic agents on hypoxia-induced metastasis.

The project involved the use chick embryo model and four different neuroblastoma cell lines BE2C, IMR32, Kelly and SKNAS cells were introduced to the CAM of embryos. Morphology, cellular proliferation, differentation and apoptosis was observed and the metastatic behaviour of hypoxic neuroblastoma tumours was quantifed before and after the application of drugs.

6.1.1. CAM Model validation

The chick embryo as a model system has been used extensively in multiple scientific research fields, but mainly in development (Stern, 2005). CAM model has been used in cancer studies, including the use of the CAM on which to grow cells from a variety of tumours such as colon carcinoma (Cecilia Subauste *et al.*, 2009), multiple myeloma (Ribatti *et al.*, 2003), uveal melanoma (Kalirai *et al.*, 2015) and neuroblastoma (Herrmann *et al.*, 2015), and analyse the extent of angiogenesis and metastasis. However its value for testing the efficacy of drugs has been more limited to date (Kim *et al.*, 2016; Sathe *et al.*, 2016).

The chick embryo complies with widely accepted guidelines designed to reduce animal numbers, refine and replace animal models (the 3Rs) (Alexander, 1998). In our experiments we xenograft the cells on CAM at E7, the earliest time point at which the CAM is sufficiently developed, and complete experiments at E14. Therefore these experiments, although *in vivo*, are not considered animal experiments under UK legislation and therby replace the use of animals. Many cell lines form tumours on the CAM however some do not (Balke *et al.*, 2010; Kalirai *et al.*, 2015; Swadi *et al.*, 2018) a feature we have also observed with neuroblastoma cell lines. Tumour cells need to invade through the epithelial layer of the CAM and this may require functioning MMPs to be secreted by the tumour cells. Whilst many neuroblastoma secrete MMPs only SKNAS cells, of those tested, was expressing the biological activator of MMP (Sugiura *et al.*, 1998; Bjørnland *et al.*, 2001). This provides an explanation for the greater efficiency of tumour formation by SKNAS cells (Herrmann *et al.*, 2015) and the rationale for the use of trypsin to enhance tumour formation for IMR32, Kelly and especially BE2C cells. Use of trypsin may enhance the use of the CAM tumour model by expanding the range of cell lines that will form tumours efficiently.

A blinded assessment, by a pathologist, on CAM-derived and primary sarcoma tumours established that the CAM-derived tumours were histologically similar to the primary sarcoma tumours (Sys *et al.*, 2013). We used similar approach to evaluate the neuroblastoma CAM tumours looking to the histology of tumours.

Drugs can be introduced to the embryo and extra embryonic tumours by topical addition, intravenous (IV) injection or injection into the allantois (Vargas *et al.*, 2007). We used allantois injection as a drug delivery for our experiments. Yet we were interested in determining the dose required to detect a statistically significant effects of RA and while a daily dose of 10µM RA showed the appropriate trend it required two doses of 40µM RA at E11 and E13 to give statistically significant changes in proliferation and a change in cell morphology. This fourfold increase over the concentration used in culture may be due to sequestration of the RA by the receptors present in

cells in the embryo (Kampmann and Mey, 2007) thus potentially reducing the effective concentration. In addition, the cells within the tumour maybe less responsive than those in culture; perhaps reflecting the differing microenvironment (Chen *et al.*, 2015).

Here we have established a method of enhancing tumour development on the CAM, delivering water-insoluble drugs to the tumours and three outcomes that confirm differentiation of cells (reduction in proliferation, change in cell morphology and qPCR of differentiation markers).

Ultimately, chick embryos develop rapidly with a window of only 7 days between a sufficiently developed CAM (E7) and the age embryos come under UK Home Office regulation (E14). Nevertheless tumours can form on the CAM and respond to drug treatments in this time window making the model highly time efficient. It is especially useful for analysing the cellular response to drug treatment as changes in gene expression, leading to different cell behaviours typically occur on a time scale of hours to days. These changes rather than, for example, changes in tumour size suit the short term nature of the model. Here we wanted to extend our results in order to rapidly and cost effectively test other potential agents to tackle resistant neuroblastoma tumours.

6.1.2. Testing potential therapeutic agents on the CAM model

Following the validation of the CAM model with RA, discussed previously, we next demonstrated its value as a model for testing the effect of therapeutic agents on tumour cell proliferation, differentiation, apoptosis and gene expression. We have shown that Palbociclib proved to reduce cell proliferation both *in vitro* and in tumours for BE2C cells and whilst for SKNAS cells it initiated apoptosis *in vitro* and a reduction in cell proliferation *in vivo.* RO-3306 promoted apoptosis in both cell lines *in vitro* and yet surprisingly there was little or no increase in apoptosis *in vivo*. This may be due to differing concentration of inhibitor experienced by the cells however at lower concentrations in culture (1µm) there was no change in either proliferation or decrease in cell viability. Thus the cellular response to agents in the complex 3D environment of a tumour can be different to that seen in 2D cultures as has been observed by others (Gandellini *et al.* 2015, Anastasiou 2017).

Taken together, the outcomes from testing Palbociclib and RO-3306 on CAM tumours were promising. Whilst SKNAS cells are resistant to differentiation therapy by retinoic acid, both Palbociclib and RO-3306 were able to reduce cell proliferation in SKNAS tumours. Thus testing the response mechanisms to Palbociclib and RO-3306 on hypoxia –induced metastasis using CAM model was of interest.

6.1.3. Hypoxia- induced metastasis

Recently, it has been shown that preconditioning neuroblastoma cell lines with either 1% oxygen or DMOG promotes metastasis of cells into the embryo, a phenomenon never see in these cell lines from tumours formed from cells grown in atmospheric oxygen (Herrmann *et al.* 2015). SKNAS cells form CAM tumours very efficiently and they continue to do so when treated with either 1% oxygen or DMOG. BE2C cells form tumours less efficiently and addition of trypsin to the CAM along with the cells enhances this. Surprisingly, treating BE2C cells with DMOG prior to CAM implantation reduced the efficiency so cells were grown in 1% oxygen for 3 days prior to implantation as this did not affect the efficiency of tumour formation. Metastasis was judged to have occurred if fluorescent cell(s) were found in the embryo by dissection under a fluorescent stereomicroscope. Single cells within in the embryo could be identified making this more efficient than previous methods of detecting metastatic cells (Zhao *et al.*, 2015). Rigorous dissection of many embryos here and previously (Rice, 2013) revealed the typical locations for the metastatic cells. Highly favoured locations for tumour cell invasion were the intestines, adjoining tissues in the trunk and crucially, the liver with one or more small clumps of cells were observed groups of individual cells. These locations are very common site for tumour metastasis in patients with neuroblastoma. No metastatic cells were seen prior to the formation of a primary tumour on the CAM and they were only seen in embryos that formed a primary tumour. This confirms that the cells within the embryo were derived from the primary tumour rather than from the initial implantation of cells on the CAM at E7.

6.1.4. The effect of Palbociclib and RO-3306 on hypoxic tumours

In proliferation quantification, Palbociclib and Ro-3306 did not show the same effect that seen on normoxic CAM tumours, both drugs were less effective on hypoxic cells of CAM tumours. Two possible explanations can be suggested here. Firstly it is possibly that the tumours derived from hypoxic cells are more resistant to drug treatment and secondly it is perhaps due to the change in timing of treatments. For the tumours derived from hypoxic cells, drugs were introduced on E10 and E12 whilst for the normoxic tumours they were introduced on E11 and E13.

6.1.5. The effect of RO-3306 on gene expression of hypoxic tumours

We selected the RO-3306 to analyse the mechanism by which those drugs were reducing the metastatic behaviour in both cell lines. Similar to experiments published earlier (Herrmann *et al.*, 2015), we showed that the expression of a number of genes thought to be involved in metastasis was changed in response to pre-treatment with 1% oxygen or DMOG. Interestingly, most genes showed a reduction in their expression in response to RO-3306. For example HIF- 1α target genes such as GLUT1 and VEGF (Herrmann *et al.*, 2015) and genes that more closely associated with metastasis like MMP9 (Hiratsuka *et al.*, 2002; Xiao *et al.*, 2016), ADAMTS1 (Ricciardelli *et al.*, 2011), VCAM (Chen and Massagué, 2012), ITGαV and ITGβ5 (Gladson *et al.*, 1997) showed a statistically significant down regulation compared to hypoxia in both cell lines. These results were obtained four days after a single injection of the RO-3306 suggesting that, like the initial changes resulting from hypoxia, these changes might be long-lasting.

6.1.6. Limitation of the CAM model

All *in vivo* models have inherent strengths and limitations. An appreciation of these limitations is essential in interpreting results obtained through their use and aids decisions about which model is suitable in which context. As a xenograft model, the chick embryo involves the addition of human

neuroblastoma cells into the chick embryo environment. This non-human environment may have an effect on aspects of cell behaviour and interactions between tumour cells and the local microenvironment may not be faithfully recreated. The natural immunodeficiency of the chick embryo, though aiding xenografting, prevents the investigation of compounds acting in an immune mediated fashion and does not recreate the interaction between host immune system and the tumour. Similar to chick embryo, mouse xenograft models have same drawbacks but do have longer time window. Whilst, GEMM do not have this drawback but the neuroblastoma cells are not human.

The second limiting factor of using the CAM model is the short time period available for the application of treatments. Whilst the time frame in this model is appropriate for the more rapid screening of compounds, three or four days of treatment makes this model less than ideal to study the therapeutic effect of a particular drug. This could be potentially amended by transplanting tumours which have had three days of treatment back into an E11 or E7 embryo for further treatment or continuing drug delivery up until E18 under a Home Office licence.

In preclinical models, the use of a single cell line does not accurately represent the extreme heterogeneity seen within neuroblastoma tumours in patients. It is known from previous work that certain cell lines are resistant to the effects of RA, and so the results found using a single cell line may not be applicable to all cell lines found in tumours (Reynolds *et al.*, 2000). Experimentation creating tumours using mixture of more than one cell line for drug testing may be advantageous in the understanding of tumour resistance.

The use of cell lines in this model, which although well characterised, are subject to genetic drift and may not represent primary disease accurately. They may also fail to reproduce the heterogeneity of genetic changes characteristic of primary tumours and therefore exaggerate or fail to respond to the therapeutic effect of targeted therapies

As the pharmacokinetics of the drugs in chick embryos is as yet unknown, the rapidly changing nature of the embryonic environment may affect factors such as the rate of drug metabolism, diffusion and distribution within the model.

In accordance to the UK home office legislations, chicks were not permitted to survive beyond the age of embryonic day 14. As such, the metastasis experiments had to be completed within a seven day period from implantation at E7 to dissection at E14.

Moreover, similar to other preclinical testing models, it is expected cells would behave in a similar manner to neuroblastoma growing in humans, however by its very nature, this study does not relate exactly to the human condition due to the fact that it has been carried out in a different species.

6.1.7. Future directions

The work carried out in these experiments used four neuroblastoma cell lines and four drugs. The success of these experiments makes it possible to extend this approach to other neuroblastoma cell lines, additional drugs and drug combinations and indeed other cancers

Presently, the pharmacokinetics of Palbociclib and RO-3306 in chick embryos has not yet been investigated so it remains to be seen whether the drugs are still present and at what concentration 48hr post injection. Therefore analysing the half-life and metabolites of the drugs would be useful and will assist in the determination of the timing, number and concentration of these drugs used in this model.

Studies with Palbociclib and RO-3306 have begun in order to test for differentiation in RA-resistant neuroblastoma cells, SKNAS cells, and hence both drugs reduced cell proliferation in SKNAS tumours it would be interesting to investigate whether the cells did begin to move down the differentiation pathway by qPCR using the previously characterised markers.

This work has shown that Palbociclib and RO-3306 reduce overall metastasis. Next we could identify which steps in the multistep metastatic process are targeted by these drugs. For example, *in vitro*

experiments such as trans-well migration assay, scratching assay and matrigel invasion assay can be carried out with and without the treatment to determine the effect of drugs on cells. In addition, the intravasation and extravasation steps can be separated out and extravasation alone can be investigated by injected the cells into the blood stream. This would provide a better understanding of the mechanism of action of these drugs and potentially enable the development of combinatorial therapies.

Here the cells were manipulated by preconditioning in hypoxia or DMOG. This approach could be extended by manipulating the cells with siRNA or CRISPR technology to identify the role so specific proteins in the behaviour of tumour cells in the CAM model.

6.1.8. Conclusions

Neuroblastoma is a malignancy of childhood that demonstrates significant clinical and biological heterogeneity. For high risk patients mortality remains tragically, and unacceptably, very high. Thus new treatments able to target the distinct biological and molecular features of these patients' disease are urgently required. In the field of paediatric therapeutic research, preclinical models are vital. With an increasing number of potential therapeutic targets being identified, the need for economically viable, high through put *in vivo* models is escalating. The chick embryo is low cost, highly practical and well characterised by centuries of research, and may provide a suitable xenograft model for work in this field.

We have demonstrated that chick embryo is valuable model for analysing tumour formation and metastatic behaviour of tumour cells. We have seen that allantois injections provide an effective way to deliver compounds in this model. Using elements of standard therapy we have identified RA dose (40µM) which reduced proliferation, induced change in cell morphology and changed the expression of differentiation genes in CAM tumours. We also demonstrated that 20µM Palbociclib or

R-3306 reduced tumour growth and metastasis significantly. Palbociclib and RO-3306 reduced cell proliferation of neuroblastoma cell in normoxic CAM tumours; however this effect is muted on tumours grown from hypoxic cells. We presumed that the change of dose timing alongside the resistance of hypoxic tumours made the results differ from that seen in normoxic tumours. Hypoxia triggered the expression of genes putative in the metastasis process but this is reversed following the application of single dose of RO-3306.

Our findings add to existing works which highlight the suitability of the chick embryo as a model system for cancer research. In addition, we identified two potential therapeutic agents that may act alone or in combination to tackle neuroblastoma resistance. We hope this research may serve as blueprint for future works allowing the full spectrum of drug effects to be investigated. We hope that further drug screening programs carrying out on this model may eventually lead to compounds offering the novel treatment for neuroblastoma patients.

In conclusion, this project has shown the potential the chick CAM has at being the model of choice during initial preclinical testing of drugs for treating cancer patients, potentially leading to an increase in the event free survival of individuals with neuroblastoma.

References:

A., S., Graf, R. and G., D. (2013) 'Neuroblastoma Integrins', in *Neuroblastoma*. InTech, pp. 190–206. doi: 10.5772/55991.

Abdullah, C., Wang, X. and Becker, D. (2011) 'Expression analysis and molecular targeting of cyclin-dependent kinases in advanced melanoma.', *Cell cycle (Georgetown, Tex.)*, 10(6), pp. 977–88. doi: 10.4161/cc.10.6.15079.

Abel, F. *et al.* (2005) 'Imbalance of the mitochondrial pro- and anti-apoptotic mediators in neuroblastoma tumours with unfavourable biology', *European Journal of Cancer*, 41(4), pp. 635–646. doi: 10.1016/j.ejca.2004.12.021.

Al-Dasooqi, N. *et al.* (2010) 'Matrix metalloproteinases are possible mediators for the development of alimentary tract mucositis in the dark agouti rat', *Experimental Biology and Medicine*, 235(10), pp. 1244–1256. doi: 10.1258/ebm.2010.010082.

Albanese, C. *et al.* (2013) 'Preclinical magnetic resonance imaging and systems biology in cancer research: current applications and challenges.', *The American journal of pathology*, 182(2), pp. 312–8. doi: 10.1016/j.ajpath.2012.09.024.

Aleem, E. and Arceci, R. J. (2015) 'Targeting cell cycle regulators in hematologic malignancies.', *Frontiers in cell and developmental biology*, 3, p. 16. doi: 10.3389/fcell.2015.00016.

Alexander, J. (1998) 'Confusing debriefing and defusing postnatally: The need for clarity of terms, purpose and value', *Midwifery*, 14(2), pp. 122–124. doi: 10.1016/S0266-6138(98)90010-9.

Ali, F. R. *et al.* (2014) 'The phosphorylation status of Ascl1 is a key determinant of neuronal differentiation and maturation in vivo and in vitro.', *Development*, 141(11), pp. 2216–24. doi: 10.1242/dev.106377.

Alizadeh, F. *et al.* (2014) 'Retinoids and their biological effects against cancer.', *International immunopharmacology*, 18(1), pp. 43–9. doi: 10.1016/j.intimp.2013.10.027.

Ambros, P. F. *et al.* (2009) 'International consensus for neuroblastoma molecular diagnostics: report from the International Neuroblastoma Risk Group (INRG) Biology Committee.', *British journal of cancer*, 100(9), pp. 1471–82. doi: 10.1038/sj.bjc.6605014.

Aminzadeh, S. *et al.* (2015) 'Energy metabolism in neuroblastoma and Wilms tumor.', *Translational pediatrics*, 4(1), pp. 20–32. doi: 10.3978/j.issn.2224-4336.2015.01.04.

Anastasiou, D. (2017) 'Tumour microenvironment factors shaping the cancer metabolism landscape.', *British journal of cancer*, 116(3), pp. 277–286. doi: 10.1038/bjc.2016.412.

Andrews, W. *et al.* (2008) 'The role of Slit-Robo signaling in the generation, migration and morphological differentiation of cortical interneurons', *Developmental Biology*, 313(2), pp. 648–658. doi: 10.1016/j.ydbio.2007.10.052.

Andrews, W. D., Barber, M. and Parnavelas, J. G. (2007) 'Slit–Robo interactions during cortical development', *Journal of Anatomy*. Blackwell Science Inc, 211(2), pp. 188–198. doi: 10.1111/j.1469-7580.2007.00750.x.

Ara, T. *et al.* (1998) 'Immunohistochemical expression of MMP-2, MMP-9, and TIMP-2 in neuroblastoma: Association with tumor progression and clinical outcome', *Journal of Pediatric Surgery*, 33(8), pp. 1272–1278. doi: 10.1016/S0022-3468(98)90167-1.

Armstrong, P. B., Quigley, J. P. and Sidebottom, E. (1982) 'Transepithelial Invasion and Intramesenchymal Infiltration of the Chick Embryo Chorioallantois by Tumor Cell Lines', *Cancer Research*, 42(5), pp. 1826–1837. doi: 10.1158/0008-5472.can-04-1112.

Arumugam, P. *et al.* (2016) 'Thymoquinone inhibits the migration of mouse neuroblastoma (Neuro-2a) cells by down-regulating MMP-2 and MMP-9', *Chinese Journal of Natural Medicines*, 14(12), pp. 904–912. doi: 10.1016/S1875-5364(17)30015-8.

Asgharzadeh, S. *et al.* (2012) 'Clinical Significance of Tumor-Associated Inflammatory Cells in Metastatic Neuroblastoma', *Journal of Clinical Oncology*, 30(28), pp. 3525–3532. doi: 10.1200/JCO.2011.40.9169.

Attiyeh, E. F. *et al.* (2005) 'Chromosome 1p and 11q Deletions and Outcome in Neuroblastoma', *New England Journal of Medicine*, 353(21), pp. 2243–2253. doi: 10.1056/NEJMoa052399.

Azab, A. K. *et al.* (2012) 'Hypoxia promotes dissemination of multiple myeloma through acquisition of epithelial to mesenchymal transition-like features', *Blood*, 119(24), pp. 5782–5794. doi: 10.1182/blood-2011-09-380410.

Azmi, A. S. and Mohammad, R. M. (2014) 'Rectifying cancer drug discovery through network pharmacology.', *Future medicinal chemistry*, 6(5), pp. 529–39. doi: 10.4155/fmc.14.6.

Bader, A. G., Kang, S. and Vogt, P. K. (2006) 'Cancer-specific mutations in PIK3CA are oncogenic in vivo.', *Proceedings of the National Academy of Sciences of the United States of America*, 103(5), pp. 1475–9. doi: 10.1073/pnas.0510857103.

Badmaev, V., Prakash, S. and Majeed, M. (1999) 'Vanadium: A Review of its Potential Role in the Fight Against Diabetes', *The Journal of Alternative and Complementary Medicine*, 5(3), pp. 273–291. doi: 10.1089/acm.1999.5.273.

Baeriswyl, V. and Christofori, G. (2009) 'The angiogenic switch in carcinogenesis.', *Seminars in cancer biology*. Berlin, Heidelberg: Springer Berlin Heidelberg, 19(5), pp. 329–37. doi: 10.1016/j.semcancer.2009.05.003.

Balciūniene, N. *et al.* (2009) 'Histology of human glioblastoma transplanted on chicken chorioallantoic membrane.', *Medicina (Kaunas, Lithuania)*, 45(2), pp. 123–131. doi: 0902-05 [pii].

Balke, M. *et al.* (2010) 'Morphologic characterization of osteosarcoma growth on the chick chorioallantoic membrane.', *BMC research notes*, 3(1), p. 58. doi: 10.1186/1756-0500-3-58.

Banfield, M. J. *et al.* (2001) 'Specificity in Trk receptor:neurotrophin interactions: The crystal structure of TrkB-d5 in complex with neurotrophin-4/5', *Structure*, 9(12), pp. 1191–1199. doi: 10.1016/S0969-2126(01)00681-5.

Barone, G. *et al.* (2013) 'New strategies in neuroblastoma: Therapeutic targeting of MYCN and ALK', *Clinical Cancer Research*, 19(21), pp. 5814–5821. doi: 10.1158/1078-0432.CCR-13-0680.

Beilharz, E. J. *et al.* (1998) 'Neuronal activity induction of the stathmin-like gene RB3 in the rat hippocampus: possible role in neuronal plasticity.', *The Journal of neuroscience : the official journal of the Society for Neuroscience*, 18(23), pp. 9780–9. Available at: http://www.ncbi.nlm.nih.gov/pubmed/9822737.

Bell, E. *et al.* (2006) 'The role of MYCN in the failure of MYCN amplified neuroblastoma cell lines to G1arrest after DNA damage', *Cell Cycle*, 5(22), pp. 2639–2647. doi: 10.4161/cc.5.22.3443.

Bellail, A. C., Olson, J. J. and Hao, C. (2014) 'SUMO1 modification stabilizes CDK6 protein and drives the cell cycle and glioblastoma progression', *Nature Communications*, 5(1), p. 4234. doi: 10.1038/ncomms5234.

Bendas, G. and Borsig, L. (2012) 'Cancer Cell Adhesion and Metastasis: Selectins, Integrins, and the Inhibitory Potential of Heparins', *International Journal of Cell Biology*, 2012, pp. 1–10. doi: 10.1155/2012/676731.

Bergers, G. and Benjamin, L. E. (2003) 'Tumorigenesis and the angiogenic switch', *Nature Reviews Cancer*, 3(6), pp. 401–410. doi: 10.1038/nrc1093.

Bernards, R., Dessain, S. K. and Weinberg, R. A. (1986) 'N-myc amplification causes down-modulation of MHC class I antigen expression in neuroblastoma.', *Cell*, 47(5), pp. 667–74. doi: 10.1016/0092-8674(86)90509-X.

Berry, T. *et al.* (2012) 'The ALKF1174L Mutation Potentiates the Oncogenic Activity of MYCN in Neuroblastoma', *Cancer Cell*, 22(1), pp. 117–130. doi: 10.1016/j.ccr.2012.06.001.

Bishayee, A. *et al.* (2010) 'Vanadium in the detection, prevention and treatment of cancer: The in vivo evidence', *Cancer Letters*. Elsevier Ireland Ltd, 294(1), pp. 1–12. doi: 10.1016/j.canlet.2010.01.030.

Bjørnland, K. *et al.* (2001) 'Expression of matrix metalloproteinases and the metastasis-associated gene S100A4 in human neuroblastoma and primitive neuroectodermal tumor cells', *Journal of Pediatric Surgery*, 36(7), pp. 1040–1044. doi: 10.1053/jpsu.2001.24735.

Bjornstad, S. *et al.* (2015) 'Cracking the Egg: Potential of the Developing Chicken as a Model System for Nonclinical Safety Studies of Pharmaceuticals', *Journal of Pharmacology and Experimental Therapeutics*, 355(3), pp. 386–396. doi: 10.1124/jpet.115.227025.

Bluhm, E. *et al.* (2008) 'Prenatal and perinatal risk factors for neuroblastoma.', *International journal of cancer. Journal international du cancer*, 123(12), pp. 2885–2890. doi: 10.1002/ijc.23847.

Bobek, V. *et al.* (2004) 'Development of a green fluorescent protein metastatic-cancer chick-embryo drug-screen model', *Clinical and Experimental Metastasis*, 21(4), pp. 347–352. doi: 10.1023/B:CLIN.0000046138.58210.31.

Bollard, J. *et al.* (2017) 'Palbociclib (PD-0332991), a selective CDK4/6 inhibitor, restricts tumour growth in preclinical models of hepatocellular carcinoma', *Gut*, 66(7), pp. 1286–1296. doi: 10.1136/gutjnl-2016-312268.

Borah, A. *et al.* (2015) 'Targeting self-renewal pathways in cancer stem cells: clinical implications for cancer therapy.', *Oncogenesis*, 4(11), p. e177. doi: 10.1038/oncsis.2015.35.

Borriello, A. *et al.* (2000) 'p27(Kip1) accumulation is associated with retinoic-induced neuroblastoma differentiation: Evidence of a decreased proteasome-dependent degradation', *Oncogene*, 19(1), pp. 51–60. doi: 10.1038/sj.onc.1203231.

Borriello, L. *et al.* (2016) 'More than the genes, the tumor microenvironment in neuroblastoma', *Cancer Letters*, 380(1), pp. 304–314. doi: 10.1016/j.canlet.2015.11.017.

Bottino, C. *et al.* (2014) 'Natural killer cells and neuroblastoma: tumor recognition, escape mechanisms, and possible novel immunotherapeutic approaches.', *Frontiers in immunology*, 5, p. 56. doi: 10.3389/fimmu.2014.00056.

Bourdeaut, F. *et al.* (2005) 'Germline mutations of the paired-like homeobox 2B (PHOX2B) gene in neuroblastoma', *Cancer Letters*, 228(1–2), pp. 51–58. doi: 10.1016/j.canlet.2005.01.055.

Bowden, E. T., Stoica, G. E. and Wellstein, A. (2002) 'Anti-apoptotic signaling of pleiotrophin through its receptor, anaplastic lymphoma kinase', *Journal of Biological Chemistry*, 277(39), pp. 35862–35868. doi: 10.1074/jbc.M203963200.

Brodeur, G. M. *et al.* (1993) 'Revisions of the international criteria for neuroblastoma diagnosis, staging, and response to treatment', *Journal of Clinical Oncology*, 11(8), pp. 1466–1477. doi: 10.1200/JCO.1993.11.8.1466.

Brodeur, G. M. (2003) 'Neuroblastoma: biological insights into a clinical enigma', *Nature Reviews Cancer*, 3(3), pp. 203–216. doi: 10.1038/nrc1014.

Brodeur, G. M. *et al.* (2009) 'Trk Receptor Expression and Inhibition in Neuroblastomas', *Clinical Cancer Research*, 15(10), pp. 3244–3250. doi: 10.1158/1078-0432.CCR-08-1815.

Brodeur, G. M. (2018) 'Spontaneous regression of neuroblastoma', *Cell and Tissue Research*, 372(2), pp. 277–286. doi: 10.1007/s00441-017-2761-2.

Brodeur, G. M. and Bagatell, R. (2014) 'Mechanisms of neuroblastoma regression', *Nature Reviews Clinical Oncology*, 11(12), pp. 704–713. doi: 10.1038/nrclinonc.2014.168.

De Brouwer, S. *et al.* (2010) 'Meta-analysis of neuroblastomas reveals a skewed ALK mutation spectrum in tumors with MYCN amplification', *Clinical Cancer Research*, 16(17), pp. 4353–4362. doi: 10.1158/1078-0432.CCR-09-2660.

Brower, V. (2014) 'Cell Cycle Inhibitors Make Progress', *JNCI: Journal of the National Cancer Institute*, 106(7), pp. 2–3. doi: 10.1093/jnci/dju221.

Cairns, R. A., Kalliomaki, T. and Hill, R. P. (2001) 'Acute (cyclic) hypoxia enhances spontaneous metastasis of KHT murine tumors', *Cancer Research*, 61(24), pp. 8903–8908. doi: 10.1158/0008-5472.can-10-1350.

Calegari, F. *et al.* (2005) 'Selective lengthening of the cell cycle in the neurogenic subpopulation of neural progenitor cells during mouse brain development.', *The Journal of neuroscience : the official journal of the Society for Neuroscience*, 25(28), pp. 6533–6538. doi: 10.1523/JNEUROSCI.0778-05.2005.

Capecchi, M. R. (1989) 'Altering the genome by homologous recombination.', *Science (New York, N.Y.)*, 244(4910), pp. 1288–92. doi: 10.1126/science.2660260.

Carpenter, E. L. and Mossé, Y. P. (2012) 'Targeting ALK in neuroblastoma—preclinical and clinical advancements', *Nature Reviews Clinical Oncology*, 9(7), pp. 391–399. doi: 10.1038/nrclinonc.2012.72.

Carr, J. *et al.* (2006) 'Increased frequency of aberrations in the p53/MDM2/p14(ARF) pathway in neuroblastoma cell lines established at relapse.', *Cancer research*, 66(4), pp. 2138–45. doi: 10.1158/0008-5472.CAN-05-2623.

Carter, R. *et al.* (2012) 'Exploitation of chick embryo environments to reprogram MYCN-amplified neuroblastoma cells to a benign phenotype, lacking detectable MYCN expression', *Oncogenesis*, 1(8), pp. e24–e24. doi: 10.1038/oncsis.2012.24.

CASCIANO, I. (2004) 'Caspase-8 Gene Expression in Neuroblastoma', *Annals of the New York*

Academy of Sciences, 1028(1), pp. 157–167. doi: 10.1196/annals.1322.017.

Castel, V., Segura, V. and Berlanga, P. (2013) 'Emerging drugs for neuroblastoma', *Expert Opinion on Emerging Drugs*, 18(2), pp. 155–171. doi: 10.1517/14728214.2013.796927.

Cecilia Subauste, M. *et al.* (2009) 'Evaluation of metastatic and angiogenic potentials of human colon carcinoma cells in chick embryo model systems', *Clinical & Experimental Metastasis*, 26(8), pp. 1033–1047. doi: 10.1007/s10585-009-9293-4.

Cekanova, M. and Rathore, K. (2014) 'Animal models and therapeutic molecular targets of cancer: utility and limitations', *Drug Design, Development and Therapy*, 8, p. 1911. doi: 10.2147/DDDT.S49584.

Celik, I. *et al.* (2005) 'Therapeutic Efficacy of Endostatin Exhibits a Biphasic Dose-Response Curve', *Cancer Research*, 65(23), pp. 11044–11050. doi: 10.1158/0008-5472.CAN-05-2617.

Cesare, A. J. and Reddel, R. R. (2010) 'Alternative lengthening of telomeres: models, mechanisms and implications', *Nature Reviews Genetics*, 11(5), pp. 319–330. doi: 10.1038/nrg2763.

Chakraborty, T. *et al.* (2006) 'Molecular basis of anticlastogenic potential of vanadium in vivo during the early stages of diethylnitrosamine-induced hepatocarcinogenesis in rats', *Mutation Research/Genetic Toxicology and Environmental Mutagenesis*, 609(2), pp. 117–128. doi: 10.1016/j.mrgentox.2006.04.023.

Chan, E. L. *et al.* (2007) 'Favorable histology, MYCN-amplified 4S neonatal neuroblastoma', *Pediatric Blood and Cancer*, 48(4), pp. 479–482. doi: 10.1002/pbc.20705.

Chen, F. *et al.* (2015) 'New horizons in tumor microenvironment biology: challenges and opportunities', *BMC Medicine*, 13(1), p. 45. doi: 10.1186/s12916-015-0278-7.

Chen, L. *et al.* (2010) 'p53 Is a Direct Transcriptional Target of MYCN in Neuroblastoma', *Cancer Research*, 70(4), pp. 1377–1388. doi: 10.1158/0008-5472.CAN-09-2598.

Chen, M.-C. *et al.* (2012) 'Retinoic Acid Induces Apoptosis of Prostate Cancer DU145 Cells through Cdk5 Overactivation.', *Evidence-based complementary and alternative medicine : eCAM*, 2012, p. 580736. doi: 10.1155/2012/580736.

Chen, Q. and Massagué, J. (2012) 'Molecular Pathways : VCAM-1 as a Potential Therapeutic Target in Metastasis', 18(17), pp. 5520–5526. doi: 10.1158/1078-0432.CCR-11-2904.

Chen, Y. *et al.* (2008) 'Oncogenic mutations of ALK kinase in neuroblastoma (Supplementary table)', *Nature*, 455(7215), pp. 971–4. doi: 10.1038/nature07399.

Chen, Y., Tsai, Y. H. and Tseng, S. H. (2013) 'Inhibition of cyclin-dependent kinase 1-induced cell death in neuroblastoma cells through the microRNA-34a-MYCN-survivin pathway', *Surgery (United States)*, 153(1), pp. 4–16. doi: 10.1016/j.surg.2012.03.030.

Cheng, A. J. *et al.* (2007) 'Cell lines from MYCN transgenic murine tumours reflect the molecular and biological characteristics of human neuroblastoma', *European Journal of Cancer*, 43(9), pp. 1467–1475. doi: 10.1016/j.ejca.2007.03.008.

Chesler, L. *et al.* (2007) 'Malignant Progression and Blockade of Angiogenesis in a Murine Transgenic Model of Neuroblastoma', *Cancer Research*, 67(19), pp. 9435–9442. doi: 10.1158/0008-5472.CAN-07-1316.

Chesler, L. and Weiss, W. A. (2011) 'Genetically engineered murine models – Contribution to our

understanding of the genetics, molecular pathology and therapeutic targeting of neuroblastoma', *Seminars in Cancer Biology*, 21(4), pp. 245–255. doi: 10.1016/j.semcancer.2011.09.011.

Cheung, N.-K. V. and Dyer, M. A. (2013) 'Neuroblastoma: developmental biology, cancer genomics and immunotherapy', *Nature Reviews Cancer*, 13(6), pp. 397–411. doi: 10.1038/nrc3526.

Chilosi, M. *et al.* (1998) 'Differential expression of cyclin-dependent kinase 6 in cortical thymocytes and T-cell lymphoblastic lymphoma/leukemia.', *The American Journal of Pathology*, 152(1), pp. 209–217. Available at: http://www.ncbi.nlm.nih.gov/pmc/articles/PMC1858129/.

Chlenski, A. *et al.* (2002) 'SPARC is a key Schwannian-derived inhibitor controlling neuroblastoma tumor angiogenesis.', *Cancer research*, 62(24), pp. 7357–63. Available at: http://www.ncbi.nlm.nih.gov/pubmed/12499280.

Chlenski, A., Liu, S. and Cohn, S. L. (2003) 'The regulation of angiogenesis in neuroblastoma', *Cancer Letters*, 197(1–2), pp. 47–52. doi: 10.1016/S0304-3835(03)00082-X.

Clark, O. *et al.* (2015) 'Oxovanadium-based inhibitors can drive redox-sensitive cytotoxicity in neuroblastoma cells and synergise strongly with buthionine sulfoximine', *Cancer Letters*, 357(1), pp. 316–327. doi: 10.1016/j.canlet.2014.11.039.

Clark, O., Daga, S. and Stoker, A. W. (2013) 'Tyrosine phosphatase inhibitors combined with retinoic acid can enhance differentiation of neuroblastoma cells and trigger ERK- and AKT-dependent, p53-independent senescence', *Cancer Letters*, 328(1), pp. 44–54. doi: 10.1016/j.canlet.2012.09.014.

Cohn, S. L. *et al.* (2000) 'MYCN expression is not prognostic of adverse outcome in advanced-stage neuroblastoma with nonamplified MYCN', *Journal of Clinical Oncology*, 18(21), pp. 3604–3613. doi: 10.1200/JCO.2000.18.21.3604.

Cohn, S. L. *et al.* (2009) 'The International Neuroblastoma Risk Group (INRG) classification system: An INRG task force report', *Journal of Clinical Oncology*, 27(2), pp. 289–297. doi: 10.1200/JCO.2008.16.6785.

Coleman, J. F. (2010) 'Robbins and Cotran's Pathologic Basis of Disease, 8th Edition', *The American Journal of Surgical Pathology*, 34(1), p. 132. doi: 10.1097/PAS.0b013e3181bc5f0f.

Collet, G. *et al.* (2014) 'Hypoxia-regulated overexpression of soluble VEGFR2 controls angiogenesis and inhibits tumor growth.', *Molecular cancer therapeutics*, 13(1), pp. 165–78. doi: 10.1158/1535-7163.MCT-13-0637.

Comstock, C. E. S. *et al.* (2009) 'Cyclin D1 splice variants: polymorphism, risk, and isoform-specific regulation in prostate cancer.', *Clinical cancer research : an official journal of the American Association for Cancer Research*, 15(17), pp. 5338–49. doi: 10.1158/1078-0432.CCR-08-2865.

Connolly, R. M., Nguyen, N. K. and Sukumar, S. (2013) 'Molecular Pathways: Current Role and Future Directions of the Retinoic Acid Pathway in Cancer Prevention and Treatment', *Clinical Cancer Research*, 19(7), pp. 1651–1659. doi: 10.1158/1078-0432.CCR-12-3175.

Cook Sangar, M. L. *et al.* (2017) 'Inhibition of CDK4/6 by Palbociclib Significantly Extends Survival in Medulloblastoma Patient-Derived Xenograft Mouse Models', *Clinical Cancer Research*, 23(19), pp. 5802–5813. doi: 10.1158/1078-0432.CCR-16-2943.

Corral, T. *et al.* (2007) 'High level expression of soluble glycoproteins in the allantoic fluid of embryonated chicken eggs using a Sendai virus minigenome system.', *BMC biotechnology*, 7(1), p. 17. doi: 10.1186/1472-6750-7-17.

Cotterman, R. and Knoepfler, P. S. (2009) 'N-Myc regulates expression of pluripotency genes in neuroblastoma including lif, klf2, klf4, and lin28b', *PLoS One*, 4(6), p. e5799. doi: 10.1371/journal.pone.0005799.

Craene, B. De and Berx, G. (2013) 'Regulatory networks defining EMT during cancer initiation and progression', *Nature Reviews Cancer*, 13(2), pp. 97–110. doi: 10.1038/nrc3447.

Craig, B. T. *et al.* (2016) 'Induced differentiation inhibits sphere formation in neuroblastoma', *Biochemical and Biophysical Research Communications*, 477(2), pp. 255–259. doi: 10.1016/j.bbrc.2016.06.053.

Cunningham, T. J. and Duester, G. (2015) 'Mechanisms of retinoic acid signalling and its roles in organ and limb development.', *Nature reviews. Molecular cell biology*, 16(2), pp. 110–23. doi: 10.1038/nrm3932.

Curinga, G. and Smith, G. M. (2008) 'Molecular/genetic manipulation of extrinsic axon guidance factors for CNS repair and regeneration', *Experimental Neurology*, 209(2), pp. 333–342. doi: 10.1016/j.expneurol.2007.06.026.

D'Cruz, O. J. and Uckun, F. M. (2002) 'Metvan: a novel oxovanadium(IV) complex with broad spectrum anticancer activity', *Expert Opinion on Investigational Drugs*, 11(12), pp. 1829–1836. doi: 10.1517/13543784.11.12.1829.

Dąbroś, W. *et al.* (2011) 'Vanadium compounds affect growth and morphology of human rhabdomyosarcoma cell line.', *Polish journal of pathology : official journal of the Polish Society of Pathologists*, 62(4), pp. 262–8. Available at: http://www.ncbi.nlm.nih.gov/pubmed/22246913.

DeBerardinis, R. J. *et al.* (2008) 'The Biology of Cancer: Metabolic Reprogramming Fuels Cell Growth and Proliferation', *Cell Metabolism*, 7(1), pp. 11–20. doi: 10.1016/j.cmet.2007.10.002.

Deryugina, E. I. and Quigley, J. P. (2008) 'Chick embryo chorioallantoic membrane model systems to study and visualize human tumor cell metastasis.', *Histochemistry and cell biology*, 130(6), pp. 1119–30. doi: 10.1007/s00418-008-0536-2.

Deyell, R. J. and Attiyeh, E. F. (2011) 'Advances in the understanding of constitutional and somatic genomic alterations in neuroblastoma', *Cancer Genetics*, 204(3), pp. 113–121. doi: 10.1016/j.cancergen.2011.03.001.

Diril, M. K. *et al.* (2012) 'Cyclin-dependent kinase 1 (Cdk1) is essential for cell division and suppression of DNA re-replication but not for liver regeneration', *Proceedings of the National Academy of Sciences*, 109(10), pp. 3826–3831. doi: 10.1073/pnas.1115201109.

Dole, M. G. *et al.* (1995) 'Bcl-xL is expressed in neuroblastoma cells and modulates chemotherapy-induced apoptosis.', *Cancer research*, 55(12), pp. 2576–82. Available at: http://www.ncbi.nlm.nih.gov/pubmed/7780971.

Duncan, J. E. *et al.* (2013) 'The Microtubule Regulatory Protein Stathmin Is Required to Maintain the Integrity of Axonal Microtubules in Drosophila', *PLoS ONE*, 8(6), pp. 1–20. doi: 10.1371/journal.pone.0068324.

Durupt, F. *et al.* (2012) 'The chicken chorioallantoic membrane tumor assay as model for qualitative testing of oncolytic adenoviruses', *Cancer Gene Therapy*, 19(1), pp. 58–68. doi: 10.1038/cgt.2011.68.

Dzieran, J. *et al.* (2018) 'MYCN-amplified neuroblastoma maintains an aggressive and undifferentiated phenotype by deregulation of estrogen and NGF signaling.', *Proceedings of the*

National Academy of Sciences of the United States of America, 115(6), pp. E1229–E1238. doi: 10.1073/pnas.1710901115.

Easton, J. *et al.* (1998) 'Disruption of the Cyclin D/Cyclin-dependent Kinase/INK4/Retinoblastoma Protein Regulatory Pathway in Human Neuroblastoma', *Cancer Research*, 58(12), p. 2624 LP-2632. Available at: http://cancerres.aacrjournals.org/content/58/12/2624.abstract.

Eggers, J. P. *et al.* (2011) 'Cyclin-Dependent Kinase 5 Is Amplified and Overexpressed in Pancreatic Cancer and Activated by Mutant K-Ras', *Clinical Cancer Research*, 17(19), pp. 6140–6150. doi: 10.1158/1078-0432.CCR-10-2288.

Eilers, M. and Eisenman, R. N. (2008) 'Myc's broad reach', *Genes & Development*, 22(20), pp. 2755–2766. doi: 10.1101/gad.1712408.

Elmore, S. (2007) 'Apoptosis: A Review of Programmed Cell Death', *Toxicologic Pathology*, 35(4), pp. 495–516. doi: 10.1080/01926230701320337.

Ernsberger, U. *et al.* (2000) 'The expression of dopamine β-hydroxylase, tyrosine hydroxylase, and Phox2 transcription factors in sympathetic neurons: Evidence for common regulation during noradrenergic induction and diverging regulation later in development', *Mechanisms of Development*, 92(2), pp. 169–177. doi: 10.1016/S0925-4773(99)00336-6.

Errico, A. *et al.* (2010) 'Identification of substrates for cyclin dependent kinases', *Advances in Enzyme Regulation*, 50(1), pp. 375–399. doi: 10.1016/j.advenzreg.2009.12.001.

Evan, G. I. and Vousden, K. H. (2001) 'Proliferation, cell cycle and apoptosis in cancer', *Nature*, 411(6835), pp. 342–348. doi: 10.1038/35077213.

Evangelou, A. M. (2002) 'Vanadium in cancer treatment', *Critical Reviews in Oncology/Hematology*, 42(3), pp. 249–265. doi: 10.1016/S1040-8428(01)00221-9.

Federico, S. M. *et al.* (2017) 'A pilot trial of humanized anti-GD2 monoclonal antibody (hu14.18K322A) with chemotherapy and natural killer cells in children with recurrent/refractory neuroblastoma', *Clinical Cancer Research*, 23(21), pp. 6441–6449. doi: 10.1158/1078-0432.CCR-17-0379.

Fergelot, P. *et al.* (2013) 'The experimental renal cell carcinoma model in the chick embryo', *Angiogenesis*, 16(1), pp. 181–194. doi: 10.1007/s10456-012-9311-z.

Flaherty, K. T. *et al.* (2012) 'Phase I, dose-escalation trial of the oral cyclin-dependent kinase 4/6 inhibitor PD 0332991, administered using a 21-day schedule in patients with advanced cancer', *Clinical Cancer Research*, 18(2), pp. 568–576. doi: 10.1158/1078-0432.CCR-11-0509.

Fletcher, C. (2013) *Diagnostic Histopathology of Tumors*. 4th edn. Philadelphia, PA, USA: Saunders/Elsevier.

Frese, K. K. and Tuveson, D. A. (2007) 'Maximizing mouse cancer models.', *Nature reviews. Cancer*, 7(9), pp. 645–58. doi: 10.1038/nrc2192.

Friedl, P. (2010) 'To adhere or not to adhere?', *Nature Reviews Molecular Cell Biology*, 11(1), pp. 3–3. doi: 10.1038/nrm2825.

Friedman, D. L. *et al.* (2005) 'Increased risk of cancer among siblings of long-term childhood cancer survivors: a report from the childhood cancer survivor study.', *Cancer epidemiology, biomarkers & prevention : a publication of the American Association for Cancer Research, cosponsored by the*

American Society of Preventive Oncology, 14(8), pp. 1922–1927. doi: 10.1158/1055-9965.EPI-05-0066.

Fry, D. W. *et al.* (2004) 'Specific inhibition of cyclin-dependent kinase 4/6 by PD 0332991 and associated antitumor activity in human tumor xenografts.', *Molecular cancer therapeutics*, 3(11), pp. 1427–38. doi: 3/11/1427 [pii].

Gabrielli, M. G. and Accili, D. (2010) 'The Chick Chorioallantoic Membrane: A Model of Molecular, Structural, and Functional Adaptation to Transepithelial Ion Transport and Barrier Function during Embryonic Development', *Journal of Biomedicine and Biotechnology*, 2010(1), pp. 1–12. doi: 10.1155/2010/940741.

Gammill, L. S. and Bronner-Fraser, M. (2003) 'Neural crest specification: Migrating into genomics', *Nature Reviews Neuroscience*, 4(10), pp. 795–805. doi: 10.1038/nrn1219.

Gammill, L. S. and Roffers-Agarwal, J. (2010) 'Division of labor during trunk neural crest development.', *Developmental biology*, 344(2), pp. 555–65. doi: 10.1016/j.ydbio.2010.04.009.

Gandellini, P. *et al.* (2015) 'Complexity in the tumour microenvironment: Cancer associated fibroblast gene expression patterns identify both common and unique features of tumour-stroma crosstalk across cancer types', *Seminars in Cancer Biology*, 35, pp. 96–106. doi: 10.1016/j.semcancer.2015.08.008.

George, R. E. *et al.* (2008) 'Activating mutations in ALK provide a therapeutic target in neuroblastoma', *Nature*, 455(7215), pp. 975–978. doi: 10.1038/nature07397.

Gerdes, J. *et al.* (1984) 'Cell cycle analysis of a cell proliferation-associated human nuclear antigen defined by the monoclonal antibody Ki-67.', *Journal of immunology (Baltimore, Md. : 1950)*, 133(4), pp. 1710–5. Available at: http://www.ncbi.nlm.nih.gov/pubmed/6206131.

Gestblom, C. *et al.* (1999) 'The Basic Helix-Loop-Helix Transcription Factor dHAND, a Marker Gene for the Developing Human Sympathetic Nervous System, Is Expressed in Both High- and Low-Stage Neuroblastomas', *Laboratory Investigation*, 79(1), p. 67. doi: 10.1261/rna.049379.114.

Gherardi, S. *et al.* (2013) 'MYCN-mediated transcriptional repression in neuroblastoma: the other side of the coin.', *Frontiers in oncology*, 3, p. 42. doi: 10.3389/fonc.2013.00042.

Gilbert, S. F. (2000) 'The Neural Crest', in *Developmental Biology*.

Gladson, C. L. *et al.* (1997) 'Vitronectin expression in differentiating neuroblastic tumors: integrin alpha v beta 5 mediates vitronectin-dependent adhesion of retinoic-acid-differentiated neuroblastoma cells.', *The American journal of pathology*, 150(5), pp. 1631–46. Available at: http://www.ncbi.nlm.nih.gov/pubmed/9137089.

Goga, A. *et al.* (2007) 'Inhibition of CDK1 as a potential therapy for tumors over-expressing MYC', *Nature Medicine*, 13(7), pp. 820–827. doi: 10.1038/nm1606.

Gogolin, S. *et al.* (2013) 'CDK4 inhibition restores G_1-S arrest in MYCN - amplified neuroblastoma cells in the context of doxorubicin-induced DNA damage', *Cell Cycle*, 12(7), pp. 1091–1104. doi: 10.4161/cc.24091.

Gordon, J. and Ruddle, F. (1981) 'Integration and stable germ line transmission of genes injected into mouse pronuclei', *Science*, 214(4526), pp. 1244–1246. doi: 10.1126/science.6272397.

Grandori, C. *et al.* (2000) 'The Myc/Max/Mad network and the transcriptional control of cell

behavior.', *Annual review of cell and developmental biology*, 16, pp. 653–699. doi: 10.1146/annurev.cellbio.16.1.653.

Greaves, M. and Maley, C. C. (2012) 'Clonal evolution in cancer', *Nature*, 481(7381), pp. 306–313. doi: 10.1038/nature10762.

Guglielmi, L. *et al.* (2014) 'MYCN gene expression is required for the onset of the differentiation programme in neuroblastoma cells', *Cell Death and Disease*, 5(2), pp. 1–14. doi: 10.1038/cddis.2014.42.

Gustafson, W. C. and Weiss, W. A. (2010) 'Myc proteins as therapeutic targets', *Oncogene*. Nature Publishing Group, 29(9), pp. 1249–1259. doi: 10.1038/onc.2009.512.

Gyöngyösi, A. *et al.* (2013) 'RDH10, RALDH2, and CRABP2 are required components of PPARγ-directed ATRA synthesis and signaling in human dendritic cells', *Journal of Lipid Research*, 54(9), pp. 2458–2474. doi: 10.1194/jlr.M038984.

Hadjidaniel, M. D. *et al.* (2017) 'Tumor-associated macrophages promote neuroblastoma via STAT3 phosphorylation and up-regulation of c-MYC', *Oncotarget*, 8(53), pp. 91516–91529. doi: 10.18632/oncotarget.21066.

Hamburger, V. and Hamilton, H. L. (1992) 'A series of normal stages in the development of the chick embryo', *Developmental Dynamics*, 195(4), pp. 231–272. doi: 10.1002/aja.1001950404.

Hamilton, E. and Infante, J. R. (2016) 'Targeting CDK4/6 in patients with cancer', *Cancer Treatment Reviews*. Elsevier Ltd, 45, pp. 129–138. doi: 10.1016/j.ctrv.2016.03.002.

Hanahan, D. and Weinberg, R. A. (2000) 'The hallmarks of cancer.', *Cell*, 100(1), pp. 57–70. doi: 10.1007/s00262-010-0968-0.

Hanahan, D. and Weinberg, R. A. (2011) 'Review Hallmarks of Cancer : The Next Generation', *Cell*, 144(5), pp. 646–674. doi: 10.1016/j.cell.2011.02.013.

Hansford, L. M. *et al.* (2004) 'Mechanisms of embryonal tumor initiation: Distinct roles for MycN expression and MYCN amplification', *Proceedings of the National Academy of Sciences*, 101(34), pp. 12664–12669. doi: 10.1073/pnas.0401083101.

Hardwick, L. J. A. and Philpott, A. (2014) 'Nervous decision-making: to divide or differentiate', *Trends in Genetics*, 30(6), pp. 254–261. doi: 10.1016/j.tig.2014.04.001.

Hayflick, L. (1997) 'Mortality and immortality at the cellular level. A review.', *Biochemistry. Biokhimiia*, 62(11), pp. 1180–90. Available at: http://www.ncbi.nlm.nih.gov/pubmed/9467840.

Heck, J. E. *et al.* (2009) 'The epidemiology of neuroblastoma: a review', *Paediatric and Perinatal Epidemiology*, 23(2), pp. 125–143. doi: 10.1111/j.1365-3016.2008.00983.x.

Henderson, D. J., Ybot-Gonzalez, P. and Copp, A. J. (1997) 'Over-expression of the chondroitin sulphate proteoglycan versican is associated with defective neural crest migration in the Pax3 mutant mouse (splotch)', *Mechanisms of Development*, 69(1–2), pp. 39–51. doi: 10.1016/S0925-4773(97)00151-2.

Herrmann, A. *et al.* (2015) 'Cellular memory of hypoxia elicits neuroblastoma metastasis and enables invasion by non-aggressive neighbouring cells', *Oncogenesis*, 4(2), pp. e138–e138. doi: 10.1038/oncsis.2014.52.

Heukamp, L. C. *et al.* (2012) 'Targeted Expression of Mutated ALK Induces Neuroblastoma in

Transgenic Mice', *Science Translational Medicine*, 4(141), p. 141ra91-141ra91. doi: 10.1126/scitranslmed.3003967.

Hiratsuka, S. *et al.* (2002) 'MMP9 induction by vascular endothelial growth factor receptor-1 is involved in lung-specific metastasis', *Cancer Cell*, 2(4), pp. 289–300. doi: 10.1016/S1535-6108(02)00153-8.

Hiyama, E. *et al.* (1995) 'Correlating telomerase activity levels with human neuroblastoma outcomes', *Nature Medicine*, 1(3), pp. 249–255. doi: 10.1038/nm0395-249.

Hogarty, M. D. *et al.* (2008) 'ODC1 Is a Critical Determinant of MYCN Oncogenesis and a Therapeutic Target in Neuroblastoma', *Cancer Research*, 68(23), pp. 9735–9745. doi: 10.1158/0008-5472.CAN-07-6866.

Holla, V. R. *et al.* (2017) 'ALK: a tyrosine kinase target for cancer therapy', *Molecular Case Studies*, 3(1), p. a001115. doi: 10.1101/mcs.a001115.

Horne, G. A. and Copland, M. (2017) 'Approaches for targeting self-renewal pathways in cancer stem cells: implications for hematological treatments', *Expert Opinion on Drug Discovery*, 12(5), pp. 465–474. doi: 10.1080/17460441.2017.1303477.

Hoshino, A. *et al.* (2015) 'Tumour exosome integrins determine organotropic metastasis', *Nature*, 527(7578), pp. 329–335. doi: 10.1038/nature15756.

Hsu, P. P. and Sabatini, D. M. (2008) 'Cancer cell metabolism: Warburg and beyond', *Cell*, 134(5), pp. 703–707. doi: 10.1016/j.cell.2008.08.021.

Hsu, S. L. *et al.* (2000) 'Retinoic acid-mediated G1 arrest is associated with induction of p27(Kip1) and inhibition of cyclin-dependent kinase 3 in human lung squamous carcinoma CH27 cells', *Experimental Cell Research*, 258(2), pp. 322–331. doi: 10.1006/excr.2000.4933.

Huang, M. and Weiss, W. A. (2013) 'Neuroblastoma and MYCN.', *Cold Spring Harbor perspectives in medicine*, 3(10), p. a014415. doi: 10.1101/cshperspect.a014415.

Huang, R. *et al.* (2011) 'MYCN and MYC regulate tumor proliferation and tumorigenesis directly through BMI1 in human neuroblastomas', *The FASEB Journal*, 25(12), pp. 4138–4149. doi: 10.1096/fj.11-185033.

Hubbi, M. E. *et al.* (2014) 'Cyclin-dependent kinases regulate lysosomal degradation of hypoxia-inducible factor 1 to promote cell-cycle progression', *Proceedings of the National Academy of Sciences*, 111(32), pp. E3325–E3334. doi: 10.1073/pnas.1412840111.

Huber, K. (2006) 'The sympathoadrenal cell lineage: Specification, diversification, and new perspectives', *Developmental Biology*, 298(2), pp. 335–343. doi: 10.1016/j.ydbio.2006.07.010.

Hughes, J. *et al.* (2011) 'Principles of early drug discovery', *British Journal of Pharmacology*, 162(6), pp. 1239–1249. doi: 10.1111/j.1476-5381.2010.01127.x.

Ikeda, H. *et al.* (2002) 'Experience with International Neuroblastoma Staging System and Pathology Classification', *British Journal of Cancer*, 86(7), pp. 1110–1116. doi: 10.1038/sj/bjc/6600231.

Iraci, N. *et al.* (2011) 'A SP1/MIZ1/MYCN Repression Complex Recruits HDAC1 at the TRKA and p75NTR Promoters and Affects Neuroblastoma Malignancy by Inhibiting the Cell Response to NGF', *Cancer Research*, 71(2), pp. 404–412. doi: 10.1158/0008-5472.CAN-10-2627.

Izbicki, T., Mazur, J. and Izbicka, E. (2003) 'Epidemiology and etiology of neuroblastoma: an

overview.', *Anticancer research*, 23(1B), pp. 755–60. Available at: http://www.ncbi.nlm.nih.gov/pubmed/12680179.

Jackson, J. K. *et al.* (1997) 'A polymer-based drug delivery system for the antineoplastic agent bis (maltolato) oxovanadium in mice', 75, pp. 1014–1020.

Jakovljević, G. *et al.* (2009) 'Vascular endothelial growth factor in children with neuroblastoma: a retrospective analysis', *Journal of Experimental & Clinical Cancer Research*, 28(1), p. 143. doi: 10.1186/1756-9966-28-143.

Jefferies, B. *et al.* (2017) 'Non-invasive imaging of engineered human tumors in the living chicken embryo', *Scientific Reports*, 7(1), p. 4991. doi: 10.1038/s41598-017-04572-1.

Jogi, A. *et al.* (2002) 'Hypoxia alters gene expression in human neuroblastoma cells toward an immature and neural crest-like phenotype', *Proceedings of the National Academy of Sciences*, 99(10), pp. 7021–7026. doi: 10.1073/pnas.102660199.

Kain, K. H. *et al.* (2014) 'The chick embryo as an expanding experimental model for cancer and cardiovascular research', *Dev. Dyn.*, 243(2), pp. 216–228. doi: 10.1002/dvdy.24093.The.

Kain, K. H. *et al.* (2014) 'The chick embryo as an expanding experimental model for cancer and cardiovascular research', *Developmental Dynamics*, 243(2), pp. 216–228. doi: 10.1002/dvdy.24093.

Kalirai, H. *et al.* (2015) 'Use of the Chick Embryo Model in Uveal Melanoma', *Ocular Oncology and Pathology*, 1(3), pp. 133–140. doi: 10.1159/000370151.

Kamijo, T. and Nakagawara, A. (2012) 'Molecular and genetic bases of neuroblastoma', *International Journal of Clinical Oncology*, 17(3), pp. 190–195. doi: 10.1007/s10147-012-0415-7.

Kampmann, E. and Mey, J. (2007) 'Retinoic acid enhances Erk phosphorylation in the chick retina', *Neuroscience Letters*, 426(1), pp. 18–22. doi: 10.1016/j.neulet.2007.07.039.

Kang, J. *et al.* (2014) 'Targeting cyclin-dependent kinase 1 (CDK1) but not CDK4/6 or CDK2 is selectively lethal to MYC-dependent human breast cancer cells', *BMC Cancer*, 14(1), pp. 1–13. doi: 10.1186/1471-2407-14-32.

Kasemeier-Kulesa, J. C. *et al.* (2006) 'Eph/ephrins and N-cadherin coordinate to control the pattern of sympathetic ganglia', *Development*, 133(24), pp. 4839–4847. doi: 10.1242/dev.02662.

Kausch, I. *et al.* (2003) 'Antisense treatment against Ki-67 mRNA inhibits proliferation and tumor growth in vitro and in vivo.', *International journal of cancer. Journal international du cancer*, 105(5), pp. 710–6. doi: 10.1002/ijc.11111.

Kavaliauskaitė, D. *et al.* (2017) 'The Effect of Sodium Valproate on the Glioblastoma U87 Cell Line Tumor Development on the Chicken Embryo Chorioallantoic Membrane and on EZH2 and p53 Expression', *BioMed Research International*, 2017, pp. 1–12. doi: 10.1155/2017/6326053.

Kembhavi, S. *et al.* (2015) 'Imaging in neuroblastoma: An update', *Indian Journal of Radiology and Imaging*, 25(2), p. 129. doi: 10.4103/0971-3026.155844.

Khanna, C. *et al.* (2002) 'Biologically relevant orthotopic neuroblastoma xenograft models: primary adrenal tumor growth and spontaneous distant metastasis.', *In vivo (Athens, Greece)*, 16(2), pp. 77–85. Available at: http://www.ncbi.nlm.nih.gov/pubmed/12073775.

Kim, J. *et al.* (2003) 'SOX10 maintains multipotency and inhibits neuronal differentiation of neural crest stem cells', *Neuron*, 38(1), pp. 17–31. doi: 10.1016/S0896-6273(03)00163-6.

Kim, Y. *et al.* (2016) 'Quantification of cancer cell extravasation in vivo', *Nature Protocols*, 11(5), pp. 937–948. doi: 10.1038/nprot.2016.050.

Klein, A. *et al.* (2008) 'Sodium orthovanadate affects growth of some human epithelial cancer cells (A549, HTB44, DU145)', *Folia Biologica*, 56(3–4), pp. 115–121. doi: 10.3409/fb.56_3-4.115-121.

Klingenberg, M. *et al.* (2014) 'The chick chorioallantoic membrane as an in vivo xenograft model for Burkitt lymphoma', *BMC Cancer*, 14(1). doi: 10.1186/1471-2407-14-339.

Klymkowsky, M. W. and Savagner, P. (2009) 'Epithelial-Mesenchymal Transition', *The American Journal of Pathology*, 174(5), pp. 1588–1593. doi: 10.2353/ajpath.2009.080545.

Knoepfler, P. S. (2002) 'N-myc is essential during neurogenesis for the rapid expansion of progenitor cell populations and the inhibition of neuronal differentiation', *Genes & Development*, 16(20), pp. 2699–2712. doi: 10.1101/gad.1021202.

Knudson, A. G. (1971) 'Mutation and Cancer: Statistical Study of Retinoblastoma', *Proceedings of the National Academy of Sciences*, 68(4), pp. 820–823. doi: 10.1073/pnas.68.4.820.

Koff, J., Ramachandiran, S. and Bernal-Mizrachi, L. (2015) 'A Time to Kill: Targeting Apoptosis in Cancer', *International Journal of Molecular Sciences*, 16(2), pp. 2942–2955. doi: 10.3390/ijms16022942.

Kostova, I. (2009) 'Titanium and Vanadium Complexes as Anticancer Agents', *Anti-Cancer Agents in Medicinal Chemistry*, 9(8), pp. 827–842. doi: 10.2174/187152009789124646.

Kotliarova, S. *et al.* (2008) 'Glycogen synthase kinase-3 inhibition induces glioma cell death through c-MYC, nuclear factor-kappaB, and glucose regulation.', *Cancer research*, 68(16), pp. 6643–51. doi: 10.1158/0008-5472.CAN-08-0850.

Kroemer, G. *et al.* (2009) 'Classification of cell death: recommendations of the Nomenclature Committee on Cell Death 2009', *Cell Death & Differentiation*, 16(1), pp. 3–11. doi: 10.1038/cdd.2008.150.

Krull, C. E. *et al.* (1997) 'Interactions of Eph-related receptors and ligands confer rostrocaudal pattern to trunk neural crest migration', *Current Biology*, 7(8), pp. 571–580. doi: 10.1016/S0960-9822(06)00256-9.

Kuan, I.-I. *et al.* (2017) 'EpEX/EpCAM and Oct4 or Klf4 alone are sufficient to generate induced pluripotent stem cells through STAT3 and HIF2α', *Scientific Reports*, 7(1), p. 41852. doi: 10.1038/srep41852.

Kulesa, P. M. and Gammill, L. S. (2010) 'Neural crest migration: Patterns, phases and signals', *Developmental Biology*, 344(2), pp. 566–568. doi: 10.1016/j.ydbio.2010.05.005.

Kumar, S. *et al.* (2012) 'Preclinical models for pediatric solid tumor drug discovery: current trends, challenges and the scopes for improvement', *Expert Opinion on Drug Discovery*, 7(11), pp. 1093–1106. doi: 10.1517/17460441.2012.722077.

Kushner, B. H. *et al.* (2001) 'Extending Positron Emission Tomography Scan Utility to High-Risk Neuroblastoma: Fluorine-18 Fluorodeoxyglucose Positron Emission Tomography as Sole Imaging Modality in Follow-Up of Patients', *Journal of Clinical Oncology*, 19(14), pp. 3397–3405. doi: 10.1200/JCO.2001.19.14.3397.

Lamouille, S., Xu, J. and Derynck, R. (2014) 'Molecular mechanisms of epithelial–mesenchymal

transition', *Nature Reviews Molecular Cell Biology*, 15(3), pp. 178–196. doi: 10.1038/nrm3758.

De Lange, F. J. *et al.* (2004) 'Lineage and morphogenetic analysis of the cardiac valves', *Circulation Research*, 95(6), pp. 645–654. doi: 10.1161/01.RES.0000141429.13560.cb.

Lapenna, S. and Giordano, A. (2009) 'Cell cycle kinases as therapeutic targets for cancer', *Nature Reviews Drug Discovery*, 8(7), pp. 547–566. doi: 10.1038/nrd2907.

Lim, K. C. *et al.* (2000) 'Gata3 loss leads to embryonic lethality due to noradrenaline deficiency of the sympathetic nervous system', *Nature Genetics*, 25(2), pp. 209–212. doi: 10.1038/76080.

Van Limpt, V. *et al.* (2004) 'The Phox2B homeobox gene is mutated in sporadic neuroblastomas', *Oncogene*, 23(57), pp. 9280–9288. doi: 10.1038/sj.onc.1208157.

Lin, M.-J. and Lee, S.-J. (2016) 'Stathmin-like 4 is critical for the maintenance of neural progenitor cells in dorsal midbrain of zebrafish larvae', *Scientific Reports*, 6(1), p. 36188. doi: 10.1038/srep36188.

Liu, D. *et al.* (2012) 'IL-15 protects NKT cells from inhibition by tumor-associated macrophages and enhances antimetastatic activity.', *The Journal of clinical investigation*, 122(6), pp. 2221–33. doi: 10.1172/JCI59535.

Lokman, N. A. *et al.* (2012) 'Chick chorioallantoic membrane (CAM) assay as an in vivo model to study the effect of newly identified molecules on ovarian cancer invasion and metastasis', *International Journal of Molecular Sciences*, 13(8), pp. 9959–9970. doi: 10.3390/ijms13089959.

Lonergan, G. J. *et al.* (2003) 'Neuroblastoma, ganglioneuroblastoma, and ganglioneuroma: radiologic-pathologic correlation.', *Radiographics : a review publication of the Radiological Society of North America, Inc*, 22(4), pp. 911–34. doi: 10.1148/radiographics.22.4.g02jl15911.

Longo, L. *et al.* (2008) 'PHOX2A and PHOX2B genes are highly co-expressed in human neuroblastoma', *International Journal of Oncology*, 33(5), pp. 985–991. doi: 10.3892/ijo_00000086.

Lu, X. and Kang, Y. (2010) 'Hypoxia and Hypoxia-Inducible Factors: Master Regulators of Metastasis', *Clinical Cancer Research*, 16(24), pp. 5928–5935. doi: 10.1158/1078-0432.CCR-10-1360.

Lutful Kabir, F., Alvarez, C. and Bird, R. (2015) 'Canine Mammary Carcinomas: A Comparative Analysis of Altered Gene Expression', *Veterinary Sciences*, 3(1), p. 1. doi: 10.3390/vetsci3010001.

MacKeigan, J. P., Murphy, L. O. and Blenis, J. (2005) 'Sensitized RNAi screen of human kinases and phosphatases identifies new regulators of apoptosis and chemoresistance', *Nature Cell Biology*, 7(6), pp. 591–600. doi: 10.1038/ncb1258.

Van Maerken, T. *et al.* (2009) 'Escape from p53-mediated tumor surveillance in neuroblastoma: switching off the p14ARF-MDM2-p53 axis', *Cell Death & Differentiation*, 16(12), pp. 1563–1572. doi: 10.1038/cdd.2009.138.

Malumbres, M. (2011) 'Physiological Relevance of Cell Cycle Kinases', *Physiological Reviews*, 91(3), pp. 973–1007. doi: 10.1152/physrev.00025.2010.

Malumbres, M. and Barbacid, M. (2001) 'To cycle or not to cycle: a critical decision in cancer', *Nature Reviews Cancer*, 1(3), pp. 222–231. doi: 10.1038/35106065.

Malumbres, M. and Barbacid, M. (2005) 'Mammalian cyclin-dependent kinases', *Trends in Biochemical Sciences*, 30(11), pp. 630–641. doi: 10.1016/j.tibs.2005.09.005.

Malumbres, M. and Barbacid, M. (2009) 'Cell cycle, CDKs and cancer: a changing paradigm', *Nature Reviews Cancer*, 9(3), pp. 153–166. doi: 10.1038/nrc2602.

Manjunathan, R. and Ragunathan, M. (2015) 'Chicken chorioallantoic membrane as a reliable model to evaluate osteosarcoma-an experimental approach using SaOS2 cell line.', *Biological procedures online*, 17, p. 10. doi: 10.1186/s12575-015-0022-x.

Maris, J. M. *et al.* (2007) 'Neuroblastoma', *The Lancet*, 369(9579), pp. 2106–2120. doi: 10.1016/S0140-6736(07)60983-0.

Maris, J. M. (2010) '2010. Maris. Recent Advances in Neuroblastoma', *New England Journal of Medicine*, 362(23), pp. 2202–2211. doi: 10.1056/NEJMra0804577.

Mark, M., Ghyselinck, N. B. and Chambon, P. (2006) 'FUNCTION OF RETINOID NUCLEAR RECEPTORS: Lessons from Genetic and Pharmacological Dissections of the Retinoic Acid Signaling Pathway During Mouse Embryogenesis', *Annual Review of Pharmacology and Toxicology*, 46(1), pp. 451–480. doi: 10.1146/annurev.pharmtox.46.120604.141156.

Marshall, G. M. *et al.* (2014) 'The prenatal origins of cancer', *Nature Reviews Cancer*, 14(4), pp. 277–289. doi: 10.1038/nrc3679.

Mather, G. (2014) *The Chick Embryo; A new drug delivery model for neuroblastoma*. University of Liverpool. Available at: https://livrepository.liverpool.ac.uk/2007502/2/BorrillMatherGra_Aug2014_2007502 (abridged).pdf.

Matthay, K. K. *et al.* (2009) 'Long-term results for children with high-risk neuroblastoma treated on a randomized trial of myeloablative therapy followed by 13-cis-retinoic acid: A children's oncology group study', *Journal of Clinical Oncology*, 27(7), pp. 1007–1013. doi: 10.1200/JCO.2007.13.8925.

Matthay, K. K. *et al.* (2016) 'Neuroblastoma', *Nature Reviews Disease Primers*, 2, p. 16078. doi: 10.1038/nrdp.2016.78.

Mayor, R. and Theveneau, E. (2013) 'The neural crest', *Development*, 140(11), pp. 2247–2251. doi: 10.1242/dev.091751.

McGowan, P. M., Kirstein, J. M. and Chambers, A. F. (2009) 'Micrometastatic disease and metastatic outgrowth: clinical issues and experimental approaches.', *Future oncology (London, England)*, 5(7), pp. 1083–98. doi: 10.2217/fon.09.73.

McLaughlin, C. C. *et al.* (2009) 'Perinatal risk factors for neuroblastoma', *Cancer Causes & Control*, 20(3), pp. 289–301. doi: 10.1007/s10552-008-9243-5.

McLennan, R. and Krull, C. E. (2002) 'Ephrin-As cooperate with EphA4 to promote trunk neural crest migration', *Gene Expression*, 10(5–6), pp. 295–305.

McMahon, S. B., Wood, M. A. and Cole, M. D. (2000) 'The Essential Cofactor TRRAP Recruits the Histone Acetyltransferase hGCN5 to c-Myc', *Molecular and Cellular Biology*, 20(2), pp. 556–562. doi: 10.1128/MCB.20.2.556-562.2000.

Meitar, D. *et al.* (1996) 'Tumor angiogenesis correlates with metastatic disease, N-myc amplification, and poor outcome in human neuroblastoma.', *Journal of Clinical Oncology*, 14(2), pp. 405–414. doi: 10.1200/JCO.1996.14.2.405.

Mendrzyk, F. *et al.* (2005) 'Genomic and protein expression profiling identifies CDK6 as novel

independent prognostic marker in medulloblastoma.', *Journal of clinical oncology : official journal of the American Society of Clinical Oncology*, 23(34), pp. 8853–62. doi: 10.1200/JCO.2005.02.8589.

Menon, A. *et al.* (2018) 'Chemical Activation of the Hypoxia-Inducible Factor Reversibly Reduces Tendon Stem Cell Proliferation, Inhibits Their Differentiation, and Maintains Cell Undifferentiation', *Stem Cells International*, 2018, pp. 1–13. doi: 10.1155/2018/9468085.

Menu, E. *et al.* (2008) 'A novel therapeutic combination using PD 0332991 and bortezomib: Study in the 5T33MM myeloma model', *Cancer Research*, 68(14), pp. 5519–5523. doi: 10.1158/0008-5472.CAN-07-6404.

Mestre-ferrandiz, J., Sussex, J. and Towse, A. (2012) *The R & D Cost of a New Medicine*.

Micalizzi, D. S., Farabaugh, S. M. and Ford, H. L. (2010) 'Epithelial-Mesenchymal Transition in Cancer: Parallels Between Normal Development and Tumor Progression', *Journal of Mammary Gland Biology and Neoplasia*, 15(2), pp. 117–134. doi: 10.1007/s10911-010-9178-9.

Miller, S. J. *et al.* (2012) 'Multimodal Imaging of Growth and Rapamycin-Induced Regression of Colonic Adenomas in Apc Mutation-Dependent Mouse', *Translational Oncology*. Neoplasia Press, Inc., 5(5), pp. 313–320. doi: 10.1593/tlo.12226.

Modak, S. and Cheung, N.-K. V. (2010) 'Neuroblastoma: Therapeutic strategies for a clinical enigma', *Cancer Treatment Reviews*, 36(4), pp. 307–317. doi: 10.1016/j.ctrv.2010.02.006.

Mohlin, S. A., Wigerup, C. and Påhlman, S. (2011) 'Neuroblastoma aggressiveness in relation to sympathetic neuronal differentiation stage', *Seminars in Cancer Biology*. Elsevier Ltd, 21(4), pp. 276–282. doi: 10.1016/j.semcancer.2011.09.002.

Molenaar, J. J., Koster, J., Ebus, M. E., *et al.* (2012) 'Copy number defects of G1-Cell cycle genes in neuroblastoma are frequent and correlate with high expression of E2F target genes and a poor prognosis', *Genes, Chromosomes and Cancer*, 51(1), pp. 10–19. doi: 10.1002/gcc.20926.

Molenaar, J. J., Domingo-Fernández, R., *et al.* (2012) 'LIN28B induces neuroblastoma and enhances MYCN levels via let-7 suppression.', *Nature genetics*, 44(11), pp. 1199–206. doi: 10.1038/ng.2436.

Molenaar, J. J., Koster, J., Zwijnenburg, D. A., *et al.* (2012) 'Sequencing of neuroblastoma identifies chromothripsis and defects in neuritogenesis genes', *Nature*, 483(7391), pp. 589–593. doi: 10.1038/nature10910.

Moreau, L. A. *et al.* (2006) 'Does MYCN amplification manifested as homogeneously staining regions at diagnosis predict a worse outcome in children with neuroblastoma? A children's oncology group study', *Clinical Cancer Research*, 12(19), pp. 5693–5697. doi: 10.1158/1078-0432.CCR-06-1500.

Moriguchi, T. (2006) 'Gata3 participates in a complex transcriptional feedback network to regulate sympathoadrenal differentiation', *Development*, 133(19), pp. 3871–3881. doi: 10.1242/dev.02553.

Mossé, Y. P. *et al.* (2008) 'Identification of ALK as a major familial neuroblastoma predisposition gene', *Nature*, 455(7215), pp. 930–935. doi: 10.1038/nature07261.

Mougiakakos, D. *et al.* (2010) 'Regulatory T Cells in Cancer', in *Advances in cancer research*, pp. 57–117. doi: 10.1016/S0065-230X(10)07003-X.

Mujtaba, S., Zeng, L. and Zhou, M.-M. (2007) 'Structure and acetyl-lysine recognition of the bromodomain', *Oncogene*, 26(37), pp. 5521–5527. doi: 10.1038/sj.onc.1210618.

Mukherjee, B. *et al.* (2004) 'Vanadium—an element of atypical biological significance', *Toxicology*

Letters, 150(2), pp. 135–143. doi: 10.1016/j.toxlet.2004.01.009.

Mullassery, D. *et al.* (2009) 'Neuroblastoma: Contemporary management', *Archives of Disease in Childhood: Education and Practice Edition*, pp. 177–185. doi: 10.1136/adc.2008.143909.

Mullassery, D. and Losty, P. D. (2016) 'Neuroblastoma', *Paediatrics and Child Health*, 26(2), pp. 68–72. doi: 10.1016/j.paed.2015.11.005.

Musgrove, E. A. *et al.* (2011) 'Cyclin D as a therapeutic target in cancer', *Nature Reviews Cancer*, 11(8), pp. 558–572. doi: 10.1038/nrc3090.

Muz, B. *et al.* (2015) 'The role of hypoxia in cancer progression, angiogenesis, metastasis, and resistance to therapy', *Hypoxia*, 3, p. 83. doi: 10.2147/HP.S93413.

Muz, B. and Azab, A. K. (2015) 'The role of hypoxia in cancer progression , angiogenesis , metastasis , and resistance to therapy', pp. 83–92.

Nakagawara, A. (2001) 'Trk receptor tyrosine kinases: A bridge between cancer and neural development', *Cancer Letters*, 169(2), pp. 107–114. doi: 10.1016/S0304-3835(01)00530-4.

Nakagawara, A. (2004) 'Neural crest development and neuroblastoma: the genetic and biological link', *Progress in Brain Research*, 146, pp. 233–242. doi: 10.1016/S0079-6123(03)46015-9.

Nakagawara, A. and Ohira, M. (2004) 'Comprehensive genomics linking between neural development and cancer: Neuroblastoma as a model', *Cancer Letters*, 204(2), pp. 213–224. doi: 10.1016/S0304-3835(03)00457-9.

Nakamura, M. *et al.* (2003) 'Retinoic acid decreases targeting of p27 for degradation via an N-myc-dependent decrease in p27 phosphorylation and an N-myc-independent decrease in Skp2', *Cell Death and Differentiation*, 10(2), pp. 230–239. doi: 10.1038/sj.cdd.4401125.

Napier, C. E. *et al.* (2015) 'ATRX represses alternative lengthening of telomeres', *Oncotarget*, 6(18), pp. 16543–16458. doi: 10.18632/oncotarget.3846.

Niederreither, K. and Dollé, P. (2008) 'Retinoic acid in development: towards an integrated view.', *Nat. Rev. Genet.*, 9(7), pp. 541–53. doi: 10.1038/nrg2340.

Niesvizky, R. *et al.* (2018) *A Phase 1 Study of PD 0332991: Complete CDK4/6 Inhibition and Tumor Response in Sequential Combination with Bortezomib and Dexamethasone for Relapsed and Refractory Multiple Myeloma*.

Nikiforov, M. A. *et al.* (2003) 'The Mad and Myc basic domains are functionally equivalent', *Journal of Biological Chemistry*, 278(13), pp. 11094–11099. doi: 10.1074/jbc.M212298200.

Niles, R. M. (2000) 'Recent advances in the use of vitamin A (retinoids) in the prevention and treatment of cancer.', *Nutrition (Burbank, Los Angeles County, Calif.)*, 16(00), pp. 1084–9. Available at: http://www.ncbi.nlm.nih.gov/pubmed/11118831.

Nowak-Sliwinska, P. *et al.* (2012) 'Angiogenesis inhibition by the maleimide-based small molecule GNX-686', *Microvascular Research*, 83(2), pp. 105–110. doi: 10.1016/j.mvr.2011.10.004.

Nowak-Sliwinska, P., Segura, T. and Iruela-Arispe, M. L. (2014) 'The chicken chorioallantoic membrane model in biology, medicine and bioengineering', *Angiogenesis*, pp. 779–804. doi: 10.1007/s10456-014-9440-7.

Oe, T. *et al.* (2005) 'Differences in gene expression profile among SH-SY5Y neuroblastoma subclones

with different neurite outgrowth responses to nerve growth factor', *Journal of Neurochemistry*, 94(5), pp. 1264–1276. doi: 10.1111/j.1471-4159.2005.03273.x.

Olivier, M., Hollstein, M. and Hainaut, P. (2010) 'TP53 mutations in human cancers: origins, consequences, and clinical use.', *Cold Spring Harbor perspectives in biology*, 2(1), p. a0010. doi: 10.1101/cshperspect.a001008.

Olsen, J. V., Ong, S.-E. and Mann, M. (2004) 'Trypsin Cleaves Exclusively C-terminal to Arginine and Lysine Residues', *Molecular & Cellular Proteomics*, 3(6), pp. 608–614. doi: 10.1074/mcp.T400003-MCP200.

Olsen, R. R. *et al.* (2017) 'MYCN induces neuroblastoma in primary neural crest cells', *Oncogene*, 36(35), pp. 5075–5082. doi: 10.1038/onc.2017.128.

Ortmann, B., Druker, J. and Rocha, S. (2014) 'Cell cycle progression in response to oxygen levels', pp. 3569–3582. doi: 10.1007/s00018-014-1645-9.

Ostrand-Rosenberg, S. and Sinha, P. (2009) 'Myeloid-derived suppressor cells: linking inflammation and cancer.', *Journal of immunology (Baltimore, Md. : 1950)*, 182(8), pp. 4499–506. doi: 10.4049/jimmunol.0802740.

Otto, T. *et al.* (2009) 'Stabilization of N-Myc Is a Critical Function of Aurora A in Human Neuroblastoma', *Cancer Cell*, 15(1), pp. 67–78. doi: 10.1016/j.ccr.2008.12.005.

Ozaki, T. and Nakagawara, A. (2011) 'Role of p53 in Cell Death and Human Cancers', *Cancers*, 3(1), pp. 994–1013. doi: 10.3390/cancers3010994.

Påhlman, S. and Mohlin, S. (2018) 'Hypoxia and hypoxia-inducible factors in neuroblastoma', *Cell and Tissue Research*, 372(2), pp. 269–275. doi: 10.1007/s00441-017-2701-1.

Palanisamy, Rp. (2016) 'Palbociclib: A new hope in the treatment of breast cancer', *Journal of Cancer Research and Therapeutics*, 12(4), p. 1220. doi: 10.4103/0973-1482.168988.

Palmer, R. H. *et al.* (2009) 'Anaplastic lymphoma kinase: signalling in development and disease.', *The Biochemical journal*, 420(3), pp. 345–361. doi: 10.1042/BJ20090387.

Palmer, T. D., Lewis, J. and Zijlstra, A. (2011) 'Quantitative analysis of cancer metastasis using an avian embryo model.', *Journal of visualized experiments : JoVE*, (51), p. e2815. doi: 10.3791/2815.

Park, J. R. *et al.* (2013) 'Children's Oncology Group's 2013 blueprint for research: Neuroblastoma', *Pediatric Blood & Cancer*. Wiley Subscription Services, Inc., A Wiley Company, 60(6), pp. 985–993. doi: 10.1002/pbc.24433.

Parrish, A. B., Freel, C. D. and Kornbluth, S. (2013) 'Cellular Mechanisms Controlling Caspase Activation and Function', *Cold Spring Harbor Perspectives in Biology*, 5(6), pp. a008672–a008672. doi: 10.1101/cshperspect.a008672.

Passos, J. F., Saretzki, G. and Von Zglinicki, T. (2007) 'DNA damage in telomeres and mitochondria during cellular senescence: Is there a connection?', *Nucleic Acids Research*, 35(22), pp. 7505–7513. doi: 10.1093/nar/gkm893.

Patel, N. *et al.* (2012) 'DNA methylation and gene expression profiling of ewing sarcoma primary tumors reveal genes that are potential targets of epigenetic inactivation.', *Sarcoma*, 2012(C), p. 498472. doi: 10.1155/2012/498472.

Pattyn, A. *et al.* (1999) 'The homeobox gene Phox2b is essential for the development of autonomic

neural crest derivatives', *Nature*, 399(6734), pp. 366–370. doi: 10.1038/20700.

Pauklin, S. and Vallier, L. (2014) 'The Cell-Cycle State of Stem Cells Determines Cell Fate Propensity', *Cell*, 156(6), p. 1338. doi: 10.1016/j.cell.2014.02.044.

Paul, S. M. *et al.* (2010) 'How to improve R&D productivity: the pharmaceutical industry's grand challenge', *Nature Reviews Drug Discovery*, 9(3), pp. 203–214. doi: 10.1038/nrd3078.

Peifer, M. *et al.* (2015) 'Telomerase activation by genomic rearrangements in high-risk neuroblastoma', *Nature*, 526(7575), pp. 700–704. doi: 10.1038/nature14980.

Perlmann, T. (2002) 'Retinoid metabolism: a balancing act', *Nature Genetics*, 31(1), pp. 7–8. doi: 10.1038/ng877.

Peuchmaur, M. *et al.* (2003) 'Revision of the International Neuroblastoma Pathology Classification', *Cancer*, 98(10), pp. 2274–2281. doi: 10.1002/cncr.11773.

Peyressatre, M. *et al.* (2015) 'Targeting Cyclin-Dependent Kinases in Human Cancers: From Small Molecules to Peptide Inhibitors', *Cancers*, 7(1), pp. 179–237. doi: 10.3390/cancers7010179.

Pistoia, V. *et al.* (2013) 'Immunosuppressive Microenvironment in Neuroblastoma', *Frontiers in Oncology*, 3(167), p. 167. doi: 10.3389/fonc.2013.00167.

Prochownik, E. V. and Vogt, P. K. (2010) 'Therapeutic Targeting of Myc', *Genes & Cancer*, 1(6), pp. 650–659. doi: 10.1177/1947601910377494.

Puaux, A.-L. *et al.* (2011) 'A Comparison of Imaging Techniques to Monitor Tumor Growth and Cancer Progression in Living Animals', *International Journal of Molecular Imaging*, 2011, pp. 1–12. doi: 10.1155/2011/321538.

Pugh, T. J. *et al.* (2013) 'The genetic landscape of high-risk neuroblastoma', *Nature Genetics*, 45(3), pp. 279–284. doi: 10.1038/ng.2529.

Puissant, A. *et al.* (2013) 'Targeting MYCN in Neuroblastoma by BET Bromodomain Inhibition', *Cancer Discovery*, 3(3), pp. 308–323. doi: 10.1158/2159-8290.CD-12-0418.

Puyol, M. *et al.* (2010) 'A Synthetic Lethal Interaction between K-Ras Oncogenes and Cdk4 Unveils a Therapeutic Strategy for Non-small Cell Lung Carcinoma', *Cancer Cell*, 18(1), pp. 63–73. doi: 10.1016/j.ccr.2010.05.025.

Qing, G. *et al.* (2010) 'Combinatorial Regulation of Neuroblastoma Tumor Progression by N-Myc and Hypoxia Inducible Factor HIF-1', *Cancer Research*, 70(24), pp. 10351–10361. doi: 10.1158/0008-5472.CAN-10-0740.

Raabe, E. H. *et al.* (2008) 'Prevalence and functional consequence of PHOX2B mutations in neuroblastoma', *Oncogene*, 27(4), pp. 469–476. doi: 10.1038/sj.onc.1210659.

Rader, J. *et al.* (2013) 'Dual CDK4/CDK6 Inhibition Induces Cell-Cycle Arrest and Senescence in Neuroblastoma', *Clinical Cancer Research*, 19(22), pp. 6173–6182. doi: 10.1158/1078-0432.CCR-13-1675.

Rahmanzadeh, R. *et al.* (2007) 'Chromophore-assisted light inactivation of pKi-67 leads to inhibition of ribosomal RNA synthesis', *Cell Proliferation*, 40(3), pp. 422–430. doi: 10.1111/j.1365-2184.2007.00433.x.

Rajagopalan, H. and Lengauer, C. (2004) 'Aneuploidy and cancer', *Nature*, 432(7015), pp. 338–341.

doi: 10.1038/nature03099.

Ramani, P., Headford, A. and May, M. T. (2013) 'GLUT1 protein expression correlates with unfavourable histologic category and high risk in patients with neuroblastic tumours', *Virchows Archiv*, 462(2), pp. 203–209. doi: 10.1007/s00428-012-1370-4.

Ray, R. S. *et al.* (2006) 'Vanadium mediated apoptosis and cell cycle arrest in MCF7 cell line', *Chemico-Biological Interactions*, 163(3), pp. 239–247. doi: 10.1016/j.cbi.2006.08.006.

Reiff, T. *et al.* (2010) 'Neuroblastoma Phox2b Variants Stimulate Proliferation and Dedifferentiation of Immature Sympathetic Neurons', *Journal of Neuroscience*, 30(3), pp. 905–915. doi: 10.1523/JNEUROSCI.5368-09.2010.

Ren, P. *et al.* (2015) 'ATF4 and N-Myc coordinate glutamine metabolism in MYCN -amplified neuroblastoma cells through ASCT2 activation', *The Journal of Pathology*, 235(1), pp. 90–100. doi: 10.1002/path.4429.

Reymond, N., D'Água, B. B. and Ridley, A. J. (2013) 'Crossing the endothelial barrier during metastasis', *Nature Reviews Cancer*, 13(12), pp. 858–870. doi: 10.1038/nrc3628.

Reynolds, C. P. *et al.* (2000) 'Retinoic-acid-resistant neuroblastoma cell lines show alteredMYC regulation and high sensitivity to fenretinide', *Medical and Pediatric Oncology*, 35(6), pp. 597–602. doi: 10.1002/1096-911X(20001201)35:6<597::AID-MPO23>3.0.CO;2-B.

Reynolds, C. P. *et al.* (2003) 'Retinoid therapy of high-risk neuroblastoma.', *Cancer letters*, 197(1–2), pp. 185–92. doi: 10.1016/S0304-3835(03)00108-3.

Ribatti, D. *et al.* (2001) 'Chorioallantoic membrane capillary bed: A useful target for studying angiogenesis and anti-angiogenesis in vivo', *Anatomical Record*, 264(4), pp. 317–324. doi: 10.1002/ar.10021.

Ribatti, D. *et al.* (2003) 'In vivo time-course of the angiogenic response induced by multiple myeloma plasma cells in the chick embryo chorioallantoic membrane', *Journal of Anatomy*, 203(3), pp. 323–328. doi: 10.1046/j.1469-7580.2003.00220.x.

Ribatti, D. (2008) 'Chick embryo chorioallantoic membrane as a useful tool to study angiogenesis.', *International review of cell and molecular biology*, 270(08), pp. 181–224. doi: 10.1016/S1937-6448(08)01405-6.

Ribatti, D. (2010) 'The Chick Embryo Chorioallantoic Membrane as an In Vivo Assay to Study Antiangiogenesis', *Pharmaceuticals*, 3(3), pp. 482–513. doi: 10.3390/ph3030482.

Ribatti, D. (2014) 'The chick embryo chorioallantoic membrane as a model for tumor biology.', *Experimental cell research*, 328(2), pp. 314–24. doi: 10.1016/j.yexcr.2014.06.010.

Ricciardelli, C. *et al.* (2011) 'The ADAMTS1 Protease Gene Is Required for Mammary Tumor Growth and Metastasis', *AJPA*. Elsevier Inc., 179(6), pp. 3075–3085. doi: 10.1016/j.ajpath.2011.08.021.

Rice, M. (2013) *The Roles of Hypoxia on Neuroblastoma Cell Migration and Invasion*. University of Liverpool, United Kingdom.

Richardson, M. and Singh, G. (2003) 'Observations on the use of the avian chorioallantoic membrane (CAM) model in investigations into angiogenesis.', *Current drug targets. Cardiovascular & haematological disorders*, 3(2), pp. 155–185. doi: 10.2174/1568006033481492.

Rihani, A. *et al.* (2015) 'Inhibition of CDK4/6 as a novel therapeutic option for neuroblastoma',

Cancer Cell International. BioMed Central, 15(1), pp. 4–11. doi: 10.1186/s12935-015-0224-y.

Robbins, S. *et al.* (2005) 'Robbins & Cotran Pathologic Basis of Disease', *Elsevier Saunders*.

Roccio, M. *et al.* (2013) 'Predicting stem cell fate changes by differential cell cycle progression patterns', *Development*, 140(2), pp. 459–470. doi: 10.1242/dev.086215.

Roomi, M. W. *et al.* (2013) 'Inhibition of the SK-N-MC human neuroblastoma cell line in vivo and in vitro by a novel nutrient mixture', *Oncology Reports*, 29(5), pp. 1714–1720. doi: 10.3892/or.2013.2307.

Rounbehler, R. J. *et al.* (2009) 'Targeting ornithine decarboxylase impairs development of MYCN-amplified neuroblastoma.', *Cancer research*, 69(2), pp. 547–53. doi: 10.1158/0008-5472.CAN-08-2968.

Rovithi, M. *et al.* (2017) 'Development of bioluminescent chick chorioallantoic membrane (CAM) models for primary pancreatic cancer cells: A platform for drug testing', *Scientific Reports*. Nature Publishing Group, 7(February), pp. 1–13. doi: 10.1038/srep44686.

Rubie, H. *et al.* (1997) 'N-Myc gene amplification is a major prognostic factor in localized neuroblastoma: Results of the French NBL 90 study', *Journal of Clinical Oncology*, 15(3), pp. 1171–1182. doi: 10.1200/JCO.1997.15.3.1171.

Ruggeri, B. A., Camp, F. and Miknyoczki, S. (2014) 'Animal models of disease: pre-clinical animal models of cancer and their applications and utility in drug discovery.', *Biochemical pharmacology*, 87(1), pp. 150–61. doi: 10.1016/j.bcp.2013.06.020.

Rytelewski, M. *et al.* (2014) 'BRCA2 inhibition enhances cisplatin-mediated alterations in tumor cell proliferation, metabolism, and metastasis', *Molecular Oncology*, 8(8), pp. 1429–1440. doi: 10.1016/j.molonc.2014.05.017.

Sakurai, M., Maseki, N. and Sakurai, M. (1987) 'Different Karyotypic Patterns in Early and Advanced Stage Neuroblastomas', *Cancer Research*, 47(1), pp. 311–318.

Sans-Fons, M. G. *et al.* (2010) 'Matrix Metalloproteinase-9 and Cell Division in Neuroblastoma Cells and Bone Marrow Macrophages', *The American Journal of Pathology*, 177(6), pp. 2870–2885. doi: 10.2353/ajpath.2010.090050.

Santamaría, D. *et al.* (2007) 'Cdk1 is sufficient to drive the mammalian cell cycle', *Nature*, 448(7155), pp. 811–815. doi: 10.1038/nature06046.

Santarius, T. *et al.* (2010) 'A census of amplified and overexpressed human cancer genes', *Nature Reviews Cancer*, 10(1), pp. 59–64. doi: 10.1038/nrc2771.

Sathe, A. *et al.* (2016) 'CDK4/6 Inhibition Controls Proliferation of Bladder Cancer and Transcription of RB1', *Journal of Urology*, 195(3), pp. 771–779. doi: 10.1016/j.juro.2015.08.082.

Schilling, F. H. *et al.* (2002) 'Neuroblastoma Screening at One Year of Age', *New England Journal of Medicine*, 346(14), pp. 1047–1053. doi: 10.1056/NEJMoa012277.

Schleiermacher, G. *et al.* (2003) 'Treatment of stage 4s neuroblastoma--report of 10 years' experience of the French Society of Paediatric Oncology (SFOP).', *British journal of cancer*, 89(3), pp. 470–6. doi: 10.1038/sj.bjc.6601154.

Schleiermacher, G., Janoueix-Lerosey, I. and Delattre, O. (2014) 'Recent insights into the biology of neuroblastoma', *International Journal of Cancer*, 135(10), pp. 2249–2261. doi: 10.1002/ijc.29077.

Schmidt, E. E. *et al.* (1994) 'CDKN2 (p16/MTS1) gene deletion or CDK4 amplification occurs in the majority of glioblastomas.', *Cancer Research*, 54(24), p. 6321 LP-6324. Available at: http://cancerres.aacrjournals.org/content/54/24/6321.abstract.

Schmidt, M. *et al.* (2009) 'The bHLH transcription factor Hand2 is essential for the maintenance of noradrenergic properties in differentiated sympathetic neurons', *Developmental Biology*, 329(2), pp. 191–200. doi: 10.1016/j.ydbio.2009.02.020.

Schmittgen, T. D. and Livak, K. J. (2008) 'Analyzing real-time PCR data by the comparative CT method', *Nature Protocols*, 3(6), pp. 1101–1108. doi: 10.1038/nprot.2008.73.

Schneider, C. *et al.* (1999) 'Bone morphogenetic proteins are required in vivo for the generation of sympathetic neurons.', *Neuron*, 24(4), pp. 861–70. doi: S0896-6273(00)81033-8 [pii].

Schönherr, C. *et al.* (2012) 'Anaplastic Lymphoma Kinase (ALK) regulates initiation of transcription of MYCN in neuroblastoma cells', *Oncogene*, 31(50), pp. 5193–5200. doi: 10.1038/onc.2012.12.

Schwab, M. *et al.* (2003) 'Neuroblastoma: biology and molecular and chromosomal pathology', *The Lancet Oncology*, 4(8), pp. 472–480. doi: 10.1016/S1470-2045(03)01166-5.

Schwermer, M. *et al.* (2015) 'Sensitivity to cdk1-inhibition is modulated by p53 status in preclinical models of embryonal tumors.', *Oncotarget*, 6(17), pp. 15425–35. doi: 10.18632/oncotarget.3908.

Seeger, R. C., Siegel, S. E. and Sidell, N. (1982) 'Neuroblastoma: clinical perspectives, monoclonal antibodies, and retinoic acid.', *Annals of internal medicine*, 97(6), pp. 873–84. Available at: http://www.ncbi.nlm.nih.gov/pubmed/6756240.

Sela, Y. *et al.* (2012) 'Human embryonic stem cells exhibit increased propensity to differentiate during the G1 phase prior to phosphorylation of retinoblastoma protein', *Stem Cells*, 30(6), pp. 1097–1108. doi: 10.1002/stem.1078.

Semenza, G. L. (2010) 'Defining the role of hypoxia-inducible factor 1 in cancer biology and therapeutics', *Oncogene*, 29(5), pp. 625–634. doi: 10.1038/onc.2009.441.

Shalinsky, D. R. *et al.* (1995) 'Retinoid-induced Suppression of Squamous Cell Differentiation in Human Oral Squamous Cell Carcinoma Xenografts (Line 1483) in Athymic Nude Mice', *Cancer Research*, 55(14), pp. 3183–3191.

Shang, X. *et al.* (2010) 'Dual-specificity phosphatase 26 is a novel p53 phosphatase and inhibits p53 tumor suppressor functions in human neuroblastoma', *Oncogene*, 29(35), pp. 4938–4946. doi: 10.1038/onc.2010.244.

Sharp, S. E. *et al.* (2009) '123I-MIBG Scintigraphy and 18F-FDG PET in Neuroblastoma', *Journal of Nuclear Medicine*, 50(8), pp. 1237–1243. doi: 10.2967/jnumed.108.060467.

Shen, Z. (2011) 'Genomic instability and cancer: an introduction.', *Journal of molecular cell biology*, 3(1), pp. 1–3. doi: 10.1093/jmcb/mjq057.

Sheppard, K. E. and McArthur, G. A. (2013) 'The cell-cycle regulator CDK4: an emerging therapeutic target in melanoma.', *Clinical cancer research : an official journal of the American Association for Cancer Research*, 19(19), pp. 5320–8. doi: 10.1158/1078-0432.CCR-13-0259.

Sherr, C. J. and McCormick, F. (2002) 'The RB and p53 pathways in cancer', *Cancer Cell*, 2(2), pp. 103–112. doi: 10.1016/S1535-6108(02)00102-2.

Shimada, H. *et al.* (1999) 'The International Neuroblastoma Pathology Classification (the Shimada

system)', *Cancer*, 86(2), pp. 364–372. doi: 10.1002/(SICI)1097-0142(19990715)86:2<364::AID-CNCR21>3.0.CO;2-7.

Shimada, H. (2003) 'The International Neuroblastoma Pathology Classification.', *Pathologica*, 95(5), pp. 240–241. doi: 10.1002/(SICI)1097-0142(19990715)86.

Shusterman, S. *et al.* (2011) 'Iodine-131–labeled Meta-Iodobenzylguanidine Therapy of Children with Neuroblastoma: Program Planning and Initial Experience', *Seminars in Nuclear Medicine*, 41(5), pp. 354–363. doi: 10.1053/j.semnuclmed.2011.06.001.

Shyamala, K. *et al.* (2015) 'Neural crest: The fourth germ layer.', *Journal of oral and maxillofacial pathology : JOMFP*, 19(2), pp. 221–229. doi: 10.4103/0973-029X.164536.

Siddikuzzaman and Grace, V. M. B. (2012) 'Inhibition of metastatic lung cancer in C57BL/6 mice by liposome encapsulated all trans retinoic acid (ATRA).', *International immunopharmacology*, 14(4), pp. 570–9. doi: 10.1016/j.intimp.2012.09.008.

Sidell, N. (1982) 'Retinoic acid-induced growth inhibition and morphologic differentiation of human neuroblastoma cells in vitro.', *Journal of the National Cancer Institute*, 68(4), pp. 589–596. doi: 10.1093/JNCI/68.4.589.

Sidell, N. *et al.* (1983) 'Effects of retinoic acid (RA) on the growth and phenotypic expression of several human neuroblastoma cell lines.', *Experimental cell research*, 148(1), pp. 21–30. doi: 10.1016/0014-4827(83)90184-2.

Simoes-Costa, M. and Bronner, M. E. (2015) 'Establishing neural crest identity: a gene regulatory recipe', *Development*, 142(2), pp. 242–257. doi: 10.1242/dev.105445.

Sjostrom, S. K. *et al.* (2005) 'The Cdk1 Complex Plays a Prime Role in Regulating N-Myc Phosphorylation and Turnover in Neural Precursors', *Developmental Cell*, 9(3), pp. 327–338. doi: 10.1016/j.devcel.2005.07.014.

Söderholm, H. *et al.* (1999) 'Human achaete-scute homologue 1 (HASH-1) is downregulated in differentiating neuroblastoma cells', *Biochemical and Biophysical Research Communications*, 256(3), pp. 557–563. doi: 10.1006/bbrc.1999.0314.

Soucek, L. *et al.* (2008) 'Modelling Myc inhibition as a cancer therapy', *Nature*, 455(7213), pp. 679–683. doi: 10.1038/nature07260.

Stern, C. D. (2005) 'The chick: A great model system becomes even greater', *Developmental Cell*, 8(1), pp. 9–17. doi: 10.1016/j.devcel.2004.11.018.

Stewart, R. A. *et al.* (2006) 'Zebrafish foxd3 is selectively required for neural crest specification, migration and survival', *Developmental Biology*, 292(1), pp. 174–188. doi: 10.1016/j.ydbio.2005.12.035.

Straub, J. A., Sholler, G. L. S. and Nishi, R. (2007) 'Embryonic sympathoblasts transiently express TrkB in vivo and proliferate in response to brain-derived neurotrophic factor in vitro.', *BMC developmental biology*, 7(1), p. 10. doi: 10.1186/1471-213X-7-10.

Strenger, V. *et al.* (2007) 'Diagnostic and prognostic impact of urinary catecholamines in neuroblastoma patients', *Pediatric Blood and Cancer*, 48(5), pp. 504–509. doi: 10.1002/pbc.20888.

Sugiura, Y. *et al.* (1998) 'Matrix metalloproteinases-2 and -9 are expressed in human neuroblastoma: Contribution of stromal cells to their production and correlation with metastasis', *Cancer Research*,

58(10), pp. 2209–2216.

Sung, P. J. *et al.* (2013) 'Identification and characterisation of STMN4 and ROBO2 gene involvement in neuroblastoma cell differentiation', *Cancer Letters*, 328(1), pp. 168–175. doi: 10.1016/j.canlet.2012.08.015.

Swadi, R. *et al.* (2018) 'Optimising the chick chorioallantoic membrane xenograft model of neuroblastoma for drug delivery', *BMC Cancer*, 18(1), p. 28. doi: 10.1186/s12885-017-3978-x.

Sys, G. M. L. *et al.* (2013) 'The in ovo CAM-assay as a xenograft model for sarcoma.', *Journal of visualized experiments : JoVE*, (77), p. e50522. doi: 10.3791/50522.

Taggart, D. R. *et al.* (2011) 'Prognostic Value of the Stage 4S Metastatic Pattern and Tumor Biology in Patients With Metastatic Neuroblastoma Diagnosed Between Birth and 18 Months of Age', *Journal of Clinical Oncology*, 29(33), pp. 4358–4364. doi: 10.1200/JCO.2011.35.9570.

Tait, S. W. G. and Green, D. R. (2013) 'Mitochondrial regulation of cell death.', *Cold Spring Harbor perspectives in biology*, 5(9), p. a008706. doi: 10.1101/cshperspect.a008706.

Tallman, M. S. *et al.* (1997) 'All- trans -Retinoic Acid in Acute Promyelocytic Leukemia', *New England Journal of Medicine*, 337(15), pp. 1021–1028. doi: 10.1056/NEJM199710093371501.

Talmadge, J. E. and Fidler, I. J. (2010) 'AACR Centennial Series: The Biology of Cancer Metastasis: Historical Perspective', *Cancer Research*, 70(14), pp. 5649–5669. doi: 10.1158/0008-5472.CAN-10-1040.

Tan, I. de A., Ricciardelli, C. and Russell, D. L. (2013) 'The metalloproteinase ADAMTS1: a comprehensive review of its role in tumorigenic and metastatic pathways.', *International journal of cancer*, 133(10), pp. 2263–76. doi: 10.1002/ijc.28127.

Tang, X.-H. and Gudas, L. J. (2011) 'Retinoids, retinoic acid receptors, and cancer.', *Annual review of pathology*, 6, pp. 345–64. doi: 10.1146/annurev-pathol-011110-130303.

Al Tanoury, Z., Piskunov, A. and Rochette-Egly, C. (2013) 'Vitamin A and retinoid signaling: genomic and nongenomic effects', *Journal of Lipid Research*, 54(7), pp. 1761–1775. doi: 10.1194/jlr.R030833.

Teitz, T. *et al.* (2000) 'Caspase 8 is deleted or silenced preferentially in childhood neuroblastomaswith amplification of MYCN', *Nature Medicine*, 6(5), pp. 529–535. doi: 10.1038/75007.

Teitz, T. *et al.* (2013) 'Th-MYCN Mice with Caspase-8 Deficiency Develop Advanced Neuroblastoma with Bone Marrow Metastasis', *Cancer Research*, 73(13), pp. 4086–4097. doi: 10.1158/0008-5472.CAN-12-2681.

Theveneau, E. and Mayor, R. (2012) 'Neural crest delamination and migration: From epithelium-to-mesenchyme transition to collective cell migration', *Developmental Biology*, 366(1), pp. 34–54. doi: 10.1016/j.ydbio.2011.12.041.

Thiele, C. J., Reynolds, C. P. and Israel, M. A. (1985) 'Decreased expression of N-myc precedes retinoic acid-induced morphological differentiation of human neuroblastoma', *Nature*, 313(6001), p. 404–6. doi: 10.1038/313404a0.

Thorner, P. S. (2014) 'The molecular genetic profile of neuroblastoma', *Diagnostic Histopathology*, 20(2), pp. 76–83. doi: 10.1016/j.mpdhp.2014.01.005.

Tiemi Egoshi, C. *et al.* (2015) *Quantification of tumor-induced angiogenesis on chicken embryo*

chorioallantoic membrane, *Bioscience Journal*.

Tonks, N. K. (2006) 'Protein tyrosine phosphatases: from genes, to function, to disease', *Nature Reviews Molecular Cell Biology*, 7(11), pp. 833–846. doi: 10.1038/nrm2039.

Tsarovina, K. (2004) 'Essential role of Gata transcription factors in sympathetic neuron development', *Development*, 131(19), pp. 4775–4786. doi: 10.1242/dev.01370.

Tsubono, Y. and Hisamichi, S. (2004) 'A halt to neuroblastoma screening in Japan.', *The New England journal of medicine*, 350(19), pp. 2010–2011. doi: 10.1056/NEJM200405063501922.

Tweddle, D. A. *et al.* (2001) 'p53 cellular localization and function in neuroblastoma: Evidence for defective G1arrest despite WAF1 induction in MYCN-amplified cells', *American Journal of Pathology*, 158(6), pp. 2067–2077. doi: 10.1016/S0002-9440(10)64678-0.

Tweddle, D. A. *et al.* (2003) 'The p53 pathway and its inactivation in neuroblastoma', *Cancer Letters*, 197(1–2), pp. 93–98. doi: 10.1016/S0304-3835(03)00088-0.

Vajdic, C. M. and Van Leeuwen, M. T. (2009) 'Cancer incidence and risk factors after solid organ transplantation', *International Journal of Cancer*, pp. 1747–1754. doi: 10.1002/ijc.24439.

Valsesia-Wittmann, S. *et al.* (2004) 'Oncogenic cooperation between H-Twist and N-Myc overrides failsafe programs in cancer cells', *Cancer Cell*, 6(6), pp. 625–630. doi: 10.1016/j.ccr.2004.09.033.

Vandamme, T. (2014) 'Use of rodents as models of human diseases', *Journal of Pharmacy and Bioallied Sciences*, 6(1), p. 2. doi: 10.4103/0975-7406.124301.

Vandesompele, J. *et al.* (2002) 'Accurate normalization of real-time quantitative RT-PCR data by geometric averaging of multiple internal control genes', *Genome Biology*, 3(711), pp. 34–1. doi: 10.1186/gb-2002-3-7-research0034.

Vargas, A. *et al.* (2007) 'The chick embryo and its chorioallantoic membrane (CAM) for the in vivo evaluation of drug delivery systems', *Advanced Drug Delivery Reviews*, 59(11), pp. 1162–1176. doi: 10.1016/j.addr.2007.04.019.

Varlakhanova, N. V. *et al.* (2010) 'Myc maintains embryonic stem cell pluripotency and self-renewal', *Differentiation*, 80(1), pp. 9–19. doi: 10.1016/j.diff.2010.05.001.

Vassilev, L. T. *et al.* (2006) 'Selective small-molecule inhibitor reveals critical mitotic functions of human CDK1', *Proceedings of the National Academy of Sciences*, 103(28), pp. 10660–10665. doi: 10.1073/pnas.0600447103.

Vergara, M. N. and Canto-Soler, M. V. (2012) 'Rediscovering the chick embryo as a model to study retinal development.', *Neural development*, 7(1), p. 22. doi: 10.1186/1749-8104-7-22.

Vinay, D. S. *et al.* (2015) 'Immune evasion in cancer: Mechanistic basis and therapeutic strategies', *Seminars in Cancer Biology*, 35, pp. S185–S198. doi: 10.1016/j.semcancer.2015.03.004.

Vogel, H. B. and Berry, R. G. (1975) 'Chorioallantoic membrane heterotransplantation of human brain tumors.', *International journal of cancer. Journal international du cancer*, 15(3), pp. 401–8. Available at: http://www.ncbi.nlm.nih.gov/pubmed/1140859.

Vu, B. T. *et al.* (2018) 'Chick chorioallantoic membrane assay as an in vivo model to study the effect of nanoparticle-based anticancer drugs in ovarian cancer', *Scientific Reports*, 8(1), p. 8524. doi: 10.1038/s41598-018-25573-8.

Wang, J., Wang, L. and Cai, L. (2009) 'Establishment of a transplantation tumor model of human osteosarcoma in chick embryo', *The Chinese-German Journal of Clinical Oncology*, 8(9), pp. 531–536. doi: 10.1007/s10330-009-0143-2.

Warfel, N. A. *et al.* (2013) 'CDK1 stabilizes HIF-1α via direct phosphorylation of Ser668 to promote tumor growth', *Cell Cycle*, 12(23), pp. 3689–3701. doi: 10.4161/cc.26930.

Wei, G. *et al.* (1999) 'CDK4 gene amplification in osteosarcoma: Reciprocal relationship withINK4A gene alterations and mapping of 12q13 amplicons', *International Journal of Cancer*, 80(2), pp. 199–204. doi: 10.1002/(SICI)1097-0215(19990118)80:2<199::AID-IJC7>3.0.CO;2-4.

Wei, J. *et al.* (2014) 'All-trans retinoic acid and arsenic trioxide induce apoptosis and modulate intracellular concentrations of calcium in hepatocellular carcinoma cells', *Journal of Chemotherapy*, 26(6), pp. 348–352. doi: 10.1179/1973947814Y.0000000200.

Weinstein, J. L. (2003) 'Advances in the Diagnosis and Treatment of Neuroblastoma', *The Oncologist*, 8(3), pp. 278–292. doi: 10.1634/theoncologist.8-3-278.

Weiss, W. A. *et al.* (1997) 'Targeted expression of MYCN causes neuroblastoma in transgenic mice', *EMBO Journal*, 16(11), pp. 2985–2995. doi: 10.1093/emboj/16.11.2985.

Westermann, F. *et al.* (2008) 'Distinct transcriptional MYCN/c-MYC activities are associated with spontaneous regression or malignant progression in neuroblastomas', *Genome Biology*, 9(10), p. R150. doi: 10.1186/gb-2008-9-10-r150.

Whitfield, M. L. *et al.* (2006) 'Common markers of proliferation', *Nature Reviews Cancer*, 6(2), pp. 99–106. doi: 10.1038/nrc1802.

Wicki, A. and Christofori, G. (2008) 'The Angiogenic Switch in Tumorigenesis', in *Tumor Angiogenesis*. Berlin, Heidelberg: Springer Berlin Heidelberg, pp. 67–88. doi: 10.1007/978-3-540-33177-3_4.

Woods, W. G. *et al.* (2002) 'Screening of Infants and Mortality Due to Neuroblastoma', *New England Journal of Medicine*, 346(14), pp. 1041–1046. doi: 10.1056/NEJMoa012387.

Wu, G. *et al.* (1998) 'Induction of axon-like and dendrite-like processes in neuroblastoma cells', *Journal of Neurocytology*, 27(1), pp. 1–14. doi: 10.1023/A:1006910001869.

Wu, T.-C. (2007) 'The role of vascular cell adhesion molecule-1 in tumor immune evasion.', *Cancer research*, 67(13), pp. 6003–6. doi: 10.1158/0008-5472.CAN-07-1543.

Wylie, L. A. *et al.* (2015) 'Ascl1 phospho-status regulates neuronal differentiation in a Xenopus developmental model of neuroblastoma', *Disease Models & Mechanisms*, 8(5), pp. 429–441. doi: 10.1242/dmm.018630.

Xiao, B. *et al.* (2016) 'Extracellular translationally controlled tumor protein promotes colorectal cancer invasion and metastasis through Cdc42/JNK/ MMP9 signaling', *Oncotarget*, 7(31), pp. 50057–50073. doi: 10.18632/oncotarget.10315.

Yan, X. *et al.* (2011) 'Cooperative cross-talk between neuroblastoma subtypes confers resistance to anaplastic lymphoma kinase inhibition', *Genes and Cancer*, 2(5), pp. 538–549. doi: 10.1177/1947601911416003.

Yang, W. *et al.* (2016) 'Accumulation of cytoplasmic Cdk1 is associated with cancer growth and survival rate in epithelial ovarian cancer', *Oncotarget*, 7(31). doi: 10.18632/oncotarget.10373.

Yang, Y. *et al.* (2017) 'Immunocompetent mouse allograft models for development of therapies to

target breast cancer metastasis.', *Oncotarget*, 8(19), pp. 30621–30643. doi: 10.18632/oncotarget.15695.

Yang, Y. and Herrup, K. (2007) 'Cell division in the CNS: protective response or lethal event in post-mitotic neurons?', *Biochimica et biophysica acta*, 1772(4), pp. 457–66. doi: 10.1016/j.bbadis.2006.10.002.

Ying, M. *et al.* (2011) 'Regulation of glioblastoma stem cells by retinoic acid: Role for Notch pathway inhibition', *Oncogene*, 30(31), pp. 3454–3467. doi: 10.1038/onc.2011.58.

Young, M. R. *et al.* (2009) 'Monitoring of Tumor Promotion and Progression in a Mouse Model of Inflammation-Induced Colon Cancer with Magnetic Resonance Colonography', *Neoplasia*, 11(3), pp. 237-IN1. doi: 10.1593/neo.81326.

Yuan, Y.-J. *et al.* (2014) 'Application of the Chick Embryo Chorioallantoic Membrane in Neurosurgery Disease', *International Journal of Medical Sciences*, 11(12), pp. 1275–1281. doi: 10.7150/ijms.10443.

Zachariae, W. and Nasmyth, K. (1999) 'Whose end is destruction: cell division and the anaphase-promoting complex', *Genes & Development*, 13(16), pp. 2039–2058. doi: 10.1101/gad.13.16.2039.

Zhang, J. *et al.* (2017) 'The CDK4/6 inhibitor palbociclib synergizes with irinotecan to promote colorectal cancer cell death under hypoxia', *Cell Cycle*, 16(12), pp. 1193–1200. doi: 10.1080/15384101.2017.1320005.

Zhang, M.-L. *et al.* (2014) 'All-trans retinoic acid induces cell-cycle arrest in human cutaneous squamous carcinoma cells by inhibiting the mitogen-activated protein kinase-activated protein 1 pathway.', *Clinical and experimental dermatology*, 39(3), pp. 354–60. doi: 10.1111/ced.12227.

Zhang, P. *et al.* (2010) 'Kruppel-like factor 4 (Klf4) prevents embryonic stem (ES) cell differentiation by regulating Nanog gene expression', *Journal of Biological Chemistry*, 285(12), pp. 9180–9189. doi: 10.1074/jbc.M109.077958.

Zhao, M. Y. *et al.* (2009) 'Phospho-p70S6K/p85S6K and cdc2/cdk1 are novel targets for diffuse large B-cell lymphoma combination therapy.', *Clinical cancer research : an official journal of the American Association for Cancer Research*, 15(5), pp. 1708–20. doi: 10.1158/1078-0432.CCR-08-1543.

Zhao, S. G. *et al.* (2015) 'Development and validation of a novel platform-independent metastasis signature in human breast cancer', *PLoS ONE*, 10(5), pp. 1–17. doi: 10.1371/journal.pone.0126631.

Zheng, J.-N. *et al.* (2009) 'Inhibition of renal cancer cell growth in vitro and in vivo with oncolytic adenovirus armed short hairpin RNA targeting Ki-67 encoding mRNA', *Cancer Gene Therapy*, 16(1), pp. 20–32. doi: 10.1038/cgt.2008.61.

Zheng, J. N. *et al.* (2006) 'Knockdown of Ki-67 by small interfering RNA leads to inhibition of proliferation and induction of apoptosis in human renal carcinoma cells', *Life Sci*, 78(7), pp. 724–729. doi: 10.1016/j.lfs.2005.05.064.

Zhu, S. *et al.* (2012) 'Activated ALK Collaborates with MYCN in Neuroblastoma Pathogenesis', *Cancer Cell*, 21(3), pp. 362–373. doi: 10.1016/j.ccr.2012.02.010.

Zijlstra, A. *et al.* (2002) 'A quantitative analysis of rate-limiting steps in the metastatic cascade using human-specific real-time polymerase chain reaction', *Cancer Research*, 62(23), pp. 7083–7092. doi: 10.1158/0008-5472.can-08-3612.

Zijlstra, A. *et al.* (2006) 'Proangiogenic role of neutrophil-like inflammatory heterophils during

neovascularization induced by growth factors and human tumor cells', *Blood*, 107(1), pp. 317–327. doi: 10.1182/blood-2005-04-1458.

Zimmerman, K. A. *et al.* (1986) 'Differential expression of myc family genes during murine development', *Nature*, 319(6056), pp. 780–783. doi: 10.1038/319780a0.

Zirath, H. *et al.* (2013) 'MYC inhibition induces metabolic changes leading to accumulation of lipid droplets in tumor cells', *Proceedings of the National Academy of Sciences*, 110(25), pp. 10258–10263. doi: 10.1073/pnas.1222404110.

Appendix I: Journal publications and conference presentations resulting from this work

Published journal papers:

[1] Swadi, R. et al. (2018) **'Optimising the chick chorioallantoic membrane xenograft model of neuroblastoma for drug delivery'**, BMC Cancer, 18(1), p. 28. doi: 10.1186/s12885-017-3978-x.

[2] Swadi, R. R. et al. (2018) **'CDK inhibitors reduce cell proliferation and reverse hypoxia-induced metastasis of neuroblastoma tumours in a chick embryo model'**, bioRxiv preprint and submitted to Scientific Reports.

Presented conference papers:

1. R. Swadi, V. See, P. Losty, D. Moss. "**Hypoxic preconditioning promotes metastasis of Neuroblastoma cells and Cyclin-Dependant Kinase inhibitors reverse this *in vivo"***. ANR 2018, San Francisco, USA. May2018.

2. P R. Swadi, V. See, P. Losty, D. Moss. "**Hypoxia prompts Neuroblastoma metastasis and CDK inhibitors reverse this in chick embryo model"**. NCRI 2017, Liverpool, UK. Nov. 2017.

3. R. Swadi, V. See, P. Losty, D. Moss. "**Cracking the Egg: Potential of Developing Chick Embryo as a Model System to Combat Metastasis of Neuroblastoma"**. NC3Rs 2017, Liverpool, UK. Oct. 2017.

4. R. Swadi, V. See, P. Losty, D. Moss**. "Hypoxia prompts Neuroblastoma metastasis and CDK inhibitors reverse this in chick embryo model"**. Poster presentation, ITM research Day 2017, University of Liverpool, UK. July 2017. *** Winner poster.**

5. R. Swadi, K. Sampat, B. Pizer, V. See, P. Losty, D. Moss. "**Multiple CDK inhibitors Palbociclib and RO-3306 suppress Neuroblastoma growth *in vivo*"**. North West Cancer Research (NWCR) 2017 symposium, University of Liverpool, UK. April 2017.

6. R. Swadi, K. Sampat, B. Pizer, V. See, P. Losty, D. Moss. "**The role of cyclin-dependent kinase inhibitors on neuroblastoma cell differentiation and apoptosis"**. ASCB 2016, San Francisco, California, US. Dec. 2016.

7. R. Swadi, G. Mather, K. Sampat, H. Greenwood, B. Pizer, V. See, P. Losty, D. Moss. "**Using the chick embryo model to investigate new therapy for Neuroblastoma"**. Poster presentation, ITM research Day 2016, University of Liverpool, UK. July 2016. *** Winner poster.**

8. R. Swadi, K. Sampat, B. Pizer, V. See, P. Losty, D. Moss. "**The role of Cyclin-Dependent Kinase inhibitors on Neuroblastoma cell proliferation, differentiation, and apoptosis"**. North West Cancer Research (NWCR) 2016 symposium, University of Liverpool, UK. March 2016.

9. R. Swadi, G. Mather, H. Greenwood, B. Pizer, V. See, P. Losty, D. Moss. **The chick embryo: a new versatile research model for Neuroblastoma**. NCRI 2015, Liverpool, UK. Nov. 2015.

10. R. Swadi, G. Mather, K. Sampat, H. Greenwood, B. Pizer, V. See, P. Losty, D. Moss. **The chick embryo: a new versatile research model for Neuroblastoma**. Neuroblastoma symposium 2015, Newcastle, UK. Nov. 2015.

Appendix II: Awards, honours and recognitions

1- First place poster presentation Award of £200 by the Institute of Translational Medicine (ITM)/ University of Liverpool in ITM Research Day 2017.

2- First place poster presentation Award of £200 by the Institute of Translational Medicine (ITM)/ University of Liverpool in ITM Research Day 2016.

3- The North West Cancer Research centre (NWCR) Travel Grant to attend the National Cancer Research Institute (NCRI) conference, 2015.

4- Ambassador at the NCRI Conference 2017.

5- Recognition as Associate Fellow of the Higher Education Academy (AFHEA) in 2018. The recognition of attainment against the UK Professional Standards Framework for teaching and learning support in higher education.

SESSION 4

UNIVERSITY OF LIVERPOOL | INSTITUTE OF TRANSLATIONAL MEDICINE

Athena SWAN Silver Award

ITM Research Day - Thursday 7 July 2016

Prize for best poster

£200 Travel Grant

Awarded to

RASHA SWADI

Physiological and Pathological Sciences

Congratulations!

To be redeemed by the prize holder against the cost of conference registration/travel booked through the ITM Finance & Research Office before 30 June 2017 itmfin@liv.ac.uk

LIFE CHANGING World Shaping

ITM Research Day - Thursday 6 July 2017

Prize for best poster

£200 Travel Grant

Awarded to

RASHA SWADI

SESSION 1

Congratulations!

To be redeemed by the prize holder against the cost of conference registration/travel booked through the ITM Finance & Research Office before 30 June 2018 itmfin@liv.ac.uk

Certificate

Higher Education Academy

This is to certify that

Rasha Swadi

has achieved the status of

Associate Fellow

of The Higher Education Academy

in recognition of attainment against the
UK Professional Standards Framework for
teaching and learning support in higher education.

Recognition reference:
PR148537
Date of recognition
05/07/2018

Alison Johns
Chief Executive Advance HE

Nigel Carrington
Chair of the Board of Directors Advance HE